Geological Survey of Finland, Bulletin 319

THE KOILLISMAA LAYERED IGNEOUS COMPLEX, FINLAND — ITS STRUCTURE, MINERALOGY AND GEOCHEMISTRY, WITH EMPHASIS ON THE DISTRIBUTION OF CHROMIUM

by

TUOMO ALAPIETI

with 37 figures in the text, 12 tables and one appended map

GEOLOGINEN TUTKIMUSLAITOS
ESPOO 1982

Alapieti, T. 1982. The Koillismaa layered igneous complex, Finland — its structure, mineralogy and geochemistry, with emphasis on the distrubution of chromium. *Geological Survey of Finland, Bulletin 319.* 116 pages, 37 figures, 12 tables and one appended map.

The Koillismaa layered igneous complex is the result of igneous activity which occurred some 2436 ± 5 Ma ago. Crystallization took place in three separate but connected magma chambers located partly within the Archaean Presvecokarelidic basement complex and partly between this basement and the Proterozoic supracrustal rocks. The total volume of magma in these three chambers may be estimated at over 2000 km^3.

The complex consists of two exposed intrusions, the eastern, or Näränkävaara, intrusion and the western intrusion, together with a hidden 'dyke' connecting them, which may well be in itself a layered intrusion. The western intrusion has been broken up by later tectonic events into the Pirivaara, Syöte, Porttivaara, Kuusijärvi, Lipeävaara, Kaukua and Murtolampi blocks, which all form discrete entities at the present erosional surface. The internal structure of the complex may be divided into three principal units: the marginal series, the layered series and the granophyre capping the rocks of the western intrusion. The layered series can then be subdivided into zones and subzones on the basis of its cryptic layering.

The crystallization conditions were different in each of the magma chambers, and this led in turn to distinct trends of differentiation. One feature that they all have in common, however, is that the marginal series shows 'reversed' fractionation compared with the layered series. The modified differentiation index varies over a very wide range, from close to 0 up to about 80, in the visible part of the Näränkävaara intrusion, but the variation is much narrower, i.e. approx. 12.5—55, in the western intrusion. The fractionation trends for the ferromagnesian silicates are short in both intrusions, and favour Mg-rich compositions. The An content of the plagioclase also varies over a relatively narrow range, except in the dioritic rocks at Näränkävaara.

The most significant ore deposit in the Koillismaa complex in economic terms is the vanadium ore of Mustavaara, which has been mined since 1976. Other potential objects of economic interest are the low grade, disseminated platinum-bearing Ni-Cu sulphide occurrences to be found mainly in the marginal series and in places in certain horizons of the layered series. The complex has proved a disappointment as far as chrome ores are concerned, however, as no chromite-rich layers have been identified, but instead it seems to be the case at least in the visible part of the complex that the chromium is largely hidden in the lattice of the pyroxenes.

Key words: intrusions, structure, mineralogy, geochemistry, crystallization, chromium, Precambrian, Koillismaa, Finland.

Tuomo Alapieti, Department of Geology, University of Oulu, Linnanmaa, SF-90570 Oulu 57, Finland.

ISBN 951-690-157-3

ISSN 0367-522X

Vammala 1982, Vammalan Kirjapaino Oy

CONTENTS

INTRODUCTION

The Koillismaa layered igneous complex, or the 'Koillismaa complex' for short, is taken here to refer to the entity formed by the extensive occurrences of layered igneous rocks located in the Koillismaa district of north-eastern Finland (Map 1 in Appendix). This includes in the west those bodies of basic intrusive rocks located in the communes of Pudasjärvi, Taivalkoski and Posio sometimes referred to earlier by the term 'Syöte-type gabbros' (Enkovaara *et al.* 1953, Väyrynen 1954), and in the east the Näränkävaara intrusion in the commune of Kuusamo, which continues across the border into the Soviet Union. In the present surface section the rocks of this complex cover altogether an area of some 240 sq. km.

The rocks of the Koillismaa complex exhibit certain features typical of layered intrusions, including cryptic and rhythmic layering (Fig. 1) and igneous laminations. Many of the radiometric datings provided by Dr. O. Kouvo give the age of the formation as 2436 ± 5 Ma, i.e. it dates from the Early Proterozoic (Fig. 2, Table 2).

The Koillismaa layered igneous complex is of the world-wide platform layered intrusion type, as represented by the Bushveld, Great Dyke, Jimberlana, Stillwater and Dufek intrusions. Of these, the Jimberlana intrusion in Australia, which intersects metamorphic rocks of age 2670 Ma, is also approximately of the same age, with radiometric datings of 2420 ± 30 Ma (Campbell *et al.* 1970, McClay &

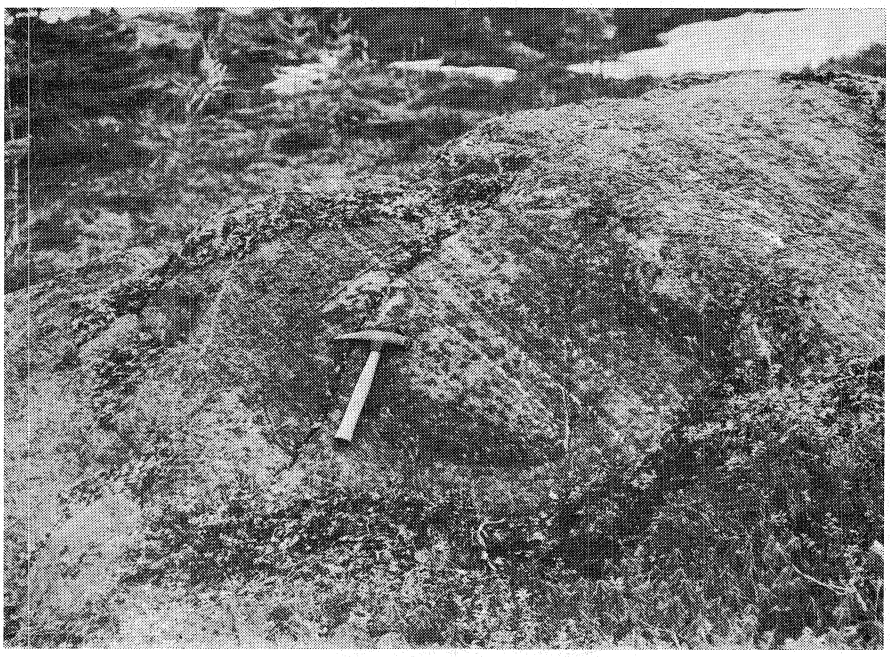

Fig. 1. Small-scale layering in the Kaukua block.

Campbell 1976). This intrusion also shows many other similarities to the Koillismaa complex in addition to its age. The other major layered intrusions of Northern Finland, including the Kemi, Penikat, Suhanko and Koitelainen intrusions, also belong to the same Early Proterozoic age group.

After crystallization the Koillismaa complex became subject to the folding and regional metamorphism associated with the Svecokarelidic orogeny. The rocks behaved almost entirely in an elastic manner during the folding process, although some brittle failure did take place, as reflected in the joint and fault system which is a conspicuous feature thoughout the complex. Some marks of metamorphism are also visible throughout the area, however, being clearest in the west. The most common feature is the alteration of the original minerals to form new, secondary minerals, e.g. the replacement of plagioclase by saussurite, olivine by serpentine, pyroxene by uralite, magnetite by amphibole and biotite, and ilmenite by leucoxene.

The present work sets out to provide a comprehensive description of the Koillismaa layered igneous complex, its structure and mineralogy and the geochemistry of the rocks and minerals contained in it. Under the last-mentioned heading the main attention will be focused on the distribution and behaviour of chromium. The aim has been to identify the primary features of the rocks at the time preceding the Svecokarelidic movements, and this has in general proved possible, since the metamorphic effects have been relatively mild, even in the western parts of the complex, so that the original structure and texture of the rocks and the original minerals are normally always in evidence.

EARLIER WORK

Bedrock mapping in the area of the Koillismaa layered igneous intrusion was commenced at the beginning of the present century, but the work was only completed in the 1950's, with the appearance of the General Geological Maps of Finland, sheets C5—B5, Oulu—Tornio (Enkovaara *et al.* 1953) and D5, Suomussalmi (Matisto 1958).

Mention is made in the description accompanying the Oulu—Tornio sheet of the rocks of the western part of the Koillismaa complex, which are referred to as 'Syöte-type gabbros' and regarded as being younger than the other formations in the area. Similarly the Näränkävaara intrusion is described in connection with the Suomussalmi sheet, where it is said to represent 'the ultrabasic type of Karelidic igneous rocks'.

The ore-prospecting organizations began to show an interest in the 'Syöte-type gabbros' in the 1950's, and Outokumpu Oy commenced ore explorations in 1962, by means of geological mapping, geophysical surveys and diamond drilling. These investigations indicated that randomly disseminated sulphides at economically interesting concentrations existed at the bottom of the 'Syöte-type gabbro' bodies. Pilot plant concentration tests were carried out by the company, but as the results were discouraging, the work was terminated in the summer of 1968. A degree dissertation was produced by V. Ohenoja (1968) based on these investigations.

Otanmäki Oy (which amalgamated with Rautaruukki Oy in 1968) carried out research in 1957—58 and 1967—71 into the vanadium-bearing magnetite gabbros occurring in the upper parts of the 'Syöte-type gabbro' bodies, which led to the discovery of economically viable vanadium ore, to the

extent that a mine was opened at Mustavaara in 1976. The genesis of the magnetite gabbro was studied by Piirainen and Juopperi (1968) from material supplied by Rautaruukki Oy and Outokumpu Oy.

The Näränkävaara intrusion attracted the attention of prospectors during the 1960's, and thus came to be re-surveyed geologically and in places geophysically. This work led to the construction by Auranen (1969) of a lithological map of the area and petrographical descriptions of the rocks of the intrusion.

The purpose of the Koillismaa Research Project, initiated by the University of Oulu in 1971, was to study basic magmatism and related metallogeny in the Koillismaa area, and the years of its operation, 1971—76, saw renewed geological mapping of the whole of the layered igneous complex and its immediate surroundings. This work covered a total of approx. 2000 sq. km. and included observations on almost 4000 sites of exposed bedrock. Various problems arising from this work were studied in Masters' and Licentiate dissertations (see Piirainen *et al.* 1978).

The research showed that the separate 'Syöte-type gabbro' bodies had not originally been discrete intrusions, but pieces of the same intrusion which had become separated in the course of subsequent movements (Piirainen *et al.* 1978). It also emerged that the Näränkävaara intrusion was organically linked with the 'Syöte-type gabbro' bodies and together with them formed an extensive layered intrusion complex. At the same time radiometric datings combined with the results of the geological mapping suggested that the formations comprising the complex were Early Proterozoic in origin, as thus very much older than had previously been assumed.

With the conclusion of the Project in 1976, processing of the extensive body of data which had been assembled remained incomplete. This work was continued later in the form of separate papers, some of which have been published. These latter include the work of Juopperi (1977) on the magnetite gabbro, and in particular the Mustavaara vanadium ore and its genesis. Hjelt *et al.* (1977) published interpretations of the magnetic and gravimetric measurements carried out in the area of the Koillismaa complex based on combinations of dipping prisms and plates, and also described the automatic interpretation program package used in obtaining these results. Piirainen *et al.* (1977) published an account of the marginal zone of the Porttivaara block and related sulphide dissemination and its genesis, and Benderitter *et al.* (1978) described magneto-telluric soundings performed in the area and compared the results with those of the seismic refraction soundings carried out by the Koillismaa Project. Separate papers have also been produced on the structure, mineralogy and geochemistry of the Näränkävaara intrusion (Alapieti *et al.* 1979 b) and of the Syöte section in the western part of the complex (Alapieti *et al.* 1979 a).

METHODS OF INVESTIGATION

SAMPLES

Over 3000 rock samples were collected in the course of the Koillismaa Project, and 17 boreholes were sunk, to a combined depth of 1670 m. A total of about 2000 thin sections and polished sections were prepared from these samples and about 800 whole-rock

chemical analyses were carried out. Out of this wide range of available samples, 127 were selected for more detailed laboratory examination for the present purposes. An attempt was made to choose these in such a way that they would span the whole area of the Koillismaa layered igneous intrusion as well as possible and would provide a clear impression of the variations occurring in the marginal series and layered series. A second criterion was that each sample should contain the maximum possible amount of primary minerals, in order to facilitate the determination of its composition and thereby the study of cryptic layering. In the western part of the layered igneous complex in particular, the minerals have often been altered as a consequence of autometamorphism and deformation caused by the Svecokarelidic movements, and in many areas it proved especially difficult to find any primary ferromagnesian silicates.

The numbering, coordinates of the sites or borehole numbers and sampling depths, estimated structural heights and mineral parageneses of the type samples are presented in Table 1, together with the relative amounts of the minerals present and indications of cumulus or intercumulus origin.

ANALYTICAL TECHNIQUES

Whole-rock analyses

The whole-rock analyses of these 127 type samples were carried out mainly at the Research Laboratory of the Raahe Steel Works of Rautaruukki Oy under the direction of Mr. E. Ojaniemi. The majority of the elements were analysed by the X-ray fluorescence technique, except that sodium was determined using an Atomic Absorption Spectrometer and that the silica content and also the high MgO concentrations of the ultramafic rocks were analysed by wet chemical methods in order to achieve greater accuracy. In addition, since the oxidation state of iron cannot be determined by the X-ray fluorescence method, the ferrous iron content was analysed titrimetrically, and ferric iron was obtained as the remainder after subtraction of the ferrous iron from the total iron content as determined by the X-ray technique. The determinations of silica and ferrous iron were performed at the Geochemical Laboratory of the Department of Geology, University of Oulu.

The REE analyses were performed by Dr. R. Rosenberg at the Reactor Laboratory of the Technical Research Centre of Finland. The method involved in the instrumental neutron activation analysis technique used for this purpose has been decribed by Rosenberg (1977).

Mineral analyses

The mineral analyses were carried out at the Institute of Electron Optics, University of Oulu, in cooperation with the staff of that Institute, mainly using a JEOL JXA-3SM electron microprobe. Altogether just over 400 quantitative microanalyses were carried out on various minerals. These were distributed between the minerals in the following manner: olivines 35 analyses, Ca-poor pyroxenes 86, Ca-rich pyroxenes 91, plagioclases 80, minerals of the spinel group 61, ilmenites 43, and other minerals 11. An average of 12

elements were determined for each mineral. A detailed account of the use of the electron microprobe technique in the study of the Koillismaa complex is in preparation (Alapieti & Sivonen), so that the description below will be restricted to those points which are most crucial for the present research.

The low X-ray take-off angle of the JXA-3SM electron microprobe places severe demands upon the polishing of the surface of the samples, since surface irregularities will affect the matrix corrections, especially those for X-ray absorption and electron backscattering (cf. Sweatman & Long 1969). Consequently a slight modification of the widely-used procedure of Moreland (1968) was employed for the preparation of the polished thin sections in order to achieve adequate results, and the preparations thus obtained then also proved highly suitable for normal petrographical work. Electrical conductivity in the thin sections, necessary for microanalysis, was achieved by means of a thin surface layer of vacuum-evaporated copper ($\sim$ 120 Å).

The minerals to be analysed were first examined by light microscope and photographed with a Polaroid camera attached to this microscope. The point for analysis was then marked on the photograph and its homogeneity often tested again with a 3-pen recorder and/or scanning images of the microprobe. Since most of the plagioclases were zoned and most of the pyroxenes and iron titanium oxides examined from the area displayed exsolution textures typical of slowly-cooled mafic rocks, these chemical inhomogeneities were inevitably reflected in the results of the analyses, in which the exsolution lamellae in particular gave rise to difficulties as the instrument available did not permit any great defocusing of the electron beam.

The conditions for the quantitative analyses were as follows: 15 kV accelerating voltage and approx. 0.05 μA specimen current (measured on metallic Cu) for Si, Ti, Al, Fe, Mg, Ca, Na and K, and 25 kV accelerating voltage and approximately 0.3 μA specimen current for the remaining elements, except in the cases of chromite and loveringite, where the accelerating voltage for Cr was 15 kV. The following standards were used: quartz for Si, TiO for Ti, synthetic sapphire for Al, hematite for Fe, periclase for Mg, wollastonite for Ca, albite for Na, sanidine for K and pure metallic standards for the remaining elements. The measured intensities were corrected for dead time and background using a separate data-processing routine developed by the Institute of Electron Optics, and the ZAF corrections for the k ratios obtained were calculated using the MKl computer program of Mason *et al.* (1969). The practical detection limit in the routine analyses was 0.05 %.

Use of a defocused beam enabled analyses to be obtained from the 'Bushveld-type orthopyroxenes', which have fine-scale exsolution lamellae parallel to (100), which closely approximate to the bulk composition of the original orthopyroxene, whereas in the case of the augites and inverted pigeonites, which show the coarse type of exsolution lamellae, a focused beam had to be used, and only the host phase could be analysed. Sometimes the lamellae were nevertheless sufficiently broad that their composition could also be determined. In spite of the breadth of the lamellae, attempts were made to perform the analyses in the (010) plane, perpendicular to the lamellae. This procedure admittedly exaggerates the Ca content in augites and underestimates it in inverted pigeonites, and also distorts the concentrations of other elements, largely Fe and Mg, although not to the same extent as that of Ca. These distortions in the results are reflected most clearly in the pyroxene fractionation trends, which in the case of augite and inverted pigeonite mainly represent subsolidus trends (Nwe 1976). Ac-

cording to Buchanan (1979), an analysis which closely approximates to the composition of the original homogeneous pyroxene phase can only be obtained for augite when using an electron beam defocused to a diameter of 200 microns.

Only partial plagioclase analyses were performed, using the 'feldspar' method of the above-mentioned program, in which only Ca, Na, K (and Fe) are measured and the program then calculates the remaining elements for correction purposes on the assumption that the minerals are stoichiometric. The other partial analyses provided for in the program, those for 'olivine' and 'pyroxene', were used only for testing the stoichiometry of these minerals. Since plagioclase crystals are zoned and are not homogenized in the same manner as ferromagnesian silicates, attempts were made to apply the plagioclase analyses to essentially unzoned inner parts or cores of discrete crystals, where the original calcic composition would tend to be preserved and part of the unzoned core of the cumulus crystals may represent the original primocryst (Wager & Brown 1968).

Attempts were generally made in the analysis of the iron—titanium oxides to use a focused beam of approx. 2 microns and to obtain individual analyses for the host oxide and the exsolution lamellae. When this was not possible, the beam was defocused to a diameter of approx. 20 microns and the bulk composition of the two phases thus obtained (cf. Gasparrini & Naldrett 1972).

The study of loveringite and of the inclusions in the chromites involved the use of both the conventional electron microprobe referred to above and also a JEOL JSM-35 scanning electron microscope (SEM) equipped with a PGT DELTA XCEL energy-dispersive spectrometer system (EDS). This combination of equipment afforded a rapid and relatively accurate means of performing such studies (cf. Metzger *et al.* 1977) and also proved to be a fairly gentle method which did not destroy the site to be examined, e.g. the minerals of an inclusion, as easily as would an instrument equipped with a wavelength dispersive spectrometer, which requires a beam current 100 times the magnitude of that of the SEM + EDS.

X-ray diffraction studies were also carried out on a few of the Fe-Cr-Ti oxides and on garnet, these being performed using a Debye-Scherrer X-ray camera.

RADIOMETRIC AGE DETERMINATIONS

The radiometric age determinations were carried out by Dr. O. Kouvo at the Geochronological Laboratory of the Geological Survey of Finland using the U-Pb method for zircon. The samples were composed of mafic pegmatoids from the basic layered intrusive rocks, granodioritic late differentiate, granophyre and metapyroxenite. The locations from which the samples were obtained are showed on the geological map (Appendix). The results of the U-Pb isotope analyses of the zircons are listed in Table 2 and a concordia diagram deduced from these results is presented in Fig. 2. All the ages are calculated using the decay constants recommended by the IUGS Subcommission on Geochronology (Steiger & Jäger 1977), and the margins of error are reported at the 95.4 % (2σ) confidence level. The zircon intersection ages with concordia are calculated according to York (1966).

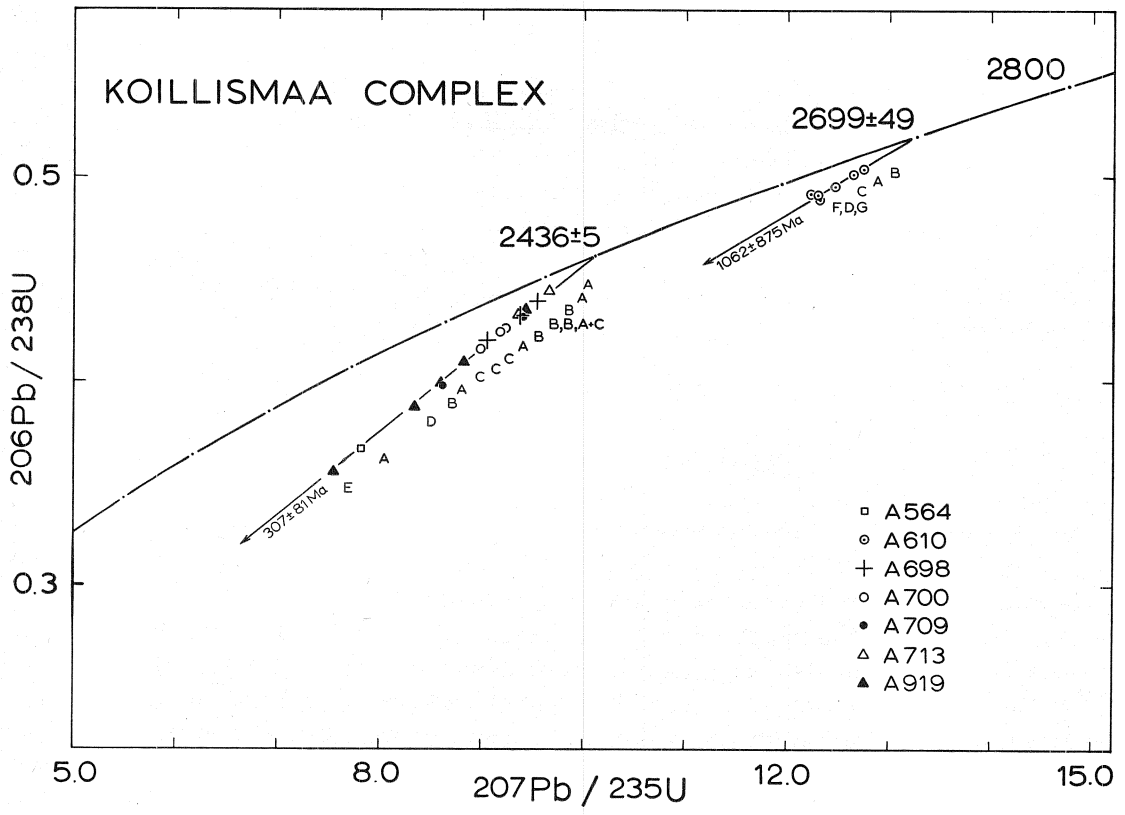

Fig. 2. U-Pb concordia diagram for zircons from the mafic pegmatoids of Lipeävaara (A698), Mustavaara in the Porttivaara block (A713), Kuusikärry in the Syöte block (A919) and Näränkävaara (A700), a granodioritic late differentiate from Näränkävaara (A709), granophyre from Valkealehto (A564) and metapyroxenite from Soukeli (A610). The numbers refer to the analyses in Table 2. Diagram compiled by O. Kouvo.

DATA PROCESSING

The data were processed on the Univac 1100/22 computer of the University of Oulu. The data required for graphical presentation were assembled on this same computer and then plotted using a CalComp 936 drum plotter system driven by a Hewlett-Packard 21 MX minicomputer. The step size of this plotter is 0,05 mm, enabling the diagrams presented here to be constructed with a high degree of accuracy.

The computer programs employed consist primarily of the PROGRA package of programs and subroutines produced by the author, and written mainly in FORTRAN 77, although with a few programs in FORTRAN V. The majority of these programs were connected with the graphical presentation aspect of the work, and were used to produce the diagrams included here, while the others were constructed for the processing of the results of the mineral microanalyses. These latter include the programs for calculating the numbers of ions in the structural formulae of the minerals, the FeO/Fe_2O_3 ratios in the Fe—Cr—Ti oxides, based of the method of Charmichael (1967), and the equi-

libration temperatures for the orthopyroxene-augite pairs following the methods of Wells (1977) and Wood and Banno (1973).

A number of existing programs were also used in addition to the PROGRA package described above. The numbers of ions in the chemical formulae of the micas were calculated using the program of Rieder (1977), the normative minerals were calculated using the HARDROCK package of programs (Till 1977), modified slightly for the Univac 1100 computer system and to allow the calculation of certain new parameters, e.g. the modified differentiation index (MDI) of von Gruenewaldt (1973), and the statistical multivariate analyses were performed using the HYLPS statistical and mathematical program package developed by the Computing Centre of the University of Helsinki.

GENERAL GEOLOGICAL SETTING

The western part of the Koillismaa complex is composed of basic intrusive rocks exposed at a number of separate stratigraphic sections, together with conformable capping granophyres, while the eastern part consists of the Näränkävaara intrusion, connected to the western part by a hidden 'dyke' which takes the form of a major gravity anomaly.

The principal geological framework for this complex of age 2436 ± 5 Ma is formed by the Archaean Presvecokarelidic basement complex, which is over 2600 Ma old, through which the basic magmas have passed and within which they have crystallized in part, and in the west the younger supracrustal rocks forming the hanging wall to the granophyre, variously interpreted as either Proterozoic or Archaean in age.

The Presvecokarelidic basement complex comprises both paragneisses and orthogneisses, often containing basic and ultrabasic, metamorphic extrusive and intrusive rocks. The interstitial zircon of the Soukeli metapyroxenite belonging to the last-mentioned group has been dated by the U-Pb method to 2699 ± 49 Ma (Map 1, Fig. 2, Table 2). Close to the contact the influence of the Koillismaa complex has led to thermometamorphic and metasomatic alterations (Piirainen *et al.* 1977), giving rise to a zone of 'albite-quartz rock' of varying thickness in which the original gneissic texture is usually always distinguishable, even in the immediate vicinity of the contact itself.

The supracrustal rocks of the hanging wall consist of polymictic conglomerate, greenstone and sericite quartzite, in this order from bottom to top. Various of the rocks making up the basement complex are encountered as fragments in the conglomerate, but no instances of the intrusive rocks of the Koillismaa complex have been observed.

FORM OF THE KOILLISMAA COMPLEX

The present surface sections of the Koillismaa layered complex, which has been exposed by a long-term process of erosion, show a relatively scattered distribution, and the original continuous form of the complex has evidently been greatly altered in later tectonic events in the course of the Svecokarelidic orogeny. Consequently it is impossible

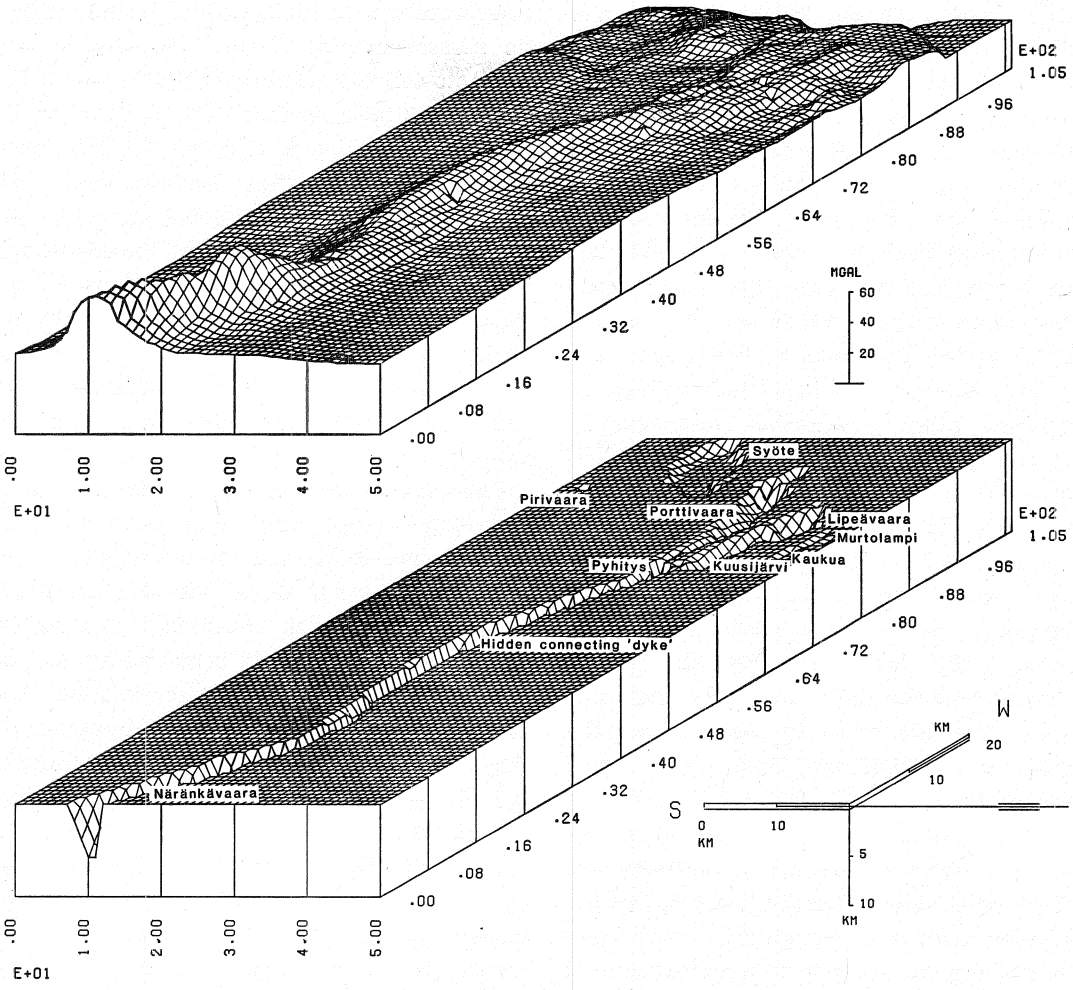

Fig. 3. Perspective block diagrams of the gravity field (above) and the Koillismaa complex (below) seen from the east. The effects of the heavy basic igneous rocks causing the gravity anomaly, together with the rock masses lying above these, are depicted negatively in the lower plot, which thus represents, in fact, the present-day basement of the Koillismaa complex. This three-dimensional geological computer plot is based on the geological map and in the vertical direction on the geophysical interpretations of Ruotsalainen (1977).

to provide any very detailed account of its primary structure. The present structure, on the other hand, is fairly well known, by virtue of the detailed geological mapping and wide range of geophysical measurements carried out by the Koillismaa Project and the interpretations provided for them. These results have enabled the construction of a three-dimensional geological computer plot depicting the form of the complex at the present time (Fig. 3). A perspective block diagram of the gravity field is also supplied for comparison purposes.

As may be seen from the block diagram (Fig. 3) and the geological map (Map 1), the present-day Koillismaa complex is a formation of over 100 km in length which is divided up into a number of smaller parts. The western part comprises a number of occurrences of basic layered intrusive rocks over-

lain by granophyre, and the eastern part the Näränkävaara intrusion, joined to the former by a hidden connecting 'dyke'.

The occurrences of intrusive rocks in the west take the form of tilted blocks having more or less the configuration of a sheet and varying in their vertical dimensions from a few hundred metres to 2.5 km below the present erosional surface. The blocks concerned, from south to north, are those of Pirivaara, Syöte, Porttivaara, Kuusijärvi, Lipeävaara, Kaukua and Murtolampi (Map 1), designated after significant landmarks in their respective areas, i.e. the hills of Pirivaara (310 m a.s.l.), Syötetunturi (431 m), Porttivaara (345 m) and Lipeävaara (337 m) and the lakes Kuusijärvi, Kaukuanjärvi and Murtolampi. These blocks vary in their dip of layering, with the four southernmost ones showing a dip of 30—40° approximately to the north and the more northerly ones dipping to the south or south-west, so that the overall form is that of a broad, interrupted synclinal formation.

The Näränkävaara intrusion, which receives its name from the hill of Näränkävaara (380 m) which dominates the landscape of the area concerned, is an elongated layered body with a triangular cross-section and extending in a downwards direction for something of the order of six kilometres. The contacts with the surrounding rocks are steep, but the layering dips only very gently, at least in the part of the intrusion visible at present. Magnetic interpretations suggest a steeper layering at greater depths, however.

The hidden connecting 'dyke' is exposed only at its western end, and there only in one branch, so that for the most part only geophysical data are available on it. Its strike is indicated on the surface by a narrow 'vein' of conglomerate, which can be followed for as much as 25 km. This suggests that the original fracture extended at least to the level of the present bedrock surface. The interpretations of the gravimetric and magnetic measurements, verified by seismic and magneto-telluric soundings (Hjelt *et al.* 1977), show the upper surface of the 'dyke' to lie at an average depth of about 1.4 km below the present erosional surface, and the anomalous mass to be about 3 km wide and very deep, going down almost vertically and becoming narrower at the same time. In addition the interpretations suggest that it rises at its western end to reach the surface at Kostonjärvi, after which it bifurcates into two 'dykes', the more southerly of which is exposed at the fell of Pyhitys (Map 1).

The above information on the present structure of the complex and analogies with other better exposed layered intrusions permit us to construct a model for the original structure, although it is admittedly difficult to take those parts already removed by erosion into account in such an interpretation. The resulting reconstruction is the hypothetical three-dimensional model for the Koillismaa layered igneous intrusion in its original guise presented in Fig. 4.

According to this model the various bodies of layered igneous rocks comprising the western part originally formed a more or less sheet-like *western intrusion* of thickness 1—3 km, a hypothetical cross-section for which is presented in Fig. 5. In the course of the Svecokarelidic orogeny this western intrusion became broken up into a number of blocks, which also tilted, some to dip towards the north and some towards the south. The consequence of this tilting is that they lie some distance apart one from another at the point where they reach the present surface, with rocks which belonged to the original basement of the complex visible in between. Separate research is in progress to study these movements in detail.

Gravimetric interpretations suggest that the deep feeders from the east do not extend very far below the western intrusion, or else

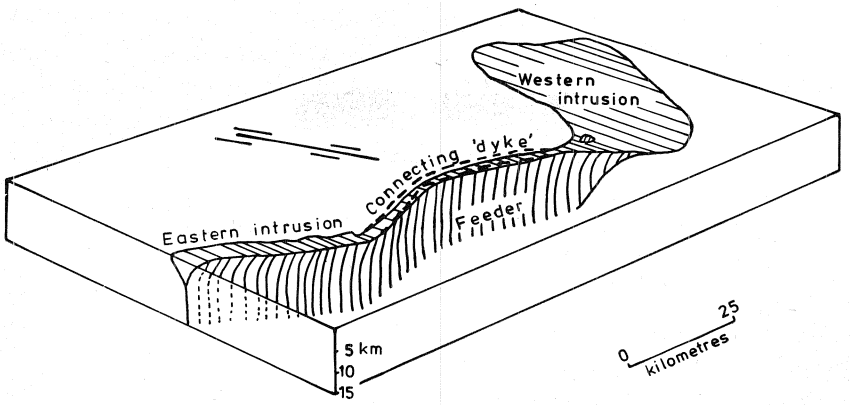

Fig. 4. Three-dimensional model of the Koillismaa complex in its original form, cut off at the level which corresponds approximately to the present ground surface.

they must be so narrow that they have no influence on the gravity field. Thus this intrusion must have filled up chiefly from the side. The magma must have opened up a subhorizontal crack between the Presvecokareleidic basement complex and the supracrustal rocks overlying it, to form a thick sequence of basic igneous rocks capped by a thinner layer of granophyre. It is on account of this mode of formation that the western intrusion is of sheet form and lacks the funnel-shaped structure so typical of many layered intrusions. In addition, the lower contact with the wall rocks and the layering of the intrusion were both originally practically horizontal and almost conformable. Thus the layered rocks bordering on the inner lower contact between the marginal and layered series represent stratigraphically only slightly higher members in the area close to the margin than do the rocks of the central part bordering on the same contact. This is particularly true in a north-south direction, whereas the basement of the intrusion would appear to rise more steeply from east to west.

The *eastern intrusion,* or *Näränkävaara intrusion,* would seem to have retained practically its original form, having been, as it is now, an elongated, roughly V-shaped layered intrusion (Figs. 3—5). Its outer contacts were steep and its layering subhorizontal, at least in the upper parts, but apparently steeper at greater depths, and particularly near the contacts. In totality it represents the type of layered intrusion which has formed directly on top of its feeder channel, with the closing of the feeder after intrusion presumably having been the result of crystallization in the feeder itself, possibly together with tectonic movements. In view of the thick ultramafic cumulates in the intrusion, the original magma chamber must have been larger than that depicted in Fig. 4, where the upper surface represents approximately the present land surface (cf. Alapieti *et al.* 1979 b).

The *connecting 'dyke'* was presumably similarly a strongly elongated V-shaped layered intrusion. Hence the use of the term 'dyke', by analogy with the corresponding formation in the Jimberlana intrusion (McClay & Campbell 1976), is misleading in that this is not a customary tabular dyke but an actual layered intrusion, which once had below it, and extending beneath the Näränkävaara intrusion at one end and some way beneath the western intrusion at the other, the feeder which 'supplied' all three of these magma chambers.

The Näränkävaara intrusion and the connecting 'dyke' together form an entity which

shows clear analogies with the Jimberlana and Muskox intrusions on the one hand (cf. McClay & Campbell 1976, Campbell 1977, Irvine & Smith 1967) and with the Great Dyke intrusion on the other (cf. Podmore 1970), while the western intrusion possesses similarities in shape with the extensive sheet-form Dufek intrusion in Antarctica (cf. Ford 1970).

The total volume of the basic magma which went to make up the Koillismaa complex may be estimated at over 2000 km^3, a figure more than four times larger than that of the Skaergaard intrusion (Wager & Brown 1968), and practically twice as large as that of Jimberlana. Since the Koillismaa complex may at times have conformed to the open-system type of layered intrusion (Alapieti *et al.* 1979 a), the volume of magma must in fact have been still greater than this, as mobile rock material would have been discharged onto the land surface of the time through overlying surface volcanoes.

STRUCTURAL UNITS OF THE KOILLISMAA COMPLEX AND THEIR ROCK TYPES

STRATIGRAPHIC SECTIONS

As explained in the previous chapter, the Koillismaa complex consists of two separate intrusions, the eastern, or Näränkävaara intrusion and the western intrusion, together with the 'dyke' connecting these. On account of the gentle dip of its layering, only about one kilometre of stratigraphic section of the Näränkävaara intrusion is visible, i.e. about one sixth of the whole vertical extent of the intrusion. The location of this *Näränkävaara stratigraphic section* with respect to the original form of the intrusion is indicated in Fig. 5. The only part of the connecting 'dyke' to be exposed at the surface is the *Pyhitys stratigraphic section* (Map 1), on the more southerly of the branches at the western end. This section represents in a vertical direction only a few hundred metres of the upper part of the whole connecting 'dyke'.

In contrast to the above, good stratigraphic sections are available for the western intrusion, which has been dissected into the *Pirivaara, Syöte, Porttivaara, Kuusijärvi, Lipeävaara, Kaukua* and *Murtolampi blocks* on account of the tilting of these blocks. This permits cross-sections to be constructed to depict the nature of the original intrusion from its basement through to the roof. Only the largest of the blocks, those of *Syöte, Porttivaara, Kuusijärvi* and *Lipeävaara,* are examined in detail here, however. The location of these with respect to the western intrusion in its original form is indicated on the hypothetical cross-section (Fig. 5).

INTERNAL UNITS, ZONES AND SUBZONES

The internal structure of the Koillismaa complex may be divided on the basis of the stratigraphic sections into three principal units: the marginal series, the layered series and the granophyre. The layered series may then be subdivided into zones and subzones with reference to its cryptic layering. The term 'series' is retained in this division in ac-

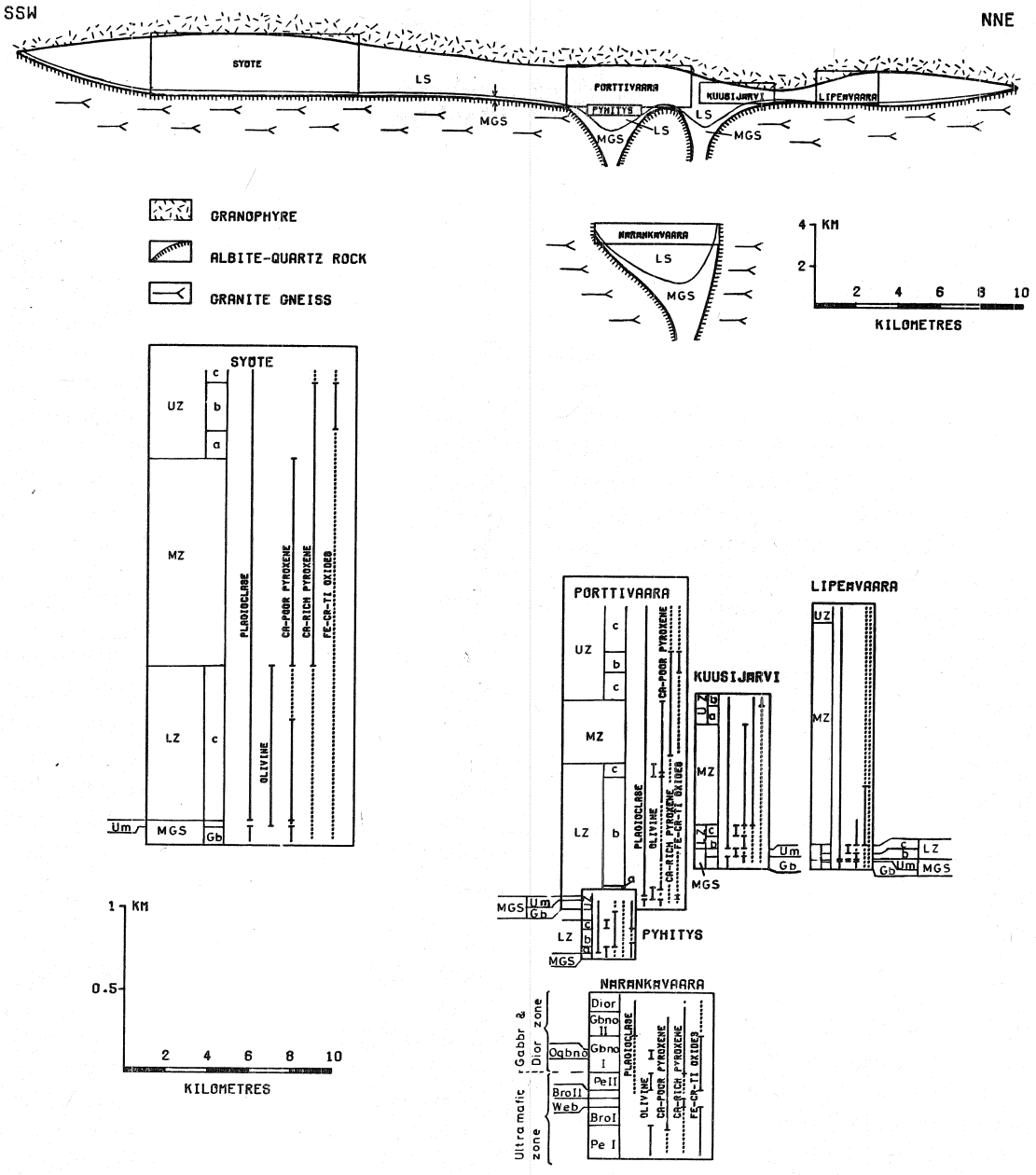

Fig. 5. Hypothetical cross-sections of the western intrusion and associated stretch of the connecting 'dyke' and the eastern, or Näränkävaara, intrusion during the period preceding the Svecokarelidic movements. The locations of the Syöte, Porttivaara, Kuusijärvi and Lipeävaara blocks and the exposed parts of Pyhitys and Näränkävaara in the original Koillismaa complex are also indicated on the cross-sections. The lower part of the diagram has the vertical scale magnified by a factor of eight in order to show the internal stratigraphy and zonation of the complex (abbreviations explained in the text). The diagram also shows the presence and absence of the most important minerals: plagioclase, olivine, Ca-poor pyroxene, Ca-rich pyroxene and iron–chromium–titanium oxides. Cumulus minerals are indicated by solid lines and intercumulus minerals by broken lines.

cordance with the convention for layered intrusions, even though in order to conform with the standard stratigraphic nomenclature it would really be better to use the term 'group'.

Marginal series

The marginal series (MGS) is a gradational series of rock types which paralled the margins of the complex and are generally discordant with respect to the layered series. The unit shows 'reversed' fractionation, grading inward from gabbroic rocks, 'contact gabbros' (Gb), at the outer contact to ultramafitolites (Um), usually through pyroxenites to peridotites, which are then followed by the rocks of the layered series. In other words, the proportion of plagioclase decreases and that of mafic minerals increases in an inward direction. This change in the abundance of the minerals is accompanied by a change in mineral composition, with the mafic minerals becoming more magnesian and the plagioclase more calcic in an inward direction, in the same manner as in the Jimberlana and Muskox intrusions (McClay & Campbell 1976, Smith 1962).

The MGS borders on thermally and metasomatically altered gneisses, 'albite—quartz rocks', which form a breccia with the contact gabbro. The chilled margin is not encountered anywhere in its original position, i.e. at the contact with the albite—quartz rock, probably as a consequence of magmatic erosion, but remnants of it are to be found in the contact gabbro, often in the form of elongated autoliths, and sometimes even in the ultramafitolite.

Marginal series of the Näränkävaara intrusion

The rocks of the MGS are exposed at the northern border of the north-western tip of the Näränkävaara intrusion (Map 1). The main rock type here is a heterogenic, metamorphic contact gabbro, which borders onto albite—quartz rock to the north. In the light of the considerable vertical dimensions of the Näränkävaara intrusion and its analogies with the better exposed Jimberlana intrusion, the proportion of the hidden MGS possessing 'reversed' fractionation must be very much larger at greater depths than it is in the part visible at present.

Marginal series of the Pyhitys section

Only the peridotitic ultramafitolite layer of the MGS is exposed in the Pyhitys section. There are nevertheless erratic blocks which indicate that contact gabbro must also occur in this series, and just as in the Näränkävaara intrusion, the proportion of the MGS must evidently be considerable in other parts of the connecting 'dyke'.

Marginal series of the western intrusion

The MGS in the western intrusion varies in thickness from 50 to 200 m. The rock types are generally heterogeneous, containing hazy streaks and veinlets of albite—quartz rock. Even so, the striking features of this unit are frequently the originally almost horizontal layering and various 'cumulate' textures, which cannot have formed by normal gravity settling, since their fractionation is the reverse of that in the layered series. Copper—nickel—iron sulphides occur sporadically in the MGS, mainly in the contact gabbro (Piirainen *et al.* 1977).

Layered series

The layered series (LS) which forms the major part of the Koillismaa complex, is characterized by cryptic and rhythmic layering and igneous lamination, where the rhythmic layering can vary in scale from the order of less than one centimetre up to macro-rhythmic layering of some hundreds of metres. The individual rock types of the series can generally be conveniently classified using the cumulate terminology of Wager and Brown (1968), since regardless of whether the genetic concepts from which this terminology is derived are valid ones, it is usually possible to distinguish in these rocks both 'cumulus' minerals and 'postcumulus' minerals which are either interstitial to or reaction products of former phases.

The LS may be further divided into zones and subzones in order to facilitate the discussion. This subdivision is based on the cryptic layering, according to the entry and exit of certain minerals as cumulus crystals. The decision as to which zone a given rock falls into requires a clear distinction to be made between the cumulus and intercumulus minerals, and this can often be difficult. At the same time, local variations may be found in the occurrence of the minerals, so that the zone boundaries may fluctuate. This is also frequently difficult to observe in the field, and it is for this reason that not all zone boundaries are indicated on the map (Map 1). The subdivision of the LS and the occurrence of the principal cumulus and intercumulus minerals in the various zones and subzones are indicated in Fig. 5.

Layered series of the Näränkävaara intrusion

The subdivision of the LS of the Näränkävaara intrusion in terms of the rock type designations remains broadly similar to that proposed earlier (see Alapieti *et al.* 1979 b). Even though different criteria were used earlier, the results correspond fairly well with the present division based on cryptic layering.

Ultramafic zone (Pe I, Bro I, Web, Bro II and Pe II)

The visible part of the Näränkävaara intrusion begins with a zone of ultramafic cumulates, which covers the major part of the area of the whole intrusion (Map 1). This comprises the following subzones, from bottom to top: peridotite I (Pe I), pyroxenites, and peridotite II (Pe II) (Fig. 5). On account of the rhythmic layering, the peridotites do not by any means always fulfil the requirement of an olivine content of over 40 % (Streckeisen 1976), but instead the term must be taken here to refer simply to ultramafic rocks containing olivine as an essential cumulus mineral.

The vertical extent of the subzone Pe I is not known, but in view of the high Mg/Fe ratio in the mafic minerals of the lowermost cumulates exposed, one might expect distinct changes to take place with depth in the lower parts of the hidden layered series, probably involving 'reversed' fractionation of the type found in the Jimberlana and Muskox intrusions. Subzone Pe I is composed principally of harzburgites. Its visible part begins with olivine(—chrome spinel) orthocumulates, which are then overlain by alternate layers of olivine(—chrome spinel) heteradcumulates and olivine—bronzite(—chrome spinel) adcumulates. Bronzite occurs in the heteradcumulates in the form of large poikilitic crystals enclosing cumulus olivine and

chrome spinel grains. Employing the abbreviation technique proposed by Todd *et al.* (1979), the olivine(—chrome spinel) cumulates may be denoted by *o(s)C* and the olivine-bronzite(—chrome spinel) cumulates by *ob(s)C*. In each case the cumulus phase indicated in parentheses is present in subordinate amounts.

Pe I is followed in the series by the pyroxenites, which are bronzitites in the upper and lower parts of the subzone and websterites (Web) in the middle part, the transitions between these often being marked by a clear magmatic layering. The rocks of the lower bronzitite layer (Bro I) are virtually monomineralic bronzite adcumulates (*bC*) (Fig. 6), whereas the upper bronzitites (Bro II) have a much higher proportion of augite and plagioclase intercumulus material, so that they are in effect bronzite orthocumulates or mesocumulates, and frequently also possess a typical distinct igneous lamination. In the websterites the augite began to crystallize temporarily to form a cumulus mineral alongside the bronzite, thus making these rocks bronzite—augite adcumulates (*baC*) with roughly even proportions of orthopyroxenes and clinopyroxenes (see Alapieti *et al.* 1979 b, Fig. 7).

The pyroxenites are overlain in the series by the subzone Pe II, the rocks of which are largely olivine—bronzite(—chrome spinel) cumulates with augite and often also plagioclase as their intercumulus minerals (*ob(s)C*), in other words lherzolites. This rock type is now taken to refer only to those peridotitic rocks which occur between the pyroxenites and gabbroids and border on both (cf. Alapieti *et al.* 1979 b). This subzone is poorly exposed, and apparently consists of a number of separate lensoid bodies, a mode of occurrence presumably attributable to magmatic erosion at the time of accumulation. This view is also supported by the presence of flow structures in the gabbronorite I subzone immediately above the upper Pe II contact, suggesting strong magmatic currents which swept across the then floor of the magma chamber and which may possibly have been associated with a fresh influx of basic magma.

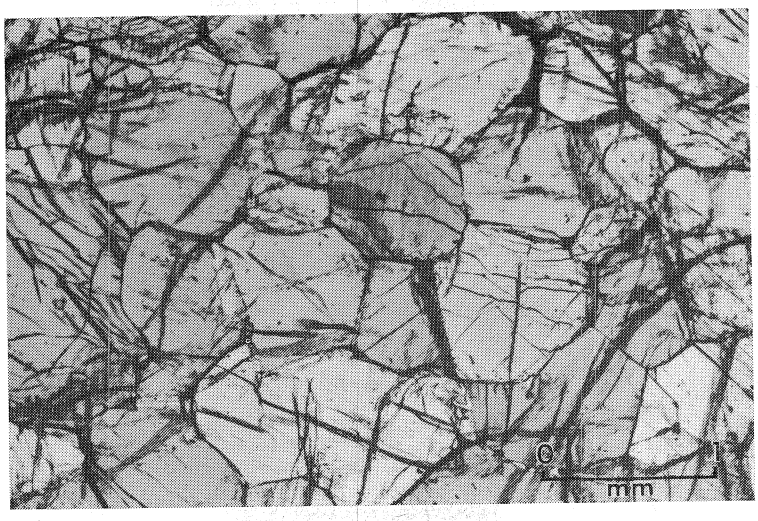

Fig. 6. Monomineralic bronzite adcumulate from the ultramafic zone of the Näränkävaara intrusion. Sample 17Nä. Magn. 23x, without analyzer.

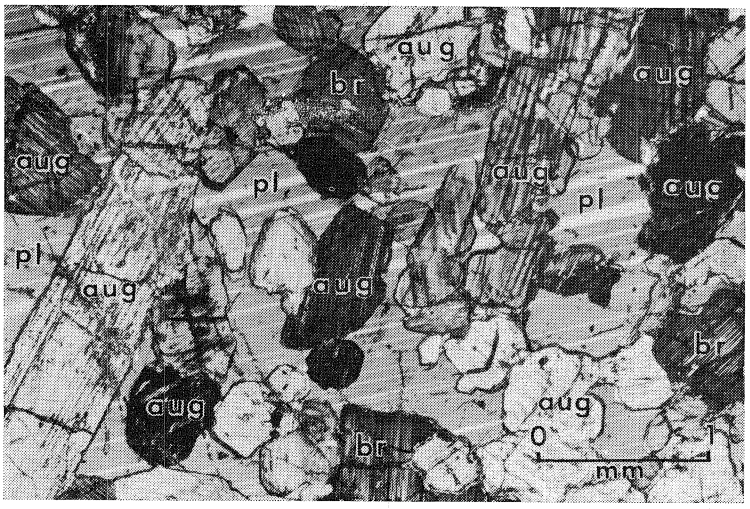

Fig. 7. Photomicrograph of part of a single, virtually unzoned poikilitic plagioclase crystal (pl) enclosing several cumulus bronzite (br) and augite (aug) crystals. Bronzite—augite heteradcumulate (Gbno I) from the Näränkävaara intrusion. Sample 39Nä. Magn. 23x. Crossed nicols.

Gabbroic and dioritic zone (Gbno I, Gbno II and Dior)

The ultramafic cumulates are followed in the stratigraphy by gabbroic rocks and later differentiates. The following subzones are recognized, from bottom to top: gabbronorite I (Gbno I), gabbronorite II (Gbno II), and quartz diorite and granodiorite (Dior) (Map 1, Fig. 5). All these rock types are massive, with no layered structures or igneous lamination, with the exception of the basal part of the gabbronorite I subzone bordering on Pe II.

Augite reappears as a cumulus mineral in Gbno I, and at the same time the amount of intercumulus plagioclase increases considerably. These rocks are bronzite—augite heteradcumulates (*baC*) containing extensive fields of virtually unzoned poikilitic plagioclase enclosing a number of cumulus bronzite and augite crystals (Fig. 7). This subzone also features a poorly exposed interlayer of olivine gabbronorite (Ogbno), or using the above cumulate terminology, olivine—bronzite—augite heteradcumulates *(obaC),* which nevertheless does not differ from the surrounding rock other than in the presence of olivine and is therefore not set aside as a separate subzone.

Plagioclase makes its appearance as a permanent cumulus mineral in the stratigraphy in the subzone Gbno II, the rocks of this subzone being plagioclase—hypersthene—augite mesocumulates or orthocumulates (*phaC*) (see Alapieti *et al.* 1979 b, Fig. 9). Plagioclase accounts for about a half of the total mineral content.

The later differentiates or dioritic rocks do not differ greatly from the Gbno II rock types in their external appearance, but are of a mineral composition which places them in the transitional area between the quartz diorites, granodiorites, tonalites and quartz monzodiorites in the classification of Streckeisen (1976).

Layered series of the Pyhitys section

The LS of the poorly exposed Pyhitys section may be divided into two zones, a lower zone (LZ) and an upper zone (UZ) (Map 1, Fig. 5). This is based on variations in mineral abundances, which are associated here with a clear macro-rhythmic layering. The lower zone may then be subdivided on the basis of the occurrence of olivine as a cumulus mineral to give the subzones LZa, LZb and LZc.

Lower zone (LZa, LZb and LZc)

The rocks of subzone LZa are mela-olivine norites, or in the cumulate terminology, olivine—plagioclase heteradcumulates (*opC*), with bronzite as the poikilitic intercumulus mineral. The occurrence of cumulus olivine is then interrupted in subzone LZb, where the rocks are bronzite—plagioclase cumulates (*bpC*) with mainly augite as an intercumulus phase. These are characterized by pronounced rhythmic layering and leucocratic plagioclase-rich varieties indicative of igneous lamination. Here plagioclase is frequently found in glomerophyric clusters (Fig. 8). In subzone LZc olivine is again found as a cumulus mineral, together with plagioclase, bronzite and ilmenomagnetite, the last-mentioned phase being present in subordinate amounts (*opb(m)C*).

Upper zone (UZ)

Olivine is no longer present in the upper zone, and granophyric intergrowths of quartz and alkali feldspar now constitute the typical pore material. Ca-poor pyroxene is represented by cumulus bronzite in the lower part of this zone, which then gives way in the upper part to poikilitic inverted pigeonite, which shows homogeneous extension due to heteradcumulate growth. Only plagioclase and ilmenomagnetite are found as cumulus minerals in this upper part of the zone.

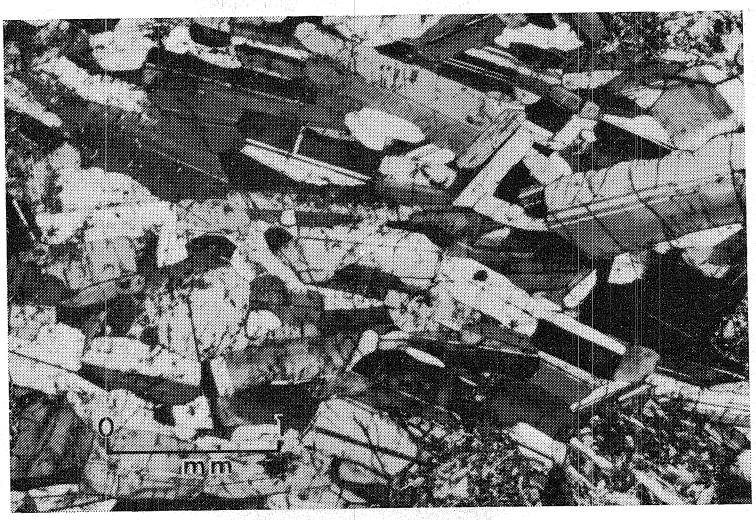

Fig. 8. Photomicrograph of a glomerophyric cluster (plagioclase adcumulate) in *bpC* from subzone LZb in the Pyhitys layered series, showing igneous lamination. Sample 4Py. Magn. 23x. Crossed nicols.

Layered series of the western intrusion

The LS of the extensive sheet-form western intrusion is to a sufficient degree an internally consistent unit that practically identical zonations are observed at all the stratigraphic sections. The differences appearing in the lower parts of the intrusion would seem to be due to an angular discordance between the marginal and layered series, causing the succession at the margins of the intrusion to begin with higher members than that in the central parts. Since this angular discordance is nevertheless relatively small, it does not give rise to any very appreciable differences. The differences found in the upper part of the layered series are most probably due to depressions in the hanging wall of the intrusion, and it seems to be for this reason that the upper part of the Lipeävaara block in particular crystallized in a quite different manner from that of the other blocks.

The layered series of this intrusion is divided into three zones: a lower zone (LZ), middle zone (MZ) and upper zone (UZ). The lower and upper zones are then each subdivided into three parts, to give the subzones LZa, LZb, LZc, UZa, UZb and UZc (Map 1, Fig. 5). These divisions are based on the presence or absence of olivine, plagioclase, Ca-poor and Ca-rich pyroxene and ilmenomagnetite as cumulus minerals. Geophysical observations suggest, however, that rocks of the hidden layered series, increasing in thickness towards the east, are to be found underlying subzone LZa in the Porttivaara block, so that this series should be taken as representing a fourth zone.

Lower zone (LZa, LZb and LZc)

Subzone LZa, with its typical pronounced fine-scale layering, is visible only in the very lowest exposed parts of the intrusion, i.e. in the lowermost layers of the Porttivaara section. The rocks are olivine norites, or in the cumulate terminology, olivine—plagioclase mesocumulates (*opC*), in the lower part of LZa and olivine—plagioclase—bronzite adcumulates (*opbC*) in the upper part. The intercumulus bronzite in the former rock type is seen to have extended by virtue of heteradcumulate growth.

LZb is the subzone which overlies LZa at Porttivaara and begins the layered series in the Kuusijärvi and Lipeävaara sections. Its lower parts are characterized by layering on a scale of 0.5—5 cm and its uppermost parts by layering of 5—15 cm, while the central parts have no layering structures at all. The rocks are bronzite—plagioclase cumulates (*bpC*), which may be interpreted as either gabbronorites or gabbros according to the amount of augite occurring as an intercumulus phase. At Porttivaara, where LZb is at its greatest observed thickness, the macrorhythmic layering may temporarily give rise to a small amount of cumulus olivine in places, in which case the bronzite becomes an intercumulus mineral (*opC*).

Olivine resumes its role as a major cumulus mineral in subzone LZc, which is now taken to account for the whole of the lower zone in the Syöte block (cf. Alapieti *et al.* 1979 a), with subzones LZa and LZb absent entirely as a consequence of an angular discordance between the MGS and LS. The rocks of LZc are principally olivine gabbronorites with olivine and plagioclase as the cumulus minerals and poikilitic bronzite and augite as intercumulus minerals. In the Porttivaara and Syöte sections bronzite is nevertheless encountered as a cumulus phase in some layers (*op* ± *bC*).

Middle zone (MZ)

Olivine, a mineral typical of the LZ, ceases to occur as a cumulus mineral in the MZ,

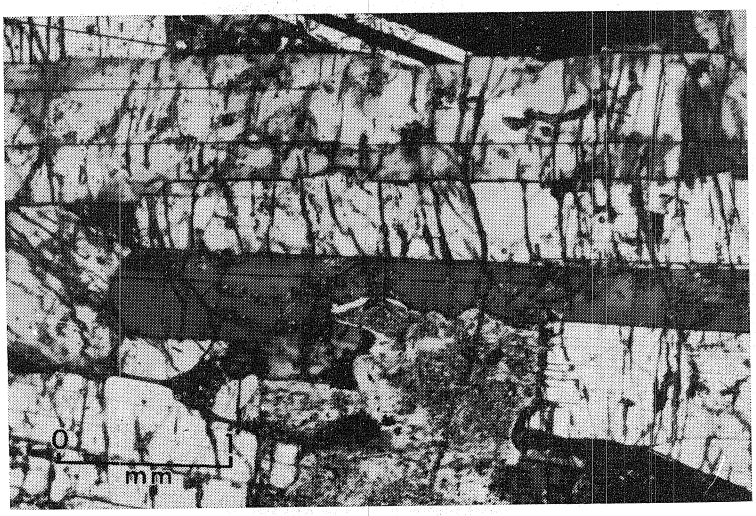

Fig. 9. Photomicrograph of a relatively coarse-grained plagioclase-rich layer in *phaC* from the middle zone of the Porttivaara layered series, showing igneous lamination. Sample 12Po. Magn. 23x. Crossed nicols.

while Ca-poor pyroxene takes its place as a cumulus mineral alongside plagioclase. This Ca-poor pyroxene may still be bronzitic in composition in the very lowest layers in this zone, in which case augite is found as an intercumulus mineral (*pbC*), but at the same time as bronzite gives way to hypersthene, augite appears as a cumulus mineral (*phaC*). Quartz and granophyric intergrowths of quartz and alkali feldspar now emerge as a major pore material. One striking and typical feature of the rocks of the MZ is frequently their coarse-scale layering, in which the layers can vary in thickness from one metre to as much as ten metres or more. Igneous lamination is also quite common (Fig. 9).

Fractionation in the Lipeävaara block obviously began to follow a pattern of its own after the deposition of the lowermost cumulates of the MZ. Firstly the crystallization of hypersthene ceased entirely at this site, and a little later on the augite reverted to an intercumulus phase. From this point on the rocks of the Lipeävaara block are plagioclase cumulates (*pC*), in which the plagioclase frequently assumes the form of glomerophyric clusters. Ilmenomagnetite-rich gabbropegmatoids are often encountered in the lower parts of these plagioclase cumulates. This idiosyncratic fractionation trend is apparently attributable to the depression in the hanging wall of the magma chamber referred to above (Fig. 5), which must have cut off the connection with the principal magma chamber to the south.

Upper zone (UZa, UZb and UZc)

The boundaries between the MZ and UZ and between the subzones of the UZ are so readily discernible in the field that they have in most cases been included in geological maps of the area. The one exception concerns subzones UZa and UZc in the Kuusijärvi block, which are so narrow that they have been impossible to draw on a map of that scale (Map 1), the latter subzone also failing to appear in the cross-section diagram (Fig. 5). The narrowness in this latter case

must also be due to the above-mentioned depression in the hanging wall.

Hypersthene, a mineral characteristic of the middle zone, no longer occurs at all in the UZa, whereas the proportion of plagioclase, which appears as a cumulus mineral alongside augite, increases steeply, allowing this mineral to achieve dominance over the latter. The rocks are leucogabbros or anorthosites ($p \pm aC$). Granophyric intergrowths are usually found in abundance.

Pronounced accumulation of titaniferous magnetite began in subzone UZb, and the amount of cumulus augite also increased again in relation to the third cumulus mineral, plagioclase. The resulting rocks are magnetite gabbros, or in the cumulate terminology plagioclase—augite—magnetite adcumulates or mesocumulates (*pamC*), in which the amount of pore material is fairly small. This subzone contains the only ore deposit in the Koillismaa complex to be mined to date, the Mustavaara vanadium-bearing iron—titanium oxide deposit at the eastern end of the Porttivaara block (Map 1).

The rocks of subzone UZc no longer have any mafic mineral as cumulus crystals, being simply plagioclase cumulates (*pC*). On the other hand, the granophyric intergrowths which form the pore material reach their maximum for the whole layered series in this subzone. Small amounts of augite and ilmenomagnetite are found as intercumulus minerals. No layering has been observed, and laminations are rare and very poorly developed. At the top of the zone one finds coarse-grained pyrite-bearing plagioclase cumulates in which the lath-like plagioclase grains may be up to 2 cm in length and enclosed within poikilitic augite of grain size up to almost 5 cm. The corresponding position in the Lipeävaara section is occupied by highly altered anorthosite with augite, ilmenomagnetite and biotite as intercumulus minerals. This is set apart as an upper zone of its own at this site, to distinguish it from the plagioclase cumulates of the MZ, which are gabbros, their poikilitic intercumulus augite amounting to almost 50 %.

Granophyre

Granophyric intergrowths of quartz and alkali feldspar form a typical pore material in the middle and upper zones of the layered series everywhere except for the Näränkävaara intrusion, in amounts which increase towards the top of the sequences. The only exception to the latter pattern is found in the magnetite gabbro, which in any case has very small quantities of pore material. These intergrowths are usually irregular in texture, although regular micrographic textures are present locally.

Of greater significance quantitatively is the true granophyre (Map 1, Fig. 5), which forms a grey-coloured, relatively homogeneous layer about one kilometre thick which constitutes a conformable cap to the layered series of the western intrusion. Its lower contact zone is exposed at only four sites, and in each case it is separated from the layered series proper by a bed 20—30 m thick composed of basic volcanic conglomerate, which may well represent an older allochthonous non-fused relict. The granophyres correspond in their composition to alkali-feldspar granites and have no layered structures or laminations. The rocks are commonly porphyritic or microphyric, showing subhedral phenocrysts of albite with granophyric intergrowths of quartz and alkali feldspar in the matrix. Biotite and hornblende, probably of metamorphic origin, occur as mafic minerals.

MINERALS AND MINERAL CHEMISTRY

The chief constituent minerals of the Koillismaa complex are olivine, Ca-poor and Ca-rich pyroxene and plagioclase, with spinellids also encountered frequently, but only locally as main components. With the exception of olivine, which only occurs as a cumulus phase, all the above have been found both as cumulus and as intercumulus minerals, whereas independent ilmenite, mica and quartz have only been encountered as minerals of intercumulus origin. Sulphides occur in traces throughout the complex, and enriched deposits of varying metal content can occur locally. The accessory minerals include loveringite, garnet, apatite and zircon. Secondary minerals such as uralite, serpentine and epidote can be very common locally, but these are not discussed in any great depth in the present connection. Some account of the occurrence of the most important minerals in the various rock types has been provided on a general level in the above, and the intention in this section of the work is to expand this description for each of the minerals separately, with particular attention being paid to their chemistry and the changes in their composition taking place in the course of fractionation.

OLIVINE

Olivine is a typical mineral of the peridotitic rocks of the marginal series of the complex and of the cumulates in the lower parts of the layered series, although in the former case it has been almost entirely altered to serpentine, so that it has been possible to analyse it only from one sample.

It is characteristic of the olivine of the layered series that it is restricted in occurrence to certain layers and subzones, i.e. interruptions must have taken place in its accumulation. These interruptions are also manifested in the form of compositional breaks, which serve as typical idiosyncratic features of individual parts of the complex and the fractionation trends detectable in these.

Taken all in all, the olivine of the Koillismaa complex varies in composition within a relatively narrow range, approximately from Fo_{88} to Fo_{68} (Table 3, Fig. 10). The fayalitic olivines typical of the upper parts of the Bushveld and Skaergaard layered intrusions (Wager & Brown 1968) are absent entirely in this case, a fact which would suggest a much lower level of Fe^{2+} enrichment during the final stages of fractionation.

Näränkävaara layered series. Within the Näränkävaara intrusion, olivine occurs as a chief mineral in the peridotites of the ultramafic zone of the layered series and in the *obaC* layer of subzone Gbno I. In the almost dunitic orthocumulates of the lower parts of subzone Pe I it appears as highly euhedral crystals. In the case of the pyroxenites an interruption in olivine accumulation is observed, but it is encountered sporadically in the very lowest *bC* layers, close to the Pe I contact and sometimes as an accessory mineral in the upper *bC* layer. The eight samples analysed suggest that the olivine of subzone Pe I varies in composition in the range $Fo_{87.6}$—$Fo_{84.4}$, with a mean value of $Fo_{86.2}$. That found in subzone Pe II is slightly richer in iron, with a mean of $Fo_{84.3}$, while the olivine in the gabbroids is fairly rich in magnesium and has a Fo value higher than

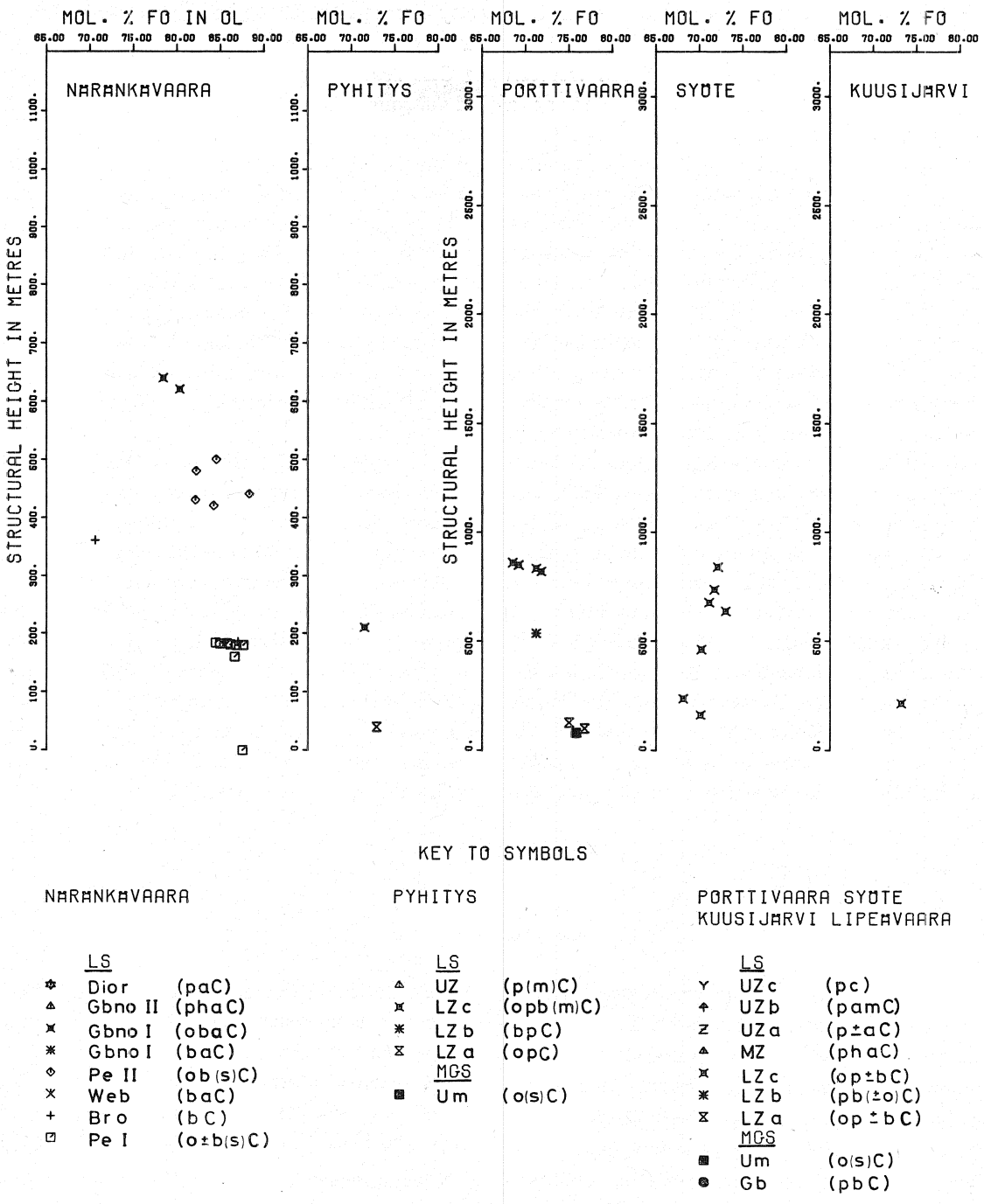

Fig. 10. Forsterite content of olivines in the Koillismaa complex plotted against height. The symbols used in this and subsequent diagrams are explained in the lower part of the figure. C = cumulate; p = plagioclase; o = olivine; b = bronzite; h = hypersthene; a = augite; s = chrome spinel; m = magnetite. The cumulus phases listed in parentheses occur in subordinate amounts. The zone and subzone abbreviations are explained in the text.

78. No more fayalitic compositions than this are recorded.

Layered series of Pyhitys and the western intrusion. The occurrence of olivine as a principal mineral in the layered series of Pyhitys and the western intrusion is restricted to two subzones, LZa and LZc, which are distinguished precisely on the criterion of olivine accumulation. The richest in forsterite are the olivines of subzone LZa at Porttivaara ($Fe_{76.8}$—$Fo_{75.0}$), which represents the lowermost visible part of the western intrusion. The forsterite content of the rocks lying below this in the marginal series is also of the same order. Olivine compositions in subzone LZc of the western intrusion show irregular fluctuations with height (Fig. 10), the range being Fo_{73}—Fo_{68}, with a mean for twelve samples of $Fo_{70.9}$, showing a distinct discrepancy in olivine composition between LZa and LZc, just as there was obviously also an interruption in accumulation. Only two determinations of olivine composition are available for the Pyhitys section, and these show the forsterite values of both of the olivine-rich subzones to be of the same order as in LZc in the western intrusion, so that any discrepancy in composition between them would be a very minor one.

One feature typical of the mesocumulates of subzone LZa in the western intrusion, and sometimes of those of LZc, is the replacement of the cumulus olivine by interstitial bronzite or augite, as shown by the presence of resorption textures. This occurs as a result of a reaction between the settled crystals and the pore liquid (Jackson 1961). This event, like the corresponding replacement of cumulus bronzite by augite (Fig. 16), can often be made use of to decide which minerals are of cumulus and which of intercumulus origin in difficult cases.

It is typical of the olivine in the Näränkävaara intrusion and at Pyhitys that its nickel content does not diminish along with the decline in the Mg/Fe ratio (Table 3, Fig. 11), a feature also observed in the Stillwater complex (Todd *et al.* 1979). The Fo and Ni values in the Porttivaara layered series vary in broadly similar directions, whereas in the Syöte section they show opposing trends, i.e. Fo values increase from the lower parts of the layered series towards the upper parts while Ni values decrease.

PYROXENES

Ca-poor pyroxene

Marginal series. Ca-poor pyroxene is found in both the mafic and the ultramafic rocks of the marginal series, possessing obvious 'cumulus' features in the former, but being poikilitic in texture in the harzburgitic rocks of the latter group. Only a few determinations of the composition of the orthopyroxenes in the marginal series could be carried out an account of pronounced uralitization (Table 4), the results obtained suggesting that the orthopyroxene of the harzburgites is bronzite, with a composition of $Mg_{81}Fe_{19}$. The Mg/Fe ratio of the mineral then decreases from the ultramafic rocks towards the external contact with the mafic rocks (Fig. 12), as mentioned above, so that the pyroxenes have the composition of bronzite, $Mg_{74}Fe_{26}$, at first, and later that of hypersthene, $Mg_{69}Fe_{31}$.

Näränkävaara layered series. Ca-poor pyroxene is encountered throughout the ultramafic and mafic sequence of the Näränkävaara intrusion as far as subzone Gbno II. The only pyroxene present in the dioritic rocks can be assumed on the basis of the pseudo-

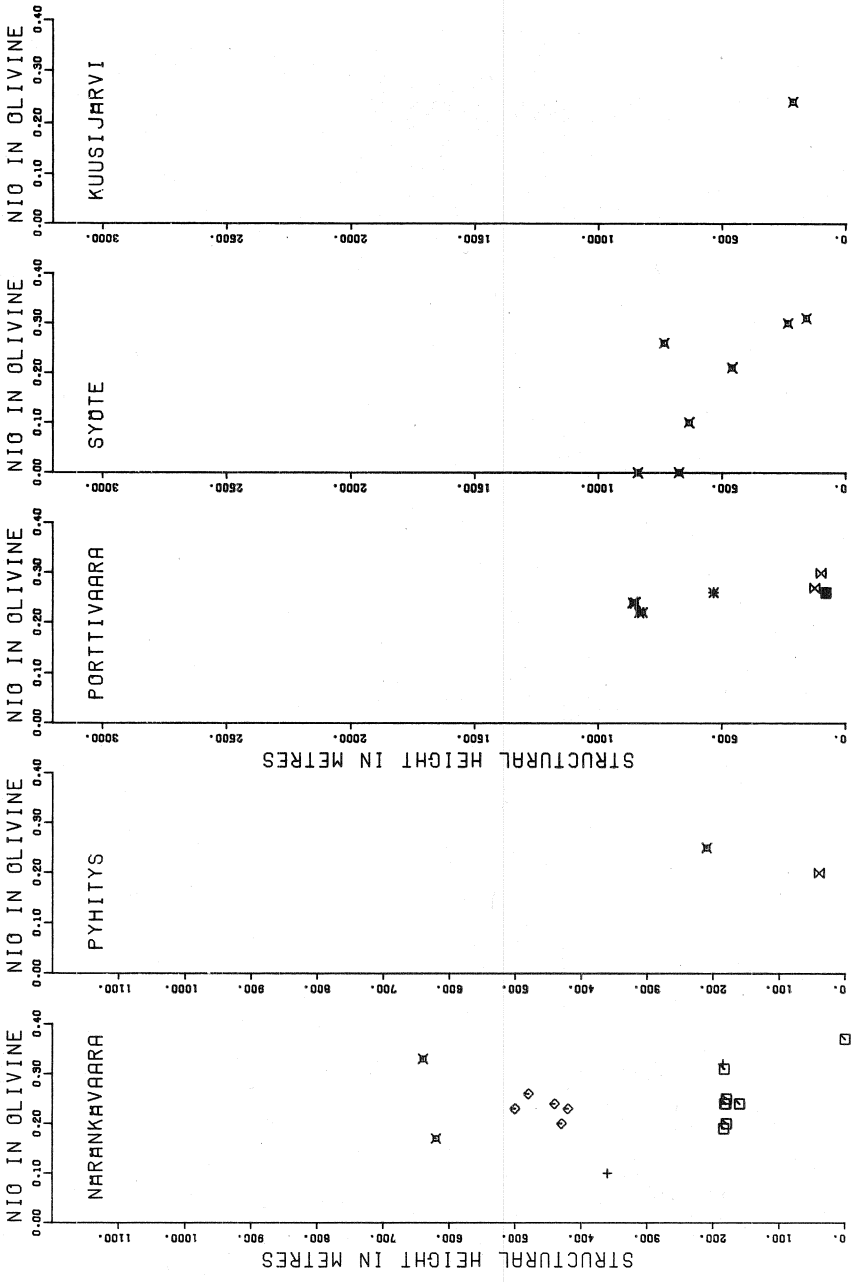

Fig. 11. NiO content of olivines in the Koillismaa complex plotted against height. For key to symbols, see Fig. 10.

morphs to have been augite. Ca-poor pyroxene is always found as a cumulus phase, except in subzone Pe I, the earliest orthopyroxenes of which are of intercumulus origin and the later ones, according to petrographic evidence, are alternatively either of heteradcumulus origin or of cumulus origin with enlargement by adcumulus growth, the latter type being dominant in the upper part of the subzone referred to here. No clear difference in composition emerges between these orthopyroxenes of differing origin.

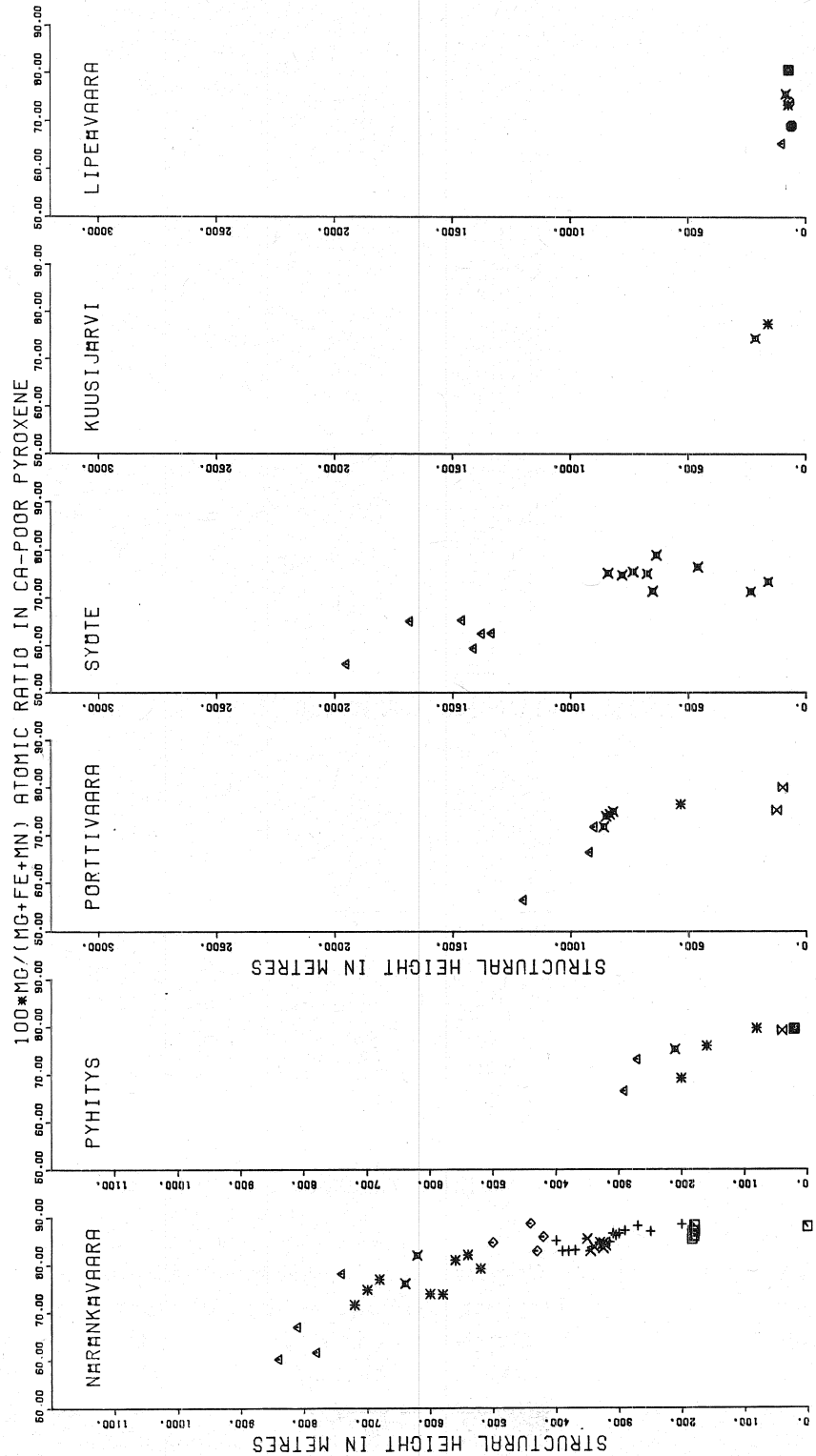

Fig. 12. Cryptic variation in Ca-poor pyroxene in the Koillismaa complex. For key to symbols, see Fig. 10.

The earliest Ca-poor pyroxenes from the ultramafic zone at Näränkävaara to be analysed are bronzites, with a composition of $Mg_{88}Fe_{12}$, thus corresponding in composition to those of the lowest cumulates in the Bushveld and Jimberlana intrusions, for example (Atkins 1969, Campbell & Borley 1974). Higher En values than this are indeed rare in layered intrusions. The Mg/Fe ratio then begins to fall towards the upper parts of the layered series (Fig. 12), although iron enrichment is not entirely progressive in nature, for the iron content decreases slightly in subzone Pe II and abruptly at the base of subzone Gbno II, before increasing again in the last part of the sequence. After this last jump, bronzite is replaced as the Ca-poor pyroxene by hypersthene.

Exsolution lamellae of augite parallel to the (100) plane of the main Ca-poor pyroxene crystal are dominant throughout the sequence at Näränkävaara, although hypersthenes more iron-rich than $Mg_{61}Fe_{39}$ also show a second set of thin lamellae arranged obliquely to the (100) set, indicating these minerals to be inverted pigeonites which have crystallized above the orthorhombic—monoclinic inversion temperature (Brown 1957). For most mafic magmas the changeover from orthopyroxene to pigeonite takes place at a ratio of about $Mg_{70}Fe_{30}$, although $Mg_{60}Fe_{40}$ has also been recorded (Phillpots 1966). The most iron-rich hypersthene found here, $Mg_{60.3}Fe_{39.7}$, represents as far as Ca-poor pyroxene is concerned the extreme limit of the compositional field in which two pyroxene phases will crystallize together, termed the 'two-pyroxene boundary'. This is reflected here at Näränkävaara in an exceptionally high En value by comparison with other layered intrusions with the exception of those of Jimberlana and Sudbury (cf. Campbell & Nolan 1974).

Pyhitys layered series. The Ca-poor pyroxene occurring in subzone LZa of the layered series in the Pyhitys section is a bronzite, with a composition of $Mg_{79.3}Fe_{20.7}$. It is of heteradcumulus origin and forms poikilitic grains of size approx. 1 cm. When Ca-poor pyroxene becomes a cumulus phase, in subzone LZb, its En value begins to fall markedly (Fig. 12), dropping into the hypersthenic composition area temporarily in the uppermost part of this subzone ($Mg_{69.2}Fe_{30.8}$). In subzone LZc olivine resumes its role as a cumulus phase and the composition of the Ca-poor pyroxene shows a simultaneous jump towards a higher Mg concentration. Beyond this point the iron content then begins to rise again, and approximately 70 m above the base of the UZ the cumulus orthopyroxene gives way to inverted pigeonite of heteradcumulus origin. This shift to a monoclinic phase is reflected in the subsolidus exsolution textures, i.e. the (100)-oriented lamellae typical of the Ca-poor pyroxenes of the lower layers are now replaced by coarser augite lamellae oriented approximately parallel to the relict (001) plane of the original pigeonite. Very thin lamellae parallel to the (100) plane of the orthopyroxene, which were exsolved after inversion, may also be found, however. The subsolidus composition of the hypersthenic orthopyroxene formed upon inversion is $Mg_{66.5}Fe_{33.5}$.

Layered series of the western intrusion. Ca-poor pyroxene is encountered in the lower and middle zones of the layered series in the western intrusion. The earliest orthopyroxenes in subzone LZa are bronzites, with a composition of $Mg_{80}Fe_{20}$, and are either of intercumulus primary origin and extended through heteradcumulate growth or else of intercumulus secondary origin and generated through olivine replacement. The later orthopyroxenes in LZa are cumulus minerals extended through adcumulate growth and enclosing small grains of plagioclase. Ca-poor pyroxene is usually a cumulus mineral in subzone LZb, except in the thick cumulates

representing this subzone at Porttivaara, where olivine occurs temporarily as a cumulus phase in the *opC* layers and bronzite is present as large poikilitic grains. In the olivine-rich subzone LZc bronzite occurs as an intercumulus mineral, with the exception of a few layers at Syöte and Porttivaara, where it is obviously of cumulus origin. Ca-poor pyroxene becomes permanently established as a cumulus phase in the middle zone, at the same time as its iron enrichment becomes more pronounced and bronzite is replaced by hypersthene. With advancing fractionation the Mg/Fe ratio of this hypersthene then declines to within the range 66.4/33.6—63.3/36.7, and the orthopyroxene gives way to inverted pigeonite, according to textural evidence, in the other words the Ca-poor pyroxene phase has now crystallized in the form of a monoclinic pigeonite (Fig. 13). The lower boundary value for the Mg/Fe ratio was obtained for the calculated composition of the original pigeonite of sample 13Sy (Alapieti *et al.* 1979 a, Table 4). The first hypersthenes formed via the subsolidus inversion of pigeonite at Pyhitys and in the western intrusion are slightly richer in the enstatite molecule than those at Näränkävaara. With further crystallization and iron enrichment of the Ca-poor pyroxene, pigeonite continues to accumulate until the two-pyroxene boundary on the Ca—Mg—Fe diagram is reached (Fig. 18), for pigeonite ceased to be precipitated by the top of the middle zone and the rocks of the upper zone contain only one pyroxene, augite. Since only the subsolidus trend is available in the case of Ca-rich pyroxene (Fig. 18), making it impossible to determine with accuracy which is the augite with the minimum Wo content, thus the pigeonite with a composition of $(Mg_{56.1}Fe_{43.9})$, the richest in the ferrosilite molecule found, provides only an extreme value for the two-pyroxene boundary, as was also the case at Näränkävaara.

The Cr_2O_3 content of Ca-poor pyroxene (Table 4, Figs. 12 and 14) also varies in a manner which may reasonably be attributed to fractional crystallization. The highest content, about 0.5 % by weight, is found in the

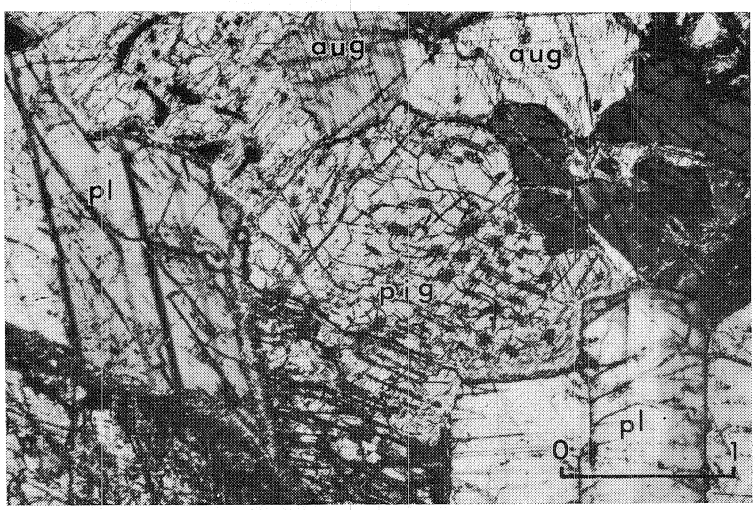

Fig. 13. Inverted pigeonite in *phaC* from the middle zone of the Syöte layered series (sample 13Sy) showing broad exsolution lamellae of augite approximately parallel to the relict (001) plane of the original pigeonite. pig = inverted pigeonite; aug = augite; pl = plagioclase. Magn. 23x. Crossed nicols.

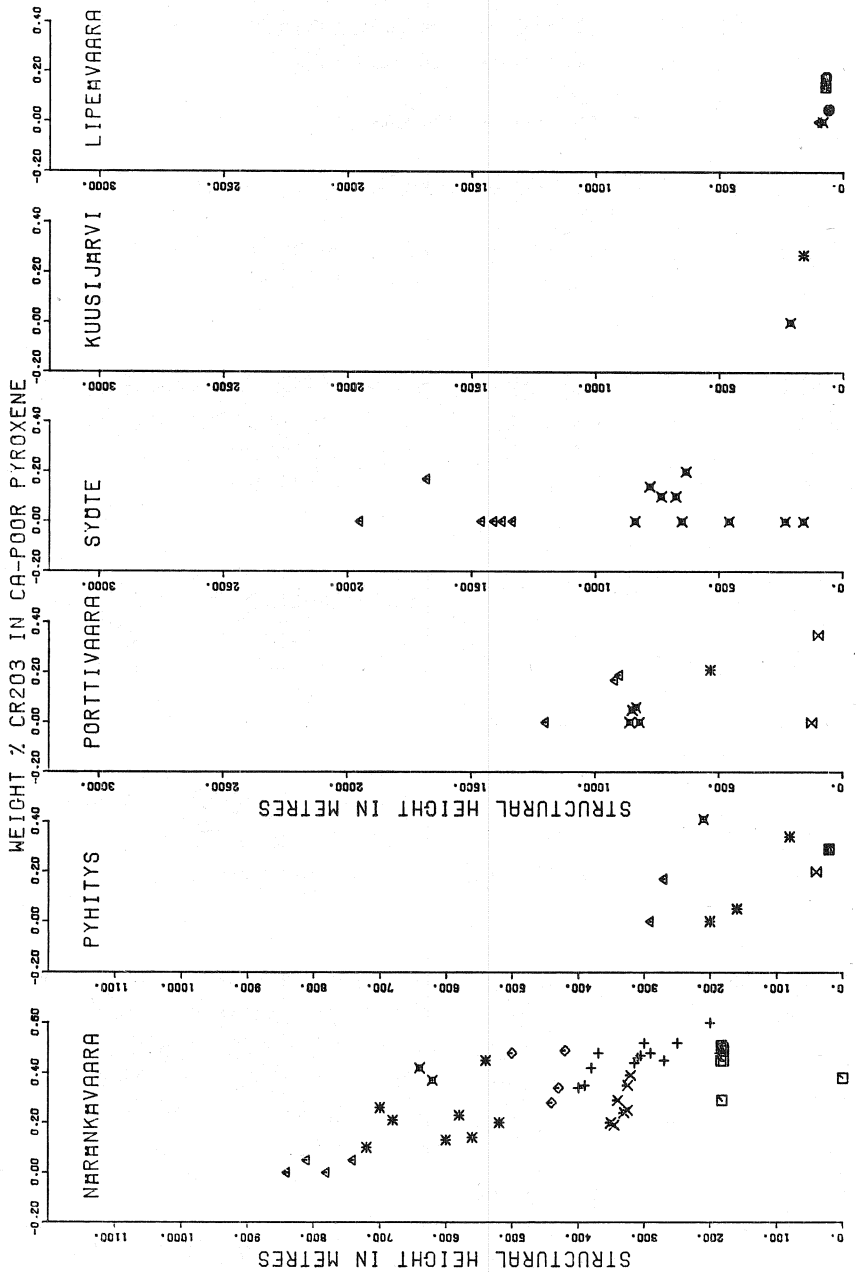

Fig. 14. Cr_2O_3 content of Ca-poor pyroxenes in the Koillismaa complex plotted against height. For key to symbols, see Fig. 10.

early pyroxenes of the ultramafic cumulates, after which the figure falls sympathetically with the Mg/Fe ratio towards the end of fractionation. There are nevertheless a few exceptions to this mutual trend. The Cr_2O_3 content of the orthopyroxenes in the websterites is on average lower than that of the orthopyroxenes in the other rocks of the ultramafic zone, the Cr_2O_3 content of the orthopyroxene at the base of subzone Gbno II is

low in spite of a relatively high En value, and there is a distinct jump in the Cr_2O_3 content of the orthopyroxenes in the middle zone at Porttivaara and Syöte which is not reflected in the Mg/Fe ratio.

Ca-rich pyroxene

Marginal series. Ca-rich pyroxene occurs as a poikilitic mineral throughout the ultramafic and mafic rocks of the marginal series. The small amount of clinopyroxene found in the harzburgite of this series takes the form of either endiopside or augite, having an approximate composition of $Ca_{44}Mg_{46}Fe_{10}$ (Table 5, sample 4Li, Figs. 15 and 18). The amount of clinopyroxene then increases in the gabbroids, while its En value falls considerably below that observed in the harzburgites. It was not possible to study in detail the variation in the Mg/Fe ratio for augite in the gabbroids, however, on account of pronounced uralitization, entirely unaltered augite being found only in sample 2Li (Table 5).

Näränkävaara layered series. Ca-rich pyroxene has been precipitated throughout the visible part of the layered series in the Näränkävaara intrusion, although it has subsequently undergone complete uralitization in the dioritic rocks. The clinopyroxene in the ultramafic cumulates follows an almost constant composition conforming to chromium-rich endiopside or diopside. Except in the websterites, this is found as an intercumulus phase, either in the form of poikilitic, net-like grains of heteradcumulus origin, or else with textural features which show the clinopyroxene to be of intercumulus secondary origin and generated through the replacement of bronzite. Above the ultramafic zone iron enrichment begins to show a progressive increase towards the top of the layered series (Fig. 15), although the detailed clinopyroxene composition exhibits irregular fluctuations with height in the sequence, the most obvious deviation from the progressive trend being the sudden drop in Fe content in the base of the gabbronorite II subzone, as was also observed in the case of the Ca-poor pyroxene. The most ferriferous member analysed from the Näränkävaara layered series had the composition $Ca_{45.6}Mg_{36.7}Fe_{17.7}$, representing at the same time the extreme iron-rich value for the two-pyroxene boundary in the case of augite (Fig. 18).

The exsolution textures of the magnesium-rich clinopyroxenes in the Näränkävaara layered series consist of lamellae of orthopyroxene parallel to the (100) plane of the main crystal. The clinopyroxenes in the websterites nevertheless feature a second, less distinct, set of lamellae which may be shown by determination on a Universal Stage to be approximately parallel to (001). The microanalyses of these latter, however, suggest that they do not differ in composition from the (100)-oriented lamellae, and they are therefore most probably simply extensions of these. Those augites which are more iron-rich than $Ca_{47}Mg_{36}Fe_{17}$ have crystallized at temperatures above that of pigeonite—orthopyroxene inversion, and thus contain pigeonite lamellae approximately parallel to the (001) plane of the augite host. Lamellae parallel to the (100) plane of the main crystal are also visible in many such pyroxenes, since the exsolved pigeonite has subsequently inverted to orthopyroxene on cooling through the monoclinic—orthorhombic inversion temperature.

Pyhitys layered series. Ca-rich pyroxene is found as an intercumulus phase in the whole of the exposed part of the Pyhitys

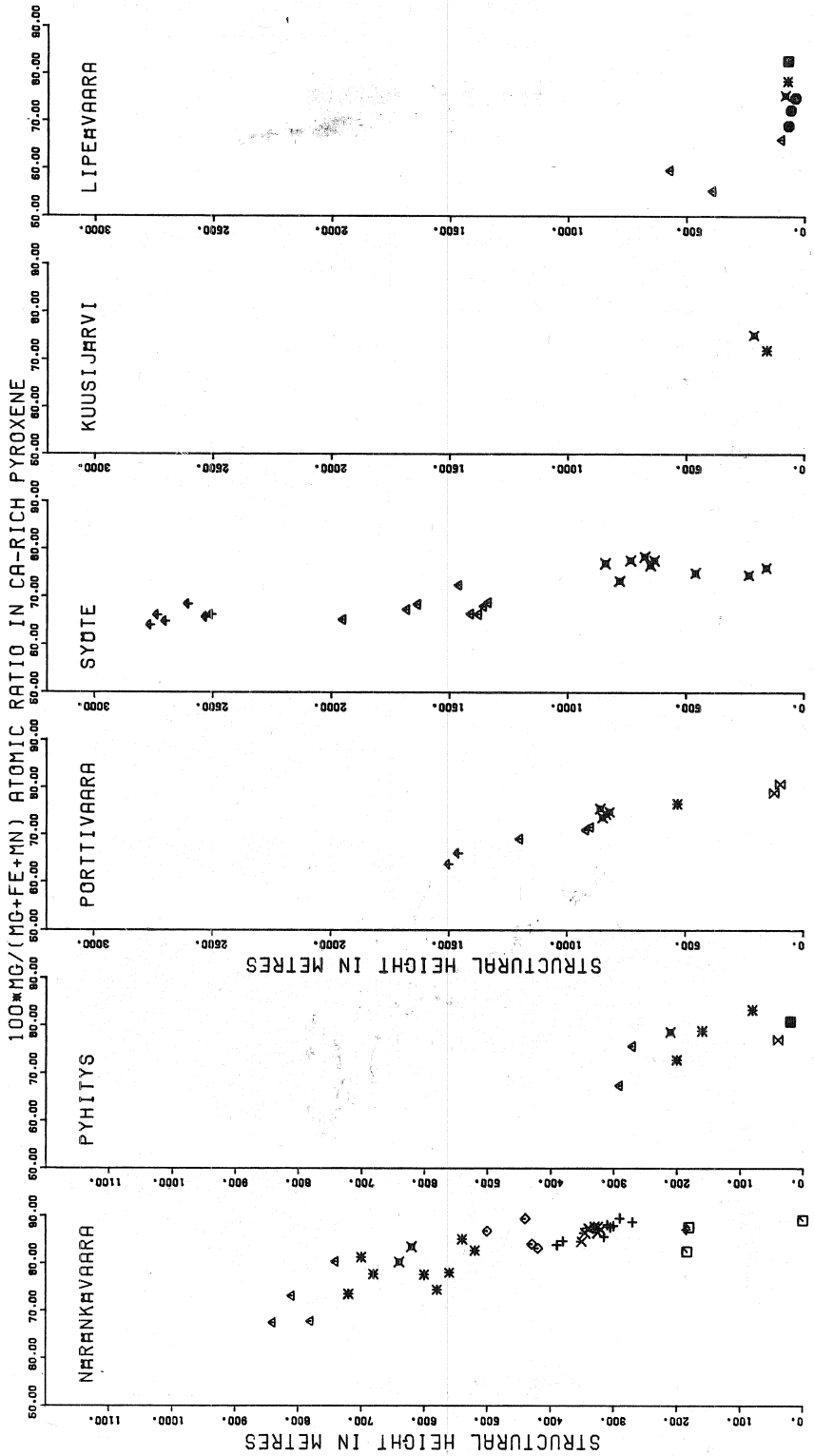

Fig 15. Cryptic variation in Ca-rich pyroxene in the Koillismaa complex. For key to symbols, see Fig. 10.

layered series. Its Mg/Fe ratio reaches its maximum in the lower part of subzone LZb (Fig. 15) and then begins to drop fairly rapidly. The augite in the upper part of the same subzone, which has a composition of $Ca_{43.2}Mg_{41.3}Fe_{15.5}$, contains exsolution lamellae parallel to the (001) plane, indicating that crystallization took place temporarily above the pigeonite—orthopyroxene inversion temperature. The composition of the augite, like that of the orthopyroxene, returns abruptly to a more Mg-rich level in subzone LZc, however, and at the same time the (001)-oriented lamellae disappear. The iron content begins to increase again in the upper zone, and crystallization again moves to the area above the inversion curve, the augite composition being $Ca_{42.8}Mg_{43.3}Fe_{13.9}$.

Layered series of the western intrusion. Ca-rich pyroxene, augitic in composition, is encountered throughout the layered series of the western intrusion with the exception of the *pC* layers of subzone UZa. Augite appears as an intercumulus phase in the lower zone, petrographical evidence suggesting that it is of intercumulus secondary origin in the earliest *opC* layers of subzone LZa and in some *pbC* horizons in LZb, being formed through the replacement of olivine and bronzite in these two subzones respectively (Fig. 16). Augite becomes a cumulus phase at last in the middle zone, where bronzite is replaced as the Ca-poor pyroxene by hypersthene, but resumes its role as an intercumulus phase in subzone UZc, or in the case of Lipeävaara approximately 350 m above the base of the middle zone.

Replacement of Mg by Fe in the layered series of the western intrusion shows a progressive increase towards the top of the sequence, although examination of this trend in greater detail reveals some irregular fluctuations (Fig. 15). The most magnesium-rich clinopyroxene analysed had the composition $Ca_{45.0}Mg_{44.5}Fe_{10.5}$, and the most ferriferous pyroxene in subzone UZb of the main magma

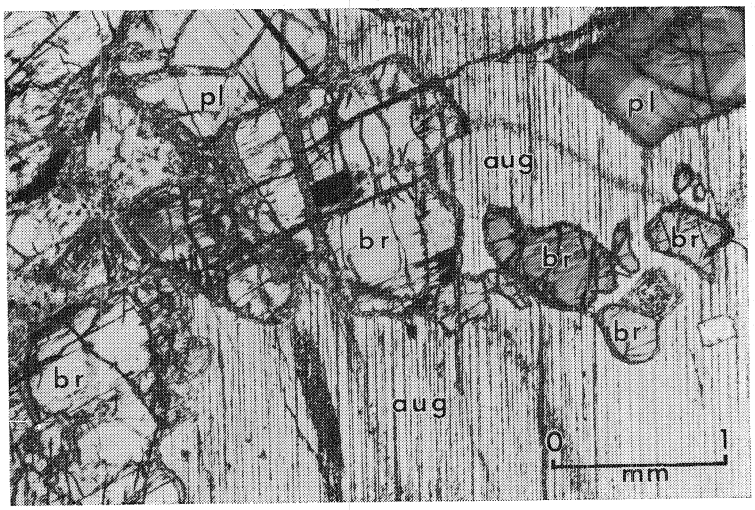

Fig. 16. Photomicrograph showing an originally single cumulus bronzite crystal (br) embayed on account of being partially enclosed by augite (aug), and the same crystal showing an original face having been in contact with plagioclase (pl). Plagioclase—bronzite cumulate from the subzone LZb of the Lipeävaara layered series (sample 5Li). Magn. 23x. Crossed nicols.

chamber in the western intrusion the composition $Ca_{42}Mg_{37}Fe_{21}$, while a still more ferriferous pyroxene was obtained from the middle zone at Lipeävaara, $Ca_{40.7}Mg_{32.8}Fe_{26.5}$. At an augite composition of $Ca_{42.5}Mg_{40.8}Fe_{16.7}$ exsolution lamellae parallel to the (001) plane make their appearance, indicating crystallization at a temperature above the curve of pigeonite—orthopyroxene inversion. Here, as in the Pyhitys layered series, augite crystallizes above the monoclinic—orthorhombic inversion temperature in earlier cumulates than does Ca-poor pyroxene. A clinopyroxene of composition $Ca_{43.2}Mg_{37.0}Fe_{19.8}$ coexisting with the most ferriferous of the inverted pigeonite provides the extreme value for the two-pyroxene boundary as far as augite is concerned (Fig. 18).

The Cr_2O_3 content and Mg/Fe ratio of Ca-rich pyroxene vary in a sympathetic manner, as in the case of Ca-poor pyroxene, and broadly speaking in the same direction, i.e. both measures decrease with greater fractionation (Table 5, Figs. 15 and 17). Similarly the deviations from this common trend are comparable in the two pyroxene types, although they are now very much clearer in the lower layers of subzone Gbno II at Näränkävaara, and particularly as regards the websterites, as a consequence of the high chromium content of the clinopyroxene (max. 1.10 % Cr_2O_3 by weight).

Estimated equilibration temperatures

Equilibration temperatures for the coexisting Ca-rich and Ca-poor pyroxenes were calculated using the best-fit two-pyroxene geothermometer of Wells (1977). The numerical results are presented in Table 6, and the variations in equilibration temperature with structural height are depicted in Fig. 19. For comparison purposes, temperatures calculated by the method of Wood and Banno (1973), widely accepted earlier although based on more restricted experimental data, are also included in Table 6. The results obtained by these two methods are seen to deviate fairly markedly one from another in many instances. Both of these temperature calculations are hampered to some extent here by recrystallization at the subsolidus stage, an effect of the method used for the microanalyses, and thus tend to be too low and to show relatively large standard deviations.

A clear decline in equilibration temperature from the base of the Näränkävaara layered series upwards is to be seen, with mean estimates of 1044°C for the ultramafic zone, 998°C for subzone Gbno I and 874°C for Gbno II. The pyroxenes of sample 47Nä, representing the base of the last-mentioned subzone, which also deviate in other ways from the other pyroxenes of this subzone, as noted earlier, give a result of 1013°C, which would correspond better to estimates for subzone Gbno I.

The equilibration temperatures in the layered series of Pyhitys and the western intrusion remain surprisingly constant in spite of the changes in structural height. A declining trend in mean temperatures is nevertheless found as one moves from the Pyhitys section to those of Porttivaara and then Syöte, with values of 1018°C, 978°C and 947°C respectively. Using the calculated composition of the original pigeonite (Alapieti *et al.* 1979 a, Table 4), the lowest pigeonite—augite couple in the Syöte layered series is assigned equilibration temperatures of 1033°C by the method of Wells (1977) and 964°C by that of Wood and Banno (1973). The Wood and Banno temperature at the point where orthopyroxene ceases to be precipitated and pigeonite begins is 1074°C for the Dufek magma (Himmelberg & Ford 1976) and 1005°C for the Bushveld magma (Wood & Banno 1973).

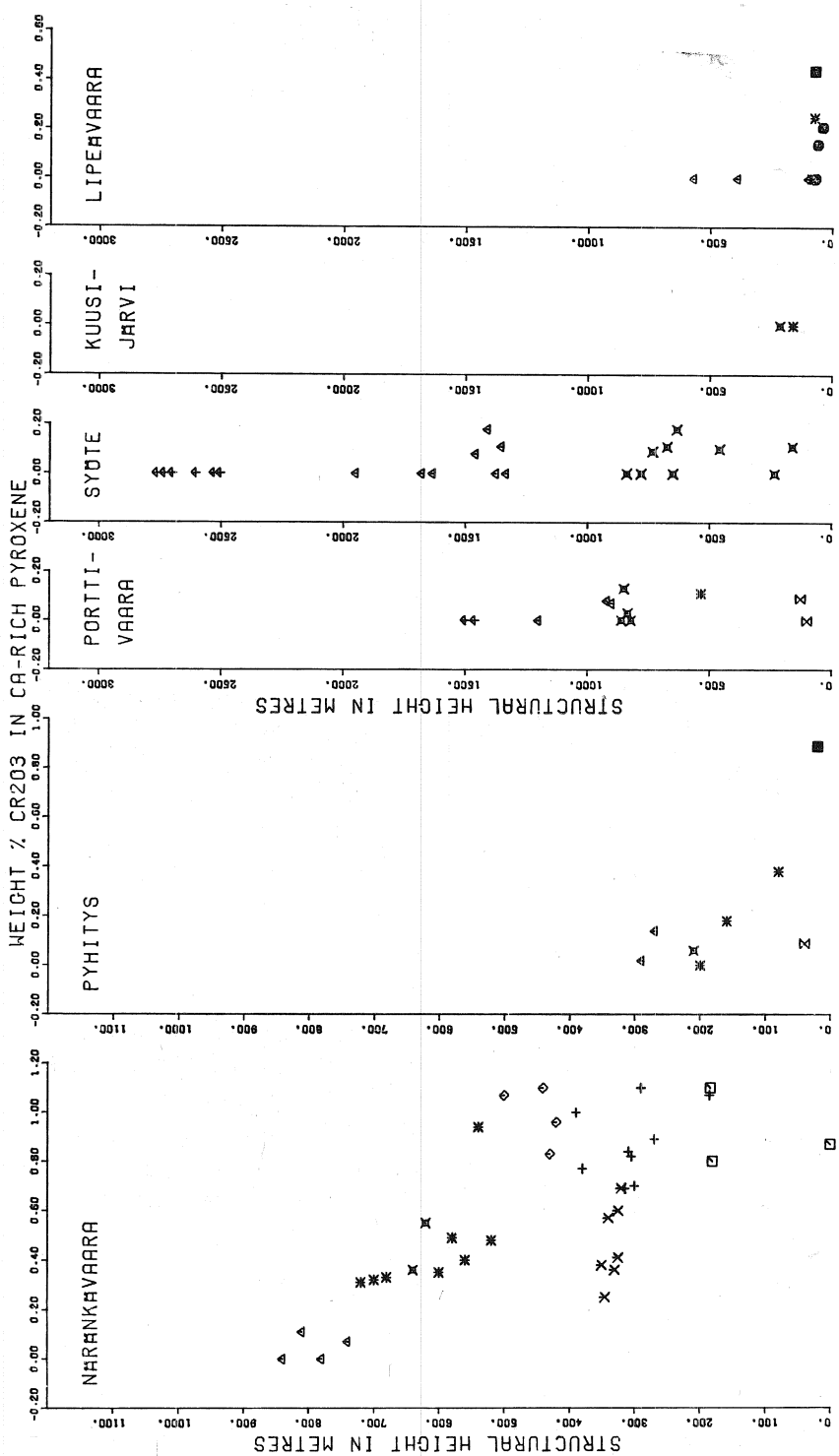

Fig. 17. Cr_2O_3 content of Ca-rich pyroxenes in the Koillismaa complex plotted against height. For key to symbols, see Fig. 10.

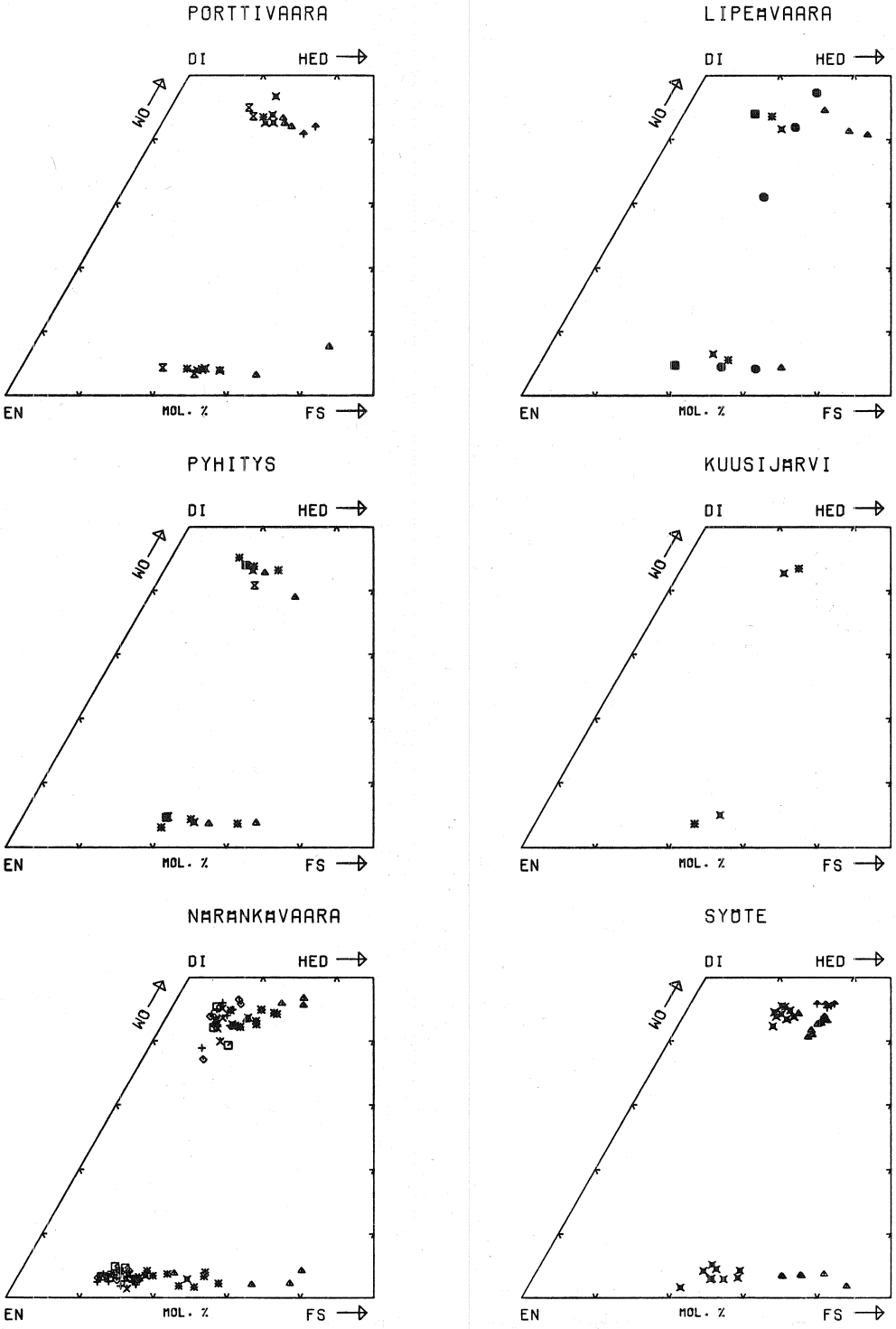

Fig. 18. Pyroxenes from the Koillismaa complex plotted on pyroxene quadrilaterals. For key to symbols, see Fig. 10.

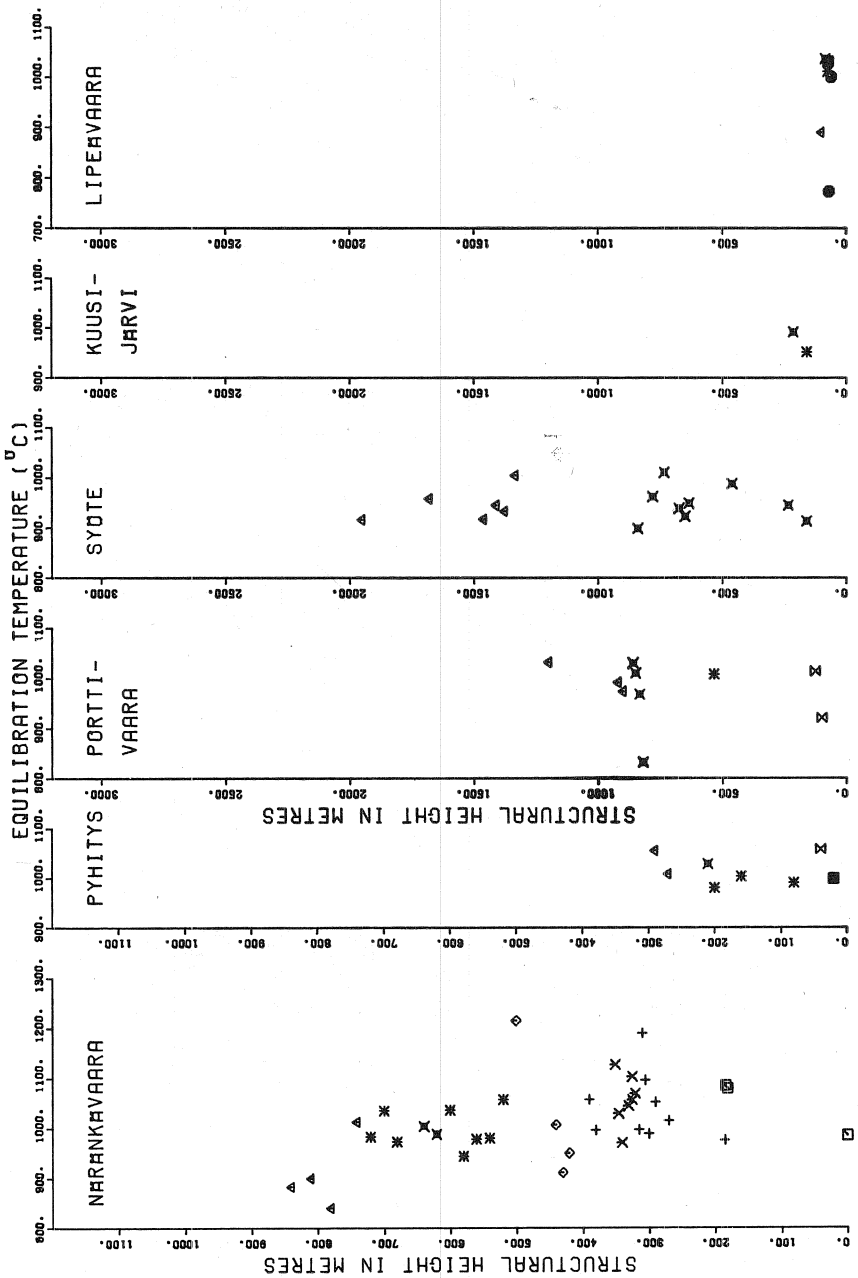

Fig. 19. Equilibration temperatures for coexisting pyroxenes in the Koillismaa complex calculated according to Wells (1977) and plotted against height. For key to symbols, see Fig. 10.

PLAGIOCLASE

Plagioclase is the most common mineral in the visible part of the Koillismaa complex, being present as a cumulus mineral in all the gabbroic and dioritic rocks with the exception of subzone Gbno I at Näränkävaara, where it is almost entirely of heteradcumulus origin. It similarly shows features typical of a cumulus phase in the gabbroic rocks

of the marginal series, and does not differ in microstructure from the corresponding cumulus minerals of the layered series. Plagioclase also occurs in small quantities as an intercumulus mineral in the ultramafic zone in the Näränkävaara layered series, i.e. in the upper *bC* layer, and in subzone Pe II above this.

Normal zoning is typical of the intercumulus plagioclase, and the pockets of plagioclase in subzone Pe II in particular are characterized by extreme zoning. On the other hand, the plagioclase of heteradcumulus origin in subzone Gbno I is virtually unzoned. The plagioclase in some of the samples representing this rock type nevertheless possesses cumulus features characterized by pronounced adcumulus growth, in which case the grains show normal zoning. Zoning is also typical of other plagioclases which are obviously of cumulus origin, and this may be of either the normal or the oscillatory — normal type, the latter being encountered particularly in the lower parts of subzone Gbno II at Näränkävaara and in the lower zone of the layered series at Pyhitys and in the western intrusion.

The compositions of the plagioclases analysed are given in Table 7 and Fig. 20. Variations in the An and Fe concentrations with height in the sequence are depicted in Figs. 21 and 22 respectively. The composition of the plagioclase is seen to vary within a relatively narrow range, from approximately $An_{53.9}$ in the upper *bC* layer at Näränkävaara to $An_{80.8}$ in the lower zone of the Syöte layered series. One exception, however, concerns the dioritic rocks of the Näränkävaara layered series and the plagioclase cumulates in the upper zone of the Lipeävaara layered series, with anorthite concentrations of An_{26} and An_5 respectively. The latter albitic plagioclase is probably a product of metamorphism.

Näränkävaara layered series. The anorthite content of the plagioclase of intercumulus origin in the Näränkävaara intrusion remains practically constant, with only minor fluctuations, in spite of changes in structural height. Once the plagioclase becomes firmly established as a cumulus phase, at the base of subzone Gbno II, however, a temporary sharp rise in An content occurs, as also noted in the En values of the pyroxenes (Figs. 12 and 15), after which it once more remains constant, before declining markedly in the dioritic rocks.

Layered series of Pyhitys and the western intrusion. The composition of the cumulus plagioclase shows pronounced fluctuations throughout the Pyhitys layered series and in subzones LZa and LZb of the layered series in the western intrusion (Fig. 21), although the average An content remains constant or even rises slightly with increasing structural height. This trend is reversed from subzone LZc onwards in the western intrusion, however, i.e. the plagioclase becomes more sodic towards the top of the layered series. This change is by no means a regular one, however, and fluctuations in composition with height are still clearly observable.

Marginal series. Contrary to the general declining trend in the anorthite content of the cumulus plagioclase towards the top of the layered series, the plagioclase in the marginal series becomes more calcic in an inward direction due to 'reversed' fractionation. Its full range of composition is from An_{58} at the base of the gabbroic rocks to An_{78} at the top of the same rock type. In spite of this reversed fractionation, the anorthite concentrations in the marginal series as a whole are still of the same order as in the layered series.

With the exception of the albite in the upper zone at Lipeävaara, the plagioclase grains also contain measurable quantities of iron. This is thought to be due to iron in the crystal structure rather than to accidental impu-

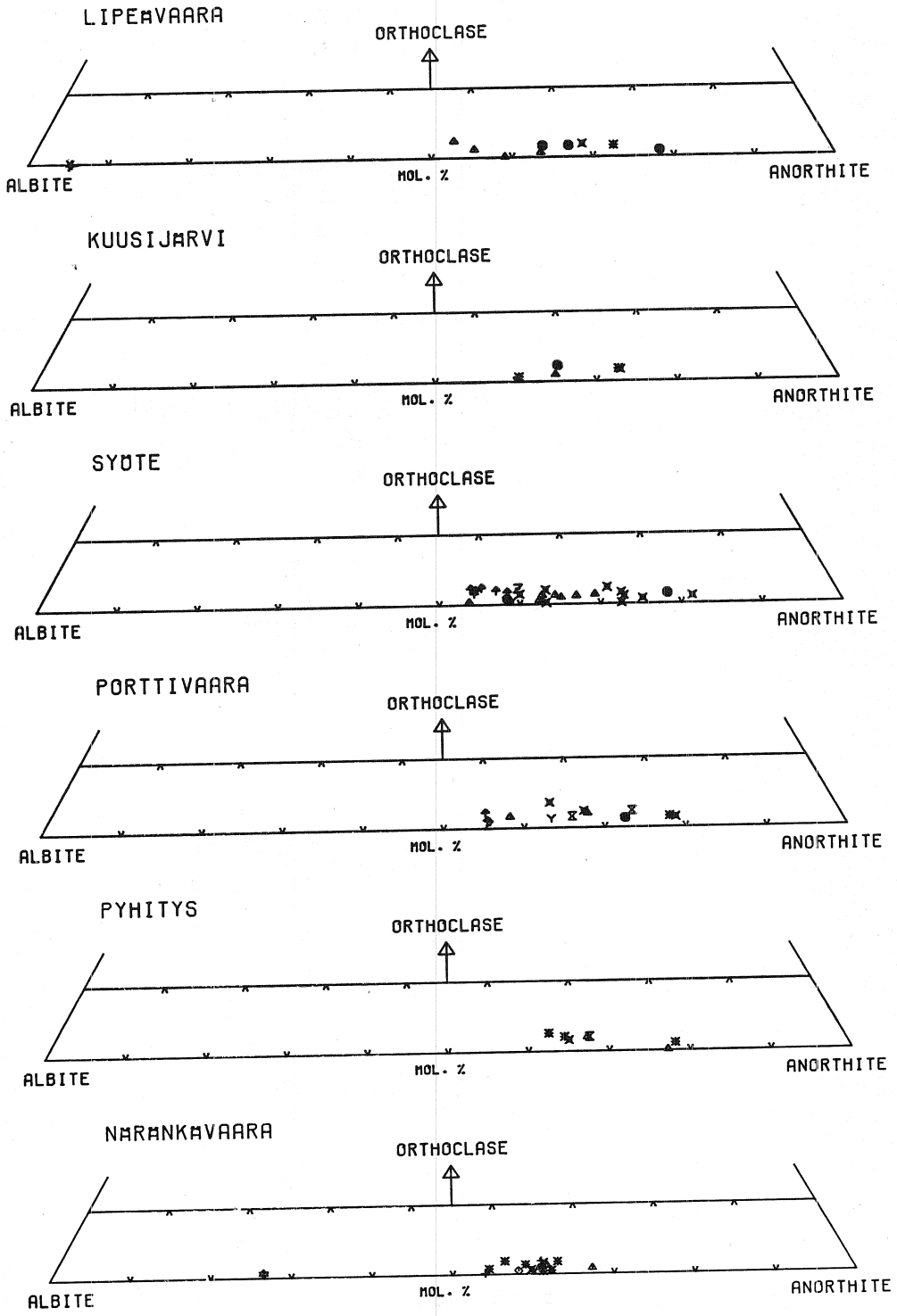

Fig. 20. Plagioclases in the Koillismaa complex plotted on Or–An–Ab diagrams. For key to symbols, see Fig. 10.

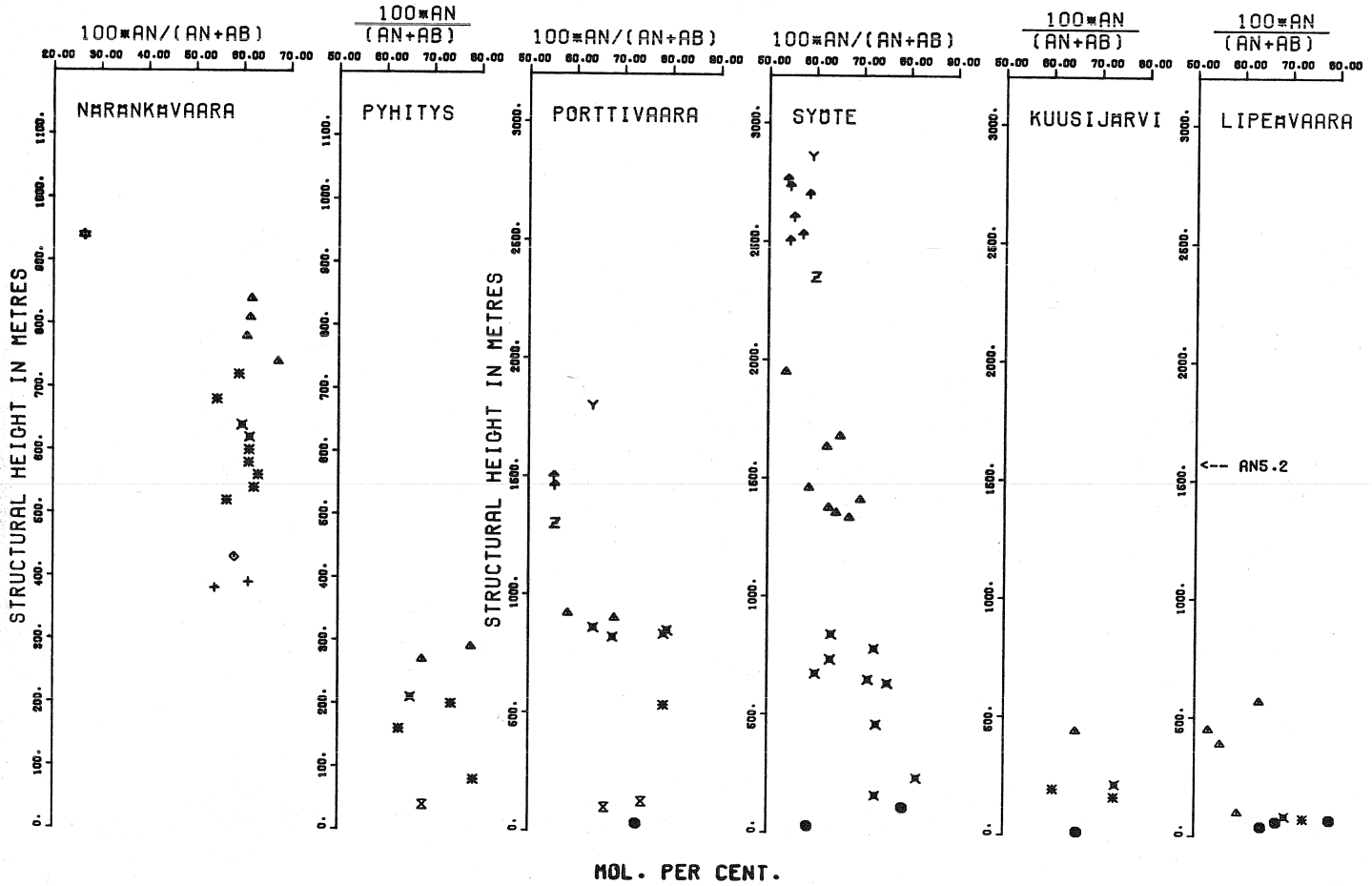

Fig. 21. Cryptic variation in plagioclase in the Koillismaa complex. For key to symbols, see Fig. 10.

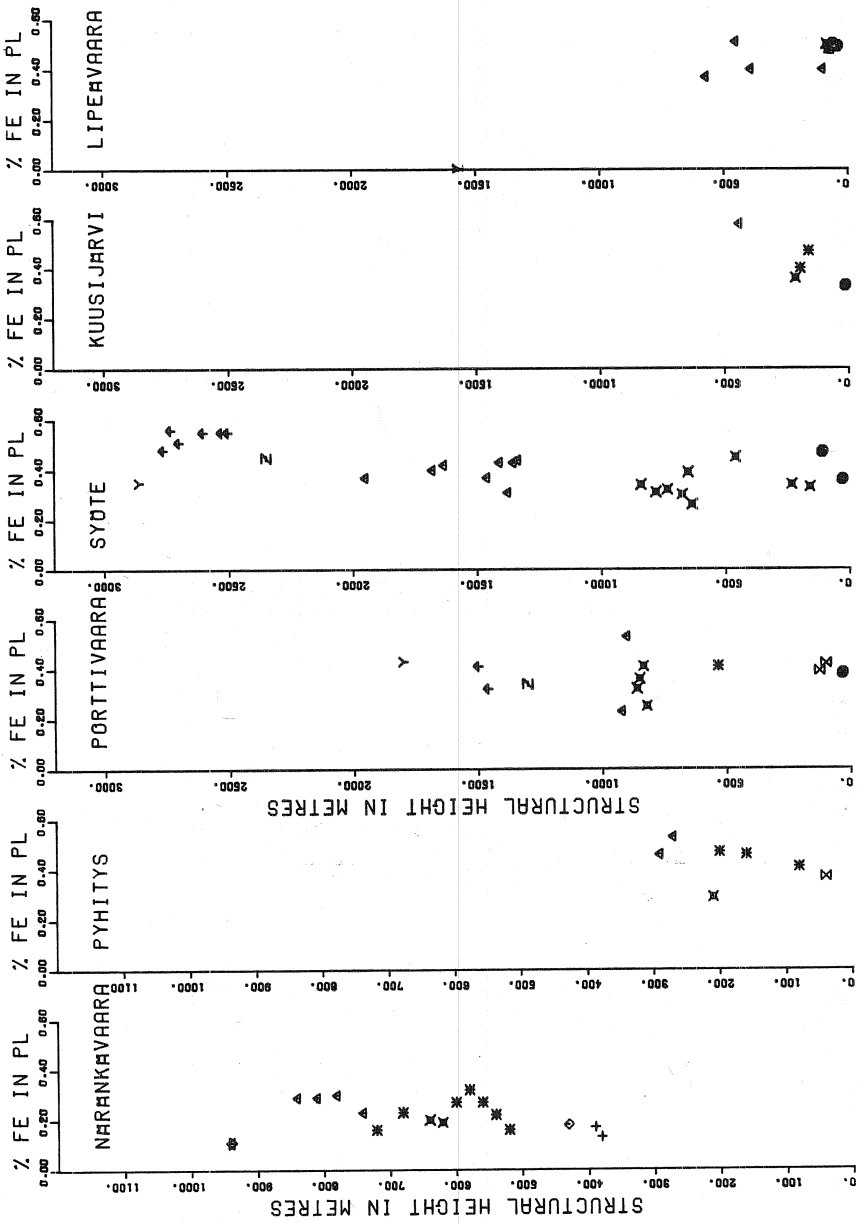

Fig. 22. Fe content of plagioclases in the Koillismaa complex plotted against height. For key to symbols, see Fig. 10.

rities (Wager & Brown 1968). The iron content plots for the plagioclases (Fig. 22) show a trend which may reasonably be attributed to fractional crystallization (cf. Longhi *et al.* 1976), and these patterns also suggest that the Fe content varies broadly speaking in an inverse manner to that of An, a tendency which is particularly obvious in the Syöte section.

IRON–CHROMIUM–TITANIUM OXIDES

Spinellids

Being members of a complex solid solution series, viz. the spinel group, the spinellids serve as sensitive indicators of the course of fractionation in layered igneous rocks. Also, many minerals of the spinel group are relatively stable under conditions of reworking caused by later tectonic events after magmatic crystallization, and thus chromite is often found in such rocks, for example, even though the ferromagnesian silicates have been completely altered. The pattern of compositional variation is complicated, however, by the reaction relation of the spinellids with associated silicates, and magnesium and ferrous iron in particular are found to have re-equilibrated during the postcumulus stage or even at subsolidus temperatures (Cameron 1975, Hamlyn & Keays 1979, Roeder *et al.* 1979).

Compositional features

The spinellids in the Koillismaa complex represent a wide range of compositions intermediate between the chromites and titanomagnetites (Table 8). In layered basic intrusions in general, the spinellids present are either Ti-rich and Cr-poor or Cr-rich and Ti-poor, as in the Bushveld complex, and the occurrence of a complete chromite — titanomagnetite series seems to be rare (Cameron 1979). Spinellids ranging from chromite to titanomagnetite have been reported in some lunar basalts, however, and in some terrestrial extrusive rocks (see Thompson 1973).

Graphical presentation of the composition of spinellids is difficult, as so many elements may enter the crystal structure. However, the microanalysis method used here is such that the titanium contents indicated for the oxide minerals are largely controlled by subsolidus reorganization and do not show any regular variation with structural height, and consequently have to be ignored, in spite of the fact that Ti was an important element in the original homogeneous magnetite–ulvöspinel solid solution. This leaves chromium, aluminium, ferric and ferrous iron and magnesium as the principal elements, and allows the major compositional features of the spinellids to be illustrated by means of a triangular prism, as described by Stevens (1944) and used widely in the literature. Since this three-dimensional diagram is difficult to comprehend, it is customarily reduced to a presentation of the contents of the three trivalent ions on a chromite–spinel–magnetite triangular graph (Fig. 23), the projections of the prism perpendicular to this triangle being used in cases where it is desired to include the variations in the bivalent ions (Figs. 24 and 25).

It may be seen from the triangular graph (Fig. 23) that there is a trend at Näränkävaara from relatively chromium-rich spinellids which fall into the field of aluminian chromite in the classification of Stevens (1944), through ferrian chromites, towards magnetites with chromite and spinel components of the order of less than one percent. The trends at Pyhitys and in the western intrusion are not so consistent, and chromium-rich magnetites are absent altogether.

The Mg/R^{2+} cation ratio in the spinellids is fairly low throughout the complex (Figs. 24, 25 and 29), even though it does reach the same order of magnitude in the Näränkävaara ultramafic zone as in the chromite-poor silicate rocks of the critical zone in the Bushveld complex (cf. Cameron 1977). In spite of its low values, however, the Mg/R^{2+} ratio for the spinellids still seems to vary in a similar

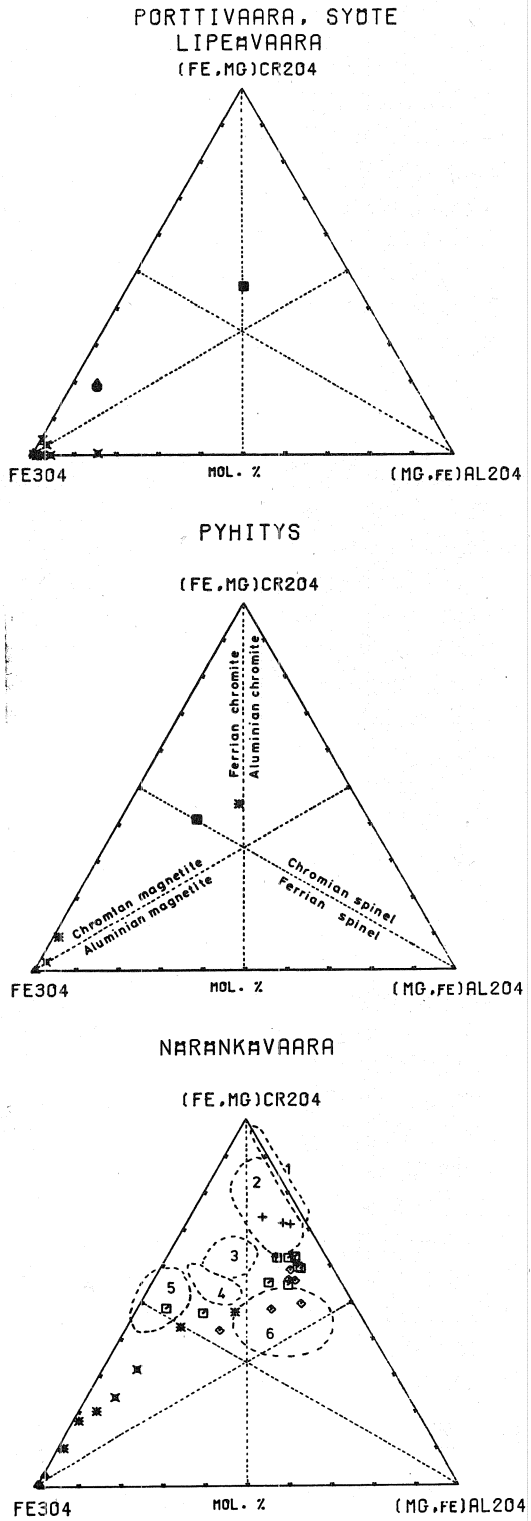

Fig. 23. Chromite–spinel–magnetite triangular diagram after Stevens (1944), showing the compositions of the minerals of the spinel group in the Koillismaa complex (R_2O_3 content). For key to symbols, see Fig. 10. The diagram for Näränkävaara also contains the provinces of chromite deposits after Weiser (1967) and Ghisler (1976): 1. Southern Europe and Asia; 2. Bushveld and Great Dyke complexes; 3. chromites from Bushveld anorthosites; 4. Kemi; 5. Western Norway; 6. Fiskenaesset.

manner to the Mg cation fractions in the ferromagnesian silicates (Figs. 10, 12, 15 and 29). The increase in Mg/R^{2+} is systematically accompanied by a rise in Al/R^{3+} (Fig. 25), and similarly Cr/R^{3+} rises steeply at first with increasing Mg/R^{2+}, but then reverts to a slight decline once the Mg cation fraction reaches a value of 0.14 (Fig. 24). A similar declining trend is reported by Hamlyn and Keays (1979) in the Panton Sill, Australia. The trends for Fe^{3+}/R^{3+} plotted against Mg/R^{2+} (Fig. 25) are antithetic to those for Cr/R^{3+} and Al/R^{3+}.

Spinellids in the marginal series and layered series

The Cr-rich spinellids of the Koillismaa complex usually occur in the form of small, idiomorphic grains which are optically, and normally also compositionally, highly homogeneous. Except in the completely serpentinized rocks, these grains are often coated with lighter, more iron-rich secondary alteration product. In contrast, Ti-rich varieties are highly heterogeneous, and as noted above, they largely show subsolidus recrystallization textures. These minerals are described here using the terminological conventions of Buddington *et al.* (1963), Anderson (1968) and Himmelberg and Ford (1977). *Titaniferous magnetite:* an optically homogeneous Fe-Ti spinel phase having an oxide stoichiometry approximating to R_3O_4. *Ilmenomagnetite:* a regular intergrowth of ferrian ilmenite lamellae in a

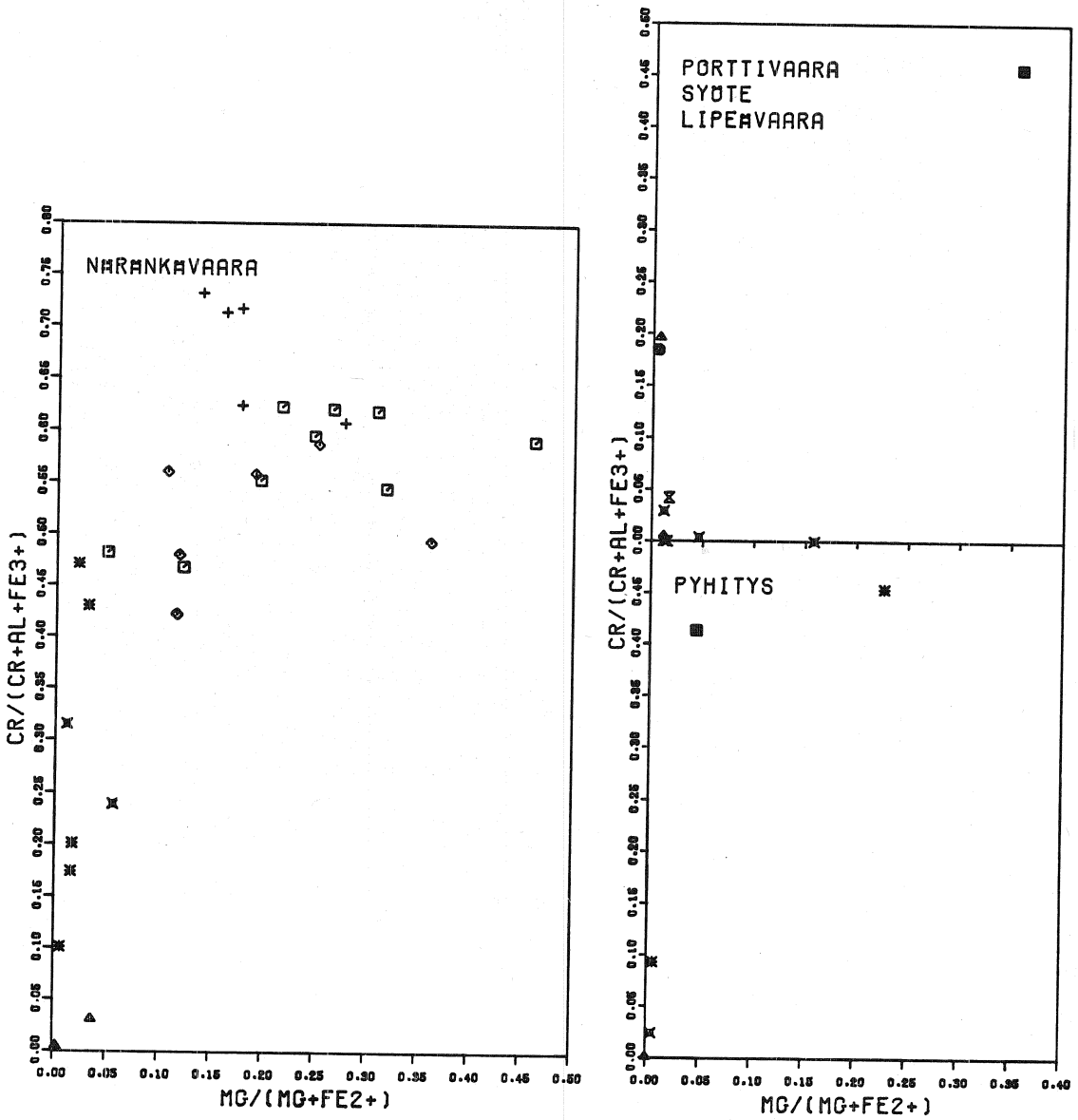

Fig. 24. Relationship between the Cr and Mg cation fractions for spinellids in the Koillismaa complex. For key to symbols, see Fig. 10.

titaniferous magnetite host. The most typical Cr-poor iron—titanium oxide mineral in the Koillismaa complex consists of a titaniferous magnetite host with octahedrally oriented ferrian ilmenite lamellae (ilmenomagnetite), intergrown with a coarse, relatively homogeneous ferrian ilmenite to form a composite ilmenomagnetite—ferrian ilmenite grain (see Alapieti *et al.* 1979 a, Fig. 10).

Marginal series. The 'reversed' fractionation in the marginal series is also reflected in the composition of the minerals of the spinel group, in that their Cr content increases and their Ti content decreases in an inward

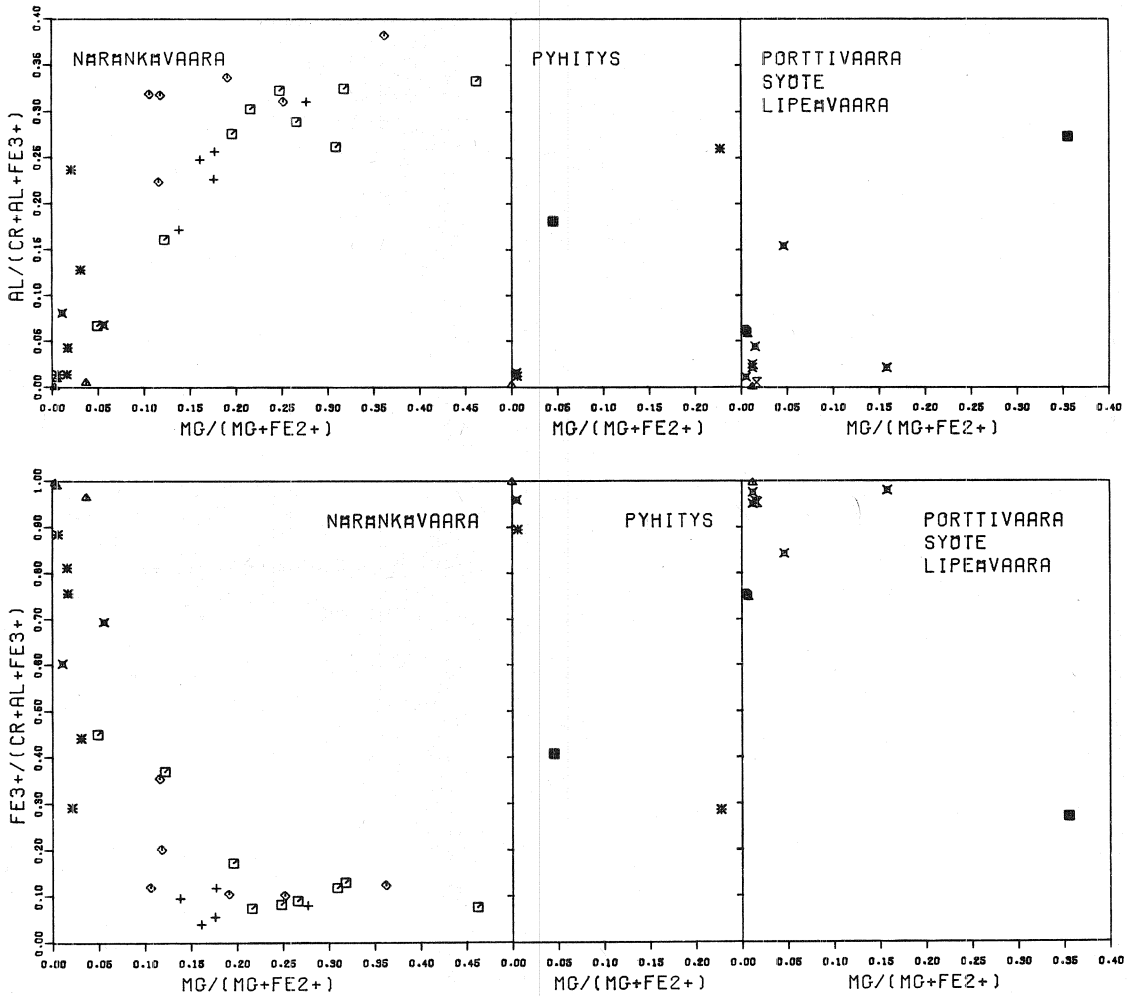

Fig. 25. Relationship between the Al and Mg and the Fe^{3+} and Mg cation fractions for spinellids in the Koillismaa complex. For key to symbols, see Fig. 10.

direction. Chromite generally occurs in accessory or trace amounts in the ultramafic rocks, with rocks containing more than 1 % by vol. chromite restricted to the marginal series at Pyhitys and that below subzone LZa at Porttivaara. This latter chromite is the richest in Cr to be found anywhere in the marginal series. The original oxide mineral in the gabbroic rocks of the marginal series was ilmenomagnetite, but due to pronounced alteration this now appears only in the form of skeletal relicts among grains of plagioclase and uralite (Piirainen *et al.* 1977). An exceptional occurrence of euhedral, relatively Cr-rich chromian magnetite is found as an inclusion in the orthopyroxene of the Lipeävaara contact gabbro (Table 8, sample 2Li, Fig. 23).

Näränkävaara layered series. The minerals of the spinel group show a general tendency for a decrease in Cr content and an increase in Ti content towards the top of the stratigraphic sequence, combined with an increase in the proportion of the ferric iron cation fraction (Figs. 25, 26 and 28) and a decline in

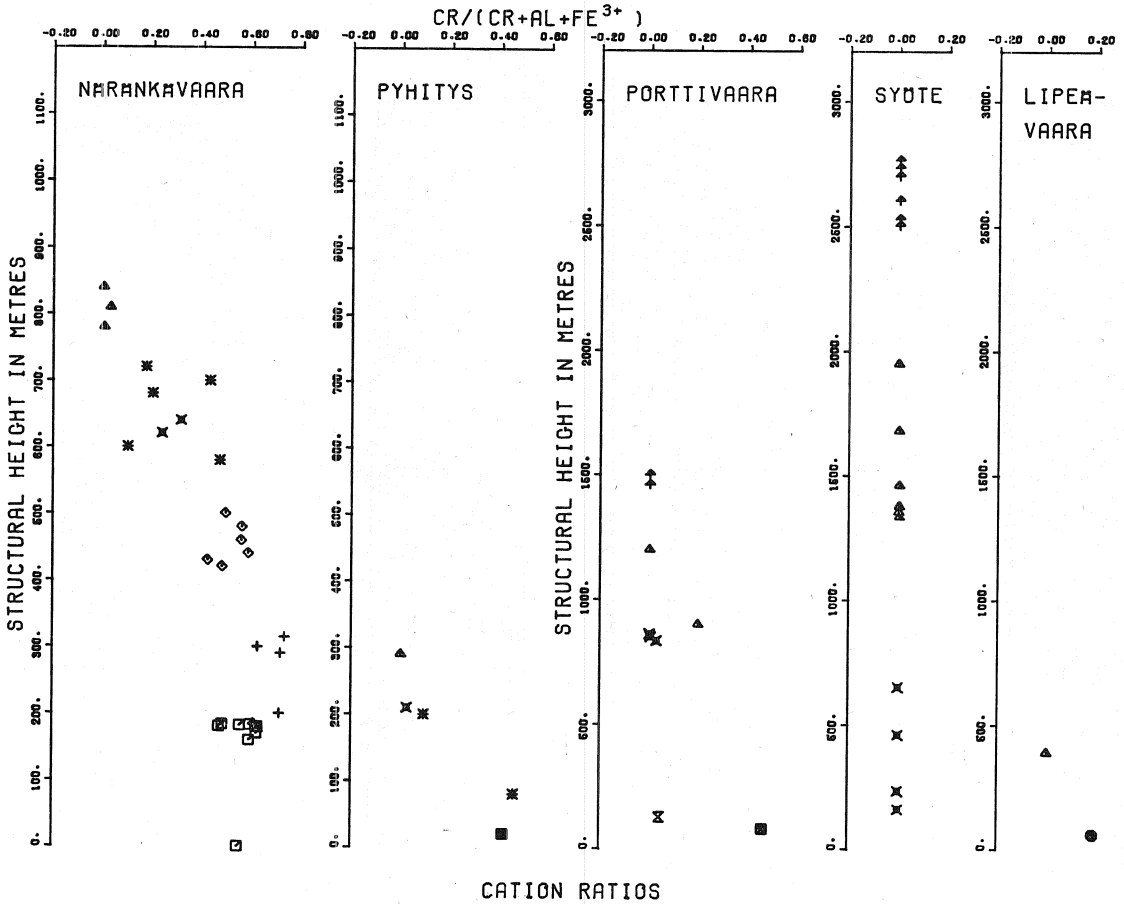

Fig. 26. Vertical variation in Cr/R^{3+} for spinellids in the Koillismaa complex. For key to symbols, see Fig. 10.

that of aluminium as fractionation advances (Figs. 25 and 27).

The chromium-rich spinellid in subzone Pe I takes the form of a minor or accessory, but nevertheless significant, cumulus phase, and mainly represents the aluminian chromites. On the other hand, the spinellids in samples 6Nä and 9Nä (Table 8), samples which contain a greater than average amount of poikilitic clinopyroxene, are located among the ferrian chromites, and are also richer in the ulvöspinel molecule and have lower Cr/R^{3+} and Mg/R^{2+} ratios than the aluminian chromites.

Subzone Bro I contains very small amounts of spinellids, and this group is absent entirely in some samples. The minerals analysed represent aluminian chromites, and some are very rich in Cr. Since they also have a relatively low Mg/R^{2+} ratio, these minerals stand out clearly as a separate group on the diagram in Fig. 24. Minerals of the spinel group are not found at all in the websterites or the upper bronzitite layer.

Chromite reappears as a significant cumulus phase in subzone Pe II, in amounts which would seem to show a clear negative correlation with those of the Ca-rich pyroxene

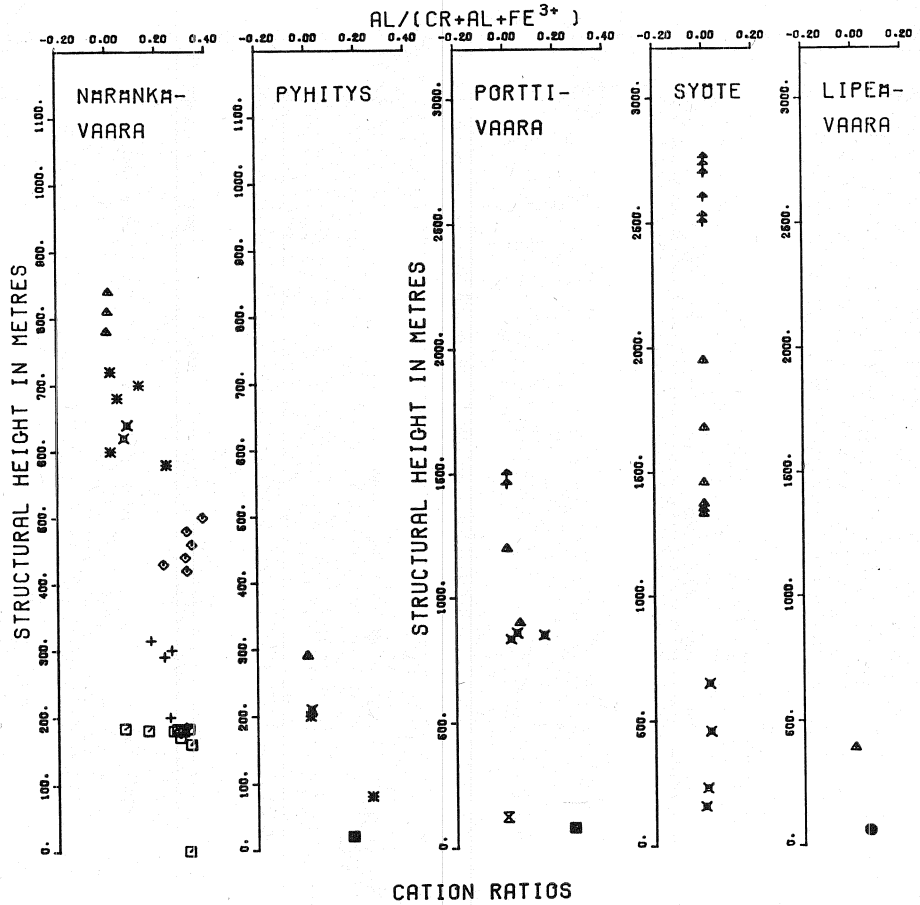

Fig. 27. Vertical variation in Al/R^{3+} for spinellids in the Koillismaa complex. For key to symbols, see Fig. 10.

which acts as an intercumulus mineral. The chromites analysed fall into the aluminian chromite field, with the exception of the ferrian chromite from sample 32Nä, a sample which contains exceptionally large amounts of clinopyroxene (Table 8, Fig. 23). In common with the ferrian chromites of subzone Pe I, this mineral is richer in titanium than the aluminian spinellids. The spinellids of subzone Pe II contain on average more spinel component and less chromite component than those found elsewhere in the ultramafic zone (Fig. 23). Since some of these also contain rather little magnesium, they again form a separate group in the diagram in which the Al cation fraction is plotted against the Mg cation fraction (Fig. 25).

The Cr/R^{3+} ratio of the spinellids reverts to a steep, though fluctuating, fall in subzone Gbno I (Fig. 26). The earliest-formed members analysed from this rock type are still ferrian chromites, and their normalized Cr/Fe^{3+} cation ratio suggests that they probably still have the structure of a normal spinel (Francombe 1957). The remainder, however, lie in the chromian magnetite field and some have an inverse structure, while others represent an intermediate form between the normal and inverse types. Once the Cr/R^{3+} ratio falls to around 0.24 (Fig. 26), correspond-

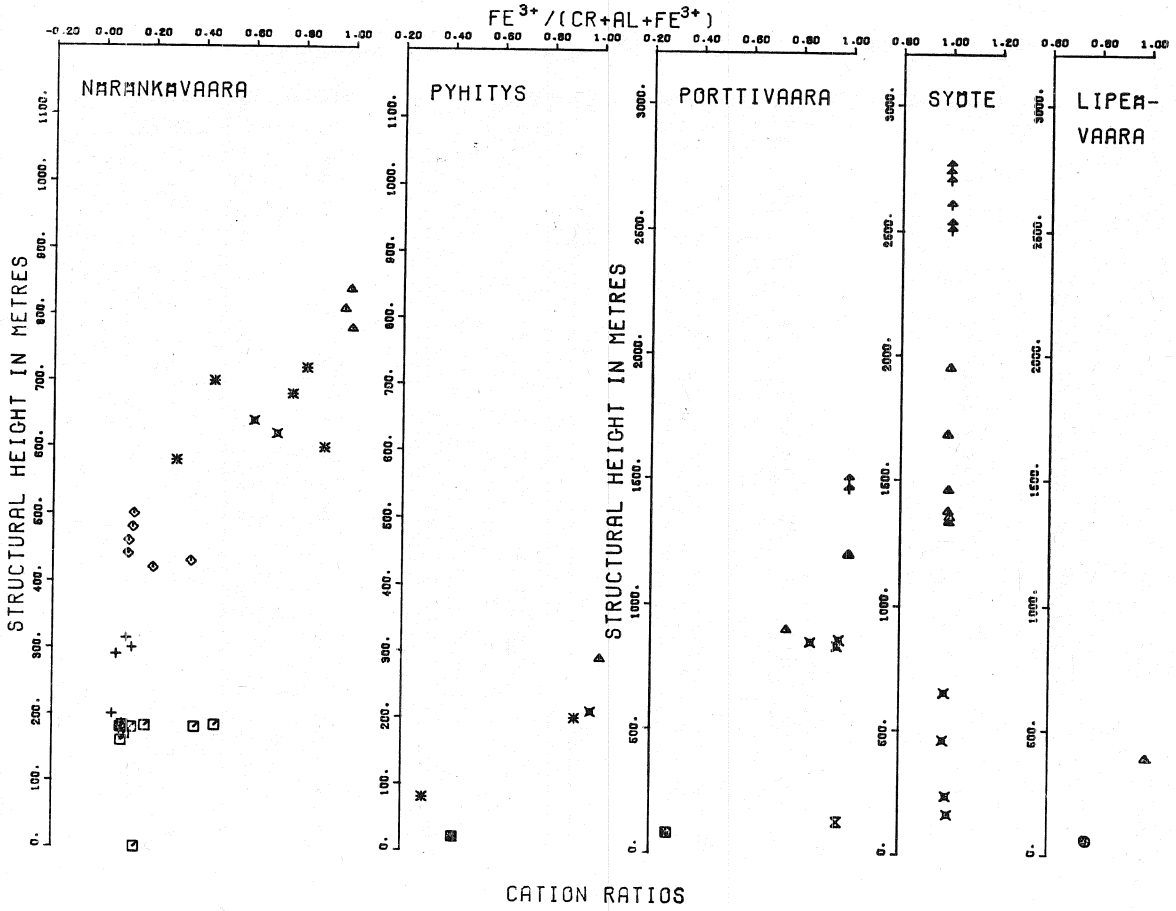

Fig. 28. Vertcial variation in Fe^{3+}/R^{3+} for spinel lids in the Koillismaa complex. For key to symbols, see Fig. 10.

ing to a Cr_2O_3 content of 14.8 % by wt. (Table 8, 42Nä), ilmenite lamellae parallel to {111} in the host appear. The normalized Cr/Fe^{3+} cation ratio suggests that the main crystal represents a composition in which the cation distribution has practically reached that of the inverse type of structure (cf. Francombe 1957). The unit-cell parameter, *a* 8.393 Å, is nevertheless slightly higher than that given by Francombe, 8.387 Å, obtained when studying a pure iron oxide—chromite solid solution. As the chromium content of the spinel phase declines slightly further to $Cr/R^{3+} \sim 0.20$, corresponding to 13.8 % Cr_2O_3 by wt., composite ilmenomagnetite—ferrian ilmenite grains appear as the typical oxide minerals. The normalized Cr/Fe^{3+} cation ratio suggests that the chromian magnetite host now has a complete inverse structure.

Composite ilmenomagnetite—ilmenite grains are also commonly encountered in subzone Gbno II, where their spinel phase has a relatively low chromium content and the unit-cell parameter, *a* 8.395 Å, begins to be typical of pure magnetite. The grains generally show a somewhat poikilitic habit, and may well be postcumulus minerals, as are the highly altered oxides in the dioritic rocks occurring above them in the stratigraphic sequence.

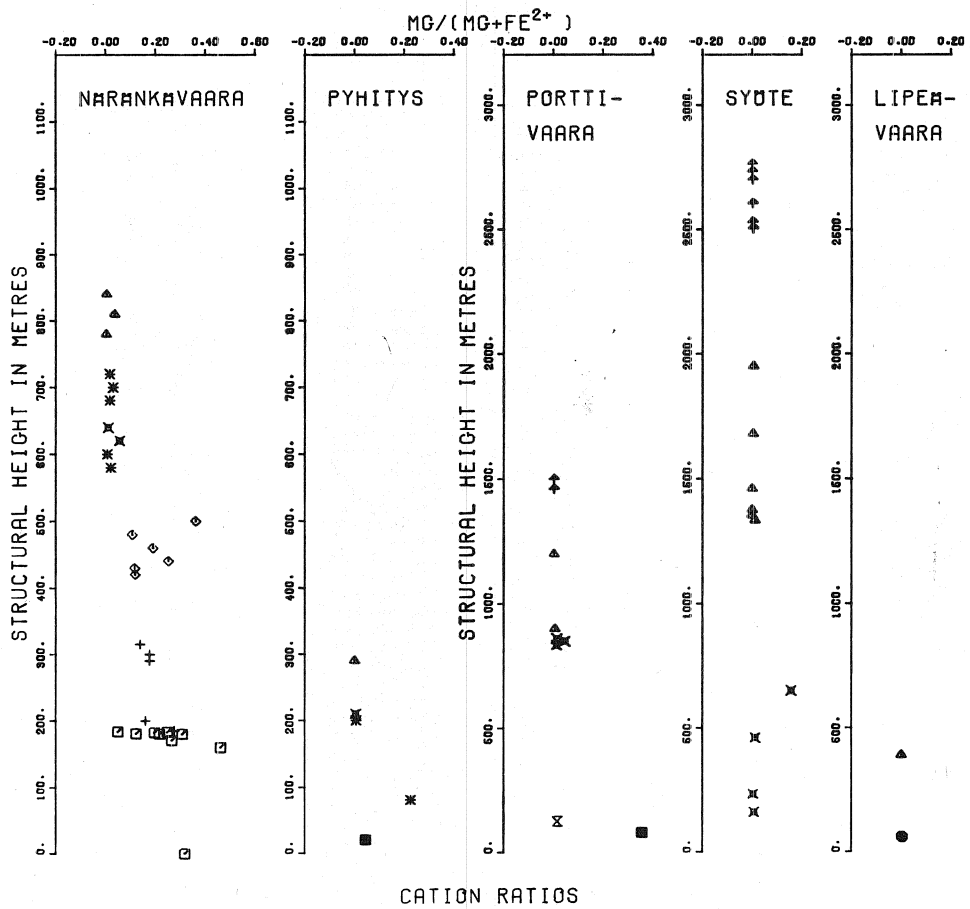

Fig. 29. Vertical variation in Mg/R^{2+} for spinellids in the Koillismaa complex. For key to symbols, see Fig. 10.

Pyhitys layered series. Members of the spinel group occur in minor or accessory amounts throughout the Pyhitys layered series. Composite ilmenomagnetite—ilmenite grains, which may well be postcumulus minerals, are found sporadically in connection with mica in subzone LZa, while the spinel phase at the base of LZb, which consists of ferrian chromite (Fig. 23), is clearly of cumulus origin. Above this one again finds composite grains, but ones in which the Cr/R^{3+} ratio of the spinel phase has plunged markedly compared with the previous layer, with a corresponding marked rise in the proportion of ulvöspinel (Fig. 26, Table 8).

Layered series of the western intrusion. Ilmenomagnetite and composite grains of ilmenomagnetite and ilmenite are typical intercumulus minerals occurring in minor amounts in the lower and middle zones of the western intrusion, containing a chromite component of over 1 Mol. % in the lower parts of the sequence (Table 8). The base of the middle zone in the Porttivaara section also contains occasional occurrences of idiomorphic magnetite which is very much richer in chromium than the above, containing 11.6 % Cr_2O_3 by wt. (Table 8, 12Po), as inclusions within the orthopyroxene. The ilmenomagnetites and composite grains become

chief minerals alongside augite and plagioclase in subzone UZb, although there are substantial fluctuations in the amount of magnetite between different parts of this subzone, with magnetite and the vanadium bound to it reaching such quantities at Mustavaara (Map 1) that the latter becomes economically exploitable.

Silicate inclusions

The chromites in the peridotites are found on rare occasions to contain small, spherical silicate inclusions of diameter less than 50 μm. These were studied in three of the present samples, two of which, 2Nä and 5Nä, represented subzone Pe I and one, 34Nä, Pe II. The inclusion in the chromite of sample 2Nä (Fig. 30) proved the richest in SiO_2 and was shown in bulk analysis to be composed of a mixture of quartz and albite (Ab_{99}) approximately in the proportions Q/Ab = 35/65. The total Na_2O content measured for it, 7.8 % by wt., is higher than would ordinarily be expected for a basaltic liquid, and according to Irvine (1975), inclusions of this kind, which are rich in alkali metals, would represent trapped droplets of a contaminant salic melt.

The inclusion in sample 5Nä proved to consist of pure olivine, which is similarly a typical mineral in inclusions in the Stillwater chromites (Jackson 1961). This olivine was shown to consist of 38.7 % SiO_2, 16.3 % FeO and 42.7 % MgO, the numbers of ions, on the basis of four oxygen atoms, being Si = 1.001, Fe = 0.353 and Mg = 1.646. The contents of any other elements remained below the detection limit. The calculated forsterite value, $Fo_{82.4}$, is considerably lower than that for the true cumulus olivine in the same sample, 87.6 (Table 3, 5Nä). Applying the olivine—spinel geothermometer to the above olivine—chromite pairs, and using the equation of Roeder *et al.* (1979), equilibration temperatures were calculated which amounted to 507°C for the inclusion olivine and cumulus chromite and 413°C for the cumulus olivine—chromite pair. Both thus represent a level well below the solidus temperature, showing that consider-

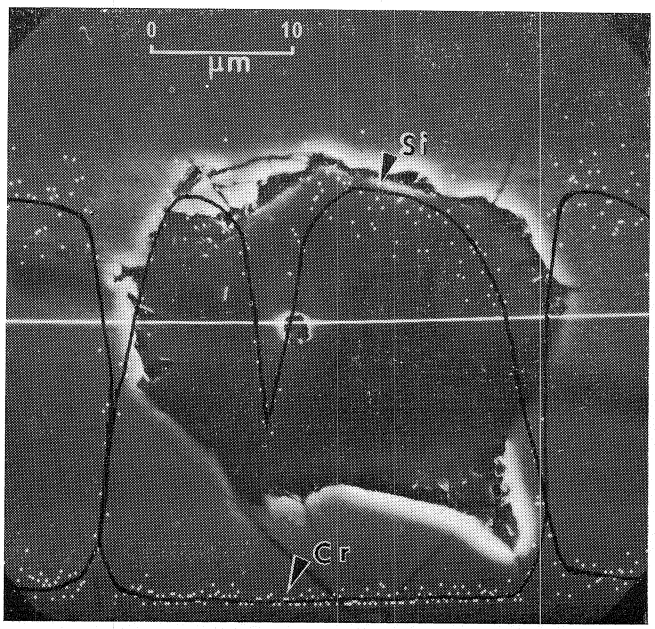

Fig. 30. Digital line scan for Si and Cr superimposed on the secondary electron image of an inclusion in chromite (sample 2Nä). The zero level for the content of each element is located at the bottom edge of the figure. The centre line represents the analysis line across the inclusion. The curves indicating composition variations were fitted to the points afterwards for the sake of clarity.

able subsolidus re-equilibration had taken place. Temperatures of the same order of magnitude (400—800°C) are also given by the coexisting olivine and chromite in the Stillwater samples (Roeder *et al.* 1979).

The third inclusion, in the chromite of a sample which had undergone complete metamorphic alteration (sample 34Nä), gave a result in bulk analysis of 39.1 % SiO_2, 10.7 % Al_2O_3, 5.7 % FeO, 33.0 % MgO, 0.10 % CaO and 0.34 % K_2O, the remainder, approx. 10 %, presumably being water. The calculated normalized mineral composition would suggest that this is a composite inclusion of olivine, orthopyroxene and phlogopite which has then homogenized in a later metamorphic process. Its high Al_2O_3 content would seem to be derived from the surrounding chromite, which is slightly altered at the edges.

Ilmenite

The term 'ilmenite' is used here to refer to the 'ferrian ilmenite' described by Buddington *et al.* (1963), Anderson (1968) and Himmelberg and Ford (1977), which is an optically homogeneous Fe—Ti rhombohedral phase having an oxide stoichiometry of about R_2O_3 with Fe_2O_3 less than 50 mole percent. In common with the ilmenites of many other plutonic rocks, those of the Koillismaa complex can be divided into two types: 1. ilmenite which crystallized originally as discrete grains, or 'primary ilmenite' in the terminology of Mathison (1975), and 2. ilmenite which is intergrown with a spinel phase and occurs either in granules or as lamellae, or in both forms, i.e. 'secondary ilmenite' after Mathison. The occurrence of ilmenite in intergrowths of the above type is nowadays accepted as being the result of an oxidation—'exsolution' process, this not being a case of exsolution in the classic sense on account of the change in composition during the process (Buddington & Lindsley 1964).

The ilmenites analysed here (Table 9) do not show any obvious cryptic variation, although admittedly it is difficult to study this accurately, since some of the analyses were carried out on independent grains while others represent 'exsolved' ilmenites. No systematic study was made of possible chemical differences between the primary and secondary ilmenites occurring in the same samples, but it nevertheless seems that the primary ilmenites (samples 44Nä, 45Nä, 46Nä, 5Po, 8Po, 10Po, 12Po, 4Li and 5Li) have higher recalculated Fe^{3+} and R_2O_3 contents than the secondary ilmenites, as also reported by Mathison (1975).

The marginal series. Primary ilmenite is encountered occasionally in the ultramafic rocks of the marginal series at Lipeävaara. As with other minerals, the ilmenite is usually highly altered in the contact gabbro, and may well be entirely of the secondary type.

Näränkävaara layered series. The lowest-lying grains of ilmenite in the Näränkävaara layered series are found in a few of the samples representing subzone Pe I, in which this ilmenite of the primary type occurs as an intercumulus mineral, usually in association with mica. After this it reappears only in the gabbroic rocks, where both primary and secondary ilmenite is found, as also in the dioritic rocks occurring at the top of the sequence. Where the simultaneously occurring spinel phase has a high chromium content the samples contain only the primary type of ilmenite, but as the Cr_2O_3 content falls to about 14,8 % by wt. trellis intergrowths of thin 'exsolved' ilmenite lamellae appear, as mentioned above. With a further slight drop in chromium content granules of secondary ilmenite also make their appearance.

Pyhitys layered series. Primary ilmenite is rare at Pyhitys, but the secondary type is encountered regularly in association with magnetite, and may account for as much as half of the composite grain, in which case the ilmenite granules frequently contain minute exsolution lamellae of hematite.

Layered series of the western intrusion. Primary ilmenite is found, along with the secondary type, in most parts of the lower zone of the western intrusion, but it becomes somewhat rarer in the middle zone, and by the upper zone only the secondary type is found. Myrmekitic intergrowths of orthopyroxene and primary ilmenite are typical of the lower cumulates of the Syöte layered series (Alapieti *et al.* 1979 a).

Loveringite

A complex, titanium-rich oxide mineral was identified in the upper bronzitite layer at Näränkävaara, in which no other oxide minerals were found, in connection with the microanalyses for minerals of the spinel group in spring 1976, at about the same time as minerals practically identical to this in chemical composition were being discovered in the critical zone of the Bushveld complex (Cameron 1978, 1979) and the bronzite–cumulate layers of the Jimberlana intrusion (Campbell & Kelly 1978, Gatehouse *et al.* 1978, Kelly *et al.* 1979). The mineral described at the latter site was given the name loveringite.

The loveringite at Näränkävaara occurs together with pyrrhotite in the interstitial spaces between the intercumulus clinopyroxene grains, and presumably represents the last phases to have crystallized from the residual intercumulus liquid, as in Jimberlana (Kelly *et al.* 1979). A chemical composition based on the elements detected in qualitative analysis is presented in Table 10. Iron is calculated entirely in terms of FeO, although Fe_2O_3 is probably also present, and this may in part explain the low total. The formula, normalized to 38 oxygen atoms, is:

$(Ca, REE)_{1.0}$ (Ti, Fe, Cr, Mg, Zr, Al, Mn, $Si)_{21.4}O_{38}$,

which is very close to the general formula of $AM_{21}O_{38}$, in which M = small cations and A = large cations. The grain of loveringite analysed was covered by a shell of thickness approx. 5 μm and obviously richer in manganese (Fig. 31), which appears in polarized light to be clearly more anisotropic than the core. This shell layer also deviates chemically from the core in that its iron content is higher and its concentrations of zirconium, chromium, titanium and calcium are correspondingly lower.

SULPHIDES AND PLATINUM-GROUP MINERALS

Enrichments of sulphide minerals are largely concentrated in the marginal series of the western intrusion (Piirainen *et al.* 1977, 1978), although two types of enrichment are also to be found in the layered series, one in the middle zone of the western intrusion at the western ends of the Porttivaara and Syöte blocks (Piirainen *et al.* 1978) and the other in the contact zone between the ultramafic and gabbroic rocks in the northwestern part of the Näränkävaara intrusion. Both types also contain platinum-group minerals.

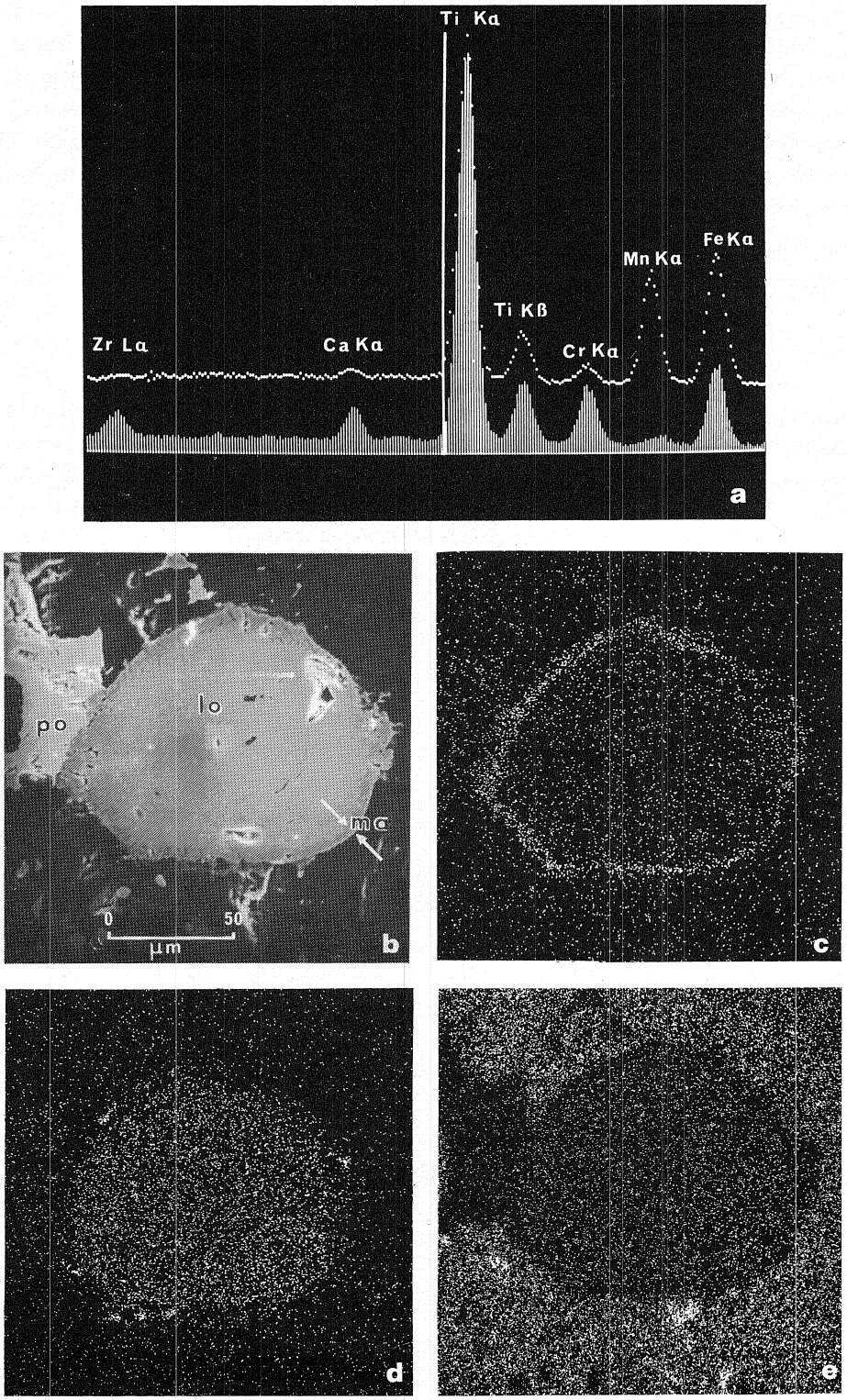

Fig. 31. (a) Energy-dispersive X-ray spectra for the core (histogram) and margin (dotted line) of a loveringite grain. (b) Secondary electron image of loveringite (lo = loveringite; ma = Mn-rich margin of loveringite; po = pyrrhotite). (c—e) X-ray scans showing the distribution of elements in loveringite: (c) manganese, (d) chromium, (e) calcium.

The sulphides in the marginal series of the western intrusion occur in the form of aggregates interstitially to silicate minerals, and consist mainly of chalcopyrite, pentlandite, pyrrhotite and smaller quantities of pyrite. The best disseminations are encountered at the top of the contact gabbro, where they take the form of unevenly distributed cloud-like enrichments. The sulphide minerals in general, and particularly the pyrrhotite and chalcopyrite, occasionally contain inclusions of platinum-group minerals, among which merenskyite, froodite, michenerite and sperrylite have been identified (Piirainen *et al.* 1977).

The sulphide enrichments in the middle zone of the western intrusion are found in connection with spotted gabbro, the spotted occurrence of this rock being due to those minerals which were late in crystallizing being concentrated in discrete, light-coloured clusters, into which the sulphides have also aggregated. These sulphide minerals chiefly consist of chalcopyrite and pentlandite and the platinum-group minerals merenskyite and michenerite.

The sulphide enrichment at Näränkävaara is associated with the contact zone between the upper bronzitite layer and the subzones Pe II and Gbno I, sulphides having been encountered in the bronzitite (sample 30Nä) and in the mela-bronzite gabbro (sample 37Nä) a distance of some 700 m apart. Those in the former are mainly composed of pyrrhotite and to a lesser extent pentlandite and chalcopyrite, and in the latter predominantly of chalcopyrite, accompanied by some pyrrhotite and pentlandite in that order. The orthopyroxene in the latter sample proved exceptionally rich in nickel, containing 0.12 % NiO by wt. (Table 4).

In addition to these enrichments, sulphides are also found in the layered series as accessory minerals, generally either interstitially to other minerals, or especially in the case of chalcopyrite, as fine-grained dust-like inclusions. This latter mode of occurrence is especially typical of the magnetite gabbros. These accessory sulphides are chiefly pyrrhotite and pentlandite at Näränkävaara, whereas chalcopyrite is predominant in the layered series of Pyhitys and the western intrusion.

MICAS

The tri-octahedral micas phlogopite and biotite are common intercumulus minerals in the layered series, and show evidence of cryptic variation manifested in the form of a distinct drop in the Mg/Fe ratio with structural height (Table 10), as a consequence of which the micas of the ultramafic zone at Näränkävaara consist of phlogopite and those found elsewhere normally of biotite.

The amounts of mica present in the Näränkävaara layered series increase markedly from the bottom of the sequence upwards (Table 1), while the reverse is true in the western intrusion, where it is common in the lower zone, much less so in the middle zone and rare in the upper zone. Mica is extremely rare in the Pyhitys layered series. In gabbroic rocks it is often found in association with the iron—titanium oxides, especially ilmenite.

The chromium content of the phlogopites is relatively high, especially in the sulphide-bearing *bC* sample 30Nä (Table 10), where the mica, which is practically opaque in the thin section, is also exceptionally rich in sodium.

GARNET

Small, roundish or slightly elongated grains of garnet, regularly enclosed in plagioclase, occur in the olivine-bearing rocks of the lower zone in the western intrusion and at Pyhitys. Frequently these are found to have been altered to the form of an isotropic, saussurite-like mass. The compositions of this garnet are shown in Table 10. The sample W146, which is not among the type samples used here, is included in this table as a cell-edge determination is available for it. It is from the eastern part of the Porttivaara block, about 5 km west of Pyhitys. Since the garnet analyses were carried out using a microprobe it was not possible to determine the ferric iron content, but instead the FeO/Fe_2O_3 ratio was adjusted iteratively by computer so as to give a figure of 4.00 for the number of ions in a R^{3+} group.

The amounts of the five end-member molecules calculated from the analytical data show these minerals to belong to the relatively rare intermediate almandine—grossular garnets, and the unit-cell parameter of a 11.70 ± 0.02 Å (Mäkelä 1975) fits extremely well with that reported for a synthetic almandine—grossular garnet of corresponding composition (cf. Cressey *et al.* 1978). It was thought at one time that there was no continuous variation between the pyralspite and ugrandite series, but as the number of analyses available has increased garnets have been found which fill the broad compositional gap, although admittedly these to date account for only about 2 % of all published garnet analyses (Hsu 1980).

OTHER MINERALS

Quartz is found as an intercumulus mineral in a few rocks representing subzone Gbno I at Näränkävaara, and is even encountered in the olivine gabbronorites (43Nä). It then increases in amount in subzone Gbno II, to reach a few percent by volume, and even exceeds 10 % by vol. in the dioritic rocks. At Pyhitys and in the western intrusion it is found in the middle and upper parts of the layered series, and frequently also in the contact gabbros of the marginal series. It generally occurs in the layered series in the form of granophyric intergrowths with alkali feldspar, and seldom as independent grains.

Zircon and apatite occur sporadically as accessory minerals in the gabbroic and dioritic rocks, particularly in their pegmatoid varieties. Grains of over one millimetre in size were even found in a few samples from the lower zone of the Syöte layered series. Independent potash feldspar was encountered only in the dioritic rocks at Näränkävaara. No primary amphibole was found, all the amphiboles present being interpreted as alteration products of pyroxenes, i.e. uralites. These also generally carry indications of cryptic variation in spite of their mode of formation (Table 10).

WHOLE-ROCK CHEMISTRY

The chemical compositions of the rocks, together with C.I.P.W. norms for the Koillismaa complex are presented in Table 11. Principal emphasis in the analysis of the minor elements was placed upon those which form ores within basic magmas, namely Cr, V, Ni, Cu, Co and S, also including Zn and Sr. In the case of the Porttivaara block the rare earth elements were also analysed (Table 12).

MAJOR AND MINOR ELEMENTS

Composition of the fine-grained border facies

Chilled margin samples from layered intrusions are sometimes used as indicators of parental magma compositions. Although this procedure has recently been questioned by various authors, it can nevertheless be assumed that they do provide certain clues to the nature of the primary liquid which originally occupied the magma chamber. Fine-grained facies of this kind are represented by the gabbronorite sample 1Ch, from the Kuusijärvi marginal series, and perhaps also the relatively highly altered small-grained contact gabbro from the Näränkävaara marginal series (Alapieti *et al.* 1979 b, Table 2, sample U482), which resembles it very closely in its chemical composition.

The Kuusijärvi sample is composed of plagioclase with a composition of $An_{54.5}Ab_{43.7}Or_{1.8}$ (0.45 % Fe by wt.) and slightly uralitized orthopyroxene and clinopyroxene. Its microstructure contains features suggestive of cumulus textures, and these, like the uralitization, have obviously had some effect on the bulk composition of the rock. The validity of sample 1Ch as an indicator of the composition of the parental magma may be evaluated in the light of the following calculations. In order to obtain a typical Mg/Fe^{2+} distribution coefficient for olivine—liquid equilibrium in basaltic magmas of $K_D = (Mg/Fe^{2+})$ liquid/(Mg/Fe^{2+})olivine = 0.33 (Roeder & Emslie 1970, Longhi *et al.* 1975), the liquid equivalent of sample 1Ch would have had to have been in equilibrium with an olivine of $Fo_{89.5}$. The composition of the lowest olivine encountered in the Näränkävaara intrusion, on the other hand, has been shown by microanalysis to be $Fo_{87.5}$ (Table 3, 1Nä), a difference with respect to the calculated value which is about of the order that one might expect. The partition of the nickel between the liquid and the olivine has been found to be dependent on the MgO content of this liquid (Hart & Davies 1978). Given a mean NiO content in the olivines of subzone Pe I at Näränkävaara of 0.255 % by wt., and assuming that these are almost the first minerals to be formed, the Ni content of the coexisting magma should be 168 ppm, which is in good agreement with the value of 170 ppm obtained in the analysis of sample 1Ch.

Sample 1Ch would suggest that the fine-grained border facies of the Koillismaa complex are characterized by a low TiO_2 and K_2O content and a relatively high MgO content. Comparison with the most recent data on other layered intrusions (Jackson 1971, Hughes 1976, Hoover 1978, Page 1979, Davies *et al.* 1980) points to both similarities and obvious differences. MgO content is slightly higher in the Bushveld and very much higher in the Great Dyke, and the Muskox, Skaergaard and Stillwater intrusions have chilled border rocks which are richer in ferrous iron and have higher CaO and TiO_2 content figures, whereas the TiO_2 content in the Bushveld and Great Dyke is very low, as is the case here.

Variations in the major and minor elements

The chemical components analysed were plotted against structural height in diagrams produced directly by computer for the purpose of illustrating cryptic layering. Even so, the value of individual chemical components evaluated in whole-rock analyses for demonstrating cryptic variation within a rhythmically layered series of igneous cumu-

lates is highly restricted by comparison with the amount of information which may be gained by studying phase-change layering and the variations in composition occurring in the course of fractionation in minerals which form solid solutions. This is chiefly due to the fact that the analyses from the leucocratic and melanocratic layers give rise to a high standard deviation in the diagrams, since it is not always possible to select 'average rocks' for analysis (Wager 1960), even though one may set out to do so. Similarly the amount of pore material present and the varying extents of alteration of the minerals will affect the total composition. In addition, the rocks of the marginal series in particular are often contaminated by the assimilation of salic country rocks, an effect which would seem to be least marked in the samples from the Syöte marginal series, since this borders onto basic volcanic rocks at the point sampled. In view of the above limitations on their usefulness, and at the same time for the sake of brevity, the variation diagrams obtained are not included here, with the exception of that for chromium (Fig. 32), the variation in which is perhaps the most clearly associated with fractionation. Instead only brief verbal comments are given.

SiO_2: The silica content remains for the most part around 50—55 % by wt. at Näränkävaara, with the exception of the peridotites and siliceous late differentiates, while at Pyhitys it increases almost linearly from 42 % in the ultramafitolite of the marginal series to 54 % in the upper zone. In the marginal series of the western intrusion, however, it declines fairly steeply in an inward direction, on account of the 'reversed fractionation', after which it shows a slight increase in the layered series, only to fall again temporarily in the magnetite gabbro.

Al_2O_3: Aluminium shows stepwise enrichment in an upwards direction at Näränkävaara, with well under 10 % Al_2O_3 in the ultramafic zone, approx. 10 % in subzone Gbno I and almost 20 % in the basal parts of Gbno II, after which it reverts to a slight fall. Elsewhere in the complex the variation in aluminium is approximately the same as that in silica.

TiO_2: At Näränkävaara TiO_2 remains below the 0.2 % level as far as subzone Gbno I, after which it begins to rise gently, reaching its maximum of approx. 1.4 % at the very top of the layered series. It also shows a gradual increase with structural height elsewhere, although still remaining below 0.5 % except in the magnetite gabbro, where it jumps to as much as 2.75 %, a value which even then exceeds the mean TiO_2 content for the gabbroic rocks by only a small amount.

Fe_2O_3: The proportion of this oxide remains below 5 % by wt. throughout the complex with the exception of the serpentinitized olivine cumulates at Näränkävaara and the *pamC* layer of the upper zone in the western intrusion, where it lies between the 5 % and 10 % levels.

FeO: This oxide shows irregular variations in the mean range 5—10 %, on account of the rhythmic layering. Very much lower values are found in the *pC* layers of the upper zone in the western intrusion and higher values in subzone UZb of the same intrusion, but even here they seldom exceed the 10 % mark.

MnO: Within the limits of accuracy employed here, manganese does not show any variations in content associated with fractionation, but remains around 0.2 % throughout.

MgO: MgO shows a rising trend in the marginal series and a falling trend in the layered series at every section, with some scatter in the results occasioned by the rhythmic layering. There are one or two outstanding deviations from these general trends, however. MgO is low in the websterites at Näränkävaara and high in subzone Pe II by comparison with this trend, and similarly jumps upwards in the magnetite gabbros of

the western intrusion at the point where augite returns as an essential cumulus mineral.

CaO: The variation here closely resembles that observed in Al_2O_3, except that the *baC* samples from Näränkävaara now stand out as a separate group on account of their high calcium content while the subzone UZb of the western intrusion no longer shows the same minimum values as for Al_2O_3 by virtue of the abundance of cumulus augite.

Na_2O and K_2O: These alkali metal oxides remain very low in the ultramafic zone at Näränkävaara, with Na_2O below 0.5 % and K_2O below 0.2 %, but they then begin to rise in a practically linear manner from subzone Gbno I onwards, to reach their maxima, 4.1 % Na_2O and 2.9 % K_2O, in the dioritic rocks. Elsewhere Na_2O increases gradually with stratigraphic height to reach its maximum in the plagioclase cumulates of the upper zone, between which there is a distinct low in subzone UZb, due to the smaller amounts of plagioclase present. K_2O remains very low throughout the layered series of Pyhitys and the western intrusion, but can rise to levels in excess of 1.5 % in those samples from the marginal series bordering onto albite-quartz rocks.

P_2O_5: This remains below 200 ppm at Näränkävaara as far up the sequence as the websterite, after which its content begins to increase almost exponentially, to reach a maximum of 4100 ppm at the top of the layered series. Elsewhere the phosphorus content fluctuates irregularly, correlating directly with the sporadic occurrences of apatite, which is most abundance in the plagioclase cumulates of the upper zone.

Cr: The chromium content achieves its highest value in the lower *bC* layer at Näränkävaara (Fig. 32), in which olivine ceased to be precipitated as a cumulus phase. Beyond this point it begins to fall more or less linearly until subzone Gbno II, where plagioclase becomes firmly established as a cumulus phase, where it drops suddently. The temporarily higher chromite content in subzone Pe II is immediately reflected in a higher chromium value. Cr content shows a practically linear decline at Pyhitys, with a deviation in the form of a minimum in subzone LZa which correlates with the replacement of chromite by ilmenomagnetite—ilmenite grains (see preceding chapter). In the western intrusion the chromium content is reduced almost to zero after relatively high values in the marginal series, then rising again temporarily in the middle zone in the same manner as the chromium content values for the pyroxenes.

V: A slight increase in vanadium content with height in the sequence takes place at Näränkävaara, the content in the ultramafic zone being 100 ppm or lower, that in the gabbroic rocks 100—200 ppm and that in the dioritic rocks even as high as 500 ppm. Elsewhere the figure remains uniformly low, with the exception of the magnetite gabbro of the western intrusion, where a major enrichment occurs, so that figures of over 2000 ppm are by no means rare.

Ni and Co: Both of these are dichotomous in their occurrence. Firstly, they both enter sulphides formed from the immiscible sulphide liquid, and thus do not participate in cryptic layering. Consequently these tended to accumulate mainly in the marginal series. Secondly, they can also easily enter ferromagnesian silicates, particular olivine, and also spinellids and ilmenite. Since the amounts of sulphides present in the layered series are usually low, it is normally the latter mode of occurrence which is dominant there, with Ni and Co most abundant in the earliest of the cumulates, after which their concentrations decline more or less linearly towards the top of the sequence.

Cu and S: Copper and sulphur may be taken together since they are both found almost exclusively in the sulphides, and thus

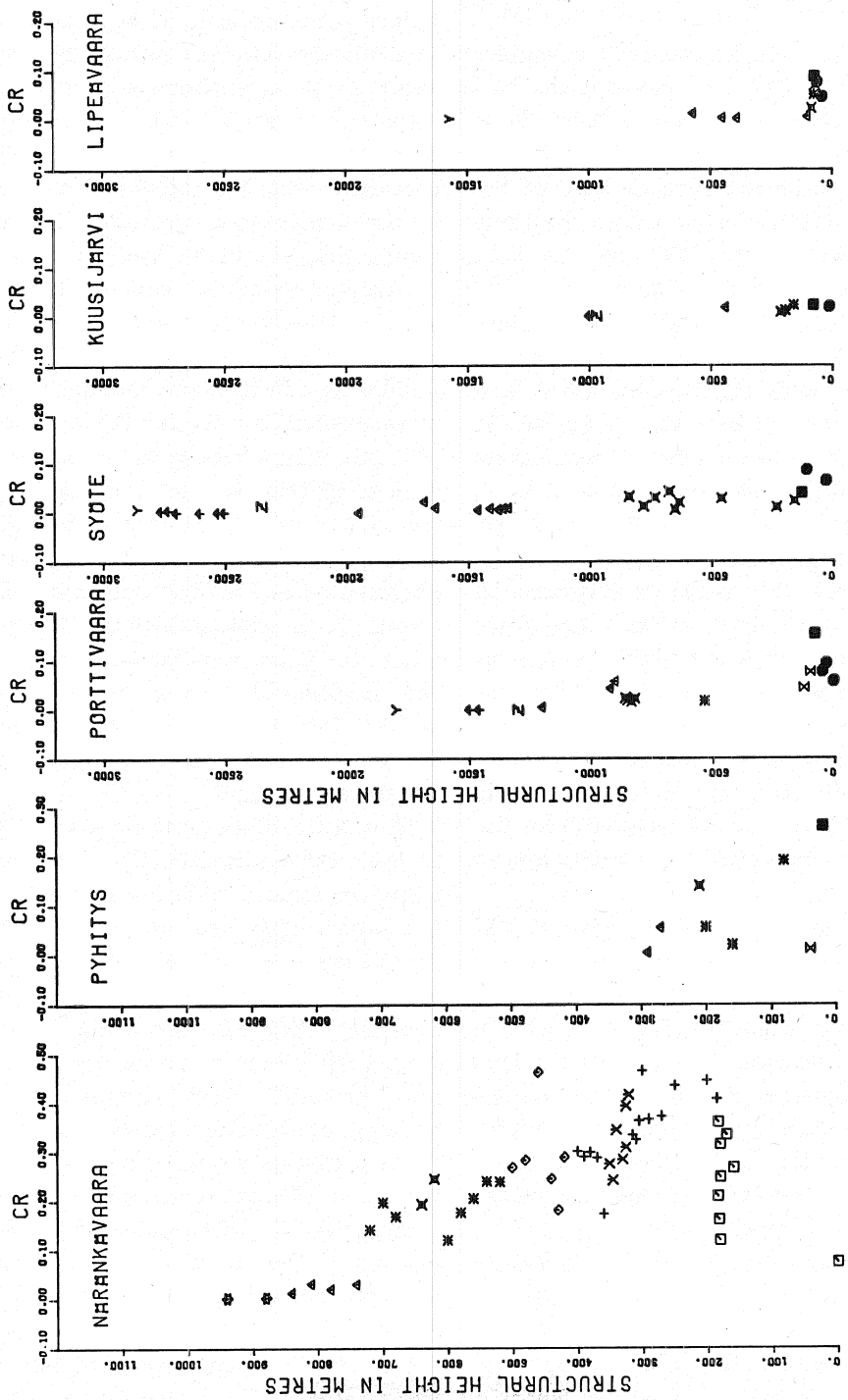

Fig. 32. Variations in the amounts of chromium in the rocks of the Koillismaa complex plotted against height. For key to symbols, see Fig. 10.

their incidence figures correlate with the variations in sulphide content described in the preceding chapter.

Zn: Zinc is concentrated in the spinellids, largely the chromites, and a figure as high as 1.1 % by wt. is obtained in the analysis of ZnO content in the spinel phase of subzone Pe II. Some enrichment of zinc is also found in the immiscible sulphide liquids, where its variations are comparable to those noted for copper.

Sr: Strontium most readily enters plagioclase, and its occurrence is thus directly analogous to the amounts of plagioclase present, the maximum of 600 ppm being recorded in the *pC* layers of the upper zone.

Variation in the modified differentiation index

More powerful than individual chemical components for the purpose of illustrating graphically the pattern of fractional crystallization are various parameters constructed from normative minerals calculated from the chemical analyses. Measures of this kind developed particularly with layered intrusions in mind are the modified differentiation index (MDI) and the modified crystallization index (MCI) (von Gruenewaldt 1973). One advantage with these is that they do not require analyses of 'average rocks' but, with certain limitations, can be based on analyses from any cumulates whatsoever. Computerized tests suggested that the MDI was the better suited of the two for comparing the various areas of the Koillismaa complex one with the other. The calculated values for this measure are given in Table 11 and depicted in relation to stratigraphic height in Fig. 33. The results show the variation in this index to be comparable to the changes in the composition of minerals belonging to solid solution series occurring in the course of fractionation (see previous chapter).

The MDI values increase very steeply with structural height in the Näränkävaara layered series, with a range of variation from about 0 to 80, which is as great as that found in the whole of the Bushveld layered series (von Gruenewaldt 1973), which has an overall stratigraphic height about eight times that encountered at Näränkävaara. Elsewhere in the Koillismaa complex the variation in the MDI, like the changes in the composition of minerals indicating cryptic variation, are very much more restricted. Comparison of the values for the layered series of Näränkävaara, Pyhitys, Porttivaara, Syöte, Kuusijärvi and Lipeävaara shows a clear increase in mean MDI to occur in this order. The MDI calculated for the fine-grained border facies, 39.65, corresponds to the values obtained from above halfway in the sequences everywhere except in the Kuusijärvi and Lipeävaara sections. The same situation prevails in the Bushveld complex (von Gruenewaldt 1973), where the more recently proposed magnesium-rich parental magma (Davies *et al.* 1980) shows a MDI of 41.35 (as calculated by the present author).

Mg–(Fe+Mn)–(Na+K) diagrams

In order to illustrate the trends in differentiation, the results of the chemical analyses were also arranged on Mg–(Fe + Mn)–(Na + K) diagrams (Fig. 34) of the kind proposed by Wager and Brown (1968). The diagram for the Kuusijärvi block also includes the results for the fine-grained border facies and the granophyre which caps the layered series of

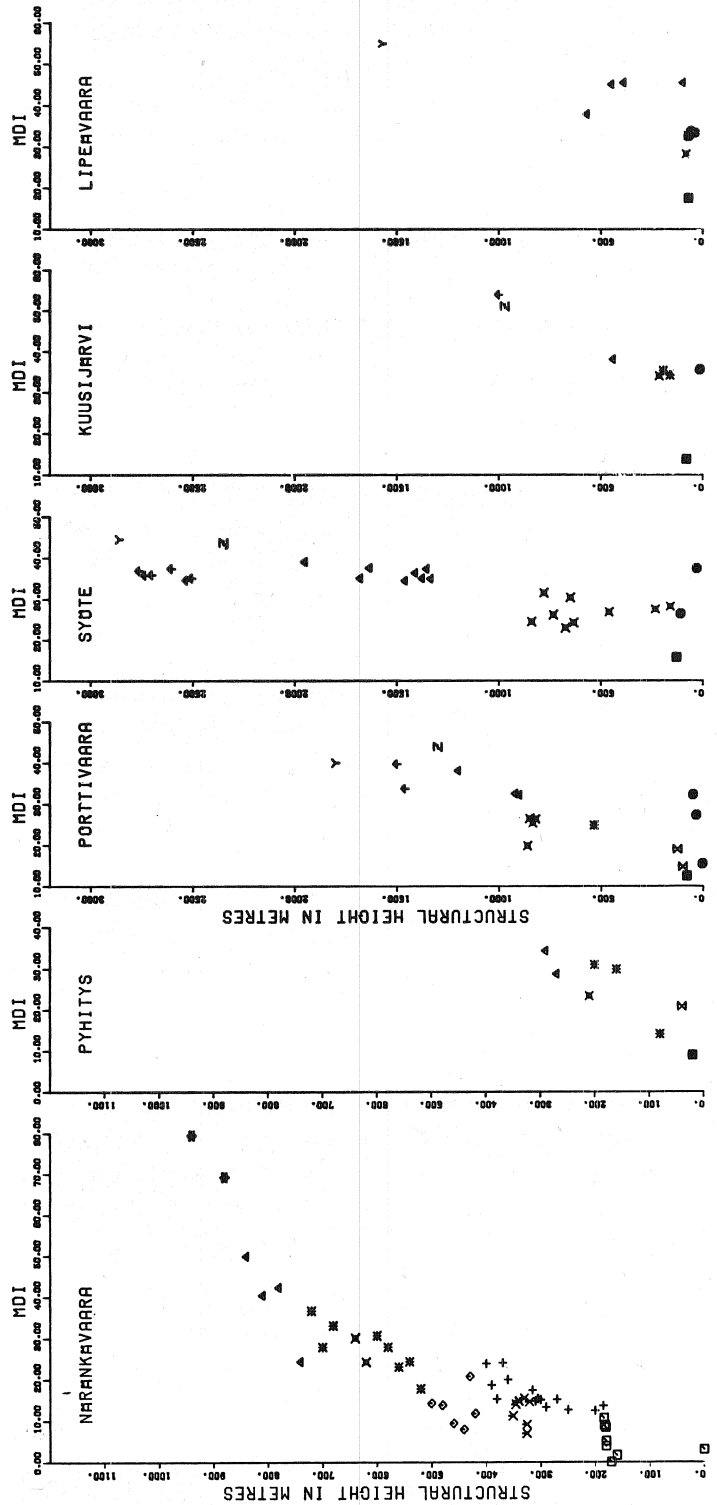

Fig. 33. Variations in the modified differentiation index in the rocks of the Koillismaa complex plotted against height. For key to symbols, see Fig. 10.

the western intrusion, the composition of which, as depicted in Table 11, bears a surprising resemblance to the granodiorite sample 52Nä from Näränkävaara.

One should also approach the use of whole-rock analyses in connection with diagrams of this kind with caution, since here again rhythmic layering and adcumulus growth can lead to a scatter of such proportions that it may even overshadow any regular trend that may exist. This effect can nevertheless be minimized by the choice of suitable samples, and the result obtained here does show reasonably easily discernible trends (Fig. 34).

The diagrams serve to reveal increasing enrichment of ferrous iron and alkali metals in relation to magnesium from the bottom of the sequence to the top in the layered series and from top to bottom in the marginal series, although to a lesser degree in the latter case. The enrichment of ferrous iron is nevertheless very much less marked here than in either the Bushveld or the Skaergaard intrusions (Wager & Brown 1968), as is also shown clearly by the shortness of the trends for olivine and pyroxenes.

RARE EARTH ELEMENTS

In addition to the major and minor elements discussed above, some attention should also be paid to the rare earths, the applicability of which to petrogenesis has been increasingly emphasized in recent times, leading to the availability of suitable comparative data from a number of major basic layered intrusions (e.g. Kuo & Crocket 1979). Research into this topic is admittedly still in its infancy as far as the Koillismaa complex is concerned, and it is not possible to provide more than some preliminary findings, and then only in respect of the Porttivaara block and the granophyre capping the Kuusijärvi block. The data concerned are listed in Table 12, and the chondrite–normalized rare earth element fractionation patterns for the samples are presented in Fig. 35. The values taken for this normalization are those of Haskin and Haskin (1968), since this is the procedure used for most of the other layered intrusions.

The rocks of the marginal series show characteristically relatively low absolute concentrations of rare earth elements, those of the layered series medium-range concentrations, and the granophyre high values. The minimum total amounts are found in the ultramafolite of the marginal series, after which the ΣREE values increase both upwards and downwards in the stratigraphical sequence (Table 12), so that the inverse relationship between the marginal series and layered series noted earlier emerges again here.

The chondrite–normalized fractionation patterns are manifestly similar for all the samples, i.e. relatively flat in the heavy rare earth element region but with higher fractionation among the lighter rare earths, although the granophyre shows a stronger enrichment of light rare earth elements relative to heavy than the other samples. One outstanding feature in the samples from the marginal series is the distinct enrichment of Lu by comparison with Yb. All the gabbroic rocks, in both the marginal and layered series, are characterized by positive Eu anomalies, while the granophyre and the ultramafitolite of the marginal series possess negative Eu anomalies. Mirror-image Eu anomaly

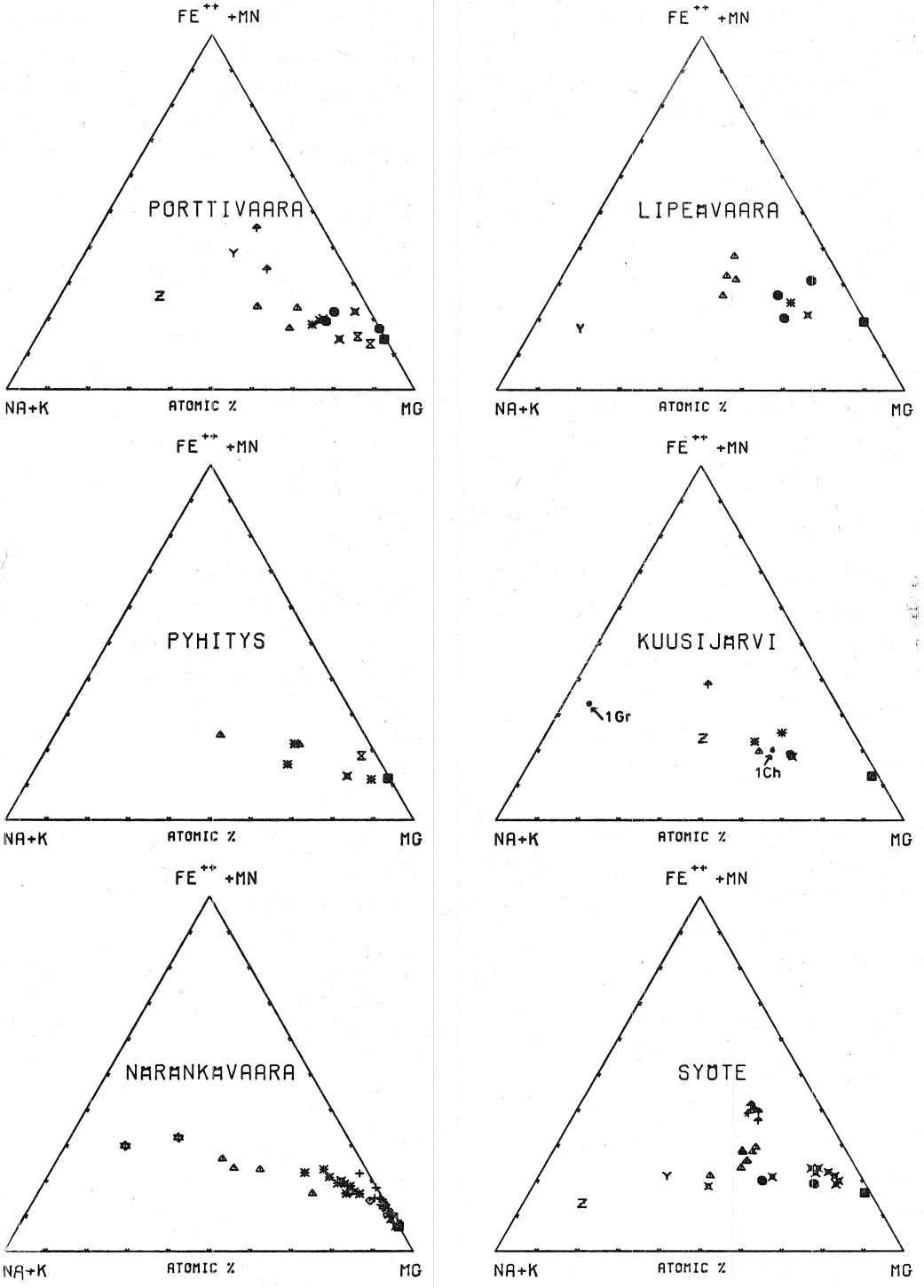

Fig. 34. Analyses of rocks from the Koillismaa complex plotted on Mg—(Fe + Mn)—(Na + K) diagram Gr = granophyre; Ch = fine-grained border facies. For key to symbols, see Fig. 10.

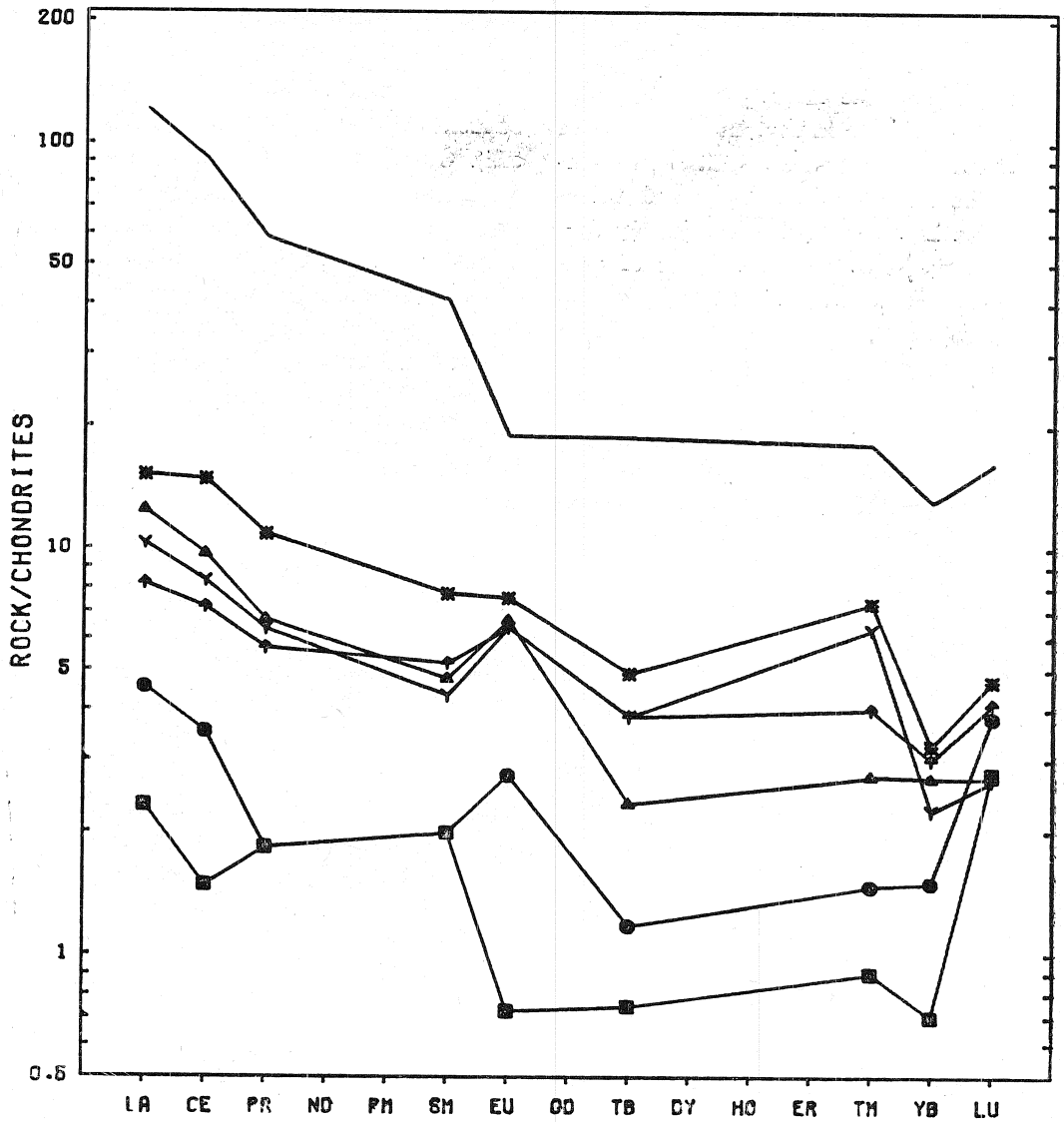

Fig. 35. Chondrite-normalized rare earth element fractionation patterns for the rocks of the Porttivaara block and capping granophyre (upper line). For key to symbols, see Fig. 10.

characteristics of this kind are also typical of many other basic layered intrusions.

In the light of the other known layered intrusions from which data are available on the rare earth elements, the Koillismaa complex would appear to resemble most the Stillwater and Muskox intrusions. Bushveld and Skaergaard show less fractionated rare earth patterns, while the Sudbury Nickel Irruptive is characterized by much higher total concentrations and a more fractionated pattern, probably due to its unusually siliceous nature.

GEOCHEMICAL BEHAVIOUR OF CHROMIUM

Chromium and the minerals which it enters are known to be important indicators of the physical and chemical conditions accompanying the formation of mafic and ultramafic rocks. In addition to these purely theoretical considerations, chromium is of considerable economic significance as an industrial raw material, and it is for this reason that any ore indicators to emerge from research into it are particularly useful. We shall look below at the behaviour of this element in the course of fractional crystallization and its distribution among the various rock types and minerals. This will involve some use of statistical methods.

The fine-grained border facies described in the preceding chapter has a chromium content of 210 ppm (Table 11), a figure which may be taken as being of the same order of magnitude as that of the parental magma of the Koillismaa complex. This value is slightly higher than the mean for basaltic rocks, but virtually the same as that for olivine—normative tholeiites, where the arithmetic mean for Cr content lies in the range 210—218 ppm (Prinz 1967, p. 302). A concentration of 210 ppm is nevertheless fairly low in comparison with those found in basic layered intrusions in which chromite-rich layers are known to occur, since the estimated concentrations for the proposed initial Muskox and Bushveld liquids are 540 and 970 ppm respectively (Irvine 1975, Davies *et al.* 1980).

The principal chromium-bearing minerals in the Koillismaa complex are the pyroxenes and those of the spinel group. Loveringite also contains large amounts of chromium, but is itself an extremely rare mineral. Other chromium-bearing minerals are ilmenite, phlogopite and olivine. In the case of ilmenite the chromium content varies from one sample to another, and values of over 1 % Cr_2O_3 are by no means rare, with the maximum recorded value as high as 3.42 % by wt., in subzone LZb at Lipeävaara (Table 9, sample 5Li). Chromium enrichment is found in the phlogopites of the ultramafic zone at Näränkävaara, the highest concentration analysed being 0.83 % Cr_2O_3 by wt., in subzone Bro II (Table 10, sample 30Nä). A chromium content in excess of the detection limit is found in the olivines only in the sample representing subzone Pe I at Näränkävaara, 0.13 % Cr_2O_3 by wt. (Table 3, sample 2Nä).

The variations in chromium content in the pyroxenes, spinellids and whole-rock samples with stratigraphical height are described above and presented in Figs. 14, 17, 26 and 32, so that no more than a summary of these is required here.

Näränkävaara layered series. The total chromium content in the *o(s)C* and *ob(s)C* layers at Näränkävaara varies over a relatively wide range, being regulated entirely by the amounts of bronzite and chrome spinel present. By the lower *bC* layer, however, the amount of chromite has declined markedly, while the cumulus olivine has been replaced by cumulus Ca-poor pyroxene. Even so, no significant changes occur in the amounts of total chromium, due to an incongruent melting relationship between Cr-rich pyroxene and chromite (Irvine 1967, Dickey *et al.* 1971, Campbell 1977). As is well-known, chromite is capable of reacting with the intercumulus liquid at the postcumulus stage, in which case the chromium which is released is absorbed into the intercumulus pyroxene as it crystallizes. Evidence of this is provided by sample 18Nä from the lower *bC* layer, for instance, where a resorbed cumulus chromite grain is found isolated in the intercumulus clinopyroxene. The spinellid concerned is the richest in chromium of all the minerals analysed from the complex (Table 8), whereas the chromium content of the surrounding pyrox-

ene is exceptionally low, only 0.18 % Cr_2O_3 by wt., compared with a value of 0.69 % by wt, elsewhere in the same rock (Table 5), so that the process can be assumed to have been interrupted.

The commencement of the accumulation of augite in the *baC* layer seems to have arrested the crystallization of chromite entirely, although this gives rise to only a small drop in the chromium content of the samples compared with the underlying *bC* layer. The total chromium in this *baC* layer is distributed between the augite and bronzite, which both show pronounced extension as a consequence of adcumulus growth, with the former binding about twice as much as the latter. Since at the same time augite has now become as plentiful as bronzite in the rock, a smaller amount of chromium has 'sufficed' for the individual mineral grains in this layer than elsewhere in the ultramafic zone (Figs. 14 and 17).

The chromium content of the pyroxenes, especially the Ca-rich pyroxene, increases once more in the upper *bC* layer, where clinopyroxene returns as an intercumulus phase. Even so, since bronzite is again dominant over the clinopyroxene and there are no minerals of the spinel group present, the total chromium content even falls slightly compared with that in the *baC* layer below. One special feature of this subzone Bro II is a new chromium-rich phase, loveringite, which was nucleated locally from the residual intercumulus liquid.

Although chromite returns as a cumulus phase in subzone Pe II, the mean value for total chromium remains practically unchanged compared with the previous subzone, since the proportion of olivine increases at the same time at the expense of pyroxenes.

A clear, if slow, decline in total chromium and in the chromium content of the various minerals begins in subzone Gbno I, although spinellids continue to be crystallized in a cumulus phase, in contrast to the situation in the Bushveld, for example, where Cameron (1979) notes that the incorporation of chromium in the clinopyroxene reduces its concentration in the magma to a point below the saturation level for chromite. Thus the spinel phase reappears in the Bushveld only once the titanomagnetite has become a stable phase.

The chromium reserves in the magma chamber would seem to have been almost exhausted by the time subzone Gbno II began to crystallize out, and consequently the pyroxenes of this subzone, although fairly rich in magnesium in the basal parts, contain very little chromium. This situation is reflected in a sudden drop in chromium content in the diagrams mentioned above.

Pyhitys layered series. Total chromium and the chromium content of the pyroxenes and spinellids all show a consistent declining trend in the Pyhitys section, with the exception of subzone LZc, where the temporary peak in total chromium is located entirely in the orthopyroxene.

Layered series of the western intrusion. The chromium content figures recorded for the marginal series in the western intrusion are on average higher than those for the layered series, the highest values of all being reached in the ultramafic rocks of the marginal series. A small jump in chromium content is found in the lower part of the middle zone in the Porttivaara section, this being reflected in all the above diagrams and also in the occurrence of chromium-rich magnetite. Higher than average values are also recorded in the middle zone at the Syöte section.

The partition of Cr^{3+} between the coexisting pyroxenes in the Näränkävaara intrusion clearly acts in favour of the Ca-rich pyroxene. The chromium content increases in both of them more or less linearly when they occur as cumulus minerals (Fig. 36), but once

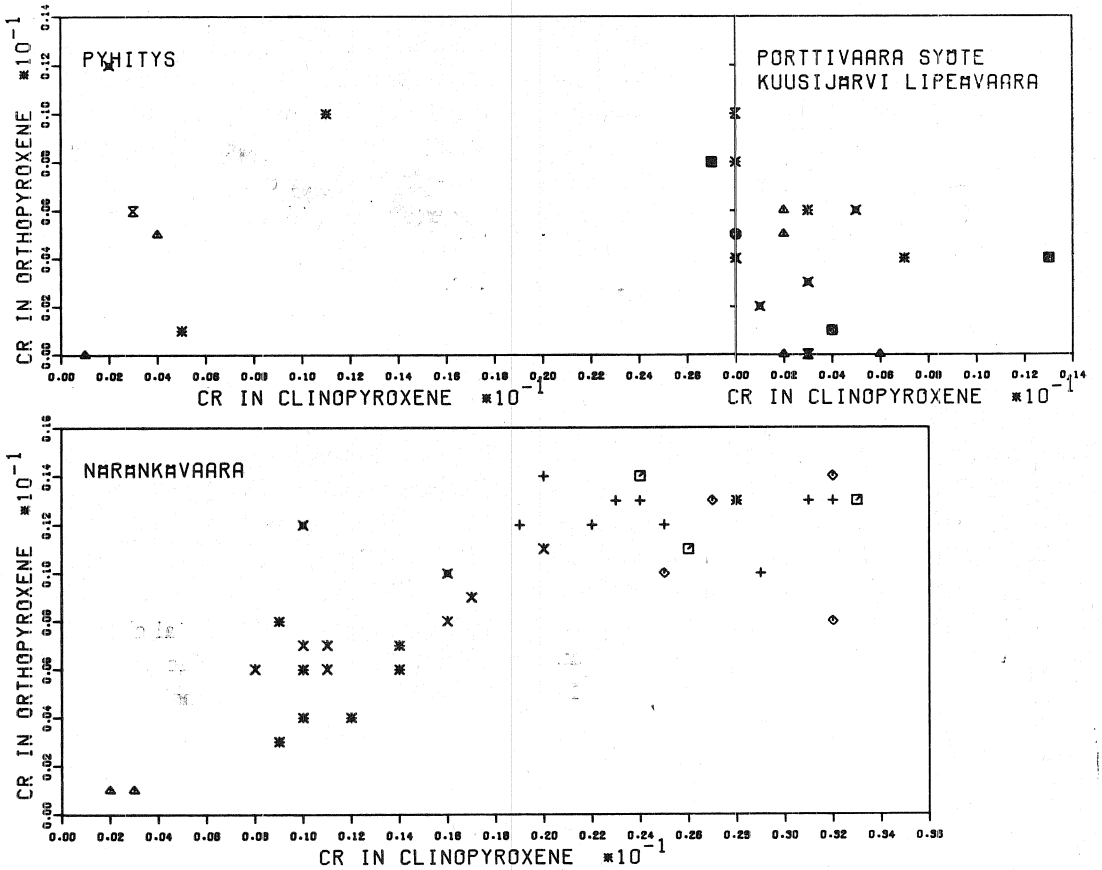

Fig. 36. Partition of Cr (recalculated on the basis of six oxygen atoms) between coexisting pyroxenes in the Koillismaa complex. No values are indicated on the diagram for samples in which both pyroxenes had a Cr content < 0.001. For key to symbols, see Fig. 10.

the Ca-rich pyroxene becomes an intercumulus phase the orthopyroxene reaches its maximum Cr content, which then remains virtually constant, while that of the clinopyroxene continues to rise. These trends become more obscure at Pyhitys and in the western intrusion, where the chromium content of the pyroxenes is lower, and even the orthopyroxenes seem to be favoured at Pyhitys.

The partition of chromium between each pyroxene and the minerals of the spinel group at Näränkävaara is also practically linear, with high coefficients of correlation (Fig. 37). The same is also true of the coexisting Ca-rich pyroxene and spinellid at Pyhitys, whereas the correlations between the Ca-poor pyroxene and spinellids at Pyhitys and between both the pyroxenes and the spinellids in the western intrusion are very much less distinct.

Chromium has a tendency to enter the first phases to crystallize from a melt, owing to its octahedral crystal-field stabilization energy, which is the highest of any transition metal ion (Burns 1970). It is for this reason that high Cr concentrations are found in the ultramafic zone at Näränkävaara, and that chromium is concentrated chiefly in the ultramafic rocks of the marginal zone in the Pyhitys section and the western intrusion. It

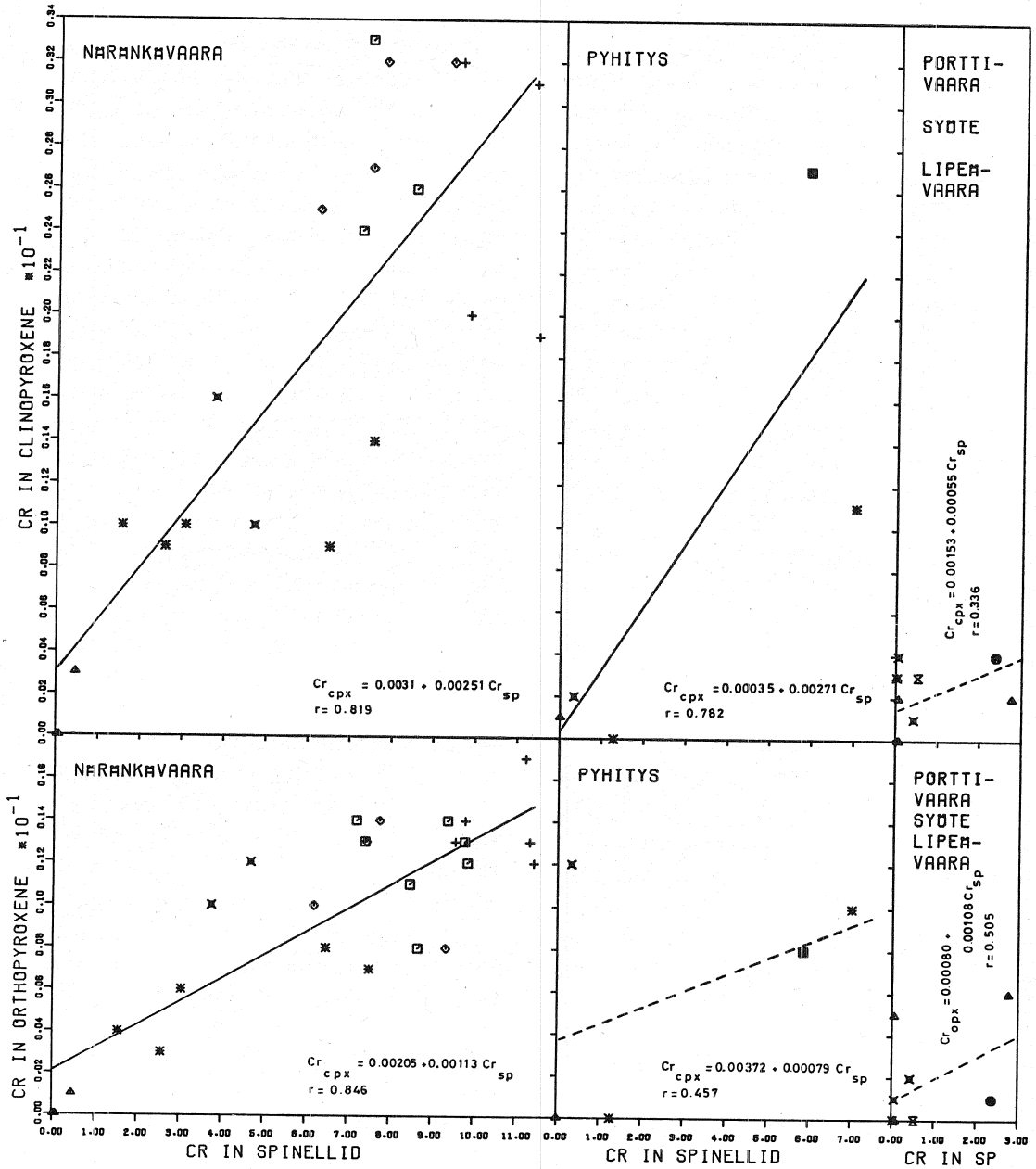

Fig. 37. Partition of Cr between a coexisting spinellid (recalculated on the basis of 32 oxygen atoms) and pyroxene pair (recalculated on the basis of 6 oxygen atoms) in the Koillismaa complex. The correlation coefficients (r) and regression equations are also shown. Values for samples with Cr $<$ 0.01 in the spinellid and Cr $<$ 0.001 in the pyroxene were rejected. For key to symbols, see Fig. 10.

is easy to understand the high partition coefficient for chromium between the pyroxenes and the melt in the light of this crystal-field theory, although it still does not explain the partition between Ca-rich and Ca-poor pyroxene, i.e. why chromium, unlike nickel,

which also has a high crystal-field stabilization energy, shows a preference for the Ca-rich pyroxene (Fig. 36, Tables 4 and 5) even though this usually crystallizes later than the Ca-poor variety. The explanation is presumably that the partition of Cr also depends on factors such as the ionic radius and charge balance. The replacement of Mg^{2+} and Fe^{2+} in pyroxenes by Cr^{3+} requires at the same time a change in the charge balance, as is achieved when a Si^{4+} ion in a tetrahedral site is replaced by an Al^{3+} ion and/or when a Na^{+} ion enters an M site (Campbell 1977). Thus the higher Cr content of the clinopyroxene is a consequence of the greater capacity of its lattice for accepting Al^{3+} in the tetrahedral sites and large cations such as Na^{+} in the M_2 sites, which in turn would seem to derive from the fact that it has a lower symmetry than orthopyroxene. This charge balance aspect also explains the low chromium content of olivine, since the amounts of aluminium and sodium present are quite negligible.

The amounts of Al^{3+} in the tetrahedral sites indicated in Tables 4 and 5 are calculated by adding the requisite amount of Al to the Si to complete the ideal two tetrahedral ions per formula unit. The relative accuracy of the microanalysis in determining SiO_2 is nevertheless only of the order of 5 %, and since, in addition, the concentration of SiO_2 is very much higher than that of Al_2O_3, these calculations do not lead to a structural formula which has an exact charge balance. If one nevertheless assumes that the majority of the aluminium will be located in the tetrahedral sites, it is still possible to examine the mutual dependency relations between Cr^{3+}, Al^{3+} and Na^{+} in the pyroxenes of the Koillismaa complex. We then find that the charge balance theory discussed above holds good to an extremely high degree. The pyroxenes in the websterites of the Näränkävaara intrusion, for instance, have fairly low Cr_2O_3 concentrations, 0.27 % by wt. in the orthopyroxenes and 0.47 % by wt. in the clinopyroxenes (Tables 4 and 5), whereas the corresponding values in the other rocks of the ultramafic zone shows means of 0.44 % and 0.91 % by wt. respectively. In the same way the pyroxenes in the websterites have low values for aluminium and sodium content, the orthopyroxenes containing on average 1.05 % Al_2O_3 by wt. and 0.01 % Na_2O, and the clinopyroxenes 1.60 % Al_2O_3 and 0.12 % Na_2O, while the orthopyroxenes in the other rocks of the ultramafic zone have mean values of 1.50 % Al_2O_3 and 0.07 % Na_2O and the clinopyroxenes 2.58 % Al_2O_3 and 0.42 % Na_2O. The clinopyroxenes of subzone Pe II are the richest in chromium of all the pyroxenes, containing 0.99 % Cr_2O_3 by wt. on average, and similarly their aluminium and sodium content figures are the highest of all, a mean of 2.93 % by wt. for Al_2O_3 and 0.49 % for Na_2O. In contrast, the pyroxenes of Gbno II are very poor in chromium, and also have low aluminium and sodium concentrations. The same is also true in other parts of the complex, although the relationship is no longer so clear-cut on account of the small concentrations of chromium involved.

Normal fractional crystallization apparently cannot in itself lead to extensive concentrations of chromite, but rather some specific mechanism is required in order to explain the enrichment of chromium by as much as 1000-fold relative to the concurrent magma. The following hypotheses have been put forward to solve this problem.

Concerning the origins of certain chromite-rich seams in the eastern Bushveld complex, Cameron & Emerson (1959) suggest that they are due fundamentally to the gravitative settling of chromite under the influence of magmatic currents.

Referring to the demonstration by Kennedy (1955) and Osborn (1959) that an increase in oxygen fugacity will lead to an increase in

the ferric/ferrous ratio in a basaltic magma and favour the crystallization of a spinel phase, Cameron & Desborough (1969), Ulmer (1969) and Cameron (1975) have postulated that the precipitation and compositional variation in the chromite in the Bushveld may have been controlled by variations in the oxygen fugacity of the magma resulting from the assimilation of groundwater or the wall rocks, or from breathing of a vent. Detailed mineralogical research has nevertheless shown that segregated chromite in layered intrusions has a lower ferric/ferrous ratio than does disseminated chromite from the adjacent layers (Jackson 1969, Cameron 1977, Hamlyn & Keays 1979).

Irvine (1975) suggests that the chromite-rich layers were formed on occasions on which the basic parental magma of the intrusion was extensively contaminated with granitic melt derived from the salic roof rocks. He is later of the opinion that this mechanism is not the correct one, however, and proposes an alternative hypothesis (Irvine 1977) which assumes that chromitites are formed when chromite-saturated picritic tholeiite liquid is blended with an earlier liquid of the same type which has differentiated to a relatively siliceous composition.

Cameron (1977) regards both of Irvine's hypotheses as inadequate for explaining the origin of chromitites, as both require a very rapid and very uniform mixing of new liquid with a magma already present in the chamber, not once, but a number of times. He also seems it improbable that such mixing could take place over distances up to a hundred kilometres or more. In his opinion changes in total pressure due to tectonism affecting the magma chamber during crystallization must have been the primary factor in the formation of the chromitites of the Eastern Bushveld.

In spite of the great volume of research devoted to chrome ores, the physical and chemical factors affecting the behaviour of this element in stratiform intrusions are still poorly understood and open to speculation. One new approach is offered by the method of multiple regression analysis employed in the present work, which allows one to estimate the total chromium content of the rock and the chromium content of the principal chromium-bearing minerals, i.e. Ca-rich and Ca-poor pyroxene and spinellid on the basis of the information supplied by the total geochemical data.

The type samples examined here included 36 for which both whole rock analyses and composition data on the above-mentioned minerals were available (Tables 4, 5 and 8). These were organized into arrays on the basis of the percentage composition of the rock by weight, the modified differation index, the number of cations and certain cation ratios in the above minerals. This gave a total of 70 variables in each array and 2520 elements in the matrix as a whole. The total chromium content and the amounts of chromium present in the pyroxenes and spinellids, expressed in cations, were then taken in turn as the dependent variable and the independent variables showing the best fit with the model were selected by computer from among the remaining elements. The one restriction placed on this was that the data derived from the same compositional array as the dependent variable were excluded from the model each time, e.g. no attempt was made to explain the total chromium content of the rock by reference to any other components of the whole rock analyses. This enabled erroneous interpretations involving variables with constant sums to be avoided. This constant sum problem, which has been discussed extensively in the literature from the late 1940's onwards (see Skala 1979), is one of the most difficult pitfalls encountered in the interpretation of geochemical data.

The results are presented in the form of four regression equations, 1—4, which are relatively short and straightforward to interpret, even though there is generally no direct causal relation between the variables, but rather their variation has a common underlying cause, the fractional crystallization event. On the other hand, there are certain variables which stand in a clear causal relationship one to another, and this dichotomous situation tends to interfere with the interpretation slightly.

The variation in total chromium content in the rock is depicted by Equation (1), in which the independent variables are the chromium content values for the spinellid and Ca-poor pyroxene. The coefficient of determination of 77.7 % shows that the model has a fairly good predictive value in spite of its simplicity.

$$Cr_{tot} = 0.0156 + 0.0196\ x_{57} + 7.6093\ x_{27}, \quad (1)$$

where

Cr_{tot} = % Cr by wt. in the whole-rock analysis,
x_{57} = Cr in the spinellid,
x_{27} = Cr in the Ca-poor pyroxene.

The chromium content of the Ca-poor pyroxene is explained best in terms of the total chromium content and the Mg/Fe cation ratio in the clinopyroxene (the corresponding ratio in the orthopyroxene was not included in the model), i.e. chromium was to be found in greater amounts in the early-formed pyroxenes.

$$Cr_{-Capx} = 0.0263 + 0.0004\ x_{52} + 0.0171\ x_{15}, \quad (2)$$

where

Cr_{-Capx} = Cr in Ca-poor pyroxene,
x_{52} = 100 Mg/(Mg + Fe) in the Ca-rich pyroxene,
x_{15} = % Cr by wt. in the whole-rock analysis.

The coefficient of determination for this sample model is 77.6 %.

The regression function for Ca-rich pyroxene presented here contains four variables, and achieves a coefficient of determination of 90.7 %. The importance of sodium, as alluded to earlier, emerges clearly in this connection in the form of the sodium content of the Ca-poor pyroxene. A parallel regression analysis in which all the variables were included, performed for comparative purposes, had the Na content of the Ca-rich pyroxene itself in this position, while whole-rock CaO was excluded. The absence of the aluminium content of the pyroxene from the model may well be due to the fact that this was represented in the computer data by the Al^{IV} and Al^{VI} values, which are insufficiently exact, as noted earlier. It is also important to remember that the samples representing the *baC* and upper *bC* layers are not included in this model, as they did not contain any spinellids.

$$Cr_{+Capx} = -0.0073 + 0.0011\ x_7 - 0.0171\ x_{69} + 0.9136\ x_{32} + 0.0015\ x_8, \quad (3)$$

where

Cr_{+Capx} = Cr in the Ca-rich pyroxene,
x_7 = % MgO by wt. in the whole-rock analysis,
x_{69} = Fe^{3+}/R^{3+} in the spinellid,
x_{32} = Na in the Ca-poor pyroxene,
x_8 = % CaO by wt. in the whole-rock analysis.

The chromium content of the spinellids is explained best in terms of the total aluminium and chromium content values for the whole-rock analyses and the amount of chromium in the Ca-rich pyroxene. The coefficient of determination is 87.6 %. Aluminium carries a negative weighting in the model, and would appear to represent chiefly the plagioclase content of the sample. The inclusion of the chromium content of the Ca-rich pyroxene would seem to be explained in part by the reaction relationship between intercumulus pyroxene and cumulus spinellid referred to earlier.

$$Cr_{sp} = 3.9285 - 0.2145\ x_3 + 9.9249\ x_{15} + 92.369\ x_{43}, \quad (4)$$

where

Cr_{sp} = Cr in the spinellid,

x_3 = % Al_2O_3 by wt. in the whole-rock analysis,

x_{15} = % Cr by wt. in the whole-rock analysis,

x_{43} = Cr in the Ca-rich pyroxene.

SUMMARY AND CONCLUSIONS

The internal structure of the Koillismaa complex, its layering and its mineralogical variation have all arisen as a result of fractional crystallization from a basic magma. Although we have no exact knowledge of the composition of this magma, some indication of the nature of the primary liquid which most probably initially filled the scattered Koillismaa chamber is provided by sample 1Ch (Table 11), which represents the fine-grained border facies. This corresponds in composition to a quartz–normative basalt, and is characterized by a relatively high MgO content and low TiO_2. This magma reached its present location, in a cold environment, by passing through a long, narrow feeder channel opening out into the Archean basement complex and forming the Näränkävaara intrusion and connecting 'dyke', with their V-shaped cross-sections. This magma then also began to escape along the practically horizontal surface of unconformity between the basement complex and the Proterozoic supracrustal rocks at the western end of the same feeder, to form the extensive sheet of the western intrusion.

The hot magma gave rise to thermometamorphic and metasomatic alterations in the gneisses adjacent to the contact, producing a zone of albite–quartz rock of varying thickness beneath the western intrusion and beside the V-shaped intrusions. At the same time a layer of granophyre formed in the hanging wall of the western intrusion, where the heating effect of the magma was greatest, although the relation between this and the basic rocks has not yet been resolved on account of the poverty of exposures. The overall similarities between the rare earth element fractionation patterns in the layered series and those in the granophyre (Fig. 35), coupled with the mirror-image Eu anomaly characteristics, would nevertheless indicate that these rocks are co-magmatic, even though contamination may well have played a significant part in the genesis of the granophyre.

One consequence of the rapid cooling of the basic magma as it came into contact with the cold environment was the formation of a fine-grained chilled margin. As the magma continued to flow, however, this broke up and became eroded away, so that now it is only encountered in the form of autoliths located further away from the contact.

While the magma was still in a state of movement, siliceous fragments of the surrounding gneisses became incorporated in it, melting either totally or partially and giving rise to pronounced local contamination. At the same time the marginal series began to crystallize in a steeply rising attitude at the sides of the V-shaped intrusions and in a horizontal position at the base of the western intrusion. During its solidification, conditions became favourable for a separation of the immiscible Ni–Cu–Fe sulphide liquid from the silicate melt, as a consequence of which a weak dissemination of sulphides with asso-

ciated platinum-group minerals is to be found in the series.

One striking feature of the marginal series is its 'overturned' layering, i.e. it shows 'reversed' fractionation, as found in Jimberlana and Muskox. Even so, the rocks with 'cumulate' textures involved in this scarcely deviate in character from those of the layered series, although since the series is 'overturned', it is difficult to explain its origins as being due to gravitative accumulation.

The modified differentiation index calculated from the chemical compositions recorded varies within a relatively wide range in the marginal series of the western intrusion, e.g. from 15.70 to 37.51 in the Syöte section (Table 11). Similarly the range in the composition of the minerals is fairly wide, e.g. with Ca-poor pyroxene varying between $Mg_{81}Fe_{19}$ and $Mg_{69}Fe_{31}$ (Table 4) and plagioclase between An_{78} and An_{58} (Table 7). All these facts point to a relatively large range for the temperature of crystallization. Thus, if an equilibrium was maintained between the magma and the Ca-poor pyroxenes of composition $Mg_{69}Fe_{31}$ and plagioclases of composition An_{58} in the marginal series and layered series, then the lower part of the marginal series must still have been in a liquid state throughout the deposition of the whole of the lower zone of the layered series. This apparent deposition on top of a liquid layer constitutes a fresh addition to the now considerable list of features of layered intrusions which do not appear to be consistent with the cumulus theory (cf. Campbell 1978, McBirney & Noyes 1979).

The crystallization conditions in these three separate but connected magma chambers, those of the Näränkävaara intrusion, the western intrusion and the connecting 'dyke', turned out to be entirely different, and thus fractionation pursued its own course in each of them, giving rise to three distinct differentiation series.

Although the vertical extent of the V-shaped Näränkävaara intrusion is of the order of some six kilometres, only about one kilometre of this is exposed to give a stratigraphic section. This begins with a zone of ultramafic cumulates, the lowermost parts of which contain practically dunitic olivine(—chrome spinel) cumulates. These cumulates have a low modified differentiation index, around 3, and high concentrations of Mg in the ferromagnesian silicates (olivine $Mg_{87.5}Fe_{12.5}$, Ca-poor pyroxene $Mg_{88}Fe_{12}$ and Ca-rich pyroxene $Mg_{89}Fe_{11}$), suggesting that fractionation was in its very early stages here. One may therefore expect a change in the direction of differentiation further down in the formation, and a marginal series of the kind found in Jimberlana and Muskox (cf. McClay & Campbell 1976) may well play a considerable role at deeper levels.

The following layers in the stratigraphy after the olivine(—chrome spinel) cumulates consist of olivine—bronzite(—chrome spinel) cumulates, bronzite cumulates, bronzite—augite cumulates and bronzite cumulates again in ascending order. These are then followed by a recurrence of olivine—bronzite (—chrome spinel) cumulates, probably as a result of a fresh influx of basic magma into the chamber, blending with the earlier liquid. This second magma need not necessarily have been of exactly the same composition as the primary magma, but may well have been modified in the lower crustal reservoirs. This new influx of magma may also have contributed to the occurrence of disseminated sulphides in the contact zone between the ultramafic and gabbroic rocks.

The ultramafic cumulates are followed by layers of mafic and intermediate cumulates. These are sufficiently limited in amount compared with the ultramafic cumulates, however, that one is forced to conclude that the intrusion must once have been more exten-

sive in its upper parts than one would assume from the present outcrop area.

The modified differentiation index for the Näränkävaara intrusion varies over a wide range, from almost zero to practically 80, and the silica content increases quite markedly in the upper parts of the layered series, as reflected in the abundance of quartz present. Although actual granophyres are not found here as they are above the basic rocks of the western intrusion, the uppermost granodiorites resemble them fairly closely in composition, being just slightly more basic. The fractionation trends of the ferromagnesian silicates are very short, and the Ca-poor pyroxene was not replaced by Fe-rich olivine once it ceased to be precipitated as is often the case in tholeiitic intrusions. Thus there is no enrichment of FeO towards the upper part of the sequence, but instead the fractionation follows the same SiO_2 enrichment — FeO depletion trend observed in Jimberlana (Campbell & Nolan 1974). Crystallization would nevertheless appear to have taken place at a lower temperature in its final stages in the case of the Näränkävaara intrusion, as is suggested by the lower En content (En_{61}) of the Ca-poor pyroxenes at the orthopyroxene–pigeonite changeover and the low calculated equilibration temperatures for the coexisting pyroxene pairs in subzone Gbno II.

Information on the layered series in the connecting 'dyke' is limited to the incomplete Pyhitys section, which is characterized by pronounced igneous lamination and rhythmic layering which varies in scale from a matter of less than one centimetre up to the level of macrorhythmic layering. The mineralogy and chemistry of the Pyhitys section suggests that it serves in its entirety as an intermediate formation between the Näränkävaara and western intrusions.

The layered series in the western intrusion consists of three mineralogically quite distinct zones, the lower, middle and upper zones, while the lower zone in the Porttivaara block would seem to be underlain by a further hidden layered series which increases in thickness towards the east and should really be regarded as constituting a fourth zone.

The lower zone, in which olivine is a significant cumulus phase at times, is typified both by fine-scale layering and also by a slightly indeterminate macrorhythmic layering, the origin of which may well be explicable in terms of the hypothesis proposed by Jackson (1961) for the formation of the macrorhythmic units of the Stillwater complex. According to this hypothesis the units were formed by bottom accumulation of crystals separating from successive relatively thin layers of stagnant magma located adjacent to the floor. The origin of the lower zone can probably be more plausibly explained, however, by the multiple injection hypothesis (Irvine & Smith 1967), since it is difficult to conceive of the extensive., side-filling western intrusion having been formed in any other way than through periodic influxes of fresh magma in which each new influx mixed with the fractionated magma already in the chamber, rendering it more basic and raising its temperature, thus resulting in the repetition of olivine-bearing cumulates, for example. The new magma pulses apparently differed from the primary magma in their composition, however, since the magma influxes entering the western intrusion periodically from the side would seem to have become progressively more differentiated in the magma chamber of the connecting 'dyke'.

The magma chamber of the western intrusion probably reached its eventual dimensions during the consolidation of the lower zone, so that in the terminology of Wager and Brown (1968) this may be designated as the integration stage in the crystallization history of the western intrusion, during which

the magma present in the chamber and that being periodically added to it were intergrated by mixing.

The commencement of formation of the middle zone marks the beginning of the true differentiation stage, in which crystallization would seem to have taken place under relatively stable conditions and in a closed system. The depression in the hanging wall nevertheless soon cut off the connection between the southern and northern parts of the magma chamber, and crystallization proceeded thereafter along a separate course in each, the northern part being characterized by the gradual emergence of plagioclase as the only cumulus phase, with progressively larger amounts of it occurring towards the top of the sequence, whereas in the southern part the deposition of the gabbronorites of the middle zone was followed at first by crystallization which led to almost monomineralic plagioclase cumulates, whereupon a simultaneous increase in oxygen fugacity led to the crystallization of vanadium-bearing titaniferous magnetite, and thus to the creation of magnetite gabbro. Following the formation of this subzoneplagioclase was then left as the only cumulus phase in this southern part of the magma chamber, too.

Like those at Näränkävaara, the fractionation trends of the minerals in the western intrusion are fairly short, but here the modified differentiation index varies within quite a narrow range and SiO_2 content values show just a slight increase towards the upper parts of the sequence, due chiefly to an increase in granophyric intergrowths of quartz and alkali feldspar as pore material. A slight enrichment of Fe^{2+} occurs as fractionation proceeds, mainly by virtue of a small jump in the amount of FeO in the magnetite gabbro. This does not result in the formation of Fe-rich silicates, however, but instead the majority of the ferrous iron is bound in the magnetite.

It would seem that the parental magma of the Koillismaa complex was rather poor in chromium, the analyses of the fine-grained border facies suggesting a content of approx. 200 ppm. None of the chromium-rich layers typical of many other layered intrusions containing ultramafic cumulates are to be found here, but rather the chromium would seem to remain largely hidden in the lattices of the pyroxenes, at least in the exposed parts of the complex. Accessory amounts of chromium-bearing minerals of the spinel group, representing a wide composition range intermediate between the chromites and titanomagnetites, are nevertheless commonly encountered, among which actual chromites are to be found in greatest abundance in the olivine-rich rocks.

An attempt has been made here to determine the variations in chromium content in the whole-rock samples and the principal chromium-bearing minerals, the pyroxenes and spinellids, by statistical means, employing multi-variant regression analysis. This yields relatively simple and fairly easily interpretable equations, in spite of the fact that in by no means all cases there is a causal relationship between the dependent and independent variable in question. Given the current rapid increase in the amount of information available on the partition of chromium between the various minerals in different layered intrusions arising from the more widespread use being made of microanalysis in such research, it should be possible to perform similar statistical analyses on material from both intrusions known to contain chrome ores and intrusions where these in all probability do not occur. Comparison of the resulting equations might then yield information of a kind which would be directly applicable to the task of prospecting for chrome ores.

Table 1.
Numbering, locations and mineral paragenesis of the type samples from the Koillismaa complex.

No.	Koil	Coordinates			Sth	Ol	Opx	Cpx	Pl	Crt	Ilm	Mag	Mic	Q&g	Sul
NÄRÄNKÄVAARA															
Peridotite I															
1Nä	O401	7276.80	487.20	255	0	***	+++	++		**			++		
2Nä	W314	7284.02	484.35	270	160	***	+++			**					
3Nä	W278-1	7283.41	485.06	285	170	greatly altered				**					
4Nä	K664I	7282.47	485.89	320	180	***	***			*					
5Nä	K649	7282.77	485.70	291	180	***	***			**					
6Nä	T219	7287.29	482.82	235	181	***	+++	+++		*	+		++		+
7Nä	W320	7286.48	483.88	235	182	***	+++			*	+				
8Nä	R692	7287.13	477.56	247	183	***	***			*					
9Nä	R691	7288.08	477.59	250	184	***	***	++		*					
Bronzitite I															
10Nä	K664II	7282.47	485.89	320	185	*	***	+		*					
11Nä	R703I	7276.97	487.71	246	200		***			*					
12Nä	K652	7282.67	485.65	325	250		***	+							
13Nä	K663	7282.38	485.29	268	270		***	+							
14Nä	K654II	7282.63	485.61	350	290		***	++		*					
15Nä	K654I	7282.63	485.61	350	300		***	++	++	*					+
16Nä	K661	7282.44	485.34	290	305		***	+							
17Nä	K660	7282.46	485.38	308	310		***	++							
18Nä	K637	7284.23	483.29	241	315		***	++	+	*					+
Websterite															
19Nä	K659II	7282.49	485.41	325	320		***	***							
20Nä	T223	7281.70	486.87	300	325		***	***							+
21Nä	R697	7281.10	486.56	260	325		***	***							
22Nä	K657	7282.59	485.43	360	330		***	***							
23Nä	K658	7282.55	485.41	348	340		***	***							
24Nä	W303-2	7284.83	482.82	245	345		***	***							
25Nä	W274-1	7282.87	484.60	270	350		***	***							
Bronzitite II															
26Nä	R699-1	7280.93	487.05	260	360	**	***	++							
27Nä	O396	7284.85	480.07	240	370		***	++							
28Nä	O395	7285.28	480.48	240	380		***	++	++						+
29Nä	W284	7285.75	481.10	241	390		***	++	++						
30Nä	U507	7287.69	478.30	249	400		***						++		++
Peridotite II															
31Nä	T204	7287.54	478.68	245	420	***	***	++		**			++		+
32Nä	W317	7285.95	482.27	246	430	***	***	+++	++	*					
33Nä	R696	7285.08	483.86	250	440	***	***	++		*					
34Nä	W281	7285.57	483.80	242	460	greatly altered				**					
35Nä	W310	7285.13	484.50	240	480	***	+++	++		*					+
36Nä	W298	7284.74	483.66	262	500	***	***	++	+++	*					
Gabbronorite I															
37Nä	K629-2	7287.29	478.89	245	520		***	***	+++						++
38Nä	W292	7284.75	483.52	272	540		***	***	+++	*	+		+		
39Nä	W318	7286.07	482.10	250	560		***	***	+++						
40Nä	K634	7286.40	481.80	246	580		***	***	+++	*					
41Nä	T220I	7286.55	481.92	250	600		***	***	+++		+	+	++	+	
Olivine gabbronorite															
42Nä	T208	7287.62	479.45	250	620	***	***	***	+++	*			+		
43Nä	T213	7287.46	480.24	250	640	***	***	***	+++	*	+		++	+	+
Gabbronorite I															
44Nä	O391	7287.51	479.98	255	680		***	***	+++	*	++	+	+++	+	+
45Nä	U502	7288.00	478.49	252	700		***	***	+++	*	+		++		+
46Nä	T212	7287.62	480.20	250	720		***	***	+++	*	++		++	++	
Gabbronorite II															
47Nä	T206	7287.44	478.74	250	740		***	***	***						+
48Nä	T210	7287.83	480.00	250	780		***	***	***		+	++	++	++	
49Nä	O392	7287.56	480.00	250	810		***	***	***	*	+	+	++	++	
50Nä	O390	7287.78	479.89	257	840		***	***	***		+	++	+++	++	+
Quartz diorite & granodiorite															
51Nä	U510I	7288.23	477.92	249	880	uralitized			***		++	+	++	+++	+
52Nä	U490	7288.36	478.81	246	940	uralitized			***			++	+++	+++	+

Table 1. Continued

No. Koil Coordinates	Sth	Ol	Opx	Cpx	Pl	Crt	Ilm	Mag	Mic	Q&g	Sul
PYHITYS											
MGS/ultramafitolite											
1Py T240 7300.10 559.85 350	20	***	+++	++		**					
Lower zone a											
2Py T239 7299.90 560.12 320	40	***	+++	++	***			+	+		
Lower zone b											
3Py W168 7300.13 559.74 354	80		***	++	***	*					+
4Py W170 7300.24 559.74 380	160		***	+++	***		+				+
5Py W171A 7300.27 559.74 380	200		***	+++	***			++			+
Lower zone c											
6Py W171B2 7300.32 559.73 390	210	***	***	++	***			*			+
Upper zone											
7Py W178 7300.64 559.67 360	270		***	+++	***		*			++	
8Py W181-2 7300.80 559.82 345	290		+++	+++	***		*	**		++	
PORTTIVAARA											
MGS/contact gabbro											
1Po M278A 7298.10 544.45 295	5	completely altered									
2Po M278D 7298.20 544.45 295	35		***	++	***						++
3Po M278I 7298.15 544.43 295	50	completely altered									
MGS/ultramafitolite											
4Po K700 7299.49 550.37 370	80	***	+++	+							+
Lower zone a											
5Po K699 7299.63 550.40 358	100	***	+++	++	***		+		+		+
6Po W112-1 7299.18 548.81 310	125	***	***	++	***			+	+		+
Lower zone b											
7Po W047 7300.06 548.81 330	535	*	+++	+++	***		+	+	++		
Lower zone c											
8Po M302 7299.23 546.09 345	820	***	+++	++	***		+	+			+
9Po W351 7300.50 548.76 320	835	***	***	+++	***		+	+	+		
10Po W059 7300.56 548.49 340	850	***	***	+++	***		+	+	+		
11Po M197B 7297.15 540.33 280	860	***	***	+++	***			+	+		
Middle zone											
12Po W060 7300.64 548.52 330	900		***	+++	***	*	+				
13Po M201A 7297.38 540.31 288	920		***	***	***			+	+		
14Po M133B1 7298.89 539.62 284	1200		***	***	***			++		++	
Upper zone a											
15Po M317 7300.14 545.78 355	1300			*	***					++	
Upper zone b											
16Po M155 7299.50 539.36 274	1460			***	***			***			
17Po M327 7300.67 545.35 386	1500			***	***			***			
Upper zone c											
18Po W077 7302.12 547.31 270	1800			+	***						
SYÖTE											
MGS/contact gabbro											
1Sy Drill-hole No.10 249.55 m	30		***	++	***	greatly uralitized+					++
2Sy Drill-hole No.10 168.80 m	110		***	+++	***						++
MGS/ultramafitolite											
3Sy Drill-hole No.10 164.60 m	130	completely altered					+				++
Lower zone c											
4Sy Drill-hole No.10 107.55 m	160	***	***	+++	***		+	+	+		+
5Sy Drill-hole No.10 33.65 m	235	***	***	+++	***		+	++	+		
6Sy H006 7280.40 531.70 265	460	***	***	+++	***			+			
7Sy K061A1 7282.49 534.71 275	635	***	***	+++	***						
8Sy K061A3 7282.49 534.71 275	650	***	***	+++	***		+	++	++		
9Sy K061C 7285.20 534.58 285	675	***	***	+++	***		+				+
10Sy K062B2 7282.66 534.53 295	735	***	***	+++	***						+
11Sy K067B2 7282.90 534.73 295	780	***	+++	+++	***		+				
12Sy K063B 7282.74 534.43 295	840	***	+++	+++	***		+	+	++		+
Middle zone											
13Sy K189 7285.55 537.06 365	1335		***	***	***			+		+	
14Sy K190 7285.58 537.04 370	1355		***	***	***			+		++	
15Sy K191 7285.60 537.01 375	1375		***	***	***			+		+	+
16Sy K192 7285.60 536.96 365	1410		***	***	***		+			++	+

Table 1. Continued

No. Koil Coordinates	Sth	Ol	Opx	Cpx	Pl	Crt	Ilm	Mag	Mic	Q&g	Sul
17Sy K193 7285.74 536.91 355	1460		***	***	***			+		++	
18Sy K106 7286.06 536.78 290	1635		***	***	***			+		+	
19Sy K112 7287.02 538.17 315	1680		***	***	***			++		++	
20Sy K209 7286.82 536.76 315	1950		***	***	***		+	+		+	+
Upper zone a											
21Sy Drill-hole No. 9 114.60 m	2350			**	***					+++	
Upper zone b											
22Sy K051B 7283.47 528.89 305	2505			***	***			***			
23Sy K050A 7283.51 528.86 315	2530			***	***			***			
24Sy K044F 7283.90 528.80 315	2605			***	***			***			+
25Sy K042D 7284.03 529.20 320	2700			***	***			***			
26Sy Drill-hole No.SR2 55.0 m	2735			***	***			***			+
27Sy Drill-hole No.SR3 132.0 m	2765			***	***			***		+	+
Upper zone c											
28Sy Drill-hole No.11 39.45 m	2860			++	***			+		++	
KUUSIJÄRVI											
MGS/contact gabbro											
1Ku U031 7306.17 551.25 240	15		***	+++	***						++
MGS/ultramafitolite											
2Ku U283 7309.47 541.63 271	80	completely altered									
Lower zone b											
3Ku U164A 7305.02 557.08 243	160		***	+++	***						
4Ku U133 7305.65 553.25 237	195		***	+++	***			+			
Lower zone c											
5Ku U132 7305.68 553.36 238	215	***	+++	+++	***		+	+	+		
Middle zone											
6Ku U122 7306.10 553.07 233	440		***	+++	***			+		++	
Upper zone a											
7Ku U119II 7307.88 553.56 239	970			**	***			+		++	
Upper zone b											
8Ku U120B 7307.91 553.40 240	1000			***	***			***			
LIPEÄVAARA											
MGS/contact gabbro											
1Li Drill-hole No.14 51.45 m	40		***	+++	***					+	++
2Li Drill-hole No.14 28.70 m	60		***	+++	***	*					+++
3Li Drill-hole No.14 20.00 m	70		***	+++	***					+	++
MGS/ultramafitolite											
4Li Drill-hole No.14 18.80 m	72	***	+++	++			+				++
Lower zone b											
5Li Drill-hole No.14 16.90 m	74		***	+++	***		+				++
Lower zone c											
6Li Drill-hole No.14 6.70 m	85	***	+++	+++	***						
Middle zone											
7Li T002I 7311.48 553.44 250	100		***	***	***		+	++	+	++	
8Li T042 7311.81 551.40 270	390			***	***			+		++	+
9Li T039II 7312.03 551.39 250	450			***	***			++		++	+
10Li T040 7311.61 551.43 290	570			+++	***			+		+	
Upper zone											
11Li U098II 7309.82 551.14 249	1570			++	***			+	+		
MGS/fine-grained gabbronorite											
1Ch U144I 7305.71 552.64 235			***	***	***						+
Granophyre											
1Gr U114 7307.07 533.66 236					***			+	+++	+++	

No. =Sample numbering used in the text and tables
Koil =Serial numbers in the Koillismaa Research Project
Coordinates=x-, y-, and z-coordinates of the outcrops. Localities of the Näränkävaara area are situated in that sector whose central meridian is 30° E and the remainder in the sector whose central meridian is 27° E.
Sth =Structural height in metres
Ol =Olivine Opx =Orthopyroxene
Cpx =Clinopyroxene Pl =Plagioclase
Crt =Chromite and chromian magnetite (not composite grains)
Ilm =Discrete ferrian ilmenite
Mag =Composite ilmeno-magnetite-ferrian ilmenite
Mic =Tri-octahedral mica
Q&g =Quartz and granophyric intergrowths
Sul =Sulphides
*** (cumulus mineral) +++ (intercumulus mineral) main rock component
** (cumulus mineral) ++ (intercumulus mineral) minor amounts
* (cumulus mineral) + (intercumulus mineral) accessory amounts

Table 2.
U-Pb analytical data for zircons from the Koillismaa complex.
(For sample numbering, see Fig. 2.)

Sample No.	Zircon fraction ($g.cm^{-3}$/size, µm)	^{238}U ppm	Radiogenic ^{206}Pb, ppm	$\frac{^{206}Pb}{^{204}Pb}$ (measured)	Isotopic abundance relative to ^{206}Pb (=100)			Radiometric ages, Ma		
					204	207	208	$\frac{^{206}Pb}{^{238}U}$	$\frac{^{207}Pb}{^{235}U}$	$\frac{^{207}Pb}{^{206}Pb}$
A564A	3.8 < d < 4.2	1853	588.5	4676	0.019989	15.790	26.735	2014 ± 12	2210 ± 7	2307 ± 3
A610A	d > 4.2 130 < m < 160	316.9	137.4	2708	0.034487	13.823	19.166	2618 ± 17	2653 ± 7	2680 ± 2
A610B	d > 4.2/m > 160	295.0	128.7	2483	0.037254	18.876	19.399	2632 ± 17	2660 ± 7	2682 ± 3
A610C	d > 4.2 70 < m < 130	309.3	132.9	2714	0.034034	13.721	19.494	2599 ± 17	2640 ± 8	2672 ± 3
A610D	d > 4.2/m < 70	286.3	121.9	3093	0.029326	18.577	20.145	2580 ± 17	2627 ± 7	2664 ± 3
A610F	d > 4.6	172.2	73.4	6990	0.010414	18.220	21.085	2582 ± 32	2622 ± 15	2653 ± 3
A610G	d > 4.2/magnetic	320.9	135.8	4094	0.019926	18.598	18.989	2567 ± 17	2628 ± 7	2676 ± 3
A698A	d > 4.2/m > 160	554.9	211.2	3859	0.024084	16.118	30.155	2350 ± 12	2391 ± 5	2427 ± 3
A698B	4.0 < d < 4.2 m > 160	920.3	344.7	4687	0.019842	16.040	33.732	2318 ± 11	2375 ± 5	2424 ± 2
A698C	3.8 < d < 4.0	1209	439.4	3610	0.025635	16.044	34.558	2261 ± 12	2343 ± 5	2416 ± 2
A700A	d > 4.2/m > 160	314.7	115.6	1368	0.070347	16.671	26.021	2231 ± 12	2356 ± 6	2422 ± 4
A700B	d > 4.2 70 < m < 130	280.5	103.3	1743	0.054420	16.521	25.879	2286 ± 11	2362 ± 6	2428 ± 4
A700C	d > 4.2/magnetic	313.5	112.9	1301	0.074095	16.712	25.267	2243 ± 11	2337 ± 6	2421 ± 5
A709A	d > 4.2/m > 160	483.0	180.5	5149	0.017678	16.124	23.131	2313 ± 11	2379 ± 5	2436 ± 3
A709B	4.0 < d < 4.2 m > 160	639.3	220.7	4618	0.019938	16.015	21.815	2164 ± 11	2299 ± 6	2421 ± 2
A709C	d > 4.2/130 < m < 160	442.3	165.1	6596	0.013325	16.060	22.541	2312 ± 11	2378 ± 5	2435 ± 2
A713A	d > 4.2	622.8	238.0	5190	0.010962	16.002	41.831	2358 ± 12	2398 ± 6	2432 ± 4
A713B	3.8 < d < 4.2	1231	461.3	8649	0.010255	15.880	38.679	2319 ± 12	2373 ± 5	2420 ± 2
A919A	4.2 < d < 4.6	486.9	167.8	1702	0.048026	16.380	33.212	2161 ± 11	2298 ± 7	2421 ± 5
A919B	4.0 < d < 4.2	872.7	328.3	1894	0.050733	16.479	42.395	2327 ± 12	2381 ± 6	2428 ± 4
A919C	3.8 < d < 4.0 m > 160	1212	429.6	3026	0.031070	16.115	37.638	2212 ± 12	2320 ± 6	2416 ± 3
A919D	3.8 < d < 4.0/m < 160	1310	438.7	2488	0.038236	16.206	40.571	2109 ± 11	2269 ± 6	2416 ± 3
A919E	3.6 < d < 3.8/m > 70	1466	450.8	1620	0.059063	16.272	38.492	1959 ± 11	2179 ± 6	2394 ± 3

Table 3.

Microprobe analyses of olivines from the Koillismaa complex. (For sample numbering, see Table 1.)

	1Nä	2Nä	4Nä	5Nä	6Nä	7Nä	8Nä	9Nä	10Nä	26Nä	31Nä	32Nä	33Nä	35Nä	36Nä	42Nä	43Nä	2Py	6Py	4Po
SiO2	42.0	38.2	43.6	38.7	39.8	40.0	40.4	38.9	43.1	37.3	41.8	41.1	40.1	39.2	39.6	37.7	38.5	37.8	38.2	38.0
TiO2	<.05	<.05	<.05	<.05	<.05	<.05	<.05	<.05	<.05	<.05	<.05	<.05	<.05	<.05	<.05	.08	<.05	<.05	.05	<.05
Al2O3	<.05	<.05	.05	<.05	<.05	.05	.07	<.05	<.05	<.05	<.05	<.05	.98	<.05	.25	.07	.08	.06	<.05	.06
FeO	11.6	12.8	12.7	12.4	13.9	14.5	13.4	15.0	12.6	27.3	14.3	16.4	11.6	16.8	14.9	18.7	20.9	24.2	26.7	22.1
MnO	.15	.18	.16	.06	.19	.20	.17	.07	.17	.48	.13	.21	.25	.26	.27	.27	.13	.38	<.05	.34
MgO	45.7	46.3	46.7	49.3	48.2	45.8	45.1	45.4	47.2	36.8	42.6	42.3	48.9	43.5	45.7	42.9	42.5	36.5	37.5	38.8
CaO	.07	.58	.07	<.05	.07	.08	.07	.05	.05	<.05	.06	.05	<.05	.06	.06	.05	<.05	.09	.13	.08
NiO	.37	.24	.25	.20	.24	.24	.31	.19	.32	.10	.23	.20	.24	.26	.23	.17	.33	.20	.25	.26
Total	99.9	98.3	103.5	100.7	102.4	100.9	99.5	99.6	103.4	102.0	99.1	100.3	102.1	100.1	101.0	99.9	102.4	99.2	102.8	99.6
Number of ions on the basis of 4 oxygen atoms																				
Si	1.035	.972	1.039	.959	.974	.994	1.011	.983	1.029	.977	1.049	1.032	.973	.994	.986	.969	.973	1.002	.985	.993
Al	-	-	.001	-	-	.001	.002	-	-	-	-	-	.028	-	.007	.002	.002	.002	-	.002
Ti	-	-	-	-	-	-	-	-	-	-	-	-	-	-	-	.002	-	-	.001	-
Fe2+	.239	.272	.253	.257	.284	.301	.280	.317	.252	.598	.300	.344	.235	.356	.310	.402	.442	.536	.576	.483
Mn	.003	.004	.003	.001	.004	.004	.004	.001	.003	.011	.003	.004	.005	.006	.006	.006	.003	.009	-	.008
Mg	1.679	1.756	1.658	1.820	1.758	1.697	1.682	1.710	1.680	1.436	1.593	1.583	1.768	1.644	1.696	1.643	1.600	1.442	1.441	1.512
Ca	.002	.016	.002	-	.002	.002	.002	.001	.001	-	.002	.001	-	.002	.002	.001	-	.003	.004	.002
Ni	.007	.005	.005	.004	.005	.005	.006	.004	.006	.002	.005	.004	.005	.005	.005	.004	.007	.004	.005	.005
Atomic ratios																				
Mg	87.5	86.6	86.8	87.6	86.1	84.9	85.7	84.4	87.0	70.6	84.2	82.1	88.3	82.2	84.5	80.3	78.4	72.9	71.5	75.8
Fe2+	12.5	13.4	13.2	12.4	13.9	15.1	14.3	15.6	13.0	29.4	15.8	17.9	11.7	17.8	15.5	19.7	21.6	27.1	28.5	24.2

Table 3. Microprobe analyses of olivines - continued.

	5Po	6Po	7Po	8Po	9Po	10Po	11Po	4Sy	5Sy	6Sy	7Sy	9Sy	10Sy	12Sy	5Ku
SiO2	38.7	39.7	38.5	37.7	37.8	39.0	38.6	37.6	37.2	38.0	37.3	37.5	38.6	37.7	38.7
TiO2	<.05	.01	<.05	.04	.02	.04	.02	<.05	<.05	<.05	<.05	<.05	<.05	.05	<.05
Al2O3	<.05	.14	.05	.07	.11	.06	.04	<.05	<.05	<.05	<.05	<.05	<.05	.06	<.05
FeO	21.6	23.5	26.8	25.8	27.0	27.9	28.0	27.0	29.0	26.5	24.6	27.0	26.7	25.6	24.7
MnO	.30	.27	.28	.27	.38	.29	.36	.34	.21	.39	.27	.32	.17	.30	.39
MgO	40.2	39.5	37.2	36.9	37.5	35.1	34.1	35.5	34.8	35.0	37.3	37.2	37.9	37.2	37.9
CaO	.07	.10	.05	.13	.09	.14	.09	.11	.09	.10	.10	.09	.09	.05	.07
NiO	.30	.27	.26	.22	.22	.24	.24	.31	.30	.21	.10	<.05	.26	<.05	.24
Total	101.2	103.5	103.1	101.1	103.1	102.8	101.4	100.9	101.6	100.2	99.7	102.1	103.7	101.0	102.0
Number of ions on the basis of 4 oxygen atoms															
Si	.993	1.000	.991	.988	.976	1.010	1.015	.994	.985	1.007	.987	.978	.987	.987	.998
Al	-	.004	.002	.002	.003	.002	.001	-	-	-	-	-	-	.002	-
Ti	-	-	-	.001	-	.001	-	-	-	-	-	-	-	.001	-
Fe2+	.463	.495	.577	.565	.583	.604	.616	.597	.642	.587	.544	.589	.571	.561	.533
Mn	.007	.006	.006	.006	.008	.006	.008	.008	.005	.009	.006	.007	.004	.007	.009
Mg	1.537	1.484	1.427	1.441	1.443	1.355	1.336	1.398	1.374	1.383	1.471	1.446	1.444	1.452	1.456
Ca	.002	.003	.001	.004	.002	.004	.003	.003	.003	.003	.003	.003	.002	.001	.002
Ni	.006	.005	.005	.005	.005	.005	.005	.007	.006	.004	.002	-	.005	-	.005
Atomic ratios															
Mg	76.8	75.0	71.2	71.8	71.2	69.2	68.5	70.1	68.1	70.2	73.0	71.1	71.7	72.1	73.2
Fe2+	23.2	25.0	28.8	28.2	28.8	30.8	31.5	29.9	31.9	29.8	27.0	28.9	28.3	27.9	26.8

Total Fe as FeO

Table 4.

Microprobe analyses of Ca-poor pyroxenes from the Koillismaa complex. (For sample numbering, see Table 1.)

	1Nä	4Nä	5Nä	6Nä	7Nä	8Nä	9Nä	10Nä	11Nä	12Nä	13Nä	14Nä	15Nä	16Nä	17Nä	18Nä	19Nä	20Nä	21Nä	22Nä
SiO2	53.8	58.9	56.4	55.8	56.8	56.8	54.8	59.7	55.4	60.0	56.6	57.5	58.8	58.0	57.7	57.2	56.2	59.2	58.8	55.0
TiO2	.37	.19	.05	.13	.08	.05	.09	.15	<.05	.12	.10	.11	.10	.09	.08	.10	.05	.08	.07	.06
Al2O3	1.60	1.70	1.40	1.40	1.32	1.60	1.80	1.70	.94	1.70	1.40	1.30	1.30	1.50	1.00	.70	1.30	1.00	1.20	.90
Cr2O3	.38	.49	.45	.50	.29	.51	.45	.48	.60	.52	.45	.48	.52	.47	.46	.44	.39	.25	.35	.24
FeO	7.60	7.90	7.60	9.00	8.57	8.70	8.90	8.10	7.00	8.10	7.70	7.90	8.70	8.60	8.50	10.0	10.5	9.90	10.4	9.50
MnO	.14	.19	.19	.18	.12	.18	.19	.16	.16	.17	.16	.19	.19	.17	.21	.18	.22	.19	.24	.22
MgO	31.8	30.3	33.1	31.6	32.9	30.8	29.9	31.9	31.0	31.1	33.0	30.8	32.2	30.8	31.5	31.9	31.6	31.2	30.3	30.2
CaO	1.70	2.50	1.80	2.20	1.68	1.80	2.40	1.70	1.19	1.30	2.00	2.10	1.90	2.30	2.20	1.40	.70	1.60	1.50	1.80
Na2O	<.05	.10	.14	.10	.09	.30	.11	<.05	<.05	.16	.05	<.05	<.05	.07	n.d.	<.05	n.d.	<.05	<.05	.06
NiO	.08	.06	.05	.07	.06	.05	<.05	.08	.07	.06	.07	.08	.06	.08	.06	.06	.07	.05	.05	.03
Total	97.5	102.3	101.2	101.0	101.9	100.8	98.6	104.0	96.4	103.2	101.5	100.5	103.8	102.1	101.7	102.0	101.0	103.5	102.9	98.0
Number of ions on the basis of 6 oxygen atoms																				
Si	1.931	2.003	1.947	1.945	1.951	1.973	1.954	1.995	1.994	2.015	1.948	1.994	1.980	1.986	1.984	1.973	1.959	2.004	2.005	1.975
AlIV	.069	-	.053	.055	.049	.027	.046	.005	.006	-	.052	.006	.020	.014	.016	.027	.041	-	-	.025
AlVI	-	.068	.004	.002	.005	.039	.029	.062	.034	.067	.004	.047	.032	.047	.025	.002	.013	.040	.048	.013
Ti	.010	.005	.001	.003	.002	.001	.002	.004	-	.003	.003	.003	.003	.002	.002	.003	.001	.002	.002	.002
Cr	.011	.013	.012	.014	.008	.014	.013	.013	.017	.014	.012	.013	.014	.013	.013	.012	.011	.007	.009	.007
Fe2+	.228	.225	.219	.262	.246	.253	.265	.226	.211	.227	.222	.229	.245	.246	.244	.289	.306	.280	.297	.285
Mn	.004	.005	.006	.005	.003	.005	.006	.005	.005	.005	.005	.006	.005	.005	.006	.005	.006	.005	.007	.007
Mg	1.701	1.536	1.703	1.642	1.685	1.595	1.589	1.589	1.663	1.557	1.693	1.592	1.616	1.572	1.615	1.640	1.642	1.574	1.540	1.616
Ca	.065	.091	.067	.082	.062	.067	.092	.061	.046	.047	.074	.078	.069	.084	.081	.052	.026	.058	.055	.069
Na	-	.007	.009	.007	.006	.020	.008	-	-	.010	.003	-	-	.005	-	-	-	-	-	.004
Ni	.002	.002	.001	.002	.002	.001	-	.002	.002	.002	.002	.002	.002	.002	.002	.002	.002	.001	.001	.001
Atomic percent																				
Mg	85.1	82.7	85.4	82.4	84.4	83.1	81.4	84.5	86.4	84.8	84.9	83.6	83.5	82.4	83.0	82.6	82.9	82.1	81.1	81.7
Fe	11.6	12.4	11.3	13.4	12.5	13.4	13.9	12.3	11.2	12.7	11.4	12.3	12.9	13.2	12.9	14.8	15.8	14.9	16.0	14.8
Ca	3.3	4.9	3.3	4.1	3.1	3.5	4.7	3.2	2.4	2.5	3.7	4.1	3.5	4.4	4.2	2.6	1.3	3.0	2.9	3.5
mg	88.0	87.0	38.3	86.0	87.1	86.1	85.4	87.3	88.5	87.0	88.2	87.2	86.6	86.2	86.6	84.8	84.0	84.6	83.5	84.7
Z	2.00	2.00	2.00	2.00	2.00	2.00	2.00	2.00	2.00	2.01	2.00	2.00	2.00	2.00	2.00	2.00	2.00	2.00	2.01	2.00
WXY	2.02	1.95	2.02	2.02	2.02	2.00	2.00	1.96	1.98	1.93	2.02	1.97	1.98	1.98	1.99	2.00	2.01	1.97	1.96	2.00

Table 4. Microprobe analyses of Ca-poor pyroxenes - continued.

	23Nä	24Nä	25Nä	27Nä	28Nä	29Nä	30Nä	31Nä	32Nä	33Nä	36Nä	37Nä	38Nä	39Nä	40Nä	41Nä	42Nä	43Nä	44Nä	45Nä
SiO2	55.7	51.2	55.2	55.3	56.7	56.3	56.1	58.1	56.3	55.2	54.6	55.1	54.1	57.1	53.8	56.6	54.3	55.7	55.7	54.3
TiO2	.07	.07	.05	.09	.15	.17	.07	.12	.20	.09	.07	.18	.12	.12	.13	.08	.23	.14	.14	.42
Al2O3	1.20	.98	.75	1.60	1.60	1.60	1.88	2.20	1.40	1.32	2.07	1.31	1.62	1.80	1.70	1.50	1.76	2.20	1.90	1.32
Cr2O3	.29	.19	.20	.48	.42	.35	.34	.49	.34	.28	.48	.20	.45	.14	.23	.13	.37	.42	.21	.26
FeO	10.4	10.5	9.58	10.7	10.3	10.5	10.0	8.20	10.3	7.65	9.16	12.6	11.1	12.2	15.8	16.2	11.7	14.9	14.1	14.7
MnO	.20	.28	.19	.19	.19	.25	.23	.21	.23	.20	.23	.25	.23	.25	.26	.26	.23	.24	.25	.29
MgO	30.7	29.3	32.4	30.0	28.7	29.3	32.7	28.8	28.7	34.5	29.1	27.4	29.2	29.8	25.4	26.1	30.6	27.1	27.0	25.0
CaO	1.50	1.56	1.83	1.20	1.00	1.50	1.00	1.30	1.30	1.68	2.10	1.83	2.18	1.80	2.00	1.70	1.81	1.50	.90	.76
Na2O	<.05	<.05	<.05	<.05	<.05	n.d.	.13	.10	.10	<.05	<.05	.19	.05	<.05	<.05	<.05	.09	<.05	<.05	<.05
NiO	.06	.07	.05	.07	.07	.05	<.05	.05	.07	.07	<.05	.12	<.05	.07	.06	.04	.05	.06	.09	<.05
Total	100.1	94.1	100.2	99.6	99.1	100.0	102.4	99.6	98.9	101.0	97.8	99.2	99.0	103.3	99.4	102.6	101.1	102.3	100.3	97.0
Number of ions on the basis of 6 oxygen atoms																				
Si	1.963	1.934	1.942	1.960	2.006	1.982	1.929	2.023	2.000	1.914	1.962	1.981	1.942	1.963	1.962	1.990	1.915	1.958	1.983	2.005
AlIV	.037	.044	.031	.040	-	.018	.071	-	-	.054	.038	.019	.058	.037	.038	.010	.073	.042	.017	-
AlVI	.013	-	-	.027	.067	.049	.005	.090	.058	-	.049	.037	.010	.036	.035	.052	-	.049	.063	.057
Ti	.002	.002	.001	.002	.004	.005	.002	.003	.005	.002	.002	.005	.003	.003	.004	.002	.006	.004	.004	.012
Cr	.008	.006	.006	.013	.012	.010	.009	.013	.010	.008	.014	.006	.013	.004	.007	.004	.010	.012	.006	.008
Fe2+	.307	.332	.282	.317	.305	.309	.288	.239	.306	.222	.275	.379	.333	.351	.482	.476	.345	.438	.420	.454
Mn	.006	.009	.006	.006	.006	.007	.007	.006	.007	.006	.007	.008	.007	.007	.008	.008	.007	.007	.008	.009
Mg	1.613	1.649	1.699	1.585	1.513	1.538	1.676	1.494	1.520	1.783	1.558	1.469	1.562	1.527	1.380	1.368	1.608	1.420	1.433	1.376
Ca	.057	.063	.069	.046	.038	.057	.037	.048	.049	.062	.081	.071	.084	.066	.078	.064	.068	.056	.034	.030
Na	-	-	-	-	-	-	.009	.007	.007	-	-	.013	.003	-	-	-	.006	-	-	-
Ni	.002	.002	.001	.002	.002	.001	-	.001	.002	.002	-	.003	-	.002	.002	.001	.001	.002	.003	-
Atomic percent																				
Mg	81.4	80.3	82.7	81.1	81.3	80.5	83.5	83.6	80.7	86.0	81.1	76.3	78.7	78.3	70.8	71.4	79.3	73.9	75.6	73.6
Fe	15.8	16.6	14.0	16.5	16.7	16.6	14.7	13.7	16.6	11.0	14.7	20.1	17.1	18.3	25.1	25.3	17.3	23.2	22.6	24.8
Ca	2.9	3.1	3.4	2.3	2.0	3.0	1.8	2.7	2.6	3.0	4.2	3.7	4.2	3.4	4.0	3.3	3.4	2.9	1.8	1.6
mg	83.8	82.9	85.5	83.1	83.0	82.9	85.1	85.9	82.9	88.7	84.7	79.2	82.1	81.0	73.8	73.9	82.0	76.1	77.0	74.8
Z	2.00	1.98	1.97	2.00	2.01	2.00	2.00	2.02	2.00	1.97	2.00	2.00	2.00	2.00	2.00	2.00	1.99	2.00	2.00	2.01
WXY	2.01	2.06	2.06	2.00	1.95	1.98	2.03	1.90	1.96	2.09	1.99	1.99	2.02	2.00	1.99	1.97	2.05	1.99	1.97	1.95

Table 4. Microprobe analyses of Ca-poor pyroxenes - continued.

	46Nä	47Nä	48Nä	49Nä	50Nä	1Py	2Py	3Py	4Py	5Py	6Py	7Py	8Py	5Po	6Po	7Po	8Po	9Po	10Po	11Po
SiO2	57.7	55.7	56.0	56.8	53.8	53.0	53.4	55.0	53.9	52.0	54.4	53.4	53.7	55.5	55.3	53.9	54.0	53.6	53.9	55.2
TiO2	.21	.24	.13	.21	.16	.15	.15	.19	.29	.23	.13	.20	.35	.18	.18	.23	.41	.14	.29	.42
Al2O3	1.40	1.00	1.10	1.40	1.10	1.73	1.49	1.59	1.06	1.04	1.19	1.00	1.03	1.75	1.32	1.40	.98	1.11	1.15	1.13
Cr2O3	.10	.05	<.05	.05	<.05	.29	.20	.34	.05	<.05	.41	.17	<.05	.35	<.05	.21	<.05	.06	.05	<.05
FeO	17.5	13.9	23.2	20.7	23.9	12.5	12.5	12.7	14.9	18.7	15.8	16.6	20.0	12.5	14.5	14.4	15.8	15.8	16.2	16.8
MnO	.32	.25	.39	.37	.41	.17	.24	.25	.25	.34	.22	.24	.35	.19	.21	.31	.26	.35	.31	.43
MgO	25.2	28.5	21.3	24.0	20.7	27.7	27.4	28.6	26.9	24.0	27.4	25.8	22.7	28.4	25.0	26.8	26.9	26.2	26.2	24.5
CaO	1.10	2.02	1.10	1.00	2.10	2.38	2.43	1.59	2.25	1.84	2.06	1.88	1.86	2.27	1.62	2.13	2.10	2.08	2.22	1.94
Na2O	.05	<.05	<.05	<.05	.06	<.05	<.05	n.d.	n.d.	n.d.	n.d.	n.d.	n.d.	.06	<.05	n.d.	n.d.	n.d.	n.d.	<.05
NiO	.06	.07	.02	.04	.02	.09	.07	.07	.07	.06	.08	.06	.05	.28	.07	.06	n.d.	.06	.08	.06
Total	103.6	101.7	103.2	104.6	102.2	98.0	97.9	100.3	99.7	98.2	101.7	99.3	100.0	101.5	98.2	99.4	100.4	99.4	100.4	100.5
Number of ions on the basis of 6 oxygen atoms																				
Si	2.012	1.964	2.014	1.994	1.977	1.937	1.953	1.956	1.955	1.951	1.942	1.958	1.981	1.954	2.016	1.955	1.950	1.958	1.953	1.994
AlIV	-	.036	-	.006	.023	.063	.047	.044	.045	.046	.050	.042	.019	.046	-	.045	.042	.042	.047	.006
AlVI	.058	.006	.047	.051	.024	.012	.017	.023	.001	-	-	.001	.026	.026	.057	.014	-	.005	.002	.042
Ti	.006	.006	.004	.006	.004	.004	.004	.005	.008	.006	.003	.006	.010	.005	.005	.006	.011	.004	.008	.011
Cr	.003	.001	-	.001	-	.008	.006	.010	.001	-	.012	.005	-	.010	-	.006	-	.002	.001	-
Fe2+	.510	.410	.698	.608	.734	.382	.382	.378	.452	.587	.472	.509	.617	.368	.442	.437	.477	.483	.491	.508
Mn	.009	.007	.012	.011	.013	.005	.007	.008	.008	.011	.007	.007	.011	.006	.006	.010	.008	.011	.010	.013
Mg	1.310	1.498	1.142	1.256	1.134	1.509	1.494	1.516	1.454	1.342	1.458	1.410	1.248	1.490	1.359	1.449	1.448	1.426	1.415	1.319
Ca	.041	.076	.042	.038	.083	.093	.095	.061	.087	.074	.079	.074	.074	.086	.063	.083	.081	.081	.086	.075
Na	.003	-	-	-	.004	-	-	-	-	-	-	-	-	.004	-	-	-	-	-	-
Ni	.002	.002	.001	.001	.001	.003	.002	.002	.002	.002	.002	.002	.001	.008	.002	.002	-	.002	.002	.002
Atomic percent																				
Mg	70.0	75.2	60.3	65.7	57.7	75.8	75.5	77.3	72.7	66.7	72.4	70.5	64.0	76.4	72.6	73.3	71.9	71.3	70.7	68.9
Fe	27.8	21.0	37.5	32.4	38.1	19.5	19.7	19.6	23.0	29.7	23.7	25.8	32.2	19.2	24.0	22.6	24.1	24.7	25.0	27.2
Ca	2.2	3.8	2.2	2.0	4.2	4.7	4.8	3.1	4.4	3.7	3.9	3.7	3.8	4.4	3.4	4.2	4.0	4.1	4.3	3.9
mg	71.6	78.2	61.7	67.0	60.3	79.6	79.3	79.7	76.0	69.2	75.3	73.2	66.5	80.0	75.2	76.4	74.9	74.3	73.9	71.7
Z	2.01	2.00	2.01	2.00	2.00	2.00	2.00	2.00	2.00	2.00	1.99	2.00	2.00	2.00	2.02	2.00	1.99	2.00	2.00	2.00
WXY	1.94	2.01	1.94	1.97	2.00	2.02	2.01	2.00	2.01	2.02	2.03	2.01	1.99	2.00	1.93	2.01	2.03	2.01	2.01	1.97

Table 4. Microprobe analyses of Ca-poor pyroxenes - continued.

	12Po	13Po	14Po	4Sy	5Sy	6Sy	7Sy	8Sy	9Sy	10Sy	11Sy	12Sy	13Sy	15Sy	16Sy	17Sy	19Sy	20Sy	3Ku	5Ku
SiO2	53.5	52.9	55.0	54.2	53.8	54.9	54.2	53.7	55.1	53.7	53.0	54.1	52.9	50.2	50.2	52.3	53.0	50.5	56.4	56.0
TiO2	.17	.17	.28	.36	.52	.17	.16	.25	.19	.16	.10	.17	.23	.36	.31	.51	.16	.25	.20	.22
Al2O3	1.15	1.27	.68	1.26	1.50	1.18	1.50	1.20	1.40	1.40	1.40	1.20	.87	1.00	.78	.92	1.10	.75	1.84	1.23
Cr2O3	.19	.17	<.05	<.05	<.05	<.05	.20	<.05	.10	.10	.14	<.05	<.05	<.05	<.05	<.05	.17	<.05	.27	<.05
FeO	17.0	20.7	25.0	16.7	17.7	14.1	13.7	18.8	16.0	15.6	14.8	15.8	23.2	22.4	23.9	22.3	21.8	26.3	13.6	15.5
MnO	.32	.40	.24	.31	.34	.31	.27	.43	.28	.29	.28	.31	.49	.46	.44	.32	.41	.50	.33	.41
MgO	24.6	23.4	18.4	26.3	25.2	26.4	29.5	26.9	27.5	27.5	25.1	27.4	22.3	21.4	20.0	23.9	23.3	19.2	27.0	25.9
CaO	2.00	1.61	3.75	1.50	2.20	2.08	.84	1.70	1.60	2.80	2.20	1.50	1.80	1.70	1.80	1.80	1.70	.86	1.85	2.55
Na2O	n.d.	n.d.	<.05	<.05	<.05	n.d.	.07	.05	<.05	<.05	n.d.	<.05	<.05	<.05	<.05	.06	<.05	<.05	<.05	<.05
NiO	.06	.05	<.05	.09	.08	.07	<.05	.06	.07	.07	<.05	<.05	<.05	<.05	<.05	<.05	<.05	<.05	.07	.07
Total	99.0	100.7	103.3	100.7	101.3	99.2	100.4	103.1	102.2	101.6	97.0	100.5	101.8	97.5	97.4	102.1	101.6	98.4	101.6	101.9
Number of ions on the basis of 6 oxygen atoms																				
Si	1.971	1.950	2.010	1.956	1.943	1.986	1.934	1.918	1.951	1.923	1.973	1.950	1.951	1.936	1.951	1.919	1.945	1.959	1.983	1.986
AlIV	.029	.050	-	.044	.057	.014	.063	.051	.049	.059	.027	.050	.038	.045	.036	.040	.048	.034	.017	.014
AlVI	.021	.005	.029	.009	.007	.037	-	-	.009	-	.034	.001	-	-	-	-	-	-	.060	.037
Ti	.005	.005	.008	.010	.014	.005	.004	.007	.005	.004	.003	.005	.006	.010	.009	.014	.004	.007	.005	.006
Cr	.006	.005	-	-	-	-	.006	-	.003	.003	.004	-	-	-	-	-	.005	-	.008	-
Fe2+	.524	.638	.764	.504	.535	.427	.409	.562	.474	.467	.461	.476	.716	.723	.777	.684	.669	.853	.400	.460
Mn	.010	.012	.007	.009	.010	.010	.008	.013	.008	.009	.009	.009	.015	.015	.014	.010	.013	.016	.010	.012
Mg	1.351	1.285	1.002	1.415	1.357	1.424	1.569	1.432	1.451	1.468	1.393	1.472	1.226	1.230	1.159	1.307	1.274	1.110	1.415	1.369
Ca	.079	.064	.147	.058	.085	.081	.032	.065	.061	.107	.088	.058	.071	.070	.075	.071	.067	.036	.070	.097
Na	-	-	-	-	-	-	.005	.003	-	-	-	-	-	-	-	.004	-	-	-	-
Ni	.002	.001	-	.003	.002	.002	-	.002	.002	.002	-	-	-	-	-	-	-	-	.002	.002
Atomic percent																				
Mg	68.8	64.3	52.2	71.2	68.3	73.4	77.7	69.1	72.8	71.6	71.4	73.0	60.5	60.4	57.2	63.1	63.0	55.1	74.7	70.6
Fe	27.2	32.5	40.2	25.9	27.4	22.5	20.7	27.7	24.2	23.2	24.1	24.1	36.0	36.2	39.1	33.5	33.7	43.1	21.6	24.4
Ca	4.0	3.2	7.6	2.9	4.3	4.2	1.6	3.1	3.0	5.2	4.5	2.9	3.5	3.4	3.7	3.4	3.3	1.8	3.7	5.0
mg	71.7	66.4	56.5	73.4	71.3	76.5	79.0	71.4	75.1	75.5	74.8	75.2	62.6	62.5	59.4	65.3	65.1	56.1	77.5	74.4
Z	2.00	2.00	2.01	2.00	2.00	2.00	2.00	1.97	2.00	1.98	2.00	2.00	1.99	1.98	1.99	1.96	1.99	1.99	2.00	2.00
WXY	2.00	2.02	1.96	2.01	2.01	1.98	2.03	2.08	2.01	2.06	1.99	2.02	2.03	2.05	2.03	2.09	2.03	2.02	1.97	1.98

Table 4. Microprobe analyses of Ca-poor pyroxenes - continued.

	2Li	3Li	4Li	5Li	6Li	7Li
SiO2	54.2	55.4	57.0	56.4	53.7	55.5
TiO2	.27	.11	.13	.17	.15	.22
Al2O3	1.38	1.91	1.46	1.17	1.34	1.13
Cr2O3	.05	.18	.14	.14	<.05	<.05
FeO	19.1	16.1	11.4	16.1	14.7	20.6
MnO	.28	.28	.15	.34	.31	.40
MgO	24.3	26.2	27.1	25.4	26.2	22.3
CaO	2.17	2.30	2.34	2.86	3.37	2.19
Na2O	<.05	<.05	<.05	<.05	<.05	<.05
NiO	.11	.08	.07	.07	.09	<.05
Total	101.9	102.6	99.8	102.6	99.9	102.3
Number of ions on the basis of 6 oxygen atoms						
Si	1.957	1.957	2.017	1.990	1.949	2.000
AlIV	.043	.043	-	.010	.051	-
AlVI	.016	.037	.061	.039	.007	.048
Ti	.007	.003	.003	.005	.004	.006
Cr	.001	.005	.004	.004	-	-
Fe2+	.577	.476	.337	.475	.446	.621
Mn	.009	.008	.004	.010	.010	.012
Mg	1.308	1.380	1.429	1.336	1.418	1.198
Ca	.084	.087	.089	.108	.131	.085
Na	-	-	-	-	-	-
Ni	.003	.002	.002	.002	.003	-
Atomic percent						
Mg	66.1	70.7	76.8	69.2	70.7	62.5
Fe	29.6	24.8	18.4	25.2	22.7	33.0
Ca	4.2	4.5	4.8	5.6	6.5	4.4
mg	69.1	74.0	80.7	73.4	75.7	65.4
Z	2.00	2.00	2.02	2.00	2.00	2.00
WXY	2.01	2.00	1.93	1.98	2.02	1.97

AlIV = Al in tetrahedral site
AlVI = Al in octahedral site
mg = 100*Mg/(Mg+Fe+Mn)
n.d. = not determined
Total Fe as FeO

Table 5.

Microprobe analyses of Ca-rich pyroxenes from the Koillismaa complex. (For sample numbering, see Table 1.)

	1Nä	6Nä	9Nä	10Nä	13Nä	14Nä	15Nä	16Nä	17Nä	18Nä	19Nä	20Nä	21Nä	22Nä	23Nä	24Nä	25Nä	28Nä	29Nä	31Nä
SiO2	50.9	52.3	49.2	49.8	54.7	55.3	54.9	53.9	54.5	54.4	55.0	56.3	57.0	54.0	53.2	49.9	52.5	52.9	51.9	52.8
TiO2	1.10	.14	.20	.27	.11	.17	.14	.20	.16	.22	.13	.10	.11	.13	.14	.20	.08	.36	.16	.54
Al2O3	2.60	2.00	3.20	2.89	2.30	2.20	2.40	2.40	1.80	2.20	1.60	1.60	1.70	1.70	1.70	1.60	1.32	2.50	3.00	3.60
Cr2O3	.87	.80	1.10	1.07	.89	1.10	.70	.82	.84	.69	.69	.41	.60	.36	.57	.25	.38	.77	1.00	.96
FeO	3.50	4.20	5.10	4.47	3.90	3.50	3.80	4.50	4.40	5.30	4.60	4.50	4.70	4.40	4.50	4.39	5.79	5.00	5.60	5.70
MnO	.10	.15	1.54	.10	.09	.12	.13	.07	.13	.11	.14	.17	.16	.11	.13	.16	.13	.11	.14	.15
MgO	16.5	17.2	17.6	17.3	17.5	17.3	16.0	18.1	18.9	18.0	18.0	18.7	17.5	18.1	18.0	16.2	18.3	15.9	16.8	16.3
CaO	21.4	19.9	19.2	22.6	22.5	21.3	21.6	21.1	19.0	23.0	21.5	22.5	20.4	22.0	23.5	20.2	20.0	21.3	20.5	23.0
Na2O	.44	.50	.50	.46	.19	.50	.40	.36	.20	.31	.01	.20	.20	.20	.13	.13	<.05	.40	.50	.50
NiO	.06	.05	.05	<.05	.04	.01	.01	.05	.06	.05	.03	.03	.05	.06	.04	.05	<.05	.03	.01	.04
Total	97.5	97.2	97.7	99.0	102.2	101.5	100.1	101.5	100.0	104.3	101.7	104.5	102.4	101.1	101.9	93.1	98.5	99.3	99.6	103.6
Number of ions on the basis of 6 oxygen atoms																				
Si	1.908	1.956	1.862	1.860	1.949	1.973	1.987	1.935	1.970	1.918	1.968	1.962	2.010	1.950	1.919	1.957	1.950	1.949	1.912	1.883
AlIV	.092	.044	.138	.127	.051	.027	.013	.065	.030	.082	.032	.038	-	.050	.072	.043	.050	.051	.088	.117
AlVI	.023	.044	.004	-	.045	.065	.090	.037	.047	.009	.035	.028	.071	.022	-	.031	.007	.057	.043	.034
Ti	.031	.004	.006	.008	.003	.005	.004	.005	.004	.006	.003	.003	.003	.004	.004	.006	.002	.010	.004	.014
Cr	.026	.024	.033	.032	.025	.031	.020	.023	.024	.019	.020	.011	.017	.010	.016	.008	.011	.022	.029	.027
Fe2+	.110	.131	.161	.140	.116	.104	.115	.135	.133	.156	.138	.131	.139	.133	.136	.144	.180	.154	.173	.170
Mn	.003	.005	.049	.003	.003	.004	.004	.002	.004	.003	.004	.005	.005	.003	.004	.005	.004	.003	.004	.005
Mg	.922	.959	.993	.963	.929	.920	.863	.969	1.018	.946	.960	.971	.920	.974	.968	.947	1.013	.873	.923	.866
Ca	.859	.797	.778	.904	.859	.814	.838	.812	.736	.869	.824	.840	.771	.851	.908	.849	.796	.841	.809	.879
Na	.032	.036	.037	.033	.013	.035	.028	.025	.014	.021	.001	.014	.014	.014	.009	.010	-	.029	.036	.035
Ni	.002	.002	.002	-	.001	-	-	.001	.002	.001	.001	.001	.001	.002	.001	.002	-	.001	-	.001
Atomic percent																				
Mg	48.7	50.7	50.1	47.9	48.7	49.9	47.4	50.5	53.8	47.9	49.8	49.9	50.2	49.7	48.0	48.7	50.8	46.7	48.3	45.1
Fe	6.0	7.2	10.6	7.1	6.2	5.9	6.5	7.2	7.2	8.1	7.4	7.0	7.8	6.9	6.9	7.7	9.2	8.4	9.3	9.1
Ca	45.4	42.1	39.3	45.0	45.0	44.2	46.0	42.3	38.9	44.0	42.8	43.1	42.0	43.4	45.1	43.6	39.9	44.9	42.4	45.8
mg	89.1	87.6	82.5	87.1	88.7	89.5	87.9	87.6	88.1	85.6	87.1	87.7	86.5	87.7	87.4	86.4	84.6	84.7	83.9	83.2
Z	2.00	2.00	2.00	1.99	2.00	2.00	2.00	2.00	2.00	2.00	2.00	2.00	2.01	2.00	1.99	2.00	2.00	2.00	2.00	2.00
WXY	2.01	2.00	2.06	2.08	1.99	1.98	1.96	2.01	1.98	2.03	1.99	2.00	1.94	2.01	2.05	2.00	2.01	1.99	2.02	2.03

Table 5. Microprobe analyses of Ca-rich pyroxenes - continued.

	32Nä	33Nä	36Nä	37Nä	38Nä	39Nä	40Nä	41Nä	42Nä	43Nä	44Nä	45Nä	46Nä	47Nä	48Nä	49Nä	50Nä	1Py	2Py	3Py
SiO2	49.7	52.7	51.1	52.7	50.4	52.0	51.1	54.3	50.2	53.9	52.9	50.8	55.2	53.4	52.8	54.2	54.8	50.0	51.7	53.3
TiO2	.24	.18	.20	.32	.20	.19	.24	.52	.12	.35	.40	1.17	.48	.46	.38	.42	.32	.36	.36	.42
Al2O3	3.50	1.67	2.96	2.44	3.06	1.80	2.80	2.90	3.10	2.50	2.80	2.56	3.10	1.94	2.10	2.10	2.20	2.81	1.91	1.88
Cr2O3	.83	1.10	1.07	.48	.94	.40	.49	.35	.55	.36	.33	.32	.31	.07	<.05	.11	<.05	.89	.09	.38
FeO	5.00	3.73	4.95	5.74	4.88	7.80	8.80	7.70	6.03	6.90	7.00	6.82	8.80	6.64	10.1	8.90	10.8	6.35	8.04	5.57
MnO	.14	.16	.19	.20	.16	.22	.17	.10	.14	.18	.20	.21	.13	.16	.24	.16	.27	.17	.21	.13
MgO	15.3	18.5	18.9	15.9	16.2	16.0	14.6	15.2	17.5	16.2	14.1	17.1	13.9	15.7	12.2	13.8	12.9	15.5	15.6	15.9
CaO	22.0	22.4	17.9	19.7	21.5	21.6	21.8	20.2	21.6	21.8	20.6	21.4	20.8	20.7	21.9	22.3	22.3	20.9	19.4	21.9
Na2O	.50	.55	.42	.51	.45	.40	.30	.40	.94	.30	.30	.40	.30	.32	.40	.30	.40	.30	.33	n.d.
NiO	.30	<.05	<.05	.06	.05	.03	n.d.	.04	<.05	.05	.06	.05	.04	.07	.03	.05	.02	.06	.05	.04
Total	97.5	101.0	97.7	98.0	97.8	100.4	100.3	101.7	100.2	102.5	98.7	100.8	103.1	99.5	100.1	102.3	104.0	97.3	97.7	99.5
Number of ions on the basis of 6 oxygen atoms																				
Si	1.883	1.913	1.904	1.963	1.896	1.925	1.904	1.961	1.859	1.937	1.969	1.870	1.974	1.970	1.973	1.968	1.972	1.900	1.954	1.962
AlIV	.117	.071	.096	.037	.104	.075	.096	.039	.135	.063	.031	.111	.026	.030	.027	.032	.028	.100	.046	.038
AlVI	.040	-	.034	.070	.032	.004	.027	.084	-	.043	.092	-	.105	.054	.065	.058	.065	.026	.039	.044
Ti	.007	.005	.006	.009	.006	.005	.007	.014	.003	.009	.011	.032	.013	.013	.011	.011	.009	.010	.010	.012
Cr	.025	.032	.032	.014	.028	.012	.014	.010	.016	.010	.010	.009	.009	.002	-	.003	-	.027	.003	.011
Fe2+	.158	.113	.154	.179	.154	.242	.274	.233	.187	.207	.218	.210	.263	.205	.316	.270	.325	.202	.254	.171
Mn	.004	.005	.006	.006	.005	.007	.005	.003	.004	.005	.006	.007	.004	.005	.008	.005	.008	.005	.007	.004
Mg	.864	1.001	1.049	.883	.908	.883	.811	.818	.966	.868	.782	.938	.741	.863	.679	.747	.692	.878	.879	.873
Ca	.893	.871	.714	.786	.867	.857	.870	.781	.857	.840	.822	.844	.797	.818	.877	.868	.860	.851	.786	.864
Na	.037	.039	.030	.037	.033	.029	.022	.028	.067	.021	.022	.029	.021	.023	.029	.021	.028	.022	.024	-
Ni	.009	-	-	.002	.002	.001	-	.001	-	.001	.002	.001	.001	.002	.001	.001	.001	.002	.002	.001
Atomic percent																				
Mg	45.0	50.3	54.5	47.6	47.0	44.4	41.4	44.6	48.0	45.2	42.8	46.9	41.0	45.6	36.2	39.5	36.7	45.3	45.6	45.6
Fe	8.5	5.9	8.3	10.0	8.2	12.5	14.3	12.8	9.5	11.1	12.3	10.8	14.8	11.1	17.2	14.6	17.7	10.7	13.5	9.2
Ca	46.5	43.8	37.1	42.4	44.8	43.1	44.4	42.6	42.6	43.7	44.9	42.2	44.2	43.3	46.7	45.9	45.6	44.0	40.8	45.2
mg	84.1	89.4	86.8	82.7	85.1	78.0	74.4	77,6	83.5	80.3	77.7	81.3	73.5	80.4	67.8	73.1	67.5	80.9	77.1	83.3
Z	2.00	1.98	2.00	2.00	2.00	2.00	2.00	2.00	1.99	2.00	2.00	1.98	2.00	2.00	2.00	2.00	2.00	2.00	2.00	2.00
WXY	2.04	2.07	2.03	1.99	2.03	2.04	2.03	1.97	2.10	2.01	1.96	2.07	1.95	1.99	1.98	1.98	1.99	2.02	2.00	1.98

Table 5. Microprobe analyses of Ca-rich pyroxenes - continued.

	4Py	5Py	6Py	7Py	8Py	5Po	6Po	7Po	8Po	9Po	10Po	11Po	12Po	13Po	14Po	16Po	17Po	4Sy	5Sy	6Sy
SiO2	53.3	50.8	53.9	52.2	50.5	52.3	51.7	51.7	50.3	49.8	51.5	51.7	50.8	51.6	52.6	52.4	50.1	52.1	52.3	51.5
TiO2	.66	.64	.77	.76	.72	.46	.49	.90	.94	.72	.72	.73	.84	.65	.54	.52	.40	.58	.88	.40
Al2O3	2.18	1.70	2.30	1.67	2.11	2.36	2.11	2.65	2.56	2.46	2.46	2.10	2.36	1.98	1.72	2.25	2.12	2.10	2.60	2.10
Cr2O3	.18	<.05	.06	.14	.02	<.05	.09	.11	<.05	.03	.13	<.05	.07	.08	<.05	<.05	<.05	.11	<.05	.10
FeO	7.46	9.18	7.50	8.52	11.9	6.57	7.37	8.08	8.34	8.78	9.13	8.53	9.80	10.2	11.2	12.3	12.6	8.00	8.40	8.40
MnO	.13	.21	.15	.17	.27	.29	.08	.15	.23	.20	.18	.18	.23	.20	.26	.21	.22	.21	.27	.21
MgO	15.9	14.1	15.9	15.2	14.1	16.2	15.6	15.0	14.3	14.6	14.6	15.1	14.2	14.3	14.4	13.6	12.6	14.7	14.3	14.5
CaO	21.9	20.5	21.3	20.9	18.6	22.8	21.3	21.0	23.3	21.3	20.5	20.6	21.1	20.7	21.0	19.8	19.9	22.3	21.6	20.6
Na2O	n.d.	n.d.	n.d.	n.d.	n.d.	.47	n.d.	n.d.	.19	n.d.	n.d.	n.d.	n.d.	n.d.	n.d.	n.d.	n.d.	.18	.21	.18
NiO	.04	.03	n.d.	n.d.	.04	.10	.04	.03	<.05	.05	.02	.03	.03	.10	n.d.	n.d.	n.d.	.07	.05	<.05
Total	101.7	97.2	101.9	99.6	98.3	101.5	98.8	99.6	100.2	97.9	99.2	99.0	99.4	99.8	101.7	101.1	97.9	100.3	100.6	98.0
Number of ions on the basis of 6 oxygen atoms																				
Si	1.936	1.949	1.948	1.946	1.930	1.910	1.935	1.923	1.884	1.901	1.930	1.938	1.913	1.934	1.941	1.947	1.935	1.932	1.931	1.950
AlIV	.064	.051	.052	.054	.070	.090	.065	.077	.113	.099	.070	.062	.087	.066	.059	.053	.065	.068	.069	.050
AlVI	.029	.025	.046	.019	.025	.011	.028	.039	-	.011	.039	.030	.018	.022	.016	.045	.031	.024	.045	.043
Ti	.018	.018	.021	.021	.021	.013	.014	.025	.026	.021	.020	.021	.024	.018	.015	.015	.012	.016	.024	.011
Cr	.005	-	.002	.004	.001	-	.003	.003	-	.001	.004	-	.002	.002	-	-	-	.003	-	.003
Fe2+	.227	.294	.227	.266	.380	.201	.231	.251	.261	.280	.286	.267	.309	.320	.346	.382	.407	.248	.259	.266
Mn	.004	.007	.005	.005	.009	.009	.003	.005	.007	.006	.006	.006	.007	.006	.008	.007	.007	.007	.008	.007
Mg	.861	.806	.857	.844	.803	.882	.870	.831	.798	.831	.815	.843	.797	.799	.792	.753	.725	.812	.787	.818
Ca	.852	.842	.825	.835	.762	.892	.854	.837	.935	.871	.823	.827	.851	.831	.830	.788	.823	.886	.855	.836
Na	-	-	-	-	-	.033	-	-	.014	-	-	-	-	-	-	-	-	.013	.015	.013
Ni	.001	.001	-	-	.001	.003	.001	.001	-	.002	.001	.001	.001	.003	-	-	-	.002	.001	-
Atomic percent																				
Mg	44.3	41.3	44.8	43.3	41.1	44.5	44.5	43.2	39.9	41.8	42.2	43.4	40.6	40.8	40.1	39.0	37.0	41.6	41.2	42.5
Fe	11.9	15.5	12.1	13.9	19.9	10.6	11.9	13.3	13.4	14.4	15.1	14.0	16.1	16.7	17.9	20.1	21.1	13.0	14.0	14.2
Ca	43.8	43.2	43.1	42.8	39.0	45.0	43.6	43.5	46.7	43.8	42.6	42.6	43.3	42.5	42.0	40.8	42.0	45.4	44.8	43.4
mg	78.9	72.8	78.7	75.7	67.4	80.8	78.9	76.5	74.8	74.3	73.6	75.5	71.6	71.0	69.1	66.0	63.7	76.1	74.6	75.0
Z	2.00	2.00	2.00	2.00	2.00	2.00	2.00	2.00	2.00	2.00	2.00	2.00	2.00	2.00	2.00	2.00	2.00	2.00	2.00	2.00
WXY	2.00	1.99	1.98	1.99	2.00	2.04	2.00	1.99	2.04	2.02	1.99	2.00	2.01	2.00	2.01	1.99	2.01	2.01	2.00	2.00

Table 5. Microprobe analyses of Ca-rich pyroxenes - continued.

	7Sy	8Sy	9Sy	10Sy	11Sy	12Sy	13Sy	14Sy	15Sy	16Sy	17Sy	18Sy	19Sy	20Sy	22Sy	23Sy	24Sy	25Sy	26Sy	27Sy
SiO2	51.0	50.9	51.5	51.5	50.1	50.2	51.9	50.9	49.1	48.8	50.7	51.5	50.2	49.2	49.3	49.0	47.3	50.6	49.5	48.7
TiO2	.30	.35	.40	.31	.88	.60	.68	.50	.62	.64	.32	.48	.74	.15	.63	.46	.47	.50	.40	.58
Al2O3	2.10	2.40	2.20	2.20	2.90	3.10	1.90	1.80	1.90	1.70	2.20	2.20	2.00	.73	3.10	2.20	1.70	2.20	1.60	1.90
Cr2O3	.18	<.05	.11	.09	<.05	<.05	<.05	.11	<.05	.18	.08	<.05	<.05	<.05	<.05	<.05	<.05	<.05	<.05	<.05
FeO	7.60	8.50	7.50	8.10	8.70	7.70	11.5	11.7	11.3	11.5	9.80	11.6	11.6	11.9	11.3	11.5	10.7	11.0	12.0	12.1
MnO	.12	.22	.14	.12	.19	.16	.29	.29	.18	.31	.21	.17	.27	.27	.25	.21	.26	.31	.25	.34
MgO	15.0	16.0	15.6	16.0	13.7	14.8	14.6	14.3	12.7	13.1	14.7	14.3	13.7	12.8	12.7	12.6	13.3	11.7	13.4	12.4
CaO	21.0	23.0	22.2	21.0	20.3	22.3	20.2	20.3	20.3	20.5	22.5	20.8	21.0	20.8	22.5	22.0	22.9	21.0	22.0	22.8
Na2O	.43	.42	.30	.39	.39	.33	.35	.18	.20	.22	.20	.34	<.05	.18	.58	.39	.42	.45	.41	.53
NiO	.05	.05	<.05	<.05	<.05	.05	<.05	<.05	<.05	<.05	<.05	<.05	<.05	<.05	<.05	<.05	<.05	<.05	<.05	<.05
Total	97.8	101.8	99.9	99.7	97.2	99.2	101.4	100.1	96.3	96.9	100.7	101.4	99.5	96.0	100.4	98.4	97.0	97.8	99.6	99.3
Number of ions on the basis of 6 oxygen atoms																				
Si	1.935	1.876	1.915	1.918	1.919	1.886	1.925	1.919	1.926	1.909	1.896	1.915	1.908	1.947	1.869	1.895	1.864	1.950	1.896	1.880
AlIV	.065	.104	.085	.082	.081	.114	.075	.080	.074	.078	.097	.085	.090	.034	.131	.100	.079	.050	.072	.086
AlVI	.029	-	.012	.015	.050	.024	.008	-	.014	-	-	.011	-	-	.007	-	-	.050	-	-
Ti	.009	.010	.011	.009	.025	.017	.019	.014	.018	.019	.009	.013	.021	.004	.018	.013	.014	.014	.012	.017
Cr	.005	-	.003	.003	-	-	-	.003	-	.006	.002	-	-	-	-	-	-	-	-	-
Fe2+	.241	.262	.233	.252	.279	.242	.357	.369	.371	.376	.306	.361	.369	.394	.358	.372	.353	.355	.384	.391
Mn	.004	.007	.004	.004	.006	.005	.009	.009	.006	.010	.007	.005	.009	.009	.008	.007	.009	.010	.008	.011
Mg	.848	.879	.865	.888	.782	.829	.807	.804	.742	.764	.819	.792	.776	.755	.718	.726	.781	.672	.765	.713
Ca	.854	.908	.885	.838	.833	.898	.803	.820	.853	.859	.901	.829	.855	.882	.914	.912	.967	.867	.903	.943
Na	.032	.030	.022	.028	.029	.024	.025	.013	.015	.017	.015	.025	-	.014	.043	.029	.032	.034	.030	.040
Ni	.002	.001	-	-	-	.002	-	-	-	-	-	-	-	-	-	-	-	-	-	-
Atomic percent																				
Mg	43.6	42.7	43.5	44.8	41.2	42.0	40.9	40.1	37.6	38.0	40.3	39.9	38.6	37.0	35.9	36.0	37.0	35.3	37.1	34.7
Fe	12.6	13.1	12.0	12.9	15.0	12.5	18.5	18.9	19.1	19.2	15.4	18.4	18.8	19.8	18.3	18.8	17.1	19.2	19.1	19.5
Ca	43.8	44.2	44.5	42.3	43.8	45.5	40.6	41.0	43.3	42.8	44.3	41.7	42.6	43.2	45.7	45.2	45.8	45.5	43.8	45.8
mg	77.6	76.6	78.4	77.6	73.3	77.0	68.8	68.0	66.3	66.4	72.4	68.4	67.3	65.2	66.2	65.7	68.4	64.8	66.1	64.0
Z	2.00	1.98	2.00	2.00	2.00	2.00	2.00	2.00	2.00	1.99	1.99	2.00	2.00	1.98	2.00	2.00	1.94	2.00	1.97	1.97
WXY	2.02	2.10	2.03	2.04	2.00	2.04	2.03	2.03	2.02	2.05	2.06	2.04	2.03	2.06	2.07	2.06	2.16	2.00	2.10	2.11

Table 5. Microprobe analyses of Ca-rich pyroxenes - continued.

	3Ku	5Ku	1Li	2Li	3Li	4LI	5Li	6Li	7Li	8Li	10Li
SiO2	51.8	51.3	54.5	50.5	50.5	52.7	51.6	51.7	52.6	50.9	51.5
TiO2	.48	.68	.09	.60	.87	.27	.33	.48	.56	.59	.61
Al2O3	2.27	2.39	3.77	2.76	2.43	2.42	2.55	2.32	1.82	1.67	2.00
Cr2O3	<.05	<.05	.21	.14	<.05	.44	.25	<.05	<.05	<.05	<.05
FeO	10.0	9.11	9.71	10.0	10.1	5.75	7.36	8.93	11.7	15.4	14.1
MnO	.23	.24	.24	.25	.30	.16	.20	.18	.29	.27	.39
MgO	14.8	15.9	16.7	15.0	13.0	16.0	15.5	15.7	13.1	10.9	12.0
CaO	22.0	21.9	13.9	20.8	23.5	21.1	21.2	20.6	22.1	18.8	19.7
Na2O	.22	.31	<.05	.25	.20	.20	.19	.22	.33	.29	.25
NiO	.06	<.05	.07	<.05	<.05	<.05	.06	<.05	.05	<.05	<.05
Total	101.9	101.8	99.2	100.3	100.9	99.0	99.2	100.1	102.5	98.8	100.5
Number of ions on the basis of 6 oxygen atoms											
Si	1.909	1.887	1.991	1.889	1.893	1.949	1.924	1.920	1.938	1.965	1.946
AlIV	.091	.104	.009	.111	.107	.051	.076	.080	.062	.035	.054
AlVI	.008	-	.154	.011	-	.055	.037	.022	.017	.041	.035
Ti	.013	.019	.002	.017	.025	.008	.009	.013	.016	.017	.017
Cr	-	-	.006	.004	-	.013	.007	-	-	-	-
Fe2+	.308	.280	.297	.313	.317	.178	.230	.277	.360	.497	.446
Mn	.007	.007	.007	.008	.010	.005	.006	.006	.009	.009	.012
Mg	.813	.872	.909	.836	.726	.882	.862	.869	.719	.627	.676
Ca	.869	.863	.544	.834	.944	.836	.847	.820	.872	.778	.797
Na	.016	.022	-	.018	.015	.014	.014	.016	.024	.022	.018
Ni	.002	-	.002	-	-	-	.002	-	.001	-	-
Atomic percent											
Mg	40.7	43.1	51.7	42.0	36.4	46.4	44.3	44.1	36.7	32.8	35.0
Fe	15.8	14.2	17.3	16.1	16.3	9.6	12.1	14.4	18.8	26.5	23.7
Ca	43.5	42.7	31.0	41.9	47.3	44.0	43.6	41.6	44.5	40.7	41.3
mg	72.0	75.2	74.9	72.3	69.0	82.8	78.5	75.4	66.1	55.3	59.6
Z	2.00	1.99	2.00	2.00	2.00	2.00	2.00	2.00	2.00	2.00	2.00
WXY	2.04	2.06	1.92	2.04	2.04	1.99	2.01	2.02	2.02	1.99	2.00

AlIV = Al in tetrahedral site
AlVI = Al in octahedral site
mg = 100*Mg/(Mg+Fe+Mn)
n.d. = not determined
Total Fe as FeO

Table 6.

Calculated equilibration temperatures (°C) for co-existing pyroxenes from the Koillismaa complex. (For sample numbering, see Table 1.)

Sample	Calculated temperature (W)	(W&B)	Sample	Calculated temperature (W)	(W&B)
1Nä	986	1063	4Py	1003	1000
6Nä	1079	1121	5Py	980	952
9Nä	1085	1121	6Py	1028	1013
10Nä	976	1050	7Py	1008	989
13Nä	1015	1088	8Py	1055	991
14Nä	1052	1110	5Po	921	960
15Nä	989	1055	6Po	1014	1003
16Na	1096	1136	7Po	1008	1006
17Nä	1190	1210	8Po	833	868
18Nä	997	1049	9Po	968	966
19Nä	1069	1099	10Po	1010	994
20Nä	1056	1093	11Po	1030	998
21Nä	1103	1121	12Po	974	958
22Nä	1044	1085	13Po	992	949
23Nä	971	1022	14Po	1031	942
24Nä	1029	1061	4Sy	913	922
25Nä	1127	1154	5Sy	945	936
28Nä	997	1036	6Sy	988	992
29Nä	1057	1083	7Sy	949	978
31Nä	950	1020	8Sy	922	920
32Nä	912	970	9Sy	938	948
33Nä	1007	1086	10Sy	1011	1003
36Nä	1215	1212	11Sy	962	964
37Nä	1057	1057	12Sy	898	919
38Nä	980	1018	13Sy	1004	944
39Nä	978	1010	13Sy	1033*	964*
40Nä	944	947	15Sy	933	896
41Nä	1036	1012	16Sy	945	895
42Nä	989	1024	17Sy	917	894
43Nä	1004	1001	19Sy	958	921
44Nä	973	984	20Sy	916	866
45Nä	1035	1017	3Ku	952	972
46Nä	983	964	5Ku	992	984
47Nä	1013	1020	2Li	1000	965
48Nä	840	829	3Li	773	819
49Nä	900	887	4Li	1032	1048
50Nä	883	855	5Li	1012	993
1Py	998	1016	6Li	1036	1023
2Py	1058	1059	7Li	890	875
3Py	991	1012			

(W) = Calculated using the method of Wells (1977).
(W&B) = Calculated using the method of Wood & Banno (1973).
* = Calculated using the estimated composition of original pigeonite.

Table 7.

Composition of plagioclases in the Koillismaa complex. (For sample numbering, see table 1.)

	28Nä	29Nä	32Nä	37Nä	38Nä	39Nä	40Nä	41Nä	42Nä	43Nä	44Nä	46Nä	47Nä	48Nä	49Nä	50Nä	52Nä	2Py	3Py	4Py
Mol. %																				
An	53.9	60.0	57.9	55.5	62.0	62.1	61.0	60.7	60.4	59.4	54.1	58.3	66.9	60.3	60.6	61.0	26.2	66.5	77.6	61.2
Ab	45.8	38.1	41.6	42.6	37.5	36.1	38.6	38.4	37.9	39.9	45.1	40.3	32.3	38.8	38.0	37.7	72.7	31.4	21.3	36.2
Or	.2	1.9	.5	1.9	.5	1.8	.4	.9	1.7	.7	.8	1.4	.8	.9	1.4	1.3	.7	2.1	1.1	2.6
Weight %																				
Fe	.13	.17	.18	.16	.22	.27	.32	.27	.19	.20	.23	.16	.23	.30	.29	.29	.11	.37	.41	.46

	5Py	6Py	7Py	8Py	2Po	5Po	6Po	7Po	8Po	9Po	10Po	11Po	12Po	13Po	15Po	16Po	17Po	18Po	1Sy	2Sy
Mol. %																				
An	63.4	64.2	66.3	77.2	71.8	65.1	72.2	77.2	66.2	77.2	78.0	61.3	66.8	57.4	55.3	54.8	54.0	62.7	58.0	77.5
Ab	22.5	34.2	31.7	21.8	26.8	33.2	25.4	21.2	31.4	21.2	20.5	35.0	31.1	40.9	44.2	44.0	43.7	36.0	41.2	21.0
Or	2.1	1.6	2.0	.1	1.4	1.7	2.4	1.6	2.4	1.6	1.5	3.7	2.1	1.7	.5	1.2	2.3	1.3	.8	1.5
Weight %																				
Fe	.47	.29	.53	.46	.38	.42	.39	.41	.25	.41	.36	.32	.53	.23	.34	.32	.41	.43	.36	.47

	4Sy	5Sy	6Sy	7Sy	8Sy	9Sy	10Sy	11Sy	12Sy	13Sy	14Sy	15Sy	16Sy	17Sy	18Sy	19Sy	20Sy	21Sy	22Sy	23Sy
Mol. %																				
An	71.7	80.8	72.3	74.8	69.6	59.2	63.1	72.5	62.1	66.4	63.7	62.1	68.6	58.1	62.1	64.6	53.5	58.6	53.5	56.0
Ab	26.6	18.1	26.6	24.4	28.0	39.3	36.6	27.3	35.7	32.3	35.0	36.6	30.0	40.9	37.3	34.4	46.1	39.1	44.8	42.0
Or	1.7	1.1	1.2	.8	2.4	1.5	.3	.2	2.1	1.2	1.3	1.3	1.4	1.0	.6	1.0	.4	2.3	1.6	2.0
Weight %																				
Fe	.33	.34	.45	.26	.39	.30	.32	.31	.34	.44	.43	.31	.43	.37	.42	.40	.37	.45	.55	.55

	24Sy	25Sy	26Sy	27Sy	28Sy	1Ku	3Ku	4Ku	5Ku	6Ku	1Li	2Li	3Li	5Li	6Li	7Li	8Li	9Li	10LI	11Li
Mol. %																				
An	54.0	57.5	53.4	52.7	58.8	64.0	71.8	60.0	72.1	64.4	62.9	66.1	77.8	71.7	67.7	59.0	54.7	51.6	63.2	5.2
Ab	43.6	40.7	44.5	45.0	40.6	33.8	26.4	39.3	26.2	34.6	35.4	32.2	21.3	26.6	30.4	40.8	44.1	46.0	36.1	94.6
Or	2.4	1.8	2.1	2.3	.6	2.3	1.8	.7	1.7	1.0	1.7	1.7	.9	1.7	1.9	.2	1.2	2.4	.7	.2
Weight %																				
Fe	.55	.51	.56	.48	.35	.33	.47	.40	.36	.58	.49	.50	.48	.48	.50	.40	.40	.51	.37	<.05

Table 8.

Microprobe analyses of spinellids from the Koillismaa complex. (For sample numbering, see Table 1.)

	1Nä	2Nä	3Nä	4Nä	5Nä	6Nä	7Nä	8Nä	9Nä	10Nä	11Nä	14Nä	15Nä	18Nä	31Nä	32Nä
SiO2	.10	n.d.	<.05	n.d.	<.05	.10	<.05	.10	n.d.	.11	<.05	n.d.	.10	.10	n.d.	.20
TiO2	1.00	.46	.37	.41	.38	1.00	.54	.50	1.30	.48	.51	.40	.47	.80	1.20	2.70
Al2O3	16.1	17.1	14.6	13.0	14.9	7.40	13.3	16.1	2.90	15.1	11.6	11.2	11.7	8.30	15.1	9.70
Cr2O3	40.3	45.3	46.7	45.8	45.7	32.0	39.6	44.2	30.9	44.0	49.7	52.6	42.3	52.8	33.9	27.2
V2O3	n.d.	.14	.18	.14	.14	.50	.22	n.d.	.18	.09	.12	.12	.18	n.d.	n.d.	n.d.
FeO	33.9	25.2	32.2	32.5	32.3	53.4	39.1	32.8	57.1	30.7	30.0	32.2	34.3	36.6	44.1	52.7
MnO	.30	.31	.89	.32	.35	.40	.49	.30	.66	.31	.62	.50	.47	.30	.40	.40
MgO	6.50	9.50	5.24	6.11	4.20	2.30	3.74	5.00	.86	5.43	2.96	3.40	3.20	2.70	2.30	2.30
ZnO	.25	.19	.36	.31	.43	.67	.44	n.d.	.80	.19	.76	.71	.47	.70	.50	.30
NiO	n.d.	.10	<.05	.08	.09	.16	.06	n.d.	.15	.13	<.05	<.05	.04	n.d.	n.d.	n.d.
CaO	n.d.	<.05	<.05	n.d.	n.d.	n.d.	<.05	<.05	<.05	n.d.	<.05	n.d.	<.05	n.d.	n.d.	n.d.
Sum	98.4	98.3	100.5	98.7	98.5	97.9	97.5	99.0	94.8	96.5	96.3	101.1	93.2	102.3	97.5	95.5
Recalculated analyses																
Ilmenite basis																
Fe2O3	10.8	6.4	7.4	9.4	5.9	27.3	13.3	6.8	31.2	6.5	3.3	4.6	8.9	7.9	15.8	26.0
FeO	24.2	19.4	25.5	24.0	27.0	28.8	27.1	26.7	29.0	24.8	27.1	28.1	26.3	29.5	29.9	29.3
Total	99.5	98.9	101.3	99.6	99.1	100.7	98.8	99.7	98.0	97.2	96.6	101.6	94.1	103.1	99.1	98.1
Ulvöspinel basis																
Fe2O3	10.1	6.1	7.1	9.2	5.7	26.6	13.0	6.4	30.3	6.1	2.9	4.3	8.5	7.3	15.0	24.0
FeO	24.8	19.7	25.8	24.3	27.2	29.5	27.4	27.0	29.8	25.2	27.4	28.3	26.6	30.0	30.6	31.1
Total	99.5	98.9	101.3	99.6	99.1	100.6	98.8	99.6	97.9	97.2	96.6	101.6	94.1	103.0	99.0	97.9
Number of ions on the basis of 32 oxygen atoms (Fe2O3/FeO from ulvöspinel basis)																
Si	.027	-	-	-	-	.028	-	.027	-	.030	-	-	.029	.027	-	.058
Al	5.050	5.251	4.574	4.139	4.786	2.482	4.343	5.088	1.036	4.889	3.905	3.596	4.035	2.680	4.937	3.297
Cr	8.481	9.332	9.814	9.782	9.848	7.201	8.674	9.370	7.402	9.556	11.222	11.329	9.786	11.435	7.435	6.202
Fe3+	2.023	1.196	1.420	1.870	1.169	5.697	2.710	1.291	6.908	1.261	.623	.882	1.872	1.505	3.131	5.209
Ti	.200	.090	.074	.083	.078	.214	.113	.101	.296	.099	.110	.082	.103	.165	.250	.586
V	-	.029	.038	.030	.031	.114	.049	-	.044	.020	.027	.026	.042	-	-	-
Mg	2.579	3.689	2.076	2.460	1.706	.976	1.544	1.998	.388	2.223	1.260	1.381	1.396	1.102	.951	.989
Ni	-	.021	-	.017	.020	.037	.013	-	.037	.029	-	-	.009	-	-	-
Fe2+	5.520	4.293	5.735	5.490	6.200	7.022	6.348	6.054	7.551	5.789	6.544	6.448	6.509	6.873	7.099	7.501
Zn	.049	.037	.071	.062	.087	.141	.090	-	.179	.039	.160	.143	.102	.142	.102	.064
Mn	.068	.068	.200	.073	.081	.096	.115	.068	.169	.072	.150	.115	.116	.070	.094	.098
Ca	-	-	-	-	-	-	-	-	-	-	-	-	-	-	-	-
Mol. %																
Fe2TiO4	2.8	1.1	.9	1.0	1.0	3.0	1.4	1.6	3.7	1.6	1.4	1.0	1.7	2.4	3.1	8.0
(Fe,Mg)Cr2O4	54.55	59.13	62.05	61.97	62.33	46.83	55.19	59.50	48.22	60.83	71.24	71.63	62.35	73.21	47.97	42.15
(Mg,Fe)Al2O4	32.49	33.27	28.92	26.22	30.29	16.14	27.63	32.31	6.75	31.12	24.79	22.74	25.71	17.16	31.85	22.41
Fe3O4	12.96	7.60	9.04	11.81	7.37	37.02	17.18	8.20	45.04	8.04	3.98	5.63	11.94	9.63	20.18	35.45

Table 8. Microprobe analyses of spinellids - continued.

	33Nä	34Nä	35Nä	36Nä	40Nä	41Nä	42Nä	43Nä	44Nä	45Nä	46Nä	48Nä	49Nä	50Nä	1Py	3Py
SiO2	<.05	<.05	n.d.	<.05	.10	.20	<.05	.10	<.05	<.05	.20	<.05	1.80	<.05	<.05	n.d.
TiO2	.18	.59	.68	.65	n.d.	.70	.24	1.90	1.25	1.75	2.10	.05	.10	4.75	3.80	1.05
Al2O3	15.9	16.8	15.4	19.8	11.3	.60	2.82	3.50	1.87	5.71	.60	<.05	.20	.34	7.41	12.3
Cr2O3	44.8	41.5	40.3	38.2	33.5	6.50	14.8	20.2	13.1	28.7	11.0	.34	1.90	.13	25.2	32.0
V2O3	.11	.13	.22	.22	n.d.	1.00	.47	.90	.92	.82	.70	1.01	.70	.64	.30	.45
FeO	34.0	35.7	38.4	32.8	52.3	85.5	68.6	70.0	78.6	61.0	82.4	93.0	88.2	88.1	56.5	46.1
MnO	.52	.49	.52	.47	.50	.20	.23	.40	.97	.32	.10	<.05	<.05	.44	.78	.36
MgO	5.02	3.76	2.00	7.55	.40	.10	.94	.20	.31	.60	.30	.05	.70	.10	.87	4.46
ZnO	.39	.92	1.10	.24	n.d.	.05	.11	.10	.19	.64	.10	.15	n.d.	<.05	.64	n.d.
NiO	.06	.10	.10	.11	n.d.	.06	<.05	.24	.25	.06	.10	.07	.07	<.05	.22	n.d.
CaO	<.05	<.05	<.05	<.05	<.05	.20	<.05	<.05	<.05	<.05	<.05	<.05	<.05	<.05	<.05	.07
Sum	101.0	100.0	98.7	100.0	98.1	95.1	88.2	97.5	97.5	99.6	97.6	94.7	93.7	94.5	95.7	96.8
Recalculated analyses																
Ilmenite basis																
Fe2O3	8.3	8.6	9.5	10.6	21.9	60.3	45.3	41.9	52.8	32.2	55.6	68.6	63.6	62.1	28.7	21.9
FeO	26.5	27.9	29.8	23.3	32.6	31.3	27.8	32.3	31.1	32.1	32.4	31.3	31.0	32.2	30.7	26.4
Total	101.8	100.9	99.7	101.1	100.3	101.1	92.7	101.7	102.7	102.8	103.2	101.5	100.0	100.7	98.6	99.0
Ulvöspinel basis																
Fe2O3	8.2	8.2	9.1	10.1	21.8	59.6	45.2	40.6	51.9	31.0	54.0	68.5	61.9	59.0	26.1	21.2
FeO	26.6	28.3	30.2	23.7	32.6	31.9	28.0	33.5	31.9	33.1	33.8	31.3	32.5	35.1	33.0	27.0
Total	101.8	100.8	99.6	101.1	100.3	101.1	92.7	101.6	102.7	102.7	103.0	101.5	99.9	100.4	98.3	98.9
Number of ions on the basis of 32 oxygen atoms (Fe2O3/FeO from ulvöspinel basis)																
Si	-	-	-	-	.028	.060	-	.029	-	-	.059	-	.547	-	-	-
Al	4.939	5.295	5.001	5.989	3.778	.213	1.068	1.211	.649	1.921	.209	-	.072	.122	2.570	4.021
Cr	9.336	8.774	8.778	7.751	7.514	1.552	3.760	4.687	3.049	6.477	2.567	.082	.456	.031	5.864	7.019
Fe3+	1.626	1.650	1.887	1.951	4.654	13.540	10.931	8.967	11.496	6.659	11.994	15.645	14.149	13.513	5.780	4.426
Ti	.036	.119	.141	.125	-	.159	.058	.419	.277	.376	.466	.011	.023	1.087	.841	.219
V	.023	.028	.049	.045	-	.242	.121	.212	.217	.188	.166	.246	.170	.156	.071	.100
Mg	1.972	1.499	.821	2.888	.169	.045	.450	.087	.136	.255	.132	.023	.317	.045	.382	1.844
Ni	.013	.022	.022	.023	-	.015	-	.057	.059	.014	.024	.017	.017	-	.052	-
Fe2+	5.864	6.329	6.958	5.087	7.735	8.054	7.525	8.223	7.853	7.901	8.343	7.945	8.256	8.934	8.122	6.264
Zn	.076	.182	.224	.045	-	.011	.026	.022	.041	.135	.022	.034	-	-	.139	-
Mn	.116	.111	.121	.102	.120	.051	.063	.099	.242	.077	.025	-	-	.113	.194	.085
Ca	-	-	-	-	-	.065	-	-	-	-	-	-	-	-	-	.021
Mol. %																
Fe2TiO4	.4	1.5	1.8	1.6	.4	2.7	.7	5.6	3.5	4.7	6.6	.1	7.1	13.6	10.5	2.7
(Fe,Mg)Cr2O4	58.71	55.78	56.06	49.39	47.09	10.13	23.87	31.55	20.05	43.02	17.38	.52	3.11	.23	41.22	45.39
(Mg,Fe)Al2O4	31.06	33.66	31.94	38.16	23.68	1.39	6.78	8.15	4.27	12.76	1.41	-	.49	.89	18.07	26.01
Fe3O4	10.22	10.55	12.00	12.45	29.23	88.47	69.35	60.30	75.68	44.22	81.21	99.48	96.40	98.88	40.71	28.61

Table 8. Microprobe analyses of spinellids - continued.

	5Py	6Py	8Py	4Po	6Po	9Po	11Po	12Po	14Po	16Po	17Po	4Sy	5Sy	6Sy	8Sy	13Sy
SiO2	n.d.	.18	<.05	<.05	<.05	<.05	<.05	<.05	<.05	<.05	<.05	.10	<.05	<.05	2.00	.07
TiO2	4.77	4.96	14.4	1.64	6.84	1.77	1.35	3.85	7.22	9.42	6.86	2.39	.70	.30	.13	.19
Al2O3	.48	.62	.05	12.7	.16	.87	1.78	2.28	.21	.20	.23	.11	.46	1.10	.85	<.05
Cr2O3	5.31	1.37	.05	31.7	2.08	1.79	<.05	11.6	<.05	<.05	<.05	.11	<.05	<.05	<.05	.34
V2O3	n.d.	.74	1.71	.26	.39	1.33	.53	.53	1.36	1.54	1.85	1.00	.60	1.10	.84	1.00
FeO	83.7	87.1	77.2	40.6	79.6	88.1	85.4	76.2	87.5	85.1	87.0	89.5	88.3	92.2	84.8	91.4
MnO	.22	.25	.57	.28	.24	.08	.09	.45	.35	.13	.12	.11	<.05	.76	.08	<.05
MgO	.11	.11	<.05	7.06	.34	.23	.27	.14	.05	.06	.06	.15	.08	.22	3.00	.21
ZnO	n.d.	n.d.	<.05	.11	<.05	<.05	<.05	<.05	<.05	<.05	<.05	<.05	.10	<.05	<.05	<.05
NiO	n.d.	.06	<.05	<.05	.05	.17	.15	<.05	<.05	.07	<.05	<.05	<.05	<.05	<.05	<.05
CaO	.03	<.05	<.05	<.05	<.05	<.05	<.05	<.05	<.05	<.05	<.05	<.05	<.05	<.05	.22	<.05
Sum	94.6	95.4	94.0	94.3	89.7	94.3	89.6	95.0	96.7	96.5	96.1	93.5	90.2	95.7	91.9	93.2
Recalculated analyses																
Ilmenite basis																
Fe2O3	57.1	60.3	47.4	20.8	54.1	62.9	61.7	49.0	59.8	56.3	59.3	64.5	64.7	68.0	64.5	67.3
FeO	32.4	32.8	34.6	21.9	30.9	31.5	29.9	32.1	33.7	34.4	33.7	31.5	30.1	31.0	26.8	30.8
Total	100.3	101.4	98.7	96.4	95.1	100.6	95.7	100.0	102.7	102.2	102.1	99.9	96.7	102.5	98.4	100.0
Ulvöspinel basis																
Fe2O3	53.9	56.9	37.8	19.7	49.5	61.7	60.8	46.4	54.9	50.0	54.7	62.8	64.2	67.8	62.6	67.1
FeO	35.2	35.9	43.2	22.9	35.0	32.6	30.7	34.4	38.1	40.1	37.8	33.0	30.5	31.2	28.5	31.0
Total	100.0	101.1	97.8	96.3	94.7	100.5	95.7	99.7	102.2	101.5	101.6	99.8	96.7	102.5	98.2	99.9
Number of ions on the basis of 32 oxygen atoms (Fe2O3/FeO from ulvöspinel basis)																
Si	-	.054	-	-	-	-	-	-	-	-	-	.031	-	-	.604	.022
Al	.172	.220	.018	4.163	.061	.311	.667	.812	.074	.071	.081	.040	.172	.387	.302	-
Cr	1.280	.327	.012	6.971	.529	.430	-	2.770	-	-	-	.027	-	-	-	.083
Fe3+	12.363	12.913	8.825	4.123	11.992	14.099	14.537	10.546	12.347	11.294	12.369	14.524	15.344	15.214	14.224	15.535
Ti	1.093	1.125	3.360	.343	1.656	.404	.323	.874	1.623	2.126	1.550	.552	.167	.067	.030	.044
V	-	.179	.425	.058	.101	.324	.135	.128	.326	.371	.446	.246	.153	.263	.203	.247
Mg	.050	.049	-	2.927	.163	.104	.128	.063	.022	.027	.027	.069	.038	.098	1.350	.096
Ni	-	.015	-	-	.013	.042	.038	-	-	.017	-	-	-	-	-	-
Fe2+	8.973	9.055	11.209	5.326	9.423	8.279	8.157	8.689	9.523	10.067	9.499	8.482	8.101	7.781	7.197	7.976
Zn	-	-	-	.023	-	-	-	-	-	-	-	-	.023	-	-	-
Mn	.057	.064	.150	.066	.065	.021	.024	.115	.089	.033	.031	.029	-	.192	.020	-
Ca	.010	-	-	-	-	-	-	-	-	-	-	-	-	-	.071	-
Mol. %																
Fe2TiO4	13.7	14.7	42.0	4.3	20.7	5.1	4.0	10.9	20.3	26.6	19.4	7.3	2.1	.8	7.9	.8
(Fe,Mg)Cr2O4	9.27	2.43	.14	45.71	4.20	2.89	-	19.61	-	-	-	.18	-	-	-	.53
(Mg,Fe)Al2O4	1.25	1.64	.21	27.30	.48	2.10	4.39	5.74	.60	.62	.65	.27	1.11	2.48	2.08	-
Fe3O4	89.49	95.93	99.65	27.00	95.31	95.01	95.61	74.65	99.40	99.38	99.35	99.54	98.89	97.52	97.92	99.47

Table 8. Microprobe analyses of spinellids - continued.

	14Sy	15Sy	17Sy	19Sy	20Sy	22Sy	23Sy	24Sy	25Sy	26Sy	27Sy	2Li	8Li
SiO2	<.05	<.05	.20	<.05	.05	<.05	.06	.09	.09	.06	.18	<.05	<.05
TiO2	.22	.26	1.10	.76	.75	7.40	10.0	7.59	10.3	11.6	10.4	6.45	4.48
Al2O3	.05	.13	.07	.23	.10	.11	.10	.15	.17	.19	.18	2.28	.28
Cr2O3	.13	.33	.28	.20	<.05	<.05	<.05	<.05	<.05	.06	<.05	10.1	<.05
V2O3	1.00	1.10	1.10	1.10	1.20	1.50	1.60	1.13	1.17	1.60	1.53	.77	1.69
FeO	94.3	92.4	87.4	90.1	91.7	85.1	82.7	83.6	83.9	80.2	83.5	76.4	88.0
MnO	.10	<.05	.13	<.05	.36	.33	.49	.39	.19	.59	.63	.10	.07
MgO	<.05	<.05	<.05	.08	.11	.08	.05	.05	.07	<.05	<.05	.11	.06
ZnO	<.05	<.05	<.05	<.05	<.05	<.05	<.05	.05	<.05	<.05	<.05	.25	<.05
NiO	<.05	<.05	<.05	<.05	<.05	<.05	<.05	<.05	<.05	<.05	<.05	<.05	<.05
CaO	<.05	<.05	<.05	<.05	<.05	<.05	<.05	.05	<.05	<.05	<.05	<.05	<.05
Sum	95.8	94.2	90.3	92.5	94.3	94.5	95.0	93.1	95.9	94.3	96.4	96.5	94.6
Recalculated analyses													
Ilmenite basis													
Fe2O3	69.4	67.7	63.4	65.8	67.3	57.9	54.4	56.8	54.9	51.4	54.6	47.7	61.6
FeO	31.9	31.5	30.3	30.9	31.1	33.0	33.8	32.5	34.5	34.0	34.4	33.5	32.6
Total	102.7	101.0	96.6	99.1	101.0	100.3	100.4	98.8	101.4	99.4	101.9	101.2	100.7
Ulvöspinel basis													
Fe2O3	69.2	67.5	62.5	65.3	66.8	53.0	47.7	51.6	48.0	43.6	47.5	43.4	58.6
FeO	32.0	31.6	31.2	31.4	31.6	37.5	39.8	37.1	40.7	41.0	40.7	37.4	35.3
Total	102.7	101.0	96.5	99.0	101.0	99.8	99.8	98.3	100.7	98.7	101.2	100.8	100.5
Number of ions on the basis of 32 oxygen atoms (Fe2O3/FeO from ulvöspinel basis)													
Si	-	-	.064	-	.015	-	.018	.028	.027	.018	.054	-	-
Al	.018	.047	.026	.084	.036	.040	.036	.055	.061	.069	.064	.801	.100
Cr	.031	.080	.070	.049	-	-	-	-	-	.015	-	2.381	-
Fe3+	15.612	15.487	14.963	15.237	15.298	12.188	10.952	12.065	10.918	10.105	10.755	9.737	13.429
Ti	.050	.060	.263	.177	.172	1.701	2.295	1.774	2.341	2.687	2.353	1.446	1.026
V	.240	.269	.281	.273	.293	.368	.391	.282	.284	.395	.369	.184	.413
Mg	-	-	-	.037	.050	.036	.023	.023	.032	-	-	.049	.027
Ni	-	-	-	-	-	-	-	-	-	-	-	-	-
Fe2+	8.023	8.057	8.301	8.143	8.043	9.584	10.156	9.641	10.289	10.560	10.242	9.325	8.990
Zn	-	-	-	-	-	-	-	.011	-	-	-	.055	-
Mn	.025	-	.035	-	.093	.085	.127	.103	.049	.154	.161	.025	.018
Ca	-	-	-	-	-	-	-	.017	-	-	-	-	-
Mol. %													
Fe2TiO4	.6	.7	4.1	2.2	2.3	21.3	28.9	22.5	29.6	33.8	30.1	18.1	12.8
(Fe,Mg)Cr2O4	.20	.51	.47	.32	-	-	-	-	-	.14	-	18.43	-
(Mg,Fe)Al2O4	.11	.30	.17	.55	.23	.32	.33	.45	.55	.68	.59	6.20	.74
Fe3O4	99.69	99.19	99.36	99.13	99.77	99.68	99.67	99.55	99.45	99.18	99.41	75.37	99.26

n.d. = not determined
Fe2O3/FeO recalculated using the method descriped by Carmichael (1967).
Content of chromite, spinel and magnetite adjusted to 100 %.

Table 9.

Microprobe analyses of ilmenites from the Koillismaa complex. (For sample numbering, see Table 1.)

	41Nä	44Nä	45Nä	46Nä	48Nä	49Nä	50Nä	51Nä	52Nä	4Py	5Py	6Py	7Py	8Py	5Po	8Po
SiO2	<.05	<.05	<.05	<.05	<.05	<.05	<.05	<.05	<.05	.15	.18	.22	<.05	<.05	<.05	<.05
TiO2	51.3	40.6	53.4	42.3	51.8	45.5	52.0	50.8	50.9	51.0	47.5	50.7	50.1	50.6	40.8	48.0
Al2O3	<.05	.10	.25	.10	<.05	<.05	<.05	<.05	.05	.15	<.05	.18	.07	<.05	.06	<.05
Cr2O3	.45	1.24	<.05	.43	<.05	<.05	<.05	<.05	<.05	.36	.81	1.58	.39	<.05	.58	.07
V2O3	.13	.17	.37	.48	.25	.25	.18	.10	.13	1.10	.39	.21	.73	.37	.59	.51
FeO	45.5	54.1	47.7	57.1	46.4	52.4	47.6	44.6	44.9	44.1	51.4	47.2	47.7	46.0	56.6	50.5
MnO	2.09	1.50	.97	1.04	1.29	.53	1.14	1.34	1.43	1.69	1.47	1.98	1.48	1.33	.70	1.24
MgO	.17	.73	.99	.26	.11	.18	.10	.05	.17	.20	.10	.19	.29	.11	1.08	.89
ZnO	<.05	<.05	.09	.16	.09	.16	.05	<.05	<.05	<.05	<.05	<.05	<.05	<.05	<.05	<.05
NiO	.06	.06	<.05	<.05	<.05	<.05	<.05	<.05	<.05	.52	<.05	<.05	<.05	<.05	.07	<.05
CaO	<.05	<.05	<.05	<.05	<.05	<.05	<.05	<.05	<.05	<.05	<.05	<.05	<.05	<.05	<.05	<.05
Sum	99.7	98.5	103.8	101.9	99.9	99.0	101.1	96.9	97.6	99.3	101.8	102.3	100.8	98.4	100.5	101.2
Recalculated analyses																
Fe2O3	2.0	22.7	2.8	23.0	1.6	13.9	2.5	.4	1.0	.1	11.3	4.1	5.2	2.3	25.1	11.3
FeO	43.7	33.7	45.2	36.4	45.0	39.9	45.4	44.2	44.0	44.0	41.3	43.5	43.0	44.0	34.1	40.3
Total	99.9	100.8	104.0	104.2	100.1	100.4	101.3	96.9	97.7	99.3	103.0	102.7	101.3	98.6	103.0	102.3
Number of ions on the basis of 6 oxygen atoms																
Si	-	-	-	-	-	-	-	-	-	.008	.009	.011	-	-	-	-
Al	-	.006	.014	.006	-	-	-	-	.003	.009	-	.010	.004	-	.003	-
Cr	.018	.049	-	.017	-	-	-	-	-	.014	.032	.061	.015	-	.023	.003
Fe3+	.076	.860	.102	.847	.061	.529	.094	.016	.039	.004	.418	.152	.195	.089	.929	.419
Ti	1.950	1.538	1.935	1.556	1.965	1.731	1.949	1.991	1.977	1.949	1.758	1.873	1.879	1.948	1.509	1.779
V	.005	.007	.014	.019	.010	.010	.007	.004	.005	.045	.015	.008	.029	.015	.023	.020
Mg	.013	.055	.071	.019	.008	.014	.007	.004	.013	.015	.007	.014	.022	.008	.079	.065
Ni	.002	.002	-	-	-	-	-	-	-	.021	-	-	-	-	.003	-
Fe2+	1.847	1.419	1.821	1.489	1.898	1.688	1.893	1.926	1.900	1.870	1.700	1.788	1.793	1.883	1.403	1.661
Zn	-	-	.003	.006	.003	.006	.002	-	-	-	-	-	-	-	-	-
Mn	.089	.064	.040	.043	.055	.023	.048	.059	.063	.073	.061	.082	.063	.058	.029	.052
Ca	-	-	-	-	-	-	-	-	-	-	-	-	-	-	-	-
Mol.% R2O3	2.5	23.1	3.2	22.2	1.7	13.5	2.5	.5	1.2	1.8	11.6	5.8	6.1	2.6	24.4	11.1

Table 9. Microprobe analyses of ilmenites - continued.

	10Po	11Po	12Po	14Po	16Po	17Po	4Sy	5Sy	6Sy	8Sy	9Sy	13Sy	14Sy	15Sy	17Sy	19Sy
SiO2	<.05	<.05	<.05	<.05	<.05	<.05	<.05	<.05	<.05	.08	<.05	.09	<.05	<.05	<.05	.07
TiO2	47.9	48.7	38.9	44.8	51.1	49.4	46.7	42.0	49.8	52.9	52.5	51.5	51.8	51.6	51.1	51.4
Al2O3	.27	<.05	.06	<.05	<.05	<.05	.06	3.40	<.05	.06	.06	.06	<.05	<.05	<.05	<.05
Cr2O3	.06	<.05	.64	<.05	<.05	<.05	<.05	<.05	<.05	.05	<.05	.05	.05	<.05	.11	.05
V2O3	.44	.24	.70	.42	.38	.40	.21	.20	.26	.21	.40	.23	.34	.22	.25	.25
FeO	52.3	46.3	55.1	51.7	50.0	50.2	52.1	47.4	47.4	47.9	48.2	45.6	47.7	45.1	46.8	45.4
MnO	.85	2.69	1.72	1.81	2.00	1.70	1.10	1.30	1.50	1.70	.82	.80	1.60	2.10	1.10	1.30
MgO	.92	.94	.24	<.05	.06	.20	.65	3.40	1.00	.08	.17	.10	.08	.11	.11	.10
ZnO	<.05	<.05	<.05	<.05	<.05	<.05	<.05	<.05	<.05	<.05	<.05	<.05	<.05	<.05	<.05	<.05
NiO	.08	<.05	<.05	<.05	<.05	<.05	<.05	<.05	<.05	<.05	<.05	<.05	<.05	<.05	<.05	<.05
CaO	<.05	<.05	<.05	<.05	<.05	<.05	<.05	.05	<.05	<.05	<.05	<.05	<.05	<.05	<.05	<.05
Sum	102.8	98.9	97.4	98.7	103.5	101.9	100.8	97.7	100.0	103.0	102.1	98.4	101.6	99.1	99.5	98.6
Recalculated analyses																
Fe2O3	13.0	7.7	24.8	14.7	6.9	8.7	13.8	19.0	6.6	2.3	2.4	.2	3.2	1.1	2.4	.7
FeO	40.6	39.4	32.8	38.5	43.8	42.3	39.7	30.3	41.5	45.8	46.1	45.4	44.8	44.1	44.6	44.8
Total	104.1	99.6	99.8	100.2	104.2	102.8	102.2	99.7	100.6	103.2	102.4	98.4	101.9	99.2	99.7	98.6
Number of ions on the basis of 6 oxygen atoms																
Si	-	-	-	-	-	-	-	-	-	.004	-	.005	-	-	-	.004
Al	.015	-	.004	-	-	-	.003	.196	-	.003	.003	.004	-	-	-	-
Cr	.002	-	.026	-	-	-	-	-	-	.002	-	.002	.002	-	.004	.002
Fe3+	.474	.293	.953	.561	.252	.323	.514	.701	.248	.085	.089	.008	.119	.042	.092	.027
Ti	1.744	1.849	1.494	1.710	1.867	1.831	1.737	1.548	1.870	1.947	1.946	1.984	1.933	1.974	1.948	1.977
V	.017	.010	.029	.017	.015	.016	.008	.008	.010	.008	.016	.009	.014	.009	.010	.010
Mg	.066	.071	.018	-	.004	.015	.048	.248	.074	.006	.012	.008	.006	.008	.008	.008
Ni	.003	-	-	-	-	-	-	-	-	-	-	-	-	-	-	-
Fe2+	1.644	1.663	1.401	1.634	1.779	1.744	1.643	1.242	1.733	1.875	1.900	1.945	1.859	1.876	1.890	1.916
Zn	-	-	-	-	-	-	-	-	-	-	-	-	-	-	-	-
Mn	.035	.115	.074	.078	.082	.071	.046	.054	.063	.070	.034	.035	.067	.090	.047	.056
Ca	-	-	-	-	-	-	-	.003	-	-	-	-	-	-	-	-
Mol.% R2O3	12.7	7.5	25.3	14.5	6.6	8.5	13.1	22.6	6.4	2.5	2.7	.6	3.4	1.3	2.7	.9

Table 9. Microprobe analyses of ilmenites - continued.

	20Sy	22Sy	23Sy	24Sy	25Sy	26Sy	27Sy	4Li	5Li	7Li	8Li
SiO2	.09	.06	<.05	.08	.05	<.05	<.05	<.05	<.05	<.05	<.05
TiO2	51.0	50.7	50.5	52.3	50.8	48.1	49.7	45.1	51.6	52.2	52.3
Al2O3	<.05	<.05	<.05	.07	<.05	<.05	<.05	.23	.53	<.05	.09
Cr2O3	<.05	<.05	<.05	<.05	<.05	<.05	<.05	1.03	3.43	<.05	<.05
V2O3	.36	.30	<.05	.40	.21	.39	.39	.51	1.58	.33	.25
FeO	45.2	46.0	46.3	47.3	46.4	48.5	47.6	44.7	45.6	45.7	46.0
MnO	1.65	2.93	.11	1.86	2.02	2.36	2.25	1.17	.66	.92	1.20
MgO	.15	.16	.14	.14	.13	.08	.11	1.35	.46	.23	.08
ZnO	<.05	<.05	<.05	<.05	<.05	.07	<.05	.07	<.05	<.05	<.05
NiO	<.05	<.05	<.05	<.05	<.05	<.05	<.05	<.05	<.05	<.05	<.05
CaO	<.05	.05	<.05	<.05	<.05	<.05	<.05	<.05	<.05	<.05	<.05
Sum	98.4	100.2	97.0	102.1	99.6	99.5	100.0	94.2	103.9	99.4	99.9
Recalculated analyses											
Fe2O3	1.3	4.1	1.4	2.6	3.3	8.7	6.0	8.7	.8	.1	.4
FeO	44.0	42.3	45.0	45.0	43.5	40.7	42.2	36.9	44.9	45.6	45.7
Total	98.6	100.6	97.2	102.4	99.9	100.4	100.6	95.0	103.9	99.4	100.0
Number of ions on the basis of 6 oxygen atoms											
Si	.005	.003	-	.004	.003	-	-	-	-	-	-
Al	-	-	-	.004	-	-	-	.014	.030	-	.005
Cr	-	-	-	-	-	-	-	.043	.131	-	-
Fe3+	.050	.155	.055	.096	.125	.331	.227	.345	.029	.004	.015
Ti	1.963	1.914	1.973	1.938	1.930	1.826	1.879	1.788	1.874	1.991	1.984
V	.015	.012	-	.016	.009	.016	.016	.022	.061	.013	.010
Mg	.011	.012	.011	.010	.010	.006	.008	.106	.033	.017	.006
Ni	-	-	-	-	-	-	-	-	-	-	-
Fe2+	1.884	1.776	1.956	1.854	1.838	1.718	1.774	1.627	1.814	1.935	1.928
Zn	-	-	-	-	-	.003	-	.003	-	-	-
Mn	.072	.125	.005	.078	.086	.101	.096	.052	.027	.040	.051
Ca	-	.003	-	-	-	-	-	-	-	-	-
Mol.% R2O3	1.6	4.1	1.4	2.9	3.3	8.7	6.1	10.6	6.3	.4	.7

Fe2O3/FeO recalculated using the method descriped by Carmichael (1967).

Table 10.

Microprobe analyses of loveringite, garnets, tri-octahedral micas and amphiboles from the Koillismaa complex. (For sample numbering, see Table 1.)

	Lover.	Garnet		Tri-octahedral mica						Amphibole	
	28Nä	9Sy	W146	1Nä	30Nä	41Nä	51Nä	52Nä	4Sy	51Nä	52Nä
SiO2	.06	35.5	37.6	39.4	38.7	38.0	38.2	37.8	38.9	40.0	44.3
TiO2	60.6	<.05	.03	3.98	5.33	4.03	2.07	2.19	4.46	.31	1.79
Al2O3	1.31	21.7	21.7	13.9	14.1	14.3	15.9	15.1	14.1	15.8	8.04
Cr2O3	9.91	<.05	<.05	.29	.83	<.05	<.05	<.05	<.05	<.05	<.05
Fe2O3		2.6	.3								
FeO	16.3	16.5	18.4	5.01	9.16	18.9	21.9	25.2	13.1	21.2	24.2
MnO	.11	2.20	1.76	<.05	<.05	.10	.07	.15	.08	<.05	.19
MgO	.97	2.00	1.83	22.0	19.3	11.6	8.83	6.89	15.0	6.07	6.19
CaO	2.29	18.9	17.4	<.05	.20	<.05	.09	<.05	.07	12.2	11.5
Na2O	<.05	.06	<.05	.39	1.02	<.05	<.05	<.05	.28	1.23	1.69
K2O	<.05	<.05	<.05	10.1	8.06	9.01	10.1	10.5	9.12	.45	1.05
NiO	<.05	<.05	<.05	<.05	<.05	<.05	<.05	<.05	.16	<.05	<.05
V2O3	<.05	<.05	<.05	<.05	<.05	<.05	<.05	<.05	<.05	<.05	<.05
ZrO2	4.61	n.d.	n.d.	n.d.	n.d.	n.d.	n.d.	n.d.	n.d.	n.d.	n.d.
Ce2O3	1.27	n.d.	n.d.	n.d.	n.d.	n.d.	n.d.	n.d.	n.d.	n.d.	n.d.
La2O3	1.30	n.d.	n.d.	n.d.	n.d.	n.d.	n.d.	n.d.	n.d.	n.d.	n.d.
Total	98.7	99.5	99.0	95.1	96.6	95.9	97.2	97.8	95.3	97.3	99.0
				Number of ions on the basis of							
	38(O)	24(O)		22(O)						23(O)	
Si	.018	5.633	5.929	5.647	5.525	5.715	5.768	5.785	5.739	6.145	6.804
Al		.367	.071	2.348	2.372	2.285	2.232	2.215	2.261	1.855	1.196
Al	.455	3.691	3.692	-	-	.250	.598	.508	.191	1.005	.259
Ti	13.438	-	.004	.429	.572	.456	.235	.252	.495	.036	.207
Cr	2.310	-	-	.032	.094	-	-	-	-	-	-
Fe3+		.310	.036								
Fe2+	4.020	2.190	2.427	.600	1.094	2.377	2.766	3.225	1.616	2.723	3.108
Mn	.027	.296	.235	-	-	.013	.009	.019	.010	-	.025
Mg	.426	.473	.430	4.700	4.107	2.601	1.987	1.572	3.299	1.390	1.417
Ca	.723	3.213	2.940	-	.031	-	.015	-	.011	2.008	1.892
Na	-	.018	-	.108	.282	-	-	-	.080	.366	.503
K	-	-	-	1.847	1.468	1.729	1.945	2.050	1.717	.088	.206
Ni	-	-	-	-	-	-	-	-	.019	-	-
Zr	.663										
Ce	.137										
La	.141										
		Z 6.00	6.00	Z 8.00	7.99	8.00	8.00	8.00	8.00	8.00	8.00
		R3+ 4.00	4.00	Y 5.76	5.77	5.70	5.60	5.58	5.63	5.15	5.02
		R2+ 6.19	6.03	X 1.96	1.78	1.73	1.96	2.05	1.81	2.46	2.60
		Alm 35.5	40.2							mg* 33.8	31.1
		And 7.5	.9								
		Gro 44.5	47.8								
		Pyr 7.7	7.1								
		Spe 4.8	3.9								

n.d. = not determined

mg* = 100*Mg/(Mg+Fe+Mn)
in garnets FeO/Fe2O3 calculated to bring the R3+ group to 4.00, in others total Fe as FeO

Table 11.

Chemical composition of the type samples from the Koillismaa complex, with C.I.P.W. norms.
(For sample numbering, see Table 1.)

	1Nä	2Nä	3Nä	4Nä	5Nä	6Nä	7Nä	8Nä	9Nä	10Nä	11Nä	12Nä	13Nä	14Nä	15Nä	16Nä
SiO2	37.18	37.83	39.73	41.69	45.10	47.18	41.73	47.31	45.99	54.82	54.60	53.31	54.76	54.51	53.86	55.25
TiO2	.20	.05	.05	.05	.07	.12	.10	.07	.15	.12	.07	.10	.10	.10	.13	.10
Al2O3	2.18	.70	.59	.63	.85	2.34	2.50	.94	5.30	1.69	1.07	1.53	1.43	1.11	2.05	1.54
Fe2O3	8.30	7.30	8.12	6.33	5.80	5.51	5.67	4.23	4.05	1.46	3.46	2.18	1.38	1.92	1.95	1.32
FeO	4.48	3.83	3.36	4.35	4.80	5.73	5.90	5.99	5.84	7.33	4.60	7.15	7.76	6.89	7.12	8.01
MnO	.21	.22	.28	.22	.23	.27	.22	.27	.26	.26	.25	.25	.27	.25	.25	.27
MgO	35.90	33.49	32.29	34.10	34.00	32.20	32.89	33.20	28.24	31.30	30.50	30.30	30.10	30.40	28.30	30.16
CaO	1.23	.17	.12	.51	.92	1.01	1.82	1.12	2.65	1.97	1.23	1.79	2.19	2.35	3.46	2.50
Na2O	.03	.04	.01	.03	.04	.11	.12	.05	.09	.08	.18	.05	.08	.05	.18	.07
K2O	.08	.01	.00	.00	.00	.07	.13	.01	.22	.04	.05	.00	.01	.00	.05	.01
P2O5	.02	.00	.00	.00	.00	.02	.00	.00	.02	.00	.00	.00	.00	.00	.00	.00
CO2	.89	1.00	.50	.40	.40	n.d.	.11	.30	.40	.40	.20	n.d.	n.d.	n.d.	n.d.	n.d.
H2O+	11.70	13.30	13.70	11.10	7.40	11.20	6.20	5.50	5.70	.90	6.00	.20	.30	.20	.30	.30
H2O-	.39	1.07	1.22	.70	.51	.19	.40	.62	.43	.18	.26	.07	.03	.04	.06	.03
Total	102.79	99.01	99.97	100.11	100.12	105.95	97.79	99.61	99.34	100.55	102.47	96.93	98.41	97.82	97.71	99.50
Cr	.074	.267	.335	.248	.315	.119	.161	.361	.209	.409	.446	.436	.373	.367	.466	.364
V	.000	.000	.000	.000	.000	.000	.010	.000	.010	.000	.000	.010	.000	.000	.010	.010
Ni	.222	.135	.119	.106	.084	.104	.100	.080	.070	.056	.046	.058	.052	.057	.054	.056
Cu	.000	.003	.004	.005	.005	.000	.000	.004	.005	.006	.006	.002	.001	.001	.002	.001
Co	.015	.015	.014	.013	.012	.012	.013	.012	.011	.009	.008	.009	.009	.009	.010	.009
Zn	.007	.004	.008	.008	.010	.007	.007	.007	.009	.008	.008	.006	.007	.006	.006	.007
S	.010	.030	.010	.020	.000	.050	.020	.010	.020	.000	.000	.000	.000	.000	.000	.000
Sr	.000	.000	.000	.000	.000	.000	.000	.000	.010	.000	.000	.000	.000	.000	.000	.000
C.I.P.W. norms (weight %)																
Q	-	-	-	-	-	-	-	-	-	-	3.90	-	.31	.75	.60	.22
or	.49	.07	.02	.02	.02	.43	.78	.07	1.38	.25	.31	.01	.07	.01	.31	.07
ab	.25	-	-	.25	.34	.93	1.02	.42	.76	.68	1.52	.42	.68	.42	1.52	.59
an	.35	-	-	-	2.04	4.88	5.89	2.30	10.49	4.13	1.96	3.94	3.51	2.80	4.63	3.85
C	1.91	.69	.59	.58	.03	.29	-	-	1.06	-	-	-	-	-	-	-
wo-di	-	-	-	-	-	-	1.02	.57	-	1.30	1.20	2.06	3.07	3.70	5.23	3.57
en-di	-	-	-	-	-	-	.83	.46	-	1.01	.99	1.60	2.34	2.88	4.03	2.71
fs-di	-	-	-	-	-	-	.06	.04	-	.16	.07	.24	.41	.42	.64	.49
en-hy	30.82	41.42	52.30	50.12	56.97	59.07	35.41	59.51	53.44	75.55	75.01	73.78	72.62	72.84	66.46	72.25
fs-hy	.64	.63	-	1.77	2.79	4.63	2.76	5.48	5.68	11.79	5.42	10.96	12.70	10.63	10.61	13.13
fo	41.05	29.44	19.72	24.41	19.44	14.80	32.00	15.94	11.86	1.00	-	.07	-	-	-	-
fa	.94	.49	-	.95	1.05	1.28	2.75	1.62	1.39	.17	-	.01	-	-	-	-
mt	12.03	10.58	11.34	9.18	8.41	7.99	8.24	6.13	5.89	2.12	5.02	3.18	2.00	2.78	2.85	1.94
hm	-	-	.30	-	-	-	-	-	-	-	-	-	-	-	-	-
il	.38	.09	.09	.09	.13	.23	.19	.13	.28	.23	.13	.19	.19	.19	.25	.19
ap	.05	-	-	-	-	.05	-	-	.05	-	-	-	-	-	-	-
cc	2.02	.30	.21	.91	.91	-	.25	.68	.91	.91	.45	-	-	-	-	-
cm	.16	.57	.72	.53	.68	.26	.35	.78	.45	.88	.96	.94	.80	.79	1.00	.78
nc	-	.07	.02	-	-	-	-	-	-	-	-	-	-	-	-	-
pr	.02	.06	.02	.04	-	.09	.04	.02	.04	-	-	-	-	-	-	-
water	12.09	14.37	14.92	11.80	7.91	11.39	6.60	6.12	6.13	1.08	6.26	.27	.33	.24	.36	.33
Total	103.20	98.78	100.25	100.66	100.72	106.31	98.20	100.28	99.81	101.25	103.21	97.68	99.04	98.45	98.50	100.14
MDI	3.03	1.63	.02	3.82	5.08	8.42	9.01	8.88	10.70	13.73	12.49	12.73	15.18	13.34	15.15	15.42

Table 11. Chemical composition of the type samples - continued.

	17Nä	18Nä	19Nä	20Nä	21Nä	22Nä	23Nä	24Nä	25Nä	26Nä	27Nä	28Nä	29Nä	30Nä	31Nä	32Nä
SiO2	55.06	54.83	54.38	54.11	53.43	54.30	54.46	52.68	53.50	51.37	58.38	52.72	53.84	51.35	46.03	49.26
TiO2	.10	.15	.13	.12	.13	.13	.13	.13	.12	.15	.13	.17	.17	.33	.12	.13
Al2O3	1.21	2.15	1.61	1.58	1.73	1.48	1.56	1.64	1.37	2.45	1.83	3.40	5.03	3.36	4.19	5.88
Fe2O3	1.45	1.69	1.05	4.43	3.51	1.12	1.17	2.34	2.99	1.34	1.39	2.94	1.80	1.60	4.92	2.87
FeO	7.44	8.64	5.54	2.90	3.90	5.98	5.33	6.22	4.91	9.99	8.32	7.30	8.30	12.00	6.83	8.06
MnO	.27	.30	.22	.19	.22	.23	.21	.26	.26	.36	.30	.27	.25	.23	.26	.25
MgO	30.10	28.90	21.50	23.19	22.82	21.90	21.40	24.30	24.92	26.64	26.90	27.80	26.42	23.78	30.20	27.00
CaO	2.73	2.79	15.14	13.73	13.79	14.11	14.85	10.22	10.81	2.72	2.34	3.40	3.58	3.58	2.48	4.07
Na2O	.08	.12	.20	.20	.19	.16	.19	.19	.16	.00	.16	.32	.45	.31	.20	.81
K2O	.01	.08	.00	.01	.00	.00	.00	.01	.02	.12	.01	.07	.06	.34	.12	.13
P2O5	.00	.02	.02	.00	.00	.02	.02	.00	.02	.02	.02	.02	.00	.02	.00	.02
CO2	n.d.	.30	n.d.	.33	.51	n.d.	n.d.	.40	.60	.10	n.d.	.10	.11	.20	n.d.	n.d.
H2O+	.20	1.10	.30	.60	.20	.30	.50	1.20	.20	4.20	2.80	.50	n.d.	2.20	6.80	4.70
H2O-	.02	.05	.05	.10	.30	.04	.04	.06	.04	.15	.16	.10	.40	.15	.30	.12
Total	98.67	101.12	100.14	101.49	100.73	99.77	99.86	99.65	99.92	99.61	102.74	99.11	100.41	99.45	102.45	103.30
Cr	.325	.335	.417	.309	.394	.284	.345	.242	.275	.173	.288	.299	.290	.301	.289	.181
V	.000	.010	.010	.010	.010	.010	.010	.010	.010	.010	.010	.010	.010	.010	.010	.010
Ni	.057	.038	.036	.038	.027	.029	.033	.031	.031	.040	.032	.039	.035	.107	.079	.063
Cu	.001	.005	.001	.000	.000	.001	.000	.004	.004	.003	.000	.006	.000	.029	.002	.003
Co	.009	.009	.007	.007	.006	.007	.007	.008	.007	.009	.009	.009	.009	.019	.013	.011
Zn	.006	.009	.005	.003	.004	.005	.004	.006	.005	.007	.007	.008	.007	.008	.009	.008
S	.000	.000	.000	.010	.000	.000	.000	.000	.000	.000	.000	.010	.020	2.120	.020	.020
Sr	.000	.000	.000	.000	.000	.000	.000	.000	.000	.000	.000	.000	.010	.000	.010	.010
C.I.P.W. norms (weight %)																
Q	.42	.49	.09	2.67	1.57	.37	.91	-	.97	-	7.46	-	-	.33	-	-
or	.07	.49	.01	.07	.01	.01	.01	.07	.13	.72	.07	.43	.43	2.03	.79	.85
ab	.68	1.02	1.69	1.69	1.61	1.35	1.61	1.61	1.35	-	1.35	2.71	3.81	2.62	1.69	6.85
an	2.91	5.08	3.49	3.38	3.86	3.32	3.40	3.59	2.96	6.32	4.24	7.63	11.49	6.76	10.14	11.98
wo-di	4.44	2.81	29.85	26.16	25.61	27.79	29.29	18.62	19.52	2.68	3.02	3.54	2.33	4.01	.90	3.37
en-di	3.41	2.11	22.86	22.17	21.00	21.09	22.54	14.37	15.62	1.93	2.25	2.73	1.74	2.87	.72	2.55
fs-di	.57	.42	3.87	.57	1.48	3.86	3.65	2.26	1.65	.51	.48	.43	.36	.78	.08	.48
en-hy	71.56	69.90	30.69	35.58	35.83	33.46	30.76	45.51	46.47	61.89	64.74	63.67	61.74	56.56	45.58	38.68
fs-hy	11.97	14.02	5.19	.92	2.53	6.12	4.98	7.16	4.91	16.35	13.71	10.01	12.78	15.34	5.18	7.22
fo	-	-	-	-	-	-	-	.46	-	1.79	-	2.02	1.62	-	20.27	18.24
fa	-	-	-	-	-	-	-	.08	-	.52	-	.35	.37	-	2.54	3.75
mt	2.10	2.47	1.55	6.45	5.11	1.65	1.72	3.42	4.36	1.97	2.04	4.29	2.63	2.34	7.16	4.18
il	.19	.28	.25	.23	.25	.25	.25	.25	.23	.28	.25	.32	.32	.63	.23	.25
ap	-	.05	.05	-	-	.05	.05	-	.05	.05	.05	.05	-	.05	-	.05
cc	-	.68	-	.75	1.16	-	-	.91	1.36	.23	-	.23	.25	.45	-	-
cm	.70	.72	.90	.67	.85	.61	.74	.52	.59	.37	.62	.64	.62	.65	.62	.39
pr	-	-	-	.02	-	-	-	-	-	-	-	.02	.04	3.97	.04	.04
water	.22	1.15	.35	.70	.50	.34	.54	1.26	.24	4.35	2.96	.60	.40	2.35	7.10	4.82
Total	99.23	101.71	100.83	102.02	101.37	100.25	100.43	100.08	100.40	99.96	103.23	99.65	100.93	101.74	103.04	103.71
MDI	14.80	17.46	14.58	6.90	9.10	15.52	14.80	14.05	11.18	20.02	24.14	15.30	18.69	23.86	11.78	20.83

Table 11. Chemical composition of the type samples - continued.

	33Nä	34Nä	35Nä	36Nä	37Nä	38Nä	39Nä	40Nä	41Nä	42Nä	43Nä	44Nä	45Nä	46Nä	47Nä	48Nä
SiO2	43.76	42.44	48.28	45.90	51.14	52.14	53.58	51.02	51.25	48.88	53.60	53.11	52.13	54.27	48.82	51.76
TiO2	.08	.12	.18	.08	.22	.20	.27	.20	.48	.37	.45	.58	.40	.62	.22	.63
Al2O3	1.20	2.04	3.79	5.27	6.58	10.51	10.50	10.31	11.01	10.16	9.00	9.85	8.85	12.44	18.99	19.30
Fe2O3	4.40	3.35	2.39	2.83	2.71	1.72	1.45	1.86	2.11	2.92	1.84	2.15	2.66	1.85	1.19	2.15
FeO	5.30	5.80	7.11	7.30	5.79	7.66	5.72	7.19	8.14	8.19	9.23	9.05	8.33	7.69	4.14	5.93
MnO	.23	.19	.22	.23	.21	.23	.19	.19	.22	.23	.25	.23	.23	.19	.14	.17
MgO	33.70	33.71	28.41	28.63	16.45	18.23	15.30	15.50	13.50	21.84	19.40	17.20	18.64	12.40	9.92	6.46
CaO	2.15	2.62	4.41	3.61	14.18	7.00	13.99	8.73	11.52	5.23	5.94	6.55	5.91	9.57	13.62	9.49
Na2O	.09	.11	.14	.24	.72	1.09	1.17	1.30	1.39	1.05	1.28	1.49	1.17	1.78	1.67	2.78
K2O	.02	.04	.10	.07	.17	.13	.20	.30	.36	.42	.49	.70	.43	.89	.31	1.26
P2O5	.02	.02	.02	.02	.02	.02	.02	.02	.02	.05	.05	.05	.05	.07	.05	.09
CO2	.30	.07	.00	.30	.30	.00	n.d.	n.d.	n.d.	.40	n.d.	n.d.	.20	n.d.	.10	.20
H2O+	7.60	9.10	5.20	4.60	.60	.90	.60	2.20	.80	1.10	.70	1.10	1.20	.60	.60	.90
H2O-	.32	.10	.09	.21	.14	.14	.05	.13	.10	.09	.08	.10	.05	.10	.12	.10
Total	99.17	99.71	100.34	99.29	99.23	99.97	103.04	98.95	100.90	100.93	102.31	102.16	100.25	102.47	99.89	101.22
Cr	.245	.463	.283	.268	.239	.240	.205	.176	.120	.245	.193	.168	.197	.141	.030	.020
V	.000	.010	.010	.000	.010	.010	.010	.010	.020	.010	.020	.020	.020	.020	.010	.020
Ni	.078	.095	.076	.061	.138	.049	.022	.036	.024	.075	.058	.050	.058	.027	.029	.011
Cu	.003	.000	.003	.008	.200	.011	.007	.007	.021	.008	.004	.007	.009	.006	.017	.009
Co	.012	.010	.009	.010	.008	.008	.006	.007	.007	.009	.009	.008	.008	.007	.004	.004
Zn	.007	.009	.007	.011	.005	.008	.005	.007	.008	.008	.008	.009	.009	.008	.004	.007
S	.010	.030	.010	.020	.710	.010	.010	.030	.050	.040	.030	.040	.030	.010	.030	.010
Sr	.000	.000	.000	.010	.010	.020	.020	.020	.020	.010	.010	.020	.020	.020	.030	.030
							C.I.P.W. norms (weight %)									
Q	-	-	-	-	-	-	-	-	-	-	-	-	.21	1.37	-	-
or	.13	.26	.61	.50	1.08	.91	1.32	1.91	2.27	2.56	2.98	4.28	2.69	5.40	2.03	7.65
ab	.76	.93	1.18	2.03	6.09	9.22	9.90	11.00	11.76	8.89	10.83	12.61	9.90	15.06	14.13	23.52
an	2.80	4.95	9.41	13.05	14.18	23.33	22.74	21.34	22.67	21.73	17.33	18.05	17.55	23.25	43.31	36.36
wo-di	2.44	3.12	5.15	1.18	22.61	4.70	19.43	9.12	14.34	.57	4.93	5.90	4.25	9.92	9.73	3.70
en-di	1.99	2.53	3.98	.91	17.37	3.36	14.24	6.43	9.65	.42	3.45	4.07	3.04	6.65	7.02	2.30
fs-di	.15	.23	.62	.14	2.85	.93	3.35	1.91	3.60	.09	1.07	1.34	.83	2.53	1.83	1.19
en-hy	42.70	31.96	45.82	41.03	24.68	41.49	21.42	32.01	20.29	34.85	40.68	35.41	43.44	24.27	7.33	12.76
fs-hy	3.19	2.90	7.12	6.41	4.06	11.43	5.04	9.51	7.57	7.83	12.60	11.66	11.85	9.24	1.91	6.59
fo	27.51	34.67	14.69	20.61	.26	.44	1.74	.15	2.68	13.44	2.95	2.38	-	-	7.34	.77
fa	2.26	3.46	2.52	3.55	.05	.13	.45	.05	1.10	3.33	1.01	.86	-	-	2.11	.44
mt	6.38	4.88	3.49	4.10	3.95	2.52	2.13	2.72	3.10	4.26	2.71	3.16	3.90	2.73	1.75	3.16
il	.15	.23	.34	.15	.42	.38	.51	.38	.91	.70	.85	1.10	.76	1.18	.42	1.20
ap	.05	.05	.05	.05	.05	.05	.05	.05	.05	.12	.12	.12	.12	.17	.12	.21
cc	.68	.16	-	.68	.68	-	-	-	-	.91	-	-	.45	-	.23	.45
cm	.53	1.00	.61	.58	.51	.52	.44	.38	.26	.53	.42	.36	.42	.30	.06	.04
pr	.02	.06	.02	.04	1.33	.02	.02	.06	.09	.07	.06	.07	.06	.02	.06	.02
water	7.92	9.20	5.29	4.81	.74	1.04	.65	2.33	.90	1.19	.78	1.20	1.25	.70	.72	1.00
Total	99.66	100.56	100.90	99.83	100.90	100.47	103.44	99.35	101.27	101.48	102.76	102.59	100.73	102.80	100.10	101.37
MDI	7.89	9.39	13.81	14.26	17.85	24.43	23.10	27.90	30.73	24.31	30.08	33.07	27.95	36.68	24.42	42.44

Table 11. Chemical composition of the type samples - continued.

	49Nä	50Nä	51Nä	52Nä	1Py	2Py	3Py	4Py	5Py	6Py	7Py	8Py	1Po	2Po	3Po	4Po
SiO2	55.08	55.06	55.82	60.51	41.95	43.22	49.86	47.35	50.00	52.40	53.29	51.83	47.18	47.68	46.64	42.16
TiO2	.53	.68	1.32	1.38	.13	.17	.18	.20	.45	.33	.25	.73	.10	.13	.13	.10
Al2O3	17.97	17.01	14.26	14.31	7.37	12.03	12.20	21.74	16.43	13.41	20.02	23.55	6.99	13.55	15.76	8.76
Fe2O3	1.59	2.17	2.79	3.17	5.79	3.88	6.43	1.49	6.00	6.66	1.88	3.11	3.37	1.48	1.29	3.88
FeO	6.24	6.65	8.91	7.14	6.70	9.10	4.70	6.30	4.30	4.30	5.60	4.60	8.68	7.88	7.47	7.70
MnO	.15	.15	.19	.13	.18	.25	.21	.13	.14	.22	.15	.13	.13	.21	.21	.15
MgO	7.92	5.88	4.20	2.00	28.75	22.37	19.95	10.01	9.63	15.67	9.20	4.46	23.80	14.30	15.30	26.36
CaO	10.15	8.90	4.96	4.70	3.61	5.24	5.49	10.42	9.46	6.76	11.12	11.60	2.93	7.26	5.27	3.56
Na2O	2.57	2.96	4.10	3.96	.07	.73	.70	2.17	2.48	1.42	1.89	2.76	.04	1.34	1.92	.04
K2O	.82	1.24	1.48	2.87	.07	.14	.24	.31	.48	.25	.18	.35	.01	.12	.28	.11
P2O5	.09	.11	.16	.41	.00	.00	.00	.00	n.d.	.02	.00	.05	.02	.00	.02	.00
CO2	n.d.	n.d.	.20	.22	.07	.07	.15	.15	n.d.	.15	.15	.11	n.d.	n.d.	n.d.	.04
H2O+	.70	.70	1.50	n.d.	6.90	3.90	n.d.	n.d.	n.d.	n.d.	n.d.	n.d.	6.70	4.70	5.80	7.00
H2O-	.08	.09	.08	n.d.	.90	.30	n.d.	n.d.	n.d.	n.d.	n.d.	n.d.	.57	.09	.27	.30
Total	103.89	101.60	99.97	100.80	102.49	101.40	100.11	100.27	99.37	101.59	103.73	103.28	100.52	98.74	100.36	100.16
Cr	.031	.013	.003	.002	.261	.012	.190	.020	.056	.140	.055	.005	.058	.094	.078	.154
V	.020	.020	.050	.030	.010	.010	.010	.000	.012	.010	.010	.030	.010	.010	.010	.000
Ni	.015	.010	.004	.001	.132	.095	.090	.061	.026	.044	.020	.019	.140	.135	.070	.123
Cu	.008	.008	.005	.000	.013	.001	.052	.015	.010	.000	.006	.007	.034	.156	.010	.004
Co	.005	.005	.004	.003	.012	.012	n.d.	n.d.	.004	n.d.	n.d.	n.d.	.010	.010	.009	.011
Zn	.006	.008	.010	.010	.008	.009	.007	.006	.008	.008	.005	.006	.009	.008	.008	.006
S	.010	.050	.010	.000	.020	.010	.050	.000	n.d.	.000	.010	.000	.020	.290	.000	.070
Sr	.030	.030	.010	.020	.010	.020	.020	.040	n.d.	.020	.030	.040	.000	.020	.030	.000
							C.I.P.W. norms (weight %)									
Q	2.39	4.13	6.14	12.67	-	-	1.98	-	1.11	5.39	2.31	2.19	-	-	-	-
or	5.05	7.54	8.83	17.11	.49	.97	1.56	2.10	2.85	1.62	1.26	2.34	.08	.85	1.86	.66
ab	21.75	25.05	34.69	33.51	.59	6.18	5.92	18.36	20.99	12.02	15.99	23.36	.34	11.34	16.25	.34
an	34.98	29.36	16.09	12.72	17.47	25.55	26.29	48.53	32.27	29.41	45.51	50.70	14.41	30.53	26.01	17.41
C	-	-	-	-	.76	1.29	1.13	-	-	-	-	-	1.63	-	2.73	2.19
wo-di	6.18	5.88	2.59	2.73	-	-	-	.92	6.12	1.27	3.64	2.43	-	2.29	-	-
en-di	3.91	3.41	1.19	1.03	-	-	-	.61	4.91	1.06	2.45	1.57	-	1.56	-	-
fs-di	1.88	2.19	1.38	1.74	-	-	-	.25	.50	.06	.91	.69	-	.55	-	-
en-hy	15.87	11.29	9.31	3.95	32.48	20.99	50.06	4.66	19.14	37.97	20.51	9.58	56.48	27.40	23.05	35.03
fs-hy	7.63	7.27	10.78	6.68	3.43	5.23	3.26	1.93	1.94	2.11	7.63	4.22	12.76	9.71	7.78	5.87
fo	-	-	-	-	27.48	24.33	-	13.85	-	-	-	-	2.13	5.46	10.60	21.47
fa	-	-	-	-	3.20	6.68	-	6.32	-	-	-	-	.53	2.13	3.95	3.97
mt	2.35	3.19	4.16	4.66	8.42	5.65	9.35	2.16	8.73	9.68	2.75	4.58	4.91	2.17	1.89	5.63
il	1.01	1.29	2.51	2.62	.25	.32	.34	.38	.85	.63	.47	1.39	.19	.25	.25	.19
ap	.21	.26	.38	.97	-	-	-	-	-	.05	-	.12	.05	-	.05	-
cc	-	-	.45	.50	.16	.16	.34	.34	-	.34	.34	.25	-	-	-	.09
cm	.07	.03	.01	-	.56	.03	.41	.04	.12	.30	.12	.01	.12	.20	.17	.33
pr	.02	.09	.02	-	.04	.02	.09	-	-	-	.02	-	.04	.54	-	.13
water	.78	.79	1.58	-	7.80	4.20	-	-	-	-	-	-	7.27	4.79	6.07	7.30
Total	104.06	101.77	100.11	100.90	103.13	101.60	100.73	100.47	99.54	101.89	103.91	103.43	100.92	99.77	100.66	100.62
MDI	40.50	50.05	69.27	79.49	8.99	20.89	14.10	29.92	30.98	23.37	28.85	34.40	15.51	27.30	32.35	12.47

Table 11. Chemical composition of the type samples - continued.

	5Po	6Po	7Po	8Po	9Po	10Po	11Po	12Po	13Po	14Po	15Po	16Po	17Po	18Po	1Sy	2Sy
SiO2	46.49	47.28	50.25	49.30	43.19	48.71	50.92	52.85	53.04	51.98	50.00	45.47	40.95	50.00	48.08	46.52
TiO2	.13	.22	.37	.22	.15	.28	.23	.32	.42	.52	.75	1.77	2.75	.83	.20	.15
Al2O3	12.93	14.09	20.73	18.56	11.59	18.77	17.33	19.27	17.89	17.26	20.78	15.48	14.94	22.12	16.23	16.87
Fe2O3	5.56	4.33	3.35	3.82	2.89	3.95	5.67	2.58	3.51	4.31	4.36	7.95	7.95	.23	2.71	1.32
FeO	5.70	6.20	5.30	6.40	11.40	7.10	4.80	4.60	6.70	5.50	4.39	8.80	13.30	9.76	5.45	5.86
MnO	.21	.19	.14	.18	.23	.18	.18	.15	.18	.19	.10	.18	.17	.15	.14	.17
MgO	21.23	18.67	10.92	12.59	21.90	13.78	14.45	9.34	9.97	6.77	2.32	6.98	6.42	5.26	8.66	12.15
CaO	5.64	6.86	10.91	9.24	4.87	8.90	8.73	9.28	9.33	11.03	11.01	10.58	8.60	10.00	8.32	10.41
Na2O	.81	1.08	1.85	1.83	.77	1.79	1.59	2.39	2.07	2.55	3.51	2.11	1.97	2.46	1.95	1.50
K2O	.13	.19	.34	.25	.11	.28	.19	.36	.25	.42	.20	.20	.20	.57	1.59	.33
P2O5	.00	.00	.02	.00	.00	.00	.00	.00	.00	.00	n.d.	.00	.00	n.d.	.07	.02
CO2	.04	.22	.15	.11	.07	.15	.15	.15	.18	.11	n.d.	.07	.07	n.d.	n.d.	n.d.
H2O+	2.10	2.50	n.d.	n.d.	2.40	n.d.	n.d.	n.d.	n.d.	1.00	n.d.	1.20	1.10	n.d.	n.d.	n.d.
H2O-	.50	.20	n.d.	n.d.	.10	n.d.	n.d.	n.d.	n.d.	.10	n.d.	.10	.30	n.d.	n.d.	n.d.
Total	101.47	102.03	104.33	102.50	99.67	103.89	104.24	101.29	103.54	101.74	97.42	100.89	98.72	101.38	93.40	95.30
Cr	.077	.045	.018	.023	.016	.020	.024	.058	.044	.006	.000	.000	.000	.001	.064	.086
V	.010	.010	.010	.010	.010	.010	.010	.010	.020	.030	.030	.160	.230	.015	.000	.000
Ni	.108	.078	.044	.052	.082	.058	.053	.018	.027	.008	n.d.	.013	.011	.015	.310	.059
Cu	.043	.016	.003	.002	.000	.001	.002	.001	.002	.012	.003	.021	.030	.002	.029	.018
Co	.011	.009	n.d.	n.d.	.011	n.d.	n.d.	n.d.	n.d.	.005	n.d.	.008	.009	.009	.012	.006
Zn	.007	.007	.006	.007	.009	.008	.009	.010	.009	.007	.006	.007	.010	.010	.008	.006
S	.040	.090	.030	.010	.000	.000	.020	.000	.040	.010	n.d.	.010	.040	n.d.	1.030	.030
Sr	.020	.020	.030	.030	.020	.030	.020	.030	.020	.030	n.d.	.020	.020	n.d.	.060	.030
C.I.P.W. norms (weight %)																
Q	-	-	-	-	-	-	-	2.24	2.90	3.46	3.29	.56	-	-	-	-
or	.91	1.26	2.21	1.68	.80	1.86	1.27	2.34	1.62	2.69	1.19	1.32	1.33	3.39	9.79	2.15
ab	6.85	9.14	15.65	15.49	6.52	15.15	13.45	20.22	17.52	21.58	29.70	17.85	16.67	20.82	16.50	12.69
an	27.73	32.64	47.16	41.59	23.72	42.25	39.52	40.68	38.71	34.31	40.35	32.11	31.26	47.62	30.64	38.22
C	1.27	.12	-	-	1.49	-	-	-	-	-	-	-	-	-	-	-
wo-di	-	-	2.46	1.48	-	.40	1.19	1.84	2.69	8.23	5.96	8.33	4.58	.83	4.25	5.55
en-di	-	-	1.79	1.06	-	.28	.94	1.33	1.82	5.61	3.57	5.55	2.44	.36	3.02	3.86
fs-di	-	-	.44	.29	-	.08	.11	.34	.66	1.98	2.07	2.16	2.00	.46	.86	1.23
en-hy	36.58	30.77	17.28	19.62	19.38	16.61	34.27	21.94	23.02	11.34	2.23	11.98	7.61	7.74	16.27	11.50
fs-hy	4.21	5.11	4.20	5.39	6.72	4.71	3.92	5.68	8.29	4.01	1.29	4.66	6.24	9.85	4.65	3.68
fo	11.64	11.10	5.71	7.49	24.64	12.22	.55	-	-	-	-	-	4.32	3.51	1.74	10.53
fa	1.48	2.03	1.53	2.27	9.41	3.82	.07	-	-	-	-	-	3.90	4.92	.55	3.71
mt	8.08	6.30	4.88	5.56	4.21	5.75	8.24	3.76	5.13	6.32	6.39	11.89	12.05	.37	3.93	1.91
il	.25	.42	.70	.42	.28	.53	.44	.61	.80	.99	1.42	3.36	5.22	1.58	.38	.28
ap	-	-	.05	-	-	-	-	-	-	-	-	-	-	-	.17	.05
cc	.09	.50	.34	.25	.16	.34	.34	.34	.41	.25	-	.16	.16	-	-	-
cm	.17	.10	.04	.05	.03	.04	.05	.12	.09	.01	-	-	-	-	.14	.19
pr	.07	.17	.06	.02	-	-	.04	-	.07	.02	-	.02	.07	-	1.93	.06
water	2.60	2.70	-	-	2.50	-	-	-	-	1.10	-	1.30	1.40	-	-	-
Total	101.93	102.36	104.49	102.66	99.85	104.05	104.40	101.45	103.73	101.89	97.48	101.26	99.25	101.45	94.82	95.62
MDI	14.84	19.03	24.81	26.34	25.30	26.38	19.85	32.22	32.46	38.05	43.92	33.68	39.71	40.04	37.51	26.36

Table 11. Chemical composition of the type samples - continued.

	3Sy	4Sy	5Sy	6Sy	7Sy	8Sy	9Sy	10Sy	11Sy	12Sy	13Sy	14Sy	15Sy	16Sy	17Sy	18Sy
SiO2	44.24	46.47	46.68	48.39	44.93	49.85	46.29	45.69	48.24	44.11	50.81	52.18	51.25	51.08	52.69	49.84
TiO2	.17	.32	.43	.18	.27	.35	.17	.15	.40	.18	.32	.52	.43	.55	.42	.43
Al2O3	7.50	16.71	17.54	17.42	14.26	24.93	14.50	15.30	20.84	12.85	20.31	21.76	19.65	18.11	21.32	17.20
Fe2O3	5.74	2.13	3.85	2.57	2.67	.72	3.24	2.71	1.10	4.30	1.74	2.07	1.63	1.63	1.66	1.70
FeO	9.05	9.34	8.28	7.94	7.77	3.34	8.32	9.28	5.52	9.23	5.96	4.31	6.01	6.87	5.40	7.51
MnO	.18	.21	.18	.19	.22	.09	.23	.22	.13	.25	.17	.14	.17	.19	.15	.19
MgO	25.79	15.40	13.30	13.80	17.50	4.50	16.40	16.80	8.60	19.80	6.60	4.90	6.60	6.90	6.40	7.20
CaO	6.13	8.79	7.50	8.94	6.91	13.90	8.03	8.49	11.05	6.42	11.80	11.76	11.94	12.10	11.92	11.90
Na2O	.36	1.44	1.55	1.54	1.00	2.86	.98	1.28	2.28	1.13	2.51	2.97	2.43	2.22	2.63	2.26
K2O	.00	.31	.27	.20	.48	.41	.18	.14	.37	.16	.30	.54	.34	.43	.36	.27
P2O5	.05	.02	.05	.00	.02	.00	.00	.00	.02	.00	.00	.05	.00	.05	.02	.00
CO2	n.d.	n.d.	n.d.	n.d.	n.d.	n.d.	n.d.	n.d.	n.d.	n.d.	n.d.	n.d.	n.d.	n.d.	n.d.	n.d.
H2O+	n.d.	1.60	2.80	1.90	4.10	.90	3.20	2.20	2.00	2.70	.70	1.10	.80	1.20	.80	1.50
H2O-	n.d.	.06	.11	.09	.16	.04	.04	.06	.04	.09	.04	.03	.04	.04	.05	.02
Total	99.21	102.80	102.54	103.16	100.29	101.89	101.58	102.32	100.59	101.22	101.26	102.33	101.29	101.37	103.82	100.02
Cr	.039	.023	.010	.028	.020	.005	.042	.030	.012	.032	.009	.008	.006	.008	.005	.010
V	.010	.010	.010	.010	.010	.010	.010	.010	.010	.010	.010	.020	.020	.020	.020	.020
Ni	.147	.070	.066	.054	.079	.017	.061	.077	.035	.090	.013	.010	.012	.010	.010	.012
Cu	.022	.008	.007	.009	.003	.007	.008	.011	.006	.006	.011	.012	.014	.008	.009	.008
Co	.012	.010	.010	.009	.009	.003	.010	.011	.006	.011	.005	.004	.005	.005	.004	.008
Zn	.007	.008	.010	.008	.012	.004	.009	.009	.006	.010	.007	.005	.006	.008	.006	.005
S	.040	.060	.080	.010	.030	.001	.040	.020	.030	.020	.010	.000	.020	.000	.010	.010
Sr	.000	.020	.030	.020	.030	.050	.020	.020	.040	.020	.030	.050	.030	.030	.030	.030
C.I.P.W. norms (weight %)																
Q	-	-	-	-	-	-	-	-	-	-	-	.62	-	.07	.10	-
or	.01	1.98	1.81	1.33	3.05	2.75	1.21	.97	2.45	1.09	1.98	3.52	2.21	2.75	2.33	1.80
ab	3.05	12.19	13.12	13.03	8.46	21.45	8.29	10.83	19.29	9.56	21.24	25.13	20.56	18.79	22.26	19.12
an	18.84	38.15	36.88	39.96	32.90	53.81	34.56	35.52	45.41	29.45	43.16	44.29	41.61	38.08	45.21	35.89
ne	-	-	-	-	-	1.49	-	-	-	-	-	-	-	-	-	-
C	-	-	1.14	-	-	-	-	-	-	-	-	-	-	-	-	-
wo-di	4.69	2.23	-	1.83	.52	6.32	2.20	2.76	3.88	1.00	6.42	5.73	7.36	9.03	5.76	9.66
en-di	3.55	1.48	-	1.24	.37	4.05	1.54	1.87	2.55	.72	3.89	3.68	4.46	5.30	3.59	5.54
fs-di	.67	.59	-	.45	.10	1.86	.48	.67	1.05	.20	2.19	1.68	2.50	3.29	1.82	3.70
en-hy	24.33	9.34	21.07	17.57	18.51	-	21.67	10.91	5.96	15.02	9.93	8.61	11.58	11.94	12.41	9.77
fs-hy	4.59	3.71	7.39	6.42	5.15	-	6.76	3.92	2.45	4.17	5.59	3.92	6.48	7.42	6.29	6.53
fo	25.59	19.34	8.48	10.95	17.32	5.05	12.40	20.42	9.08	23.56	1.89	-	.35	-	-	1.88
fa	5.32	8.47	3.28	4.41	5.31	2.55	4.26	8.09	4.11	7.20	1.17	-	.21	-	-	1.38
mt	8.35	3.11	5.60	3.75	3.89	1.07	4.72	3.95	1.62	6.26	2.55	3.05	2.41	2.41	2.45	2.51
il	.32	.61	.82	.34	.51	.66	.32	.28	.76	.34	.61	.99	.82	1.04	.80	.82
ap	.12	.05	.12	-	.05	-	-	-	.05	-	-	.12	-	.12	.05	-
cm	.08	.05	.02	.06	.04	.01	.09	.06	.03	.07	.02	.02	.01	.02	.01	.02
pr	.07	.11	.15	.02	.06	-	.07	.04	.06	.04	.02	-	.04	-	.02	.02
water	-	1.66	2.91	1.99	4.26	.94	3.24	2.26	2.04	2.79	.74	1.13	.84	1.24	.85	1.52
Total	99.58	103.05	102.79	103.36	100.52	102.02	101.83	102.56	100.76	101.47	101.39	102.48	101.44	101.49	103.95	100.16
MDI	15.70	28.17	27.46	26.79	24.17	30.44	22.95	26.14	31.46	24.36	34.98	37.41	35.11	36.43	34.48	37.56

Table 11. Chemical composition of the type samples - continued.

	19Sy	20Sy	21Sy	22Sy	23Sy	24Sy	25Sy	26Sy	27Sy	28Sy	1Ku	2Ku	3Ku	4Ku	5Ku	6Ku
SiO2	49.99	51.68	54.56	43.67	43.93	45.28	45.66	43.64	46.01	52.50	46.78	48.33	46.50	46.80	47.70	50.95
TiO2	.55	.47	.32	2.10	1.93	1.82	1.43	2.34	1.63	.50	.27	1.47	.33	.45	.48	.42
Al2O3	20.38	18.04	25.11	14.80	14.92	14.62	14.56	15.33	15.20	22.57	17.62	6.50	16.82	18.64	16.28	16.92
Fe2O3	1.90	2.50	1.57	9.28	8.51	7.52	6.49	8.94	6.53	2.33	.90	.60	2.05	1.24	1.46	1.94
FeO	6.47	7.14	1.70	11.09	10.93	11.22	9.74	11.59	9.97	4.30	6.46	6.53	7.26	5.32	5.95	5.00
MnO	.17	.21	.04	.21	.21	.21	.18	.19	.19	.10	.13	.21	.18	.12	.12	.11
MgO	6.20	6.70	1.04	6.40	7.10	6.90	6.90	6.70	6.20	3.64	12.43	25.80	9.66	7.10	11.93	8.00
CaO	10.67	11.37	11.15	10.62	10.60	10.88	11.69	10.22	11.35	9.92	7.86	5.26	10.28	10.27	8.54	8.90
Na2O	2.37	2.66	3.85	1.87	1.85	1.97	1.79	1.99	1.99	4.02	2.35	.38	2.14	2.50	2.40	2.59
K2O	.36	.27	.22	.17	.17	.17	.35	.17	.17	.36	.75	.02	.23	.25	.36	.47
P2O5	.05	.05	.02	.00	.00	.00	.00	.00	.00	.09	n.d.	n.d.	.07	.07	n.d.	n.d.
CO2	n.d.	n.d.	n.d.	n.d.	n.d.	n.d.	n.d.	n.d.	n.d.	n.d.	n.d.	n.d.	n.d.	n.d.	n.d.	n.d.
H2O+	1.20	.90	1.30	1.40	1.40	1.60	1.80	1.40	1.70	2.30	n.d.	n.d.	1.41	2.85	n.d.	n.d.
H2O-	.08	.06	.00	.03	.04	.02	.02	.06	.05	.00	n.d.	n.d.	n.d.	n.d.	n.d.	n.d.
Total	100.39	102.05	100.88	101.64	101.59	102.21	100.61	102.57	100.99	102.63	95.55	95.10	96.93	95.61	95.22	95.30
Cr	.023	.000	.014	.000	.000	.000	.000	.004	.003	.007	.020	.023	.023	.012	.009	.019
V	.020	.020	.010	.220	.190	.190	.160	.210	.150	.010	.003	.005	.010	.010	.008	.007
Ni	.013	.009	.003	.017	.015	.015	.013	.014	.013	.005	.250	.012	.039	.027	.052	.015
Cu	.010	.020	.000	.034	.029	.054	.035	.045	.052	.000	.340	.020	.010	.004	.006	.005
Co	.005	.006	.008	.009	.009	.010	.008	.011	.009	.003	.011	.009	.006	.004	.007	.005
Zn	.008	.007	.002	.009	.009	.010	.010	.010	.009	.006	.013	.007	.008	.007	.006	.005
S	.010	.020	.010	.020	.020	.030	.010	.080	.180	.010	n.d.	n.d.	.000	.000	n.d.	n.d.
Sr	.030	.030	.060	.020	.020	.020	.020	.020	.020	.050	n.d.	n.d.	.030	.040	n.d.	n.d.
C.I.P.W. norms (weight %)																
Q	.17	.16	6.11	-	-	-	-	-	.58	.04	-	-	-	-	-	2.20
or	2.33	1.80	1.69	1.15	1.15	1.15	2.22	1.15	1.15	2.46	4.46	.13	1.57	1.75	2.14	2.79
ab	20.06	22.51	32.58	15.82	15.65	16.67	15.15	16.84	16.84	34.02	19.89	3.22	18.11	21.16	20.31	21.92
an	43.81	36.39	50.39	31.42	31.83	30.47	30.59	32.32	31.97	42.31	35.30	15.96	35.51	38.77	32.58	33.15
wo-di	3.68	8.22	2.00	8.88	8.67	9.81	11.44	7.67	10.16	2.64	1.54	4.23	6.28	4.90	4.09	4.59
en-di	2.15	4.80	1.24	5.33	5.25	5.66	6.82	4.58	5.92	1.58	1.06	3.29	3.98	3.12	2.86	3.13
fs-di	1.34	3.03	.64	3.08	2.94	3.71	4.04	2.69	3.76	.92	.36	.48	1.90	1.46	.89	1.11
en-hy	13.36	12.03	1.35	10.71	10.12	9.84	9.57	9.31	9.90	7.49	3.09	43.37	7.34	8.38	11.07	16.83
fs-hy	8.34	7.60	.70	6.19	5.66	6.45	5.66	5.48	6.29	4.38	1.06	6.38	3.49	3.91	3.45	5.99
fo	-	-	-	.10	1.77	1.46	.73	2.18	-	-	20.51	12.43	8.97	4.35	11.09	-
fa	-	-	-	.06	1.09	1.05	.48	1.41	-	-	7.76	2.01	4.71	2.24	3.80	-
mt	2.80	3.67	2.30	13.96	12.77	11.34	9.77	13.44	9.81	3.40	1.31	.88	3.00	1.82	2.14	2.83
il	1.04	.89	.61	3.99	3.67	3.46	2.72	4.44	3.10	.95	.51	2.79	.63	.85	.91	.80
ap	.12	.12	.05	-	-	-	-	-	-	.21	-	-	.17	.17	-	-
cm	.05	-	.03	-	-	-	-	.01	.01	.02	.04	.05	.05	.03	.02	.04
pr	.02	.04	.02	.04	.04	.06	.02	.15	.34	.02	-	-	-	-	-	-
water	1.28	.96	1.30	1.43	1.44	1.62	1.82	1.46	1.75	2.30	-	-	1.41	2.85	-	-
Total	100.55	102.21	101.00	102.16	102.04	102.75	101.02	103.15	101.57	102.74	96.90	95.23	97.11	95.74	95.34	95.38
MDI	35.10	39.12	43.73	35.07	34.57	37.44	35.86	35.80	36.89	44.49	35.62	13.82	34.23	35.31	34.00	38.15

Table 11. Chemical composition of the type samples - continued.

	7Ku	8Ku	1Li	2Li	3Li	4Li	5Li	6Li	7Li	8Li	9Li	10Li	11Li	1Ch	1Gr
SiO2	52.87	48.50	48.27	45.98	47.18	44.89	48.47	46.25	50.41	48.59	50.85	49.69	53.40	51.84	64.82
TiO2	1.32	2.12	.22	.32	.25	.25	.18	.17	.53	.60	.43	.27	.50	.45	.95
Al2O3	16.58	12.58	16.38	10.26	16.18	3.66	16.74	16.76	15.42	14.86	16.47	19.85	23.88	14.60	11.04
Fe2O3	3.28	6.44	1.44	2.53	2.21	5.72	1.05	2.61	1.90	2.88	1.02	1.00	1.40	1.43	2.70
FeO	5.46	10.27	5.79	11.81	7.40	10.37	7.34	6.95	7.99	9.53	7.57	5.44	4.31	6.11	7.01
MnO	.11	.20	.14	.25	.15	.27	.17	.15	.17	.23	.15	.13	.08	.12	.10
MgO	5.24	4.97	9.75	13.40	8.70	24.70	10.10	12.20	6.30	5.70	5.40	4.90	1.65	9.65	.70
CaO	7.29	9.93	10.53	6.58	10.28	5.17	9.40	9.50	10.26	11.53	11.72	13.38	6.81	8.60	1.09
Na2O	3.73	3.00	2.28	1.20	2.04	.11	1.94	1.78	2.72	2.45	2.71	2.68	7.48	2.80	3.81
K2O	.25	.61	.23	.12	.17	.02	.16	.17	.30	.19	.24	.20	.31	.13	2.94
P2O5	n.d.	n.d.	.05	.05	.05	.05	.05	.07	.07	.07	.09	.05	.14	n.d.	.30
CO2	n.d.	n.d.	n.d.	n.d.	n.d.	n.d.	n.d.	n.d.	n.d.	n.d.	n.d.	n.d.	n.d.	n.d.	n.d.
H2O+	n.d.	n.d.	2.78	1.47	1.35	3.34	1.58	2.47	1.52	.93	1.37	.98	1.88	n.d.	1.14
H2O-	n.d.	n.d.	n.d.	n.d.	n.d.	n.d.	n.d.	n.d.	n.d.	n.d.	n.d.	n.d.	n.d.	n.d.	.53
Total	96.13	98.62	97.86	93.97	95.96	98.55	97.18	99.08	97.59	97.56	98.02	98.57	101.84	95.73	97.13
Cr	.002	.001	.046	.076	.055	.088	.050	.023	.006	.003	.004	.013	.000	.021	.000
V	.020	.080	.010	.020	.010	.010	.010	.000	.020	.040	.020	.020	.010	.005	.010
Ni	.003	.008	.084	.423	.187	.125	.047	.107	.023	.008	.011	.008	.002	.017	.001
Cu	.002	.019	.067	.233	.366	.084	.029	.067	.009	.018	.012	.001	.000	.006	.005
Co	.005	.009	.004	.014	.008	.012	.006	.009	.004	.006	.004	.003	.002	.005	.002
Zn	.007	.013	.005	.012	.007	.010	.009	.014	.009	.008	.008	.006	.002	.006	.007
S	n.d.	n.d.	.160	1.020	.810	.220	.050	.280	.000	.050	.000	.000	.000	n.d.	.000
Sr	n.d.	n.d.	.030	.020	.030	.000	.030	.030	.030	.030	.030	.030	.080	n.d.	.010
						C.I.P.W. norms (weight %)									
Q	6.15	1.74	-	-	-	-	-	-	1.02	-	.85	-	-	1.28	24.58
or	1.49	3.63	1.56	.86	1.21	.14	1.16	1.22	1.98	1.33	1.63	1.39	2.34	.78	17.45
ab	31.56	25.39	19.29	10.15	17.26	.93	16.42	15.06	23.02	20.73	22.93	22.68	45.45	23.69	32.24
an	27.75	19.05	33.68	22.18	34.39	9.42	36.39	37.13	28.88	28.89	31.96	41.44	30.41	26.88	3.45
ne	-	-	-	-	-	-	-	-	-	-	-	-	9.67	-	-
wo-di	3.51	12.62	7.61	4.23	6.80	6.64	4.14	3.98	9.01	11.63	10.69	10.28	1.03	6.59	-
en-di	2.32	6.69	5.14	2.62	4.44	4.89	2.60	2.75	4.84	5.69	5.40	5.70	.42	4.38	-
fs-di	.95	5.53	1.90	1.37	1.89	1.11	1.29	.91	3.86	5.73	5.04	4.18	.62	1.73	-
en-hy	10.75	5.82	10.57	26.12	12.06	37.41	17.12	11.73	10.91	8.33	8.13	3.52	-	19.70	1.78
fs-hy	4.39	4.81	3.90	13.63	5.12	8.51	8.48	3.90	8.71	8.39	7.59	2.58	-	7.80	9.25
fo	-	-	6.35	4.43	5.47	13.89	3.96	11.48	-	.22	-	2.10	2.59	-	-
fa	-	-	2.58	2.54	2.56	3.48	2.16	4.21	-	.24	-	1.69	4.22	-	-
mt	4.80	9.52	2.11	3.71	3.23	8.32	1.55	3.78	2.80	4.27	1.52	1.50	2.05	2.08	3.94
il	2.51	4.03	.42	.61	.47	.47	.34	.32	1.01	1.14	.82	.51	.95	.85	1.80
ap	-	-	.12	.12	.12	.12	.12	.17	.17	.17	.21	.12	.33	-	.71
cm	-	-	.10	.16	.12	.19	.11	.05	.01	.01	.01	.03	-	.05	-
pr	-	-	.30	1.91	1.52	.41	.09	.52	-	.09	-	-	-	-	-
water	-	-	2.78	1.47	1.35	3.34	1.58	2.47	1.52	.93	1.37	.98	1.88	-	1.67
Total	96.18	98.83	98.40	96.12	98.01	99.28	97.50	99.70	97.73	97.78	98.15	98.68	101.96	95.82	96.88
MDI	51.06	53.91	33.38	33.77	32.56	17.54	32.69	28.26	45.53	45.49	45.08	37.87	54.97	39.65	93.78

n.d. = not determined
MDI = Modified differentiation index (von Gruenewaldt 1973.)

Table 12.

Rare earth element abundances (ppm) in the Porttivaara section.
(For sample numbering, see Table 1.)

Sample	La	Ce	Nd	Sm	Eu	Tb	Tm	Yb	Lu	Eu/Eu*	(La/Yb)N	ΣREE
2Po	1.5	3.1	1.1	.36	.19	.055	.044	.30	.13	1.66	3.03	5.63
4Po	.77	1.3	1.1	.36	.050	.035	.027	.14	.095	0.51	3.33	2.75
7Po	5.	13.	6.5	1.4	.52	.23	.22	.65	.16	1.14	4.66	20.96
12Po	4.1	8.5	4.	.86	.46	.11	.082	.54	.092	1.80	4.60	14.66
16Po	2.7	6.3	3.4	.94	.44	.18	.12	.60	.14	1.37	2.73	11.30
18Po	3.4	7.3	3.8	.78	.44	.18	.19	.45	.091	1.56	4.58	12.64
1Gr	40.	80.	35.	7.4	1.3	.88	.54	2.6	.55	0.59	9.32	132.73

Eu/Eu* is the ratio of Eu concentration in the sample to the value, Eu*, which is obtained by interpolation between Sm and Tb from the chondrite-normalized rare earth element fractionation pattern of the sample.
(La/Yb)N is the ratio of the chondrite-normalized concentrations of La and Yb.
ΣREE is the sum of La+Ce+Sm+Eu+Tb+Yb+Lu in ppm.

ACKNOWLEDGEMENTS

The work reported here was carried out under the direction of Assoc. Prof. Tauno Piirainen, instructor in ore geology at the Department of Geology, University of Oulu, and scientific director of the Koillismaa Research Project in 1971—76. I am extremely grateful for all the advice and encouragement I have received from him in the course of innumerable discussions as he followed the progress of my work with interest. I would also wish to thank my colleagues on the Koillismaa Project for the help which they have given me in so many ways, and in particular the head geologist on the project Mr. Rauno Hugg, Phil. Mag., upon whose geological map the present Appendix Map is principally based.

Especial thanks are also due to the staff of the Institute of Electron Optics at the University of Oulu, and particularly to the head of that department, Mr. Seppo Sivonen, Dipl.Eng., for almost ten years of valuable cooperation on the subject of mineral analyses. I am also most grateful to Dr. Olavi Kouvo, who kindly made his radiometric dating results from the area available for use in this work. I similarly wish to thank the staff of the research laboratory of Rautaruukki Oy at Raahe, and most notably Mr. Erkki Ojaniemi, for carrying out the whole-rock analyses for me, and also Dr. R. Rosenberg at the Reactor Laboratory of the Technical Research Centre of Finland for performing the REE analyses.

I also wish to express my gratitude to Mr. Malcolm Hicks, M. A., who has translated the majority of the manuscript into English and revised the language of those parts which I have written directly in English. The manuscript has been read by Prof. Kauko Laajoki and Assoc. Prof. Tauno Piirainen, both of whom made valuable comments. Prof. Kalevi Kauranne, Director of the Geological Survey of Finland, kindly arranged for this paper to be published in the Survey's Bulletin series.

I was able to carry out the actual research reported here while occupying the position of Research Assistant for the Natural Sciences Research Council of the Academy of Finland, and I have also received financial support from the Outokumpu Oy Foundation.

Accepted for publication 1st December, 1981.

REFERENCES

Alapieti, T., Hugg, R. & Piirainen, T., 1979 a. Structure, mineralogy and chemistry of the Syöte section in the Early Proterozoic Koillismaa layered intrusion, northeastern Finland. Geol. Surv. Finland, Bull. 299. 43 p.

Alapieti, T., Hugg, R., Piirainen, T. & Ruotsalainen, A., 1979 b. The ultramafic and mafic intrusion at Näränkävaara, northeastern Finland. Geol. Surv. Finland, Rep. Invest. No. 35. 31 p.

Anderson, A. T., 1968. The oxygen fugasity of alkaline basalt and related magmas, Tristan da Cunha. Am. J. Sci. 266, 704—727.

Atkins, F. B., 1969. Pyroxenes of the Bushveld intrusion, South Africa. J. Petrology 10, 222—249.

Auranen, O., 1969. Näränkävaaran ultraemäksinen massiivi. Master's thesis. Manuscript at the Department of Geology, University of Turku, Finland. 55 p.

Benderitter, Y., Hérisson, C., Korhonen, H. & Pernu, T., 1978. Magneto—telluric experiments in northern Finland. Geophys. Prospecting 26, 562—571.

Brown, G. M., 1957. Pyroxenes from the early and middle stages of fractionation of the Skaergaard intrusion, East Greenland. Miner. Mag. 31, 511—543.

Buchanan, D. L., 1979. A combined transmission electron microscope and electron microprobe study of Bushveld pyroxenes from the Bethal area. J. Petrology 20, 327—354.

Buddington, A. F., Fahey, J. & Vlisidis, A., 1963. Degree of oxidation of Adirondack iron oxide and iron—titanium oxide minerals in relation to petrogeny. J. Petrology 4, 138—169.

Buddington, A. F. & Lindsley, D. H., 1964. Iron—titanium oxide minerals and synthetic equivalents. J. Petrology 5, 310—357.

Burns, R. G., 1970. Mineralogical applications of crystal field theory. Cambridge: Cambridge Univ. Press. 224 p.

Cameron, E. N., 1975. Postcumulus and subsolidus equilibration of chromite and coexisting silicates in the Eastern Bushveld Complex. Geochim. Cosmochim. Acta 39, 1021—1034.

— , 1977. Chromite in the central sector of the Eastern Bushveld Complex, South Africa. Am. Mineral. 62, 1082—1096.

— , 1978. An unusual titanium-rich oxide mineral from the Eastern Bushveld Complex. Am. Mineral. 63, 37—39.

— , 1979. Titanium-bearing oxide minerals of the Critical Zone of the Eastern Bushveld Complex. Am. Mineral. 64, 140—150.

Cameron, E. N. & Desborough, G. A., 1969. Occurrence and characteristics of chromite deposits — Eastern Bushveld Complex. Econ. Geol. Mon. 4, 23—40.

Cameron, E. N. & Emerson, M. E., 1959. The origin of certain chromite deposits of the eastern part of the Bushveld complex. Econ. Geol. 54, 1151—1213.

Cambell, I. H., 1977. A study of macrorhythmic layering and cumulate processes in the Jimberlana Intrusion, Western Australia. Part I: The upper layered series. J. Petrology 18, 183—215.

— , 1978. Some problems with cumulus theory. Lithos 11, 311—323.

Campbell, I. H. & Borley, G. D., 1974. The geochemistry of pyroxenes from the lower layered series of the Jimberlana intrusion, Western Australia. Contrib. Mineral. Petrol. 47, 281—297.

Campbell, I. H. & Kelly, P. R., 1978. The geochemistry of loveringite, a uranium-rare-earth-bearing accessory phase from the Jimberlana intrusion of Western Australia. Mineral. Mag. 42, 187—193.

Campbell, I. H. & Nolan, J., 1974. Factors effecting the stability field of Ca-poor pyroxene and origin of the Ca-poor minimum in Ca-rich pyroxenes from tholeiitic intrusions. Contrib. Mineral. Petrol. 48, 205—219.

Campbell, I. H., McCall, G. J. H. & Tyrwhitt D. S., 1970. The Jimberlana Norite, Western Australia — a smaller analogue of the Great Dyke of Rhodesia. Geol. Mag. 107, 1—12.

Charmichael, I. S. E., 1967. The iron—titanium oxides of salic volcanic rocks and their associated ferromagnesian silicates. Contrib. Mineral. Petrol. 14, 36—64.

Cressey, G., Schmid, R. & Wood, B. J., 1978. Thermodynamic properties of almandine—grossular garnet solid solutions. Contrib. Mineral. Petrol. 67, 397—404.

Davies, N. J., Cawthorn, G. R., Barton, J. M., Jr. & Morton, M., 1980. Parental magma to the Bushveld Complex. Nature 287, 33—35.

Dickey, J. S., Jr., Yoder, H. S., Jr. & Schairer, J. F., 1971. Chromium in silicate-oxide systems. Carnegie Inst. Wash. Yearb. 70, 118—122.

Enkovaara, A., Härme, M. & Väyrynen, H., 1953. Kivilajikartan selitys C5-B5, Oulu-Tornio. English summary: Explanation to the map of rocks. General Geological Map of Finland, 1: 400 000. 153 p.

Ford, A. B., 1970. Development of the layered series and capping granophyre of the Dufek intrusion of Antarctica. Geol. Soc. South Africa, Spec. Publ. 1, 492—510.

Francombe, M. H., 1957. Lattice changes in spinel-type iron chromites. J. Phys. Chem. Solids 3. 38 p.

Gasparrini, E. G. & Naldrett, 1972. Magnetite and ilmenite in the Sudbury Nickel Irruptive. Econ. Geol. 67, 605—621.

Gatehouse, B. M., Grey, I. E., Campbell, I. H. & Kelly, P., 1978. The crystal structure of loveringite — a new member of the crichtonite group. Am. Mineral. 63, 28—36.

Ghisler, M., 1976. The geology, mineralogy and geochemistry of the pre-orogenic Archaean stratiform chromite deposits at Fiskenaesset, West Greenland. Berlin, Borntraeger. 156 p.

Gruenewaldt, G. von, 1973. The modified differentiation index and the modified crystallization index as parameters of differentiation in layered intrusions. Trans. geol. Soc. S. Afr. 76, 53—61.

Hamlyn, P. R. & Keays, R. R., 1979. Origin of chromite compositional variation in the Panton Sill, Western Australia. Contrib. Mineral. Petrol. 69, 75—82.

Hart, R. H. & Davis, K. E., 1978. Nickel partitioning between olivine and silicate melt. Earth planet. Sci. Lett. 40, 203—219.

Haskin, L. A. & Haskin, M. A., 1968. Rare-earth elements in the Skaergaard intrusion. Geochim. Cosmochim. Acta 32, 433—447.

Himmelberg, G. R. & Ford, A. B., 1976. Pyroxenes of the Dufek Intrusion, Antarctica. J. Petrology 17, 219—243.

Himmelberg, G. R. & Ford, A. B., 1977. Iron—titanium oxides of the Dufek intrusion, Antarctica. Am. Mineral. 62, 623—633.

Hjelt, S.-E., Lanne, E., Ruotsalainen, A. & Heiskanen, V., 1977. Regional interpretation of magnetic and gravimetric measurements, based on combinations of dipping prisms and plates. Geol. Fören. i Stockholm, Förh. 99, 216—225.

Honkamo, M., 1979. Kallioperäkartta — Pre-Quaternary rocks. Lehti — Sheet, 3541, Rytinki. Geological map of Finland, 1: 100 000.

Hoover, J. D., 1978. Melting relations of a new chilled margin sample from the Skaergaard intrusion. Carnegie Inst. Wash. Yearb. 77, 739—745.

Hsu, L. C., 1980. Hydration and phase relations of grossular—spessartine garnets at P_{H_2O} = 2Kb. Contrib. Mineral. Petrol. 71, 407—415.

Hughes, C. J., 1976. Parental magma of the Great Dyke of Rhodesia — voluminous late Archaean high magnesium basalt. Trans. geol. Soc. S. Afr. 79, 179—182.

Irvine, T. N., 1967. Chromian spinel as a petrogenetic indicator, Part 2. Petrologic applications. Can. J. Earth Sci. 4, 71—103.

— , 1975. Crystallization sequences in the Muskox intrusion and other layered intrusions — II. Origin of chromite layers and similar deposits of other magmatic ores. Geochim. Cosmochim. Acta 39, 991—1020.

— , 1977. Origin of chromitite layers in the Muskox intrusion and other stratiform intrusions: a new interpretation. Geology 5, 273—277.

Irvine, T. N. & Smith, C. H., 1967. The ultramafic rocks of the Muskox intrusion, Northwest Territories, Canada. Pp. 38—49 in Ultramafic and related rocks, ed. by P. J. Wyllie. New York, John Wiley and Sons.

Jackson, E. D., 1961. Primary textures and mineral associations in the ultramafic zone of the Stillwater Complex, Montana. U. S. Geol. Surv. Prof. Paper 358, 1—106.

— , 1966. Liquid immiscibility in chromitite seam formation. Econ. Geol. 61, 777—780.

— , 1969. Chemical variation in coexisting chromite and olivine in chromitite zones of the Stillwater Complex. Econ. Geol. Mon. 4, 41—71.

— , 1971. The origin of ultramafic rocks by cumulus processes. Fortschr. Miner. 48, 128—174.

Juopperi, A., 1977. The magnetite gabbro and related Mustavaara vanadium ore deposit in Porttivaara layered intrusion, north-eastern Finland. Geol. Surv. Finland, Bull. 288. 68 p.

Kelly, P. R., Campbell, I. H., Grey, I. E. & Gatehouse, B. M., 1979. Additional data of

loveringite $(Ca,REE)(Ti,Fe,Cr)_{21}O_{38}$ and mohsite discredided. Can. Mineral. 17, 635—638.

Kennedy, G. C., 1955. Some aspects of the role of water in rock melts. Geol. Soc. Am. Spec. Paper 62, 489—503.

Kuo, H. Y. & Crocket, J. H., 1979. Rare earth elements in the Sudbury Nickel Irruptive: Comparison with layered gabbros and implications for Nickel Irruptive petrogenesis. Econ. Geol. 74, 590—605.

Lahti, S. I. & Honkamo, M., 1980. Kallioperäkartta — Pre-Quaternary rocks. Lehti — Sheet, 3543 Loukusa. Geological map of Finland, 1: 100 000.

Longhi, J., Walker, D. & Hayes, J. F., 1975. Fe-Mg distribution between olivine and lunar basaltic liquids (abs). EOS (Am. Geophys. Union Trans.) 56, p. 471.

Longhi, J., Walker, D. & Hayes, J. F., 1976. Fe and Mg in plagioclase. Proc. Lunar Sci. Conf. 7th, 1281—1300.

McBirney, A. R. & Noyes, R. M., 1979. Crystallization and layering of the Skaergaard intrusion. J. Petrology 20, 487—554.

McClay, K. & Campbell, I. H., 1976. The structure and shape of the Jimberlana Intrusion, Western Australia, as indicated by an investigation of the Bronzite Complex. Geol. Mag. 113, 129—139.

McDonald, J. A., 1965. Liquid immiscibility as one factor in chromitite seam formation in the Bushveld Igneous Complex. Econ. Geol. 60, 1674—1685.

— , 1967. Evolution of part of the Lower Critical Zone, Farm Ruighoek, Western Bushveld. J. Petrology 8, 165—209.

Mäkelä, T., 1975. Emäksisen magman kiteytyminen ja differentiaatio Porttivaaran alueella, Koillismaalla. Master's thesis. Manuscript at the Department of Geology, University of Oulu, Finland. 103 p.

Mason, P. K., Frost, M. T. & Reed, S. J. B., 1969. B. M.—I. C.—N. P. L. computer programs for calculating corrections in quantitative x-ray microanalysis. Nat. Phys. Lab. IMS Report 2.

Mathison, C. I., 1975. Magnetites and ilmenites in the Somerset Dam layered basic intrusion, Southeastern Queensland. Lithos 8, 93—111.

Matisto, A., 1958. Kivilajikartan selitys. Lehti — sheet, D5, Suomussalmi. English summary: Explanation to the map of rocks. General Geological Map of Finland, 1: 400 000. 115 p.

Metzger, F. W., Kelly, W. C., Nesbitt, B. E. & Essene, E. J., 1977. Scanning electron microscopy of daughter minerals in fluid inclusions. Econ. Geol. 72, 141—152.

Moreland, G. C., 1968. Preparation of polished thin sections. Am. Mineral. 53, 2070—2074.

Nwe, Y. Y., 1976. Electron-probe studies of the earlier pyroxenes and olivines from the Skaergaard intrusion, East Greenland. Contrib. Mineral. Petrol. 55, 105—126.

Ohenoja, V., 1968. Porttivaaran—Kuusijärven alueen kallioperä. Master's thesis. Manuscript at the Department of Geology, University of Oulu. 88 p.

Osborn, E. F., 1959. Role of oxygen pressure in the crystallization and differentiation of basaltic magma. Am. J. Sci. 257, 609—647.

Page, N. J., 1979. Stillwater Complex, Montana — Structure, mineralogy and petrology of the Basal zone with emphasis on the occurrence of sulfides. U. S. Geol. Surv. Prof. Paper 1038, 1—69.

Phillpotts, A. R., 1966. Origin of the anorthosite—mangerite rocks in southern Quebec. J. Petrology 7, 1—64.

Piirainen, T. & Juopperi, A., 1968. Die Titaneisenerzlagerstätte von Porttivaara und ihre Entstehung. Nordia 1968, 5. 24 p.

Piirainen, T., Alapieti, T., Hugg, R. & Kerkkonen, O., 1977. The marginal border group of the Porttivaara layered intrusion and related sulphide mineralization. Bull. Geol. Soc. Finland 49 (2), 125—142.

Piirainen, T., Hugg, R., Aario, R., Forsström, L., Ruotsalainen, A. & Koivumaa, S., 1978. Koillismaa malmikriittisten alueiden tutkimusprojektin loppuraportti 1976. English summary: The report of the Koillismaa Research Project. Geol. Surv. Finland, Rep. Invest. No. 18. 51 p.

Podmore, F., 1970. The shape of the Great Dyke of Rhodesia as revealed by gravity surveying. Geol. Soc. South Africa, Spec. Publ. 1, 610—620.

Prinz, M., 1967. Geochemistry of basaltic rocks: trace elements, 271—323 in Basalts, ed. by H. H. Hess and A. Poldervaart. John Wiley and Sons, New York.

Rieder, M., 1977. Micas: calculation of crystallochemical formulas by a FORTRAN IV computer program. Věstnik Ústředního ústavu geologického 52, 333—342.

Roeder, P. L., Campbell, I. H. & Jamieson, H. E., 1979. A re-evaluation of the olivine—spinel geothermometer. Contrib. Mineral. Petrol. 68, 325—334.

Roeder, P. L. & Emslie, R. F., 1970. Olivine-liquid equilibrium. Contrib. Mineral. Petrol. 29, 275—289.

Rosenberg, R. J., 1977. Instrumental neutron activation analysis as a routine method for rock analysis. Tech. Res. Cent. Finland, Electr. Nucl. Technol., Publ. 19. 139 p.

Ruotsalainen, A., 1977. Koillismaan intruusioiden rakenteen geofysikaalisesta tulkinnasta. Master's thesis. Manuscript at the Department of Geophysics, University of Oulu, Finland. 64 p.

Skala, W., 1979. Some effects of the constant-sum problem in geochemistry. Chem. Geol. 27, 1—9.

Smith, C. H., 1962. Notes on the Muskox intrusion, Coppermine River area, District of Mackenzie. Geol. Surv. Can. Paper 61—25. 16 p.

Steiger, R. H. & Jäger, E., 1977. Subcommission on geochronology: convention on the use of decay constants in geo- and cosmochronology. Earth Planet. Sci. Lett. 36, 359—362.

Stevens, R. E., 1944. Composition of some chromites of the Western Hemisphere. Am. Mineral. 29, 1—34.

Streckeisen, A., 1976. To each plutonic rock its proper name. Earth-Sci. Rev. 12, 1—33.

Sweatman, T. R. & Long, J. V. P., 1969. Quantitative electronprobe microanalysis of rock-forming minerals. J. Petrology 10, 332—379.

Thompson, R. N., 1973. Titanian chromite and chromian titanomagnetite from a Snake River Plain basalt, a terrestrial analoque to lunar spinels. Am. Mineral. 58, 826—830.

Till, R., 1977. The HARDROCK package, a series of FORTRAN IV computer programs for performing and plotting petrochemical calculations. Computers & Geosciences 3, 185—243.

Todd, S. G., Schissel, D. J. & Irvine, T. N., 1979. Lithostratigraphic variations associated with the platinum-rich zone of the Stillwater complex. Carnegie Inst. Wash. Yearb. 78, 461—468.

Ulmer, G. C., 1969. Experimental investigations of chromite spinels. Econ. Geol. Mon. 4, 114—131.

Väyrynen, H., 1954. Suomen kallioperä, sen synty ja geologinen kehitys. Helsinki, Otava. 260 p.

Wager, L. R., 1960. The major element variation of the layered series of the Skaergaard intrusion and a re-estimation of the average composition of the hidden layered series and of the successive residual magmas. J. Petrology 1, 364—398.

Wager, L. R. & Brown, G. M., 1968. Layered igneous rocks. Edinburgh, Oliver and Boyd. 588 p.

Weiser, T., 1967. Untersuchungen mit der Elektronenmikrosonde über die Zusammensetzung von Chromiten. Neues Jb. Miner. Abh. 107, 113—143.

Wells, P. R. A., 1977. Pyroxene thermometry in simple and complex systems. Contrib. Mineral. Petrol. 62, 129—139.

Wood, B. J. & Banno, S., 1973. Garnet-orthopyroxene and orthopyroxene-clinopyroxene relationships in simple and complex systems. Contrib. Mineral. Petrol. 42, 109—124.

York, S., 1966. Least-squares fitting on straight line. Can. J. Phys. 44, 1079—1086.